Cooperative Hydrogen-Bonding in Models of Self-Assembled Peptide Nanomaterials

by

Yung-fou Chen

A dissertation submitted to the Graduate Faculty in Chemistry in partial fulfillment of the requirements for the degree of Doctor of Philosophy,

The City University of New York

2007

UMI Number: 3292489

Copyright 2007 by
Chen, Yung-fou

All rights reserved.

UMI Microform 3292489
Copyright 2008 by ProQuest Information and Learning Company.
All rights reserved. This microform edition is protected against
unauthorized copying under Title 17, United States Code.

ProQuest Information and Learning Company
300 North Zeeb Road
P.O. Box 1346
Ann Arbor, MI 48106-1346

© Copyright 2007 by Yung-fou Chen

All Rights Reserved

APPROVAL

This manuscript has been read and accepted for the
Graduate Faculty in Chemistry in satisfaction of the
dissertation requirement for the degree of Doctor of Philosophy.

Date	Professor Joseph J. Dannenberg Chair of Examining Committee
Date	Professor Gerald W. Koeppl Executive Officer

Professor Hiroshi Matsui

Professor Nicholas D.K. Petraco

Professor Raji Viswanathan

Supervisory Committee

THE CITY UNIVERSITY OF NEW YORK

DEDICATION

I would like to dedicate this dissertation to my father Da-kai Chen, a lymphoma and leukemia fighter, my wonderful mom, Min-ming Yen, and my lovely younger sister and a future chemist, Yung-chieh Chen.

ACKNOWLEDGMENTS

To my mentor Dr. Dannenberg - for his expert mentoring, generous support and valuable advice in not only research but also in life, especially regarding the concepts of Hydrogen bonds.

To my first mentor in the early days of my Ph.D. study, Dr. Hiroshi Matsui - for introducing me to the world of peptide nanotube and nanotechnology research.

To my committee members: Dr. Nicholas D. K. Petraco, and Dr. Raji Viswanathan - for their kind guidance and helpful suggestions on my computational chemistry research.

To Thomas A. Kubic, JD, Ph.D. - for his admirable knowledge of forensic science and his encouragement for me to pursue a Ph.D. in chemistry.

To Dr. Tahsin Chow - for introducing me to the world of chemistry in College.

To Waldemar Cieniewizc - for his amazing ability to keep the Hunter cluster running.

To Dr. Florian Lengyel - for keeping the Graduate Center Monad Cluster running.

A special thank goes to Dr. Antonio Oliva - for his assistance reviewing my very first dissertation manuscript and his insightful suggestions.

To Pei-ting Hsu - a great friend and a wonderful supporter in my Ph.D. studies.

To Jim Chueh - my life-long friend and my professional ass kicker. Now I have done something to return your decade-long support and enlightenment.

To Midas Tsai - for his kind assistance and encouragement when we work together.

To all my friends in forensics and in other fields, for your faith in me and the unvarying encouragement and trust.

ABSTRACT

Cooperative Hydrogen-Bonding in Models of Self-Assembled Peptide Nanomaterials

by

Yung- fou Chen

Adviser: Professor Joseph J. Dannenberg

The effects of H-bond cooperativity of various peptide structures (glycine, diglycine and their derivatives) and various H-bond donor-accepter sequences are investigated by *ab initio* calculations. Frequency analysis of the C=O coupling effects due to H-bond cooperativity on infrared (IR) spectra of 4-pyridone and various diglycine derivatives inserted with acetylene spacers are also performed.

The H-bond interactions of carboxylic acids and amides dimers, the mixed dimers, and dimers can be manipulated by alkyl substitutions. The strengths of individual N-H···O and O-H···O H-bonds show significant variations in different structures. However, one should consider not only the strength of interactions but also the possibilities to further expand the structures in designing structures.

The influences of H-bond donor and acceptor sequences and the insertion of several spacers, such as acetylene and benzene are of interest. I investigated the groups of the DA-DA, DA-AD and AD-DA sequences. The results show the H-bond interactions are stronger when the dipole moments are aligned in opposite directions in those structures.

That the range of enthalpies for N-H···O H-bonds can vary from as little as 2 to as much 23 kcal/mol depends primarily upon the polarizability of whatever internally connects the N-H and C=O within the H-bonding molecule, which are two parallel -C=C entities in 4-pyridone. The contribution of covalent or charge-transfer interactions between the π-systems of adjacent 4-pyridones is small.

The C=O and N-H coupling in H-bonded chains of 4-pyridones was also studied. ^{14}C-substitutions are used to decouple various vibrations for purposes of illustration. The coupling of the C=O's occurs primarily via the cooperative H-bonds rather than transition dipole coupling (TDC) as demonstrated by 1) the fact that the couplings are greater than previously reported for similar studies on formamides despite the greater distance between the C=O's in the pyridone chains; and 2) the red shifts can be attributed to the changes in the geometries (particularly the C=O bond lengths) of the individual 4-pyridones in the H-bonding chains induced by the H-bonds resulting polarization of the monomers.

TABLE OF CONTENTS

LIST OF TABLES

LIST OF FIGURES

CHAPTER 1 – INTRODUCTION

Molecular systems composed of peptides or proteins can be programmed to produce intriguing and potentially useful supramolecular architectures. The formation of molecular structures with predictable patterns and properties of peptide self-assembles, especially amphiphilic peptides are discussed in several reviews. [1-4] These self-assembles can be formed via chiral, amphiphilic polymer assembly, molecular structural designing, template processes, and other template-free polymerizations. These amphihpilic peptides with particular secondary structures can self-assemble through non-covalent bond intermolecular interaction (coordination bonding, electrostatic, van der Waals force, H-bond and halogen bond) to form one, two and three-dimensional organized supramolecular structures. The ability to predict and control molecular assembly is a crucial topic in supramolecular chemistry and crystal engineering, because the properties of these self-assembled materials depend on the formed structures.[5-8] While designing structures, geometric parameters and the nature of intermolecular interactions must be carefully considered. The design and the preparation of self-assembled functional materials can bring benefits to nanotechnology. In this chapter, I will describe the background of self-assembly followed by the problems in designing nanomaterials. The introduction of computational techniques and the pros and cons of DFT methods I adopted will also be discussed. At the end of this chapter, a summary of each chapter will be described.

1.1 Background of self-assemblies

1.1.1 Molecular self-assembly

Molecular self-assembly is a process by which molecular spontaneously form ordered aggregates.[1,4] The process requires no direct synthetic approaches and the interaction involved are usually non-covalent. The hydrogen bonded self-assembled structures can form rapidly when mixing individual units together. The literature on the subject of the H-bonded self-assembly is very extensive. [1-4] Some special multiple H-bond structures including rosette/tape, artificial receptor mimics, and quadruple H-bonded systems were discussed.[4,9] Those self-assembled systems also have potential applications in electronics industry such as semiconductors and liquid crystals. Recently a new class of crowded aromatics that form 1-D semiconductor nanostructures *via* hydrogen bonding and π-π interactions (Figure 1-1).[10] Since these molecules have permanent dipole moments, the assembly of these molecular stacks can be controlled with electric fields. The side-chain structures can also be replaced to obtain desired face-on or edge-on orientation. The size of these structures can also be modified depending on the functional groups, concentrations, and solvents.

Timmerman et al. reviewed several H-bonded liquid crystal complexes with liquid crystalline such as pyridine and carboxylic acid mesogenic complexes including phenol-stilbazole, carboxylic acid - stilbazole, phenol - pyridine, alcohol - imidazole, and carboxylic acid - amidopyridine interactions.[11]

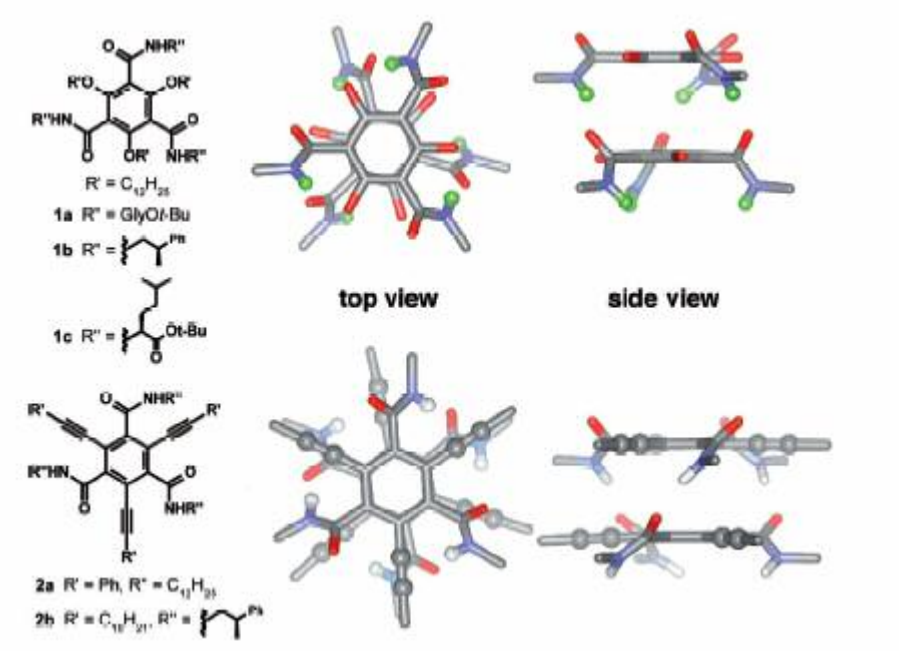

Figure 1-1. The crowded aromatics semiconductor nanostructures.[10]

1.1.2 Self-assembled peptide nanotubes

To clarify, the peptide mentioned here is defined as the structures contain four-atom functional groups -C(=O)NH- that can also be called amide groups. Peptide bonds can hold together chains of amino acids to form polypeptides or proteins. De Santis et al. first suggested that cyclic peptides including amino acids have the potential to develop tube-like stacks via H-bond in 1974.[12] It had not been achieved until about 20 years later when Ghadiri et al. reported the first assembly of organic nanotubes based on the said principle[13,14]. These cyclic nanotubes were composed of eight-membered cyclic peptide units with the sequence (L-Gln-d-Ala-l-Glu-d-Ala)$_2$. The nanotube can be extended one-dimensionally when more units are linked to each other through H-bond. This cyclic nanotube is unique in two parts. First, the cyclic nanotubes allow orthogonal stacking through the formation of eight H-bonds to extend the length of the nanotubes. Secondly, the diameter of the nanotube can be manipulated by changing the number and sequence of amino acids. As the cyclic peptide nanotubes are toxic to bacteria, they were demonstrated to serve as novel antibiotic agents.[15] As these structures can serve as nano-sized containers, it can be used for drug delivery.[16] These nanotubes can be incorporated into self-assembled monolayers (SAMs) of thiols or thioethers on gold film to construct diffusion-limited size selective sensors.[17] Cyclic voltammetry showed that the nanotubes act as selective ion channels, since only redox couples small enough to pass through the channels showed redox activity.

Peptide-based tubular structures can also self-assemble by linear peptides as was demonstrated by a family of bolaamphiphiles peptides by Matsui et al. (Figure 1-2).[18] In these structures, two glycines are separated by hydrophobic alkyl linker (heptyl), bis(N-α-amido-glycylglycine)-1,7-heptane dicarboxylates can self-assemble into either fibrils or spheres depending upon the conditions. The driving force for the formation of these structures is most likely the intermolecular H-bond to form ordered structures. These peptide nanotubes were used as templates to form metal nanowires[19] and immobilized through H-bond on gold substrates functionalized with 4-mercaptobenzoic acid SAM.[20] Another immobilization procedure was conducted by coating the peptide nanotubes with avidin and binding them to gold surfaces treated with biotinylated self-assembled monolayer. The sequenced histidine-rich peptide molecules were assembled on nanotubes, and the biological recognition of the sequenced peptide selectively trapped Au ions for the nucleation of Au nanocrystals.[21,22] Moreover, in a similar manner with different sequence peptide, nickel nanocrystals were grown onto the nanotube surface resulting in magnetic tubes that can be used as building blocks for magnetic devices and recording media.[23] This nanotube might also be applied to build nanoswitch in electronic and sensors. When the nanotube is functionalized with ferrocene and incorporated with cyclodextrin SAM coated on pattern gold substrates, the attachment and detachment of nanotube and the substrate can be controlled. This is due to the host-guest molecular interaction between ferrocene and cyclodextrin is sensitive to the redox states.[24]

Although a model suggested that the protonated bolaamphiphiles form stable acid-anion pairs (R-$COO^-$and R-COOH) with deprotonated species through unusually strong hydrogen bonds.[25] But that model did not consider the interlayer N-H···O H-bond from glycine and there is no direct evidence showing the real structure of such stable acid-anion dimer. Therefore, theoretical studies of H-bonds in such bolaamphiphiles are needed to provide experimentalists the energetic and geometric results of the H-bonded structures.

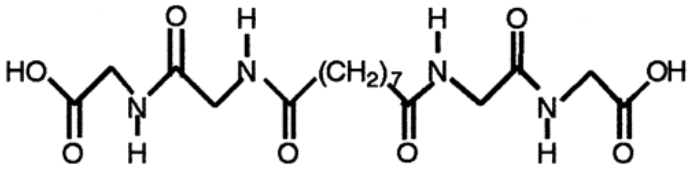

Bis(N-α-amido-glycylglycine)-1,7-heptane dicarboxylate

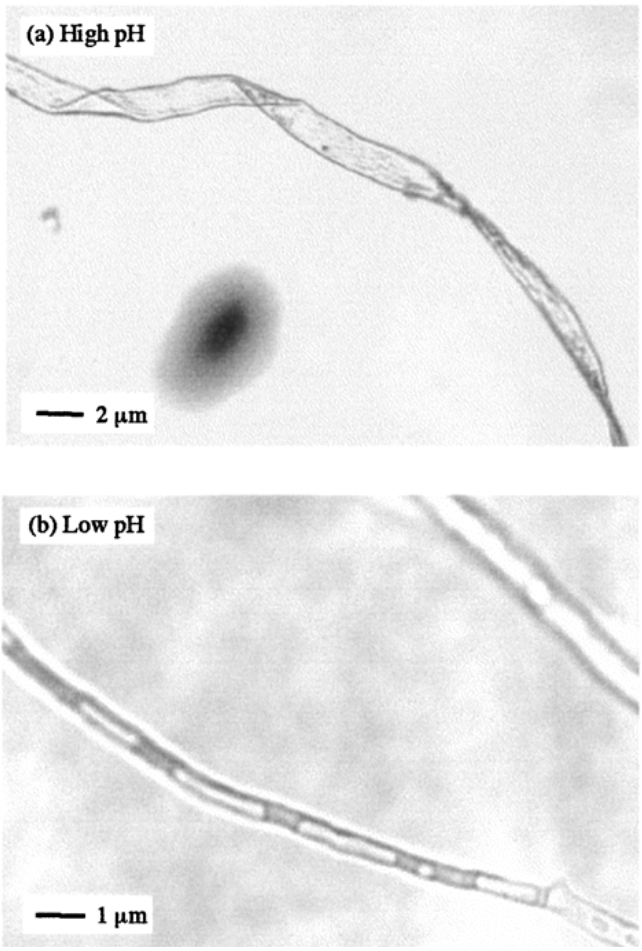

Figure 1-2. Proposed heptane bolaamphiphile assembly mechanism.[18]

Reches and Gazit reviewed several recent peptide nanotubes (Figure 1-3).[26] Those include bolaamphiphiles, hydrophilic peptides with hydrophobic alkyl tail**,** the V6D1 surfactant-like linear peptides, and the biphenyl peptides**.** The bolaamphiphile nanotubes have been discussed in the previous section (Figure 1-3A). The peptide conjugated amphiphile hydrophilic peptides with hydrophobic alkyl tail (Figure 1-3B) can be used as artificial three-dimensional scaffolds as the self-assembled nanofibers form fibrillar network. In order to encourage cell differentiation, adequate peptide sequences were incorporated.[27] The non-conjugated peptides with ordered nanoscaled structure have been demonstrated by Zhang et al. (Figure 1-3C).[28] The peptides are characterized by a hydrophilic head composed of aspartic acid and a tail composed of hydrophobic amino acids such as alanine, valine, or leucine. When dissolved in water, these peptides self-assemble by hydrophobic interactions into well-ordered nanotubes and nanovesicles. Several short peptide models containing aromatic residue (bipheylalanine) can inhibit amyloidal fibril formation are studied (Figure 1-3D and E).[29,30] Some of these motif inhibitors are under the clinical trial for the ability to treat Alzheimer's disease.[26] They found the two amino acid peptide, the biphenylalanine motif can self-assemble into a novel class of peptide nanotubes.[31] Those aromatic dipeptides can also self-assemble into nanosphere structures when a thiol group was introduced into the diphenylalanine peptide.[32]

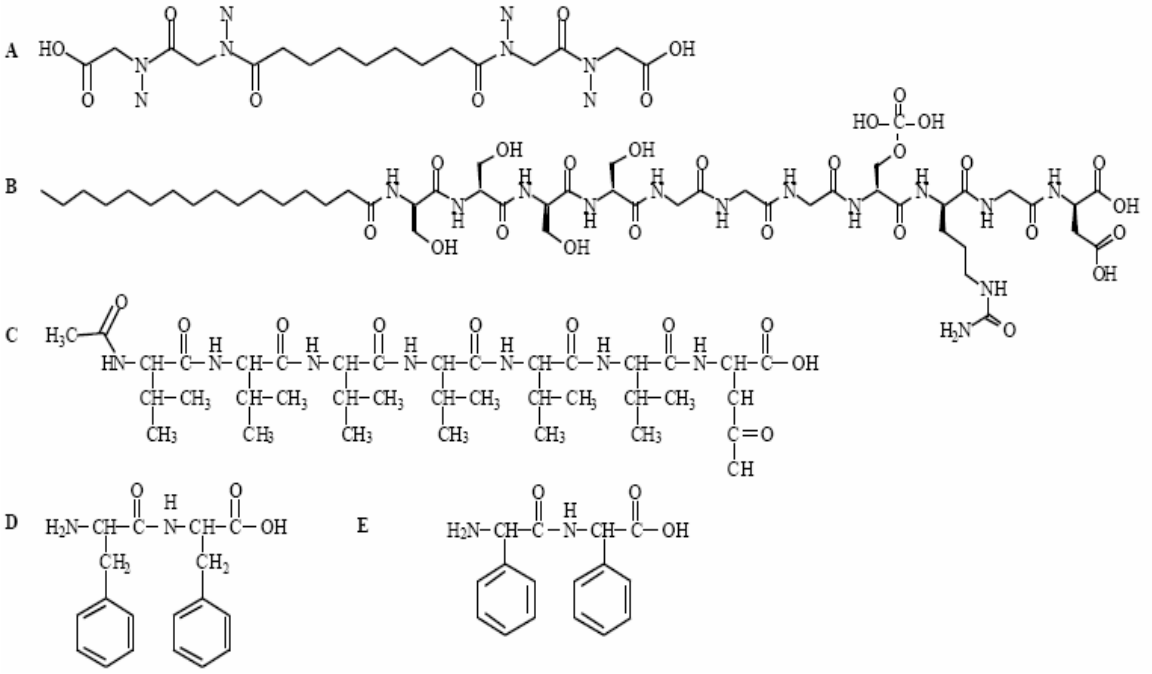

Figure 1-3. Chemical structures of the various self-assembling peptides.[26] **A.** bis(N-α-amido-glycylglycine)-1,7-heptane dicarboxylate. **B.** peptide-conjugate amphiphile composed of hydrophilic peptide with hydrophobic alkyl tail **C.** The V6D1 surfactant-like linear peptides. **D.** the diphenylalanine peptide **E.** the diphenylglycine peptide.

1.1.3 Hydrogen Bonds

The most attractive types of functional groups for general use in controlling intermolecular orientations in self-assembly are H-bonds. [1-4] The strength of H-bonding interaction ranges from about 1 to 40 kcal/mol, indicating the existence of a continuum of strength.[33] The precise definition of a hydrogen bond is still undetermined.[34] Occasionally, H-bonds are ascribed to only electrostatic or polarization interaction and others, covalent interactions are involved. Recently an International Union of Pure and Applied Chemistry (IUPAC) task group of fifteen international experts (http://www.iupac.org/projects/2004/2004-026-2-100.html) held a workshop in Pisa, Italy during 5~9 September 2005 to conclude the definition of H-bond. In the preliminary meeting report suggested the short definition and a list of criteria and characteristics for hydrogen bonds as follows:

> "*The hydrogen bond is an attractive interaction between the hydrogen from a group X–Hand an atom or a group of atoms Y, in the same or different molecule(s), where there is evidence of bond formation. The most important criteria for a hydrogen bond are: (i) the H in the X–H group is more electropositive than X and (ii) the physical forces involved in hydrogen bonding should include attractive electrostatic forces, i.e. it should not be primarily dispersive forces"*.

There are several unusual H-bond systems. The weak C-H···O and C-H···F H-bonds[35] and the binding energies of H-bonded complexes from Ar-CH_4 to $(H_3O)^+H_2O$ have a linear relationship with the electron densities and the Laplacian at the bond critical points[36] and other systems. This indicates the diversity of the H-bond interaction.

The word "cooperativity" can be considered as "the overall is greater than the sum of its parts", meaning that in a chain of H-bonds, the overall interaction is stronger than the sum of the individual interactions. There are two well-known kinds of H-bond cooperativity, σ and π-cooperativity.[33] The σ-cooperativity contains extended H-bonded linear chains or cyclic structures that increase the overall interactions. The σ-cooperativity can be found in some molecular crystals such as acetic acid[37,38], formamide[39], urea[40], nitroaniline[41], 1,3-cyclohexanedione[42,43], and 4-pyridone[44-46]. The π-cooperativity involves systems with multiple π-bonds is usually referred as the *resonance assisted hydrogen bond* (RAHB). RAHB usually found between hydroxyl groups such as carbohydrates crystal structures.[47-50] When we consider the increasing trend of cooperativity, it can be distinguished between "additive" and "nonadditive" cooperativity. Additive (pairwise) cooperativity is commonly regarded as the cooperativity associated with pairwise interactions. Nonadditive (non-pairwise) cooperativity is the cooperativity that exceeds the additive one. Only electrostatic interaction can show the pairwise cooperativity. Interactions that involve polarization are considered as a three-body problem and those involve mutual polarization and covalent interactions are many-body problems.[51] It is clear that when interactions are not pairwise additive, the cooperativities are nonadditive. The electrostatic component can be considered as composed of dipole-dipole interactions. The interactions are inversely

proportional to $1/R^3$, where R is the distance between the dipoles. If *N* dipoles are aligned linearly and evenly spaced to each other, the interactions between the first and the third dipoles (1-3 interactions) would be 1/8 ($1/2^3$) th of the 1-2 interactions as the distance between 1-3 are twice as long as the 1-2 distance. Likewise, the 1-4 interactions would be 1/27 th of the 1-2 interactions, etc. The maximum additive cooperativity in the electrostatic component would be a sum of all such pairwise interactions. In the infinite chains of dipoles, if only electrostatic interaction is involved, the strongest H-bond in the center of the chain could be 1.61 times that of a dimer. In the chains of formamide[52] and 4-pyridones[45], the strongest H-bond in both chains are greater than at least 2 times that of a dimer. This indicates the additive cooperativity is not adequate to explain this model and the importance of nonadditive cooperativity in crystal engineering and the designs of self-assemblies.

H-bonds play key roles in nanometer-scaled building blocks assembly.[53] A variety of new materials are synthesized and utilized to build desired shapes and structures through their unique self assembly properties.[54] The H-bond form peptide nanotube assemblies have been fabricating with proteins, metals, porphyrins, and nanocrystals as templates.[55] Thus great potential applications can be used in diverse fields from medicine, biotechnology, even to computer and electronics industry.[56] Amidic (N-H···O=C) H-bonds play important roles in both biochemical and synthetic self-assembling systems. The remarkable formamide H-bond[52] (almost twice as strong as the usual amide H-bond) contributes to the determination of the relative stabilities of peptide secondary structures, for example α-helices. Generally, the H-bonds involved in protein folding and DNA paring generally are more complex, and occur as cyclic dimeric or trimeric H-bonds.

1.2 Problems and Approaches

We have to understand the interaction of each hydrogen bond on the peptide structure to control or alter the functions and shape of the peptide nanomaterials. Computational studies of the cooperative hydrogen-bonding in peptide structures were investigated intensely.[57] The investigation of H-bonds in "peptide nanotube" is still in the early stages.[58] There are some studies of amphiphilic precursors self-assembly processes,[54] and computational studies by Monte Carlo study, coarse grain (CG) model, empirical force fields and atomistic molecular dynamics calculations.[59] Most of them are seeking the number of H-bond in the structures, not the quality (strength) of the H-bond. Also, some models[25] (such as acid-anion pairs) are used to explain the intra and intermolecular interactions between each monomer to cause the formation of the nanotubes. Computational study that can predict resulting structures stability is a necessary because it can offer experimentalists fundamental information while it is not obtainable due to the limitations of instruments.

An elastic theory based on liquid crystal has been applied to discuss lipid nanotube (LNT).[60] In order to describe nanotube formation, the theory assumes three scenarios, the splay, twist and bend. In a review by Shimizu et al.[3] they concluded several elastic theories successfully describe morphologies of LNTs and helical ribbon structures, however it is difficult to calculation all the parameters for a given molecular and predict nanotubes dimensions. According to their conclusion, it is because elastic theory is merely phenomenological, not directly obtained from the molecular structures. They also point out the elastic theories ignored crystalline-like molecular packing, several critical factors such as H-bond and π-π stacking are not considered and should be included later.

Macdonald and Whitesides identify the design of new solid-state materials must concern the controlling of both molecular and supramolecular structure. The reason is the solid-state properties are associated with the component molecules and the correct orientation with respect to one another in the crystal lattice.[4] Usually there are several problems in crystal engineering such as multiple possible orientations of molecules in crystals, inaccurate energies in estimation and thermodynamic and kinetic contribution to crystal growth.

Although molecular mechanics can be used as a tool in the design of supramolecular systems, Dannenberg revealed this level of calculation is not always adequate for supramolecular designs.[61] Highly accurate computational methods in rationale molecular designs of versatile H-bond supramolecules, the "molecular zipper" via Density Functional Theory (DFT) method is reported.[62] The H-bond strength of small molecule organic systems with multiple H-bonds was investigated first. Several H-bond combinations with different donor and acceptor sequences are also considered. The energies of the geometry-optimized polymers (tetramers in here) structures are compared with the monomer to determine the stability of various possible H-bond sequences. They suggested this approach could provide possible target molecules and guidelines for further design of molecular zippers. Perczel et al. performed *ab initio* calculations of strands of β-peptides and found that the sheets of β-peptides can form nanotubes rather than 2D extended sheet structures, as in α-peptides. [58]

The computational methods and proposed structures will be described in following sections in this chapter.

1.3 Computational methods

Obtaining accurate H-bond strength and geometry experimental and theoretical results are difficult tasks.[63,64] The angle of H-bond X-H···Y represents important characteristic of H-bond strength. In normal H-bond, the angle is in the range from 140 to 180° and it is directly proportional to the bond strenth.[65] When the angle is smaller, the H-bond interaction is due to the London dispersion.[66,67] It is generally known *ab initio* techniques that consider electron correlation can provide accurate description of H-bond.[68] Several methods such as second-order Møller-Plesset (MP2) perturbation theory, coupled clusters (CC) or configuration interaction (CI) can overcome the Hartree-Fock electron correlation errors that underestimate the H-bond strength.[69] The correlated methods are accurate. However, they are usually very expensive in time. A method with similar accuracy as MP2 but less computer time is a desired method. The density functional theory (DFT) method is a good candidate.[70] Traditional Hartree-Fock theory (H-F theory) is based on the complicated many-body electron wavefunction. It assumes that the exact, *N*-body wavefunction of the system can be approximated by a single Slater determinant or by a single permanent of *N* spin-orbitals. The wavefunction is dependent on 3*N* variables, three spatial variables for each of the *N* electrons. The DFT simplifies the complicated many-body electron wavefunction with the simplified electron density functional. DFT is a successful approach for the description of ground state properties of metals, semiconductors, and insulators. The success of density functional theory (DFT) not only encompasses standard bulk materials but also complex materials such as proteins and nanotubes.

The main concept of DFT is to describe an interacting system of fermions via its density and not via its many-body wave function. For *N* electrons in a solid, which follow the Pauli principle and repulse each other via the Coulomb potential. This means that the basic variable of the system depends only on three spatial coordinates x, y, and z, rather than 3*N* degrees of freedom. Kohn and Sham[71]suggested the electronic energy can be divided into several terms:

$$\mathbf{E = E^T+E^V+E^J+E^{XC}} \qquad \mathbf{(1.1)}$$

where E^T is the kinetic energy term, E^V describes the potential energy of nuclear-electron attraction and the repulsion between pairs of nuclei, E^J is the electron-electron repulsion term, and E^{XC} is the exchange-correlation term and includes the electron-electron interactions that were not described in the E^J term. $E^T+E^V+E^J$ corresponds to the classical energy of the charge distribution. E^{XC} is determined by the functional of the electron density, which is usually approximated as an integral involving only the spin density and maybe the gradient. E^{XC} is usually divided into *exchange* and *correlation* parts. The exchange and correlation parts correspond to same-spin and mix-spin interactions, respectively. Kohn and Sham[71]pointed out the self-consistent-field (SCF) DFT calculations are similar to the methodology of H-F theory. Since H-F theory also includes an exchange term in its formulation, Becke[72] established hybrid functionals that contain a mixture of H-F and DFT exchange along with DFT correlation, can be defined as:

$$\mathbf{E^{XC}_{\ hybrid} = C_{HF}E^X_{HF}+ C_{DFT}E^{XC}_{DFT}} \qquad \mathbf{(1.2)}$$

Where C's are constants and E^x is the exchange term of H-F theory.

The accuracy of DFT depends on if the selected functional can estimate the electronic exchange and correction contribution accurately as well as the need of functionals and the grids (a number of radial shells around each atom). Ireta et al.[69] pointed out some several concerns of the exchange and correlation functionals, including (1) the local-density approximation (LDA) overestimate the H-bond strength; (2) the generalized gradient approximation (GGA) and hybrid functionals are more accurate to describe the H-bonds than LDA; (3) the popular hybrid-GGAs, Lee-Yang-Parr function for correlation (LYP) and the Becke's 3-parameter nonlocal-exchange functional (B3LYP) and some other GGAs usually underestimate the H-bond strength, regarding MP2 or CC results[73]; (4) The reliability of more recently developed exchange and correlation functionals is not known yet; (5) GGAs provide low classical energy barrier for proton transfer between donor and acceptor atoms.

Ireta et al.[69] also discussed some other errors associated with the Kohn-Sham (KS) orbitals basis-set expansion. Among the three commonly used basis sets, localized Gaussian orbitals, localized numerical orbitals and plane waves, Gaussian orbitals possess rather greater basis set superposition error (BSSE). It also has to be corrected to obtain accurate H-bond interaction energies.[74] The BSSE occurs when atoms of interacting molecules approach one another, the monomers begin to use the basis set of their adjacent partner in the complex, that provides extra stabilization energy not coming from the interaction between dimer.[75] The BSSE is mostly greater in small basis sets, but gone when close to the complete-basis limit. When the distance between two molecules is shortened, the BSSE lowers gradually. The SCF BSSE can be reduced to small amount when larger base sets are applied, the correlated levels BSSE decreases in a slow trend.

BSSE can be corrected by calculating the energy of all species within the same set of basis functions. The corrected basis set used to calculate the energy of one monomer includes not only its own function but those of its adjacent partner as well. This correction is generally known as "functional counterpoise", the counterpoise (CP) correction.[76] The CP correction was proposed to correct the BSSE by Boys and Bernardi in 1970 and republished with modifications in 1992.[77] The CP correction is described as:

$$\mathbf{CP = E_{(A,\ basis\ A)} - E_{(B,\ basis\ AB)} + E_{(B,\ basis\ B)} - E_{(B,\ basis\ AB)}} \quad \mathbf{(1.3)}$$

The correction is performed by computing the energies of each individual monomer by "ghost orbitals", and later subtracts the error from the uncorrected energy to obtain the corrected interaction energies.[61,77-83]

The energies should be calculated in geometry optimization for the dimer. Turi and Dannenberg reported the CP correction for the BSSE for aggregates could be calculated by utilizing the sum of individual CP corrected results for each monomer in the basis of all monomers in the cluster.[84] Simon, Duran and Dannenberg performed an improved method of CP corrected supramolecules orbital calculation on potential energy surfaces (PES).[85] The obtained CP corrected results in interaction energies are more negative than the traditional method; the separation of intermolecular interaction is increased; and the H-bonding stretching vibrations decrease always.

In the study of the accuracy of DFT for describing H-bonds [69], the H-bond strength and geometry parameters obtained by Perdew, Burke and Ernzerhof (PBE) GGA functional show good agreement with MP2 and CC methods.[86] The results also show that the PBE functional is reliable for normal H-bond. As H-bond becomes weaker, London

dispersion plays a more important role, the accuracy of this DFT-PBE method decreases with increasing deviation from a linear D-H···A (D and A mean donor and acceptor, respectively) arrangement the accuracy of the DFT-PBE decreases. The DFT failures of describing the dispersion like interaction were also reported.[87] The error percentage of B3LYP in the H-bonded stacked tetramers can be as high as 83%.[88,89] The accuracy of X3LYP for H-bonded and van de Waals complexes shows it is feasible for the planar structures, but fails to localize any minimum at the stacked structures of the potential energy surface.[90]

The failures of DFT regarding energetic descriptions have been mentioned in several papers.[91] Those inaccurate predictions include the heats of formation of alkanes, bond energies, relative energies and molecular geometries, and many more other systematic deficiencies. [91-93] Schleyer et al. analyzed the performance of nine density functionals by comparing the isodesmic bond separation energy (BSE) of 72 hydrocarbons with available experimental results.[94]Those functionals include B3LYP, B3PW91, MPW1895, MPWB1k, PW91, M05-2X, B1B95, MPW1PW91, and PBE. The analysis reveals only Zhao and Truhlar's hybrid meta-GGA M05-2X functional can provide satisfying results.

Is DFT not good for H-bond study at all? Some studies show DFT can provide reliable results. When B3LYP combined with an adequate basis set size is used, it can provide accurate predictions of the geometries of both single and multiple hydrogen bonded structures.[73,95-97]Dannenberg et al. reported the DFT energetic and geometric results of the H-bond interaction of water dimers by D95++(d,p) basis set with CP correction. [78,82] The DFT value is even more close to the experimental value than the results obtained by HF and MP2 methods in different levels.

Molecular frequencies depend on the second derivative of the energy with respect to the nuclear positions. The vibrations of a molecule are given by its normal modes. Each absorption in a vibrational spectrum corresponds to a normal mode. Modes that have the same energy are called degenerate. In the classical treatment of molecular vibrations, each normal mode is treated as a simple harmonic oscillator (SHO). It could be considered as atoms with mass m are lined by spring with force constant k in erg/cm^2. Hook's law for an extension, x is represented as:

$$\mathbf{F = -dV/dx = -kx} \qquad \mathbf{(1.4)}$$

The potential for Hook's law can be obtained by integrating equation (1.4) to form

$$\mathbf{V = \tfrac{1}{2}\, kx^2} \qquad \mathbf{(1.5)}$$

In molecular mechanics and molecular orbital calculations, the force constant is not known. However, the force constant can be calculated from the second derivative of the potential energy.

$$\boldsymbol{k = d^2V/dx^2} \qquad \mathbf{(1.6)}$$

The Hooke's Law force is substituted into Newton' Law:

$$\boldsymbol{md^2V/dt^2 = -kx} \qquad \mathbf{(1.7)}$$

To solve the extension as the function of time

$$\boldsymbol{X(t) = Asin(2\pi\nu t)} \qquad \mathbf{(1.8)}$$

ν is the fundamental vibration frequency and A is the amplitude of the vibration. Taking the second derivative of the extension gives

$$d^2x/dt^2 = -4\pi^2\nu^2x \qquad (1.9)$$

Substituting equation (1.9) back into equation (1.7) gives:

$$-4\pi^2\nu^2 = k/m \qquad (1.10)$$

That is, if a molecule, initially in its ground vibrational state, could be excited so that it vibrated at a given frequency, then that molecule could absorb a photon that vibrates at the same frequency. Although vibrational frequencies are usually expressed as kilohertz or megahertz, in chemistry vibrational frequencies are normally expressed in terms of wavenumbers (cm^{-1}), which can be written as:

$$\nu = [1/(2\ c\pi)](k/\mu)^{1/2} \qquad (1.11)$$

In order for ν to be in cm^{-1}, c, the speed of light must be in $cm.sec^{-1}$, and μ the reduced mass in grams.

Raw computed frequency values at Hartree-Fock level contain systematic error from the negligence of electron correlation. This causes 10 to 12% overestimations (more blue shifted). The same error was also found on the calculations of zero-point energies. This systematic error can be corrected by applying scale factors that can provide values in good agreement with experimental values.

The intensities of the normal vibrational modes are extracted from the derivatives of the dipole moment, taken as linear with respect to nuclear coordinates. Within this

approximation, the intensities of the fundamentals are proportional to the square of the dipole moment derivatives with respect to normal coordinates.[98] The formation of H-bonds causes a large red-shift (> 100 cm^{-1}) of the fundamental C=O stretching vibration and occurs as a consequence of a lengthening of the C=O bond.[11] In addition, the intensity of the new band is significantly elevated, sometimes by more than two orders of magnitude and broadened.[99] The magnitude of the red-shift correlates linearly with the H-bond strength.[98-100] The strength of intermolecular H-bonds is directly related to the intensity of the H-bonded C=O frequency.

Coupling between the C=O's in proteins or peptides that lead to the amide I infrared absorption shifts often used to characterize H-bonded molecules. The coupling involved in the amide I band can occur by through-space transition dipole coupling (TDC) or by coupling of the C=O's mediated by H-bonds. The TDC method of calculating the coupling between C=O's in peptides was introduced by Krimm.[101] This method assumes that two peptides interact with each other via dipole–dipole interaction. The coupling between the oscillators is based upon the electrostatic interactions between the oscillating dipoles. As dipole-dipole interactions are electrostatic in nature, the mechanism of TDC depends upon the predominance of electrostatics in determining the interaction between the coupled entities. The coupling force constant which is constructed by the amide I vibrational coordinates of each peptide bond, can be obtained by examining the distance and relative orientation between the two relevant peptide groups in a given polypeptide.

In the final portion of this section, I would like to describe briefly the computational methods adopted in all the studies of H-bond interactions. Density

Functional Theory (DFT) calculations were performed using the Gaussian 03[102] suite computer programs on our parallelized cluster Pentium 4, and AMD Athlon computers which are parallelized using Linda.[103] All calculations used the D95(d,p) basis set and the B3LYP functional. This hybrid density functional method include Becke's 3-parameter nonlocal-exchange functional[104] with the correlation functional of Lee, Yang, and Parr[105]. This method was used for the ground-state structures with constrained degrees of freedom. The vibrational frequencies were calculated by the normal harmonic approximations employed in the Gaussian 03 program to verify the stationary points and to calculate the enthalpies of the various species. All frequencies were real except for some very low frequency imaginary vibrations. The basis set superposition error (BSSE) corrections in calculating intermolecular interactions were applied. This was achieved by the optimization on the counterpoise (CP) corrected potential energy surfaces values (CP-OPT)[78] were calculated using the procedure incorporated in Gaussian 03.

1.4 Brief Summary

The effects of H-bond cooperativity of various peptide structures (glycine, diglycine and their derivatives) and the effects of various H-bond donor and acceptor, will be discussed in Chapter 2-5. In the last two chapters, Chapter 6 and 7, the frequency analysis of the C=O coupling effects due to H-bond cooperativity on infrared (IR) spectra of 4-pyridone and various diglycine derivatives inserted with acetylene spacers will be discussed.

In Chapter 2, the H-bond strengths of carboxylic acids and amides dimers, the mixed dimers, and dimers with alkyl substitutions will be discussed. Usually one only consider the number of H-bonds in supramolecules instead of the quality of the H-bond while designing self-assembled nanomaterials.[3,106-110] I concentrate on the strengths of each N-H···O and O-H···O H-bonds (the quality of H-bond) and the effects of substitution in my study. For simplicity, the substituient adopted is a methyl group, $-CH_3$. This investigation can provide basic information necessary for categorizing the basic interactions between these moieties, so that these energetic parameters can be utilized for designing monomers that can self-assemble into desired patterns. I consider this information can be great help to explode the H-bond interaction in larger and more complex structures. The H-bond strength of individual N-H···O and O-H···O H-bond shows significant variation in different dimer systems.

The α and β mentioned stand for $-CH_3$ and $-C_2H_5$ between peptide groups (amide groups), correspondingly. Since the H-bond distances are shorter in the β-sheet than those in the α-helices, the H-bond cooperativity in the sheet structures plays an important

role.[111,112] The interaction energies/enthalpies of nylon-like, anti-parallel – sheets, extended structures, and the carboxylic acid at the terminal structures to understand the cooperativity of the H-bonds in these sheet structures and elucidate the reasons of H-bonding energies between strands are discussed in C++-hapter 3. This can help to choose appropriate functional groups to form desired vertically or horizontally extended structures. When we consider desired structures, the strength of interaction is not the only factors, the ability of specific structures to be further extended sometimes plays a more important role.

Since the β-peptides can form non-planar helical structures[58] , the influence of H-bond donor and acceptor sequence and the insertion of several spacers, such as acetylene and benzene to the H-bond strength and geometry will be covered in Chapter 4. The sequence groups of H-bond donor investigated are DA-DA, DA-AD and AD-DA. The H-bond interactions are stronger when the dipole moments are aligned in the opposite directions in those structures.

In Chapter 5, I investigated the chains of H-bond cooperativity in a linear 4-pyridones. The N-H···O H-bonding enthalpy between 4-pyridones connected in a chain of H-bonds can achieve -23 kcal/mol for the most central H-bonds, while that between two 4-pyridones is -9.90 kcal/mol based upon DFT calculations on the counterpoise-corrected potential energy surfaces. The range of enthalpies of N-H···O H-bonds vary from as little as -2 to as much -23 kcal/mol. This is because the polarizability of whatever internally connects the N-H and C=O within the H-bonding molecule. In 4-pyridone, the N-H and C=O are connected via two parallel -C=C- entities. The contribution of covalent or charge-transfer interactions between the π-systems of adjacent 4-pyridones is small.

The C=O and N-H coupling in H-bonded chains of 4-pyridones are studied in Chapter 6. ^{14}C-substitutions are used to decouple various vibrations for purposes of illustration. The coupled C=O vibrations are correlated to the H-bond in proteins and peptides. The coupling of the C=O's occurs primarily via the cooperative H-bonds rather than transition dipole coupling (TDC) as demonstrated by 1) the fact that the couplings are greater than previously reported for similar studies on formamides despite the larger distance between the C=O's in the pyridone chains (TDC coupling decreases with distance); and 2) the red shifts (also greater than for formamides) can be attributed to the changes in the geometries (particularly the C=O bond lengths) of the individual 4-pyridones in the H-bonding chains induced by the H-bonds and resulting polarization of the monomers.

The Amide I vibrations in designed structures will be described in Chapter 7. Those designed structures include various combinations of donor-acceptor sequence. We can observe how frequencies and intensities of the Amide I are influenced by the addition of various spacing molecules and the extension to form through H-bond couplings. I found longer H-bonding chains lead to lower frequency, more intense Amide I vibrations. When long H-bonding chains are present, the intensities of these low-frequency Amide I vibrations might dominate the spectra. Differences of conformations (cis and trans) of the dimers and tetramers exhibit significant spectroscopic variations. The trans structures show more intense peaks than the cis ones. The stronger H-bond interactions show more red-shifted absorptions.

CHAPTER 2—COOPERATIVE HYDROGEN BONDS: SMALL FRAGMENTS

2.1 Introduction

Self-assembled nano-structures have attracted much recent interest in general public with special attention to the applications of the development of new materials. While these structures are often thought to assemble via extensive hydrogen bond networks, the details of these H-bonding interactions remain elusive.[33,113] The same monomeric materials can self-assemble to more than one structure under different experimental conditions, mirroring the well-known phenomenon of polymorphism in crystals and the aggregation of some proteins into fibrils or plaques common to amyloid diseases. For example the bolaamphiphile molecules, bis(*N*-α-amido-glycylglycine)-1,7-heptane dicarboxylates can self-assemble into either fibrils or spheres depending upon the conditions.[114] Many self-assembled structures contain the functionality -CH_2-CO-NH-CH_2-NH-COOH or others that are similar.[114-117] Therein, they are rather biomimetic, as this structural motif is common to peptides, some of which are natural materials (e.g. silk) and similar motifs are present in well-known synthetic materials (e.g. nylon). A cursory inspection of this functionality reveals the presence of multiple donor and acceptor sites for H-bonding. Thus, a variety of various associative interactions could occur. Clearly, the design of *de nuovo* self-assembled structures would benefit significantly from an understanding of the relative energies of the interactions inherent in these interactions and how structural variations affect them.

In this chapter, I explore many different H-bonding patterns that are possible for typical interactions of these kinds off monomers. For simplicity, I first reduced each kind of interaction to its basic form, and then elaborated on these interactions with different patterns of alkyl substitutions. The particular interactions discussed in this chapter involve those between carboxylic acids, between amides, and between acids and amides. These results provide the information necessary for categorizing the interactions between these moieties, so that these energetic parameters can be used for designing monomers that can self-assemble into desired patterns. This chapter is the first step, the studies of larger and structures that are more complex will be discussed in later chapters. Several interactions that I discuss here have been previously studied by others.[41,118,119] I include them in this chapter so that all the interactions can be compared via calculations using a common method.

2.2 Calculation Details

Density Functional Theory (DFT) calculations of B3LYP functional and D95(d, p) basis set were performed by Gaussian 03[102] software. More about the computational methods are described in Chapter 1. The geometries of all species were completely optimized with the following constraints (1) each of the monomer was kept planar, (2) in the perpendicular species, each monomer was kept perpendicular with the X-H···O angle fixed at its value in the planar base pair (X is either nitrogen or oxygen in the H-bond). The vibrational frequencies were calculated for the planar structures, using the normal harmonic approximations employed in the Gaussian 03 program to verify the stationary points and to calculate the enthalpies of the various species. All frequencies were real except some very low frequency imaginary vibrations that involve out of plane rocking motions of the OH groups in some (but not all) structures. The basis set superposition error (BSSE) corrections in calculating intermolecular interactions were applied. This was achieved by the optimization on the counterpoise (CP) corrected potential energy surfaces values (CP-OPT)[78] were calculated using the procedure incorporated in Gaussian 03.

2.3 Results and Discussion

I first investigated the H-bonded dimers of the simplest functional groups, such as carboxylic acid, formic acid, the simplest amide, formamide, and their mixtures. Then I studied the possible methylated dimeric structures, since the above functional groups are connected with various structures, the methyl group is treated as the simplified structures connected with various dimeric structures. The cooperativity occurs when the total interaction of a combination of several interactions is greater than the sum of the individual interaction.

2.3.1 H-bonds of cyclic dimers and the effects of alkylation

If we only discuss simple dimers, it would not provide direct information on self-assembled materials. Other functional groups must be attached to them. Since these groups are often alkyl chains, we considered the effects of alkylation (here, methylation) at various positions. Formic acid has only one position available for alkylation, whereas formamide has two (C and N). To facilitate the following discussion, each structure is given a shortened name as follows. The structures include formic acid (FA), acetic acid (AA), formamide (FM), methyl formamide which methyl is attached to the C atom of foramide ($M_{(c)}FM$), methyl foramide which methyl group attached to the N atom of foramide ($M_{(n)}FM$). All the possible structures are shown in Figure 2-1.

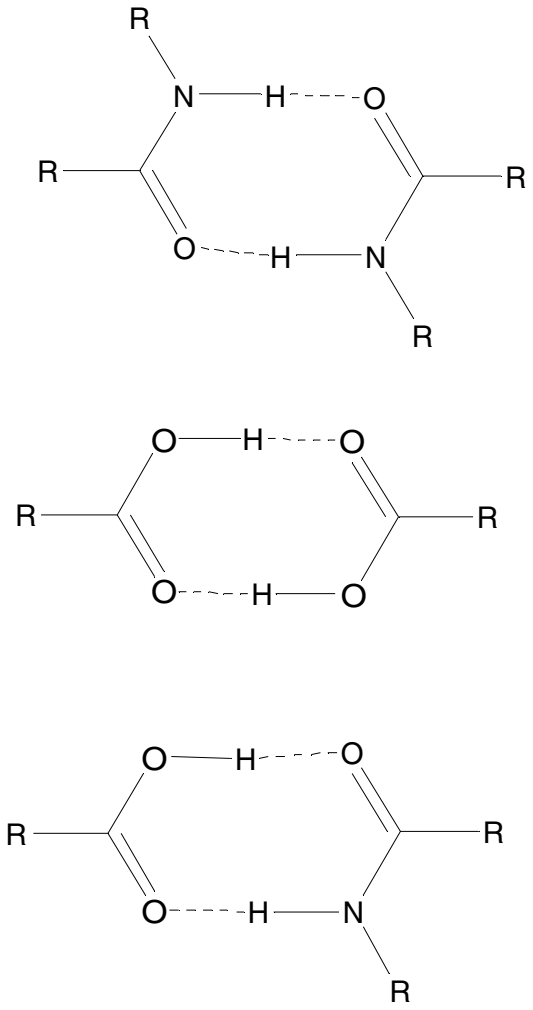

R = H or CH_3

Figure 2-1. The structures of cyclic formamide, formic acid, mixed dimers, and their derivatives.

After CP-OPT correction, the interaction enthalpies of the non-substituted FA, FM, and FA/FM dimers are -15.03, -12.12, and -14.27 kcal/mol by DFT respectively. The interaction energies of the above dimers are -16.44, -14.03, and -15.90 kcal/mol. Except the FA/FM dimers, the other dimers have C_{2H} symmetry, and all dimers contain two H-bonds. The enthalpy difference between each dimer is associated to H-bond strength difference of O-H···O and N-H···O. The energetic and geometric data of all non-substituted cyclic dimers are summarized in Table 2-1. To observe cooperativity and strength of H-bond, each monomer within a cyclic dimer is twisted at a 90-degree angle to each other to form the structure with only single N-H···O or O-H···O H-bond. In the FA/FM dimer, due to the nature of the dimer, both single H-bonds can be observed when the dimer is twisted in different ways. Sometimes, due to the C-H···O H-bond, the planar energy minimum of the single H-bond structure could be difficult to find. More details about the single H-bond interaction in structures will be discussed in later sections.

Table 2-1. Interaction energies, enthalpies and the summary of the calculated H-Bond distances and angles at the B3LYP/D95(d,p) computational levels of FM, FA, and FA/FM dimers.[α]

SPECIES	ΔE	ΔH	O-H···O	N-H···O	(OHO)degree	(NHO)degree	COOP (ΔE)
FM/FM	-14.03	-12.12		1.841		173.6	-4.37
1-HB (N-H···O)	-4.83			1.972		163.6	
FA/FA	-16.44	-15.03	1.629		178.8		-6.06
1-HB (O-H···O)	-5.19		1.822		165.9		
FA/FM	-15.90	-14.27	1.626	1.855	175.4	165.3	-4.07
1-HB (O-H···O)	-8.31		1.727		170.2		
1-HB (N-H···O)	-3.52			2.056		176.7	

[α] Energies and enthalpies are in the unit of kcal/mol. COOP means “cooperativity”. Bond distances are in angstrom and the angles are in degree.

2.3.2 H-bonds of cyclic formamide dimers

The cyclic formamide dimer is depicted in Figure 2-1. The interaction enthalpy and energy are -12.12 and -14.03 kcal/mol, respectively. Luque et al. reported the value of -13.35 for the interaction energy.[119] The longer H-bonds (relative to formic acid dimer) of 1.841 Å reflect both the lower stabilizations calculated and the larger atomic radius of nitrogen than oxygen. Varetti et al. reported in different basis sets, the N-H···O H-bond distances of cyclic formamide are 1.849 and 1.876 Å[120], and the enthalpies are -15.43 and -11.26 kcal/mol, respectively. While analyzing single H-bonds for the investigation of H-bond cooperativity, we can find a planar minimum that avoids the C-H···O complication mentioned above existing in the formic acid dimer. The calculated bond distance and interaction energy for this single N-H···O H-bond formamide dimer (opened) are 1.972 Å and -4.83 kcal/mol, respectively. The energy is much less than that the calculated per H-bond for the cyclic structure of -7.02 kcal/mol. Varetti reported in an open ring dimer (single H-bond), the enthalpies per H-bond are -4.79 to -7.53 kcal/mol in different basis sets. The N-H···O distances in different basis set are 1.965 and 2.002 Å. The geometric and energetic results in this study are similar to those of Varetti's results. The cooperativity in energy of the cyclic formamide dimer is -4.37 kcal/mol.

2.3.3 H-bonds of cyclic formic acid dimers

The calculated enthalpy of interaction of a formic acid dimer (see Figure 2-1) is -15.03 kcal/mol, while the corresponding energy is -16.44 kcal/mol. All geometric and energetic values of cyclic dimers are listed in Table 2-1. A DFT study reported the interaction energies with the range from -14.2 to -16.5 kcal/mol in different basis sets.[119] The O···O distance of the dimer in the gas phase is 2.765 Å[121] and the O-H···O crystal structure is 1.764 Å.[122] In MP2 method calculated results, the cyclic formic acid with interaction energy could be as strong as -13.27 kcal/mol, and the O-H···O bond distance is 1.756 Å.[123] While investigating single H-bond strength, I could not obtain a completely optimized structure that contains only a single H-bond as a C-H···O interaction formed in that structure. Dannenberg et al. have used this procedure previously to study the contributions of individual H-bonds and their cooperativity in the DNA base pairs.[124] This single O-H···O H-bond has the calculated interaction energy of -5.19 kcal/mol, which is significantly less than the -8.22 kcal/mol per H-bond of the cyclic dimer (we could not calculate the corresponding enthalpy for this structure because it is not a true minimum on the potential energy surface). From these two figures one can see that the H-bonding O···H distance of 1.629 Å in the cyclic dimer increases to 1.822 in structure with the single H-bond, as expected for a weaker H-bonding interaction. The cooperativity of FA/FA dimer is -6.06 kcal/mol, which is the strongest among the non-substituted dimers.

2.3.4 H-bonds of cyclic mixed dimers

The cyclic mixed dimers of formic acid and formamide (see Figure 2-1) have interaction enthalpies and energies (-14.27 and -15.90, respectively) that are intermediate between those of the two homogeneous dimers. The N-H···O distance in this dimer of 1.855 Å is longer (N-H···O 1.841), and the O-H···O distance of 1.626 is shorter (O-H···O 1.629) than those in the two homogeneous dimers. The implication of these structural variations would be that one H-bond (the O-H···O) is stronger and the other (N-H···O) weaker than in the homogeneous dimers. Chakraborty et. al. reported the interaction energies of cyclic dimers could be in the range of -14.29 to -15.12 kcal/mol, and the bond distance for O-H···O is 1.669 Å, and that for N-H···O is 1.917.[125] Table 2-1 shows that each of these single H-bonds has been lengthened relative to the cyclic structure. The interaction energies of the individual H-bonds are -3.52 (N-H···O) and -8.31 (O-H···O) kcal/mol, which follow the implications of the H-bond lengths in the cyclic dimer.

The single N-H···O and O-H···O bond distances are 1.727 and 2.056 Å, respectively. Thus, replacing an O-H (in both dimers that contains formic acid) with an NH_2 strengthens the O-H···O H-bond, while replacing an NH_2 with an O-H in both dimers that contain formamide weakens the N···H interaction. A rational explanation could be due to the values of relative electronegativity of oxygen and nitrogen. Since nitrogen is less electronegative than oxygen, donating electrons to the H-bond acceptor, C=O could be easier. Thus, the strength of H-bond is increased. The cooperativity of this mixed dimer is -4.07 kcal/mol, which is the weakest among the non-substituted dimers.

2.3.5 H-bonds of methylated formamide dimers

Figures 2-2 depicts nine cyclic dimers that can be formed from all possible combinations of mono and di-alkylated foramides. Let us first consider the effect of a single methylation at either C or N of only one formamide in the dimer. The interaction energies show that N-methylation increases the stability of the dimer by 0.11 kcal/mol, while C-alkylation decreases its stability by 0.10 kcal/mol in these cyclic dimers. Symmetric dimers of the N-methylated formamide have shorter H-bonds than the symmetric formamide dimer. The longer of the two H-bonds in this dimer with a single N-methyl group has a shorter of the two H-bonds in this last structure. The interaction energy makes this $M_{(n)}FM/M_{(n)}FM$ dimer 0.23 kcal/mole more stable than the FM/FM dimer. Thus, the effect of two N-methyl substitution is about twice the effect of just one. Methylated formamide in the dimer at C decreases the energetic stability of the dimer by 0.27 kcal/mole, which is more than twice the destabilization on a single C-methyl substitution. We can then predict the most stable structure in this system based on this additive assumption, which the most stable structure will be N-methyl substituted dimer which is 0.22 kcal/mol lower than the formamide dimer, whereas the calculated value is 0.23 kcal/mol. Nevertheless, when both methyls are on FM to form DFM, this kind of addition shows different effect. I found the interaction energy between DFM/FM is -13.89 kcal/mol, which is less stable than the FM/FM dimer by 0.14 kcal/mol. The least stable substituted dimer is DFM/DFM dimer, which is 0.41 kcal/mol higher than the FM/FM dimer. The most stable $M_{(n)}FM/M_{(n)}FM$ is more stable FM/FM dimer by 0.23 kcal/mol.

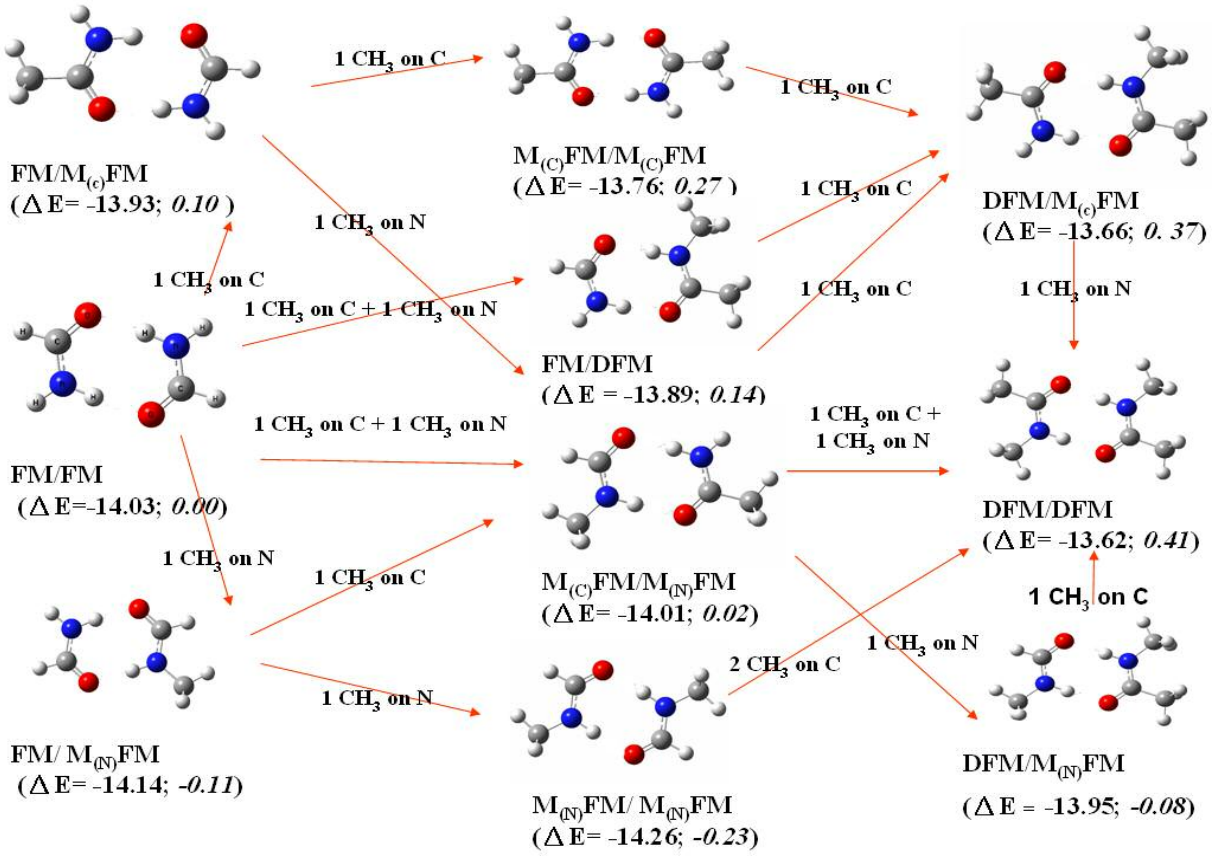

Figure 2-2. Interaction energies of formamide dimers and their derivatives. Values in *italic* stand for the energy differences (ΔΔE) between substituted dimers and formamide dimer.

2.3.6 H-bonds of formamide dimers substituted with one methyl

The detailed structures and single H-bonds of FM/FM, $M_{(n)}$FM/FM and $M_{(c)}$FM/FM dimers are illustrated in Figure 2-3. The interaction energies, enthalpies, bond distances, bond angles, and cooperativities of above three dimers are listed in Table 2-2. The effects of C- and N-methyl substitution can be observed clearly in these dimers. In the $M_{(n)}$FM/FM and $M_{(c)}$FM/FM dimers, I found that the H-bond distance is decreased with the C-methyl addition and is increased with the N-methyl addition. However, the interaction energy of $M_{(n)}$FM/FM is more stable than that of $M_{(n)}$FM/FM. This might be due to the lower cooperativity of this cyclic dimer structure compare to the formamide dimers (-3.42 vs. -4.37 kcal/mol). The single H-bonds of the C- and N-methyl substitution are -5.46 and -5.49 kcal/mol, respectively. Both bonds are stronger than per H-bond -4.83 kcal/mol in the FM/FM dimer. In a rigid cyclic dimer, if the strength of one H-bond is strengthened, this weakens the strength of the other H-bond, therefore the total interaction energies might be weakened or strengthen. If we only look at the destabilized C-methyl substituted structures, all the corresponding single H-bond is enhanced not only in interaction energy but also in the shortening of N-H···O distance, while the other single H-bond of the dimer is weakened. For the N-methyl substituted structures, the strengthened of the corresponding H-bond also strengthens the other single H-bond in the dimer even more. This dual H-bond strengthened phenomenon results in the more stable N-methyl substituted dimer than that of the C-methyl substituted ones. The changes of the interaction energies will depend on not only the C- or N-substitution, but also the cooperativity and the strength of the non-substituted H-bond.

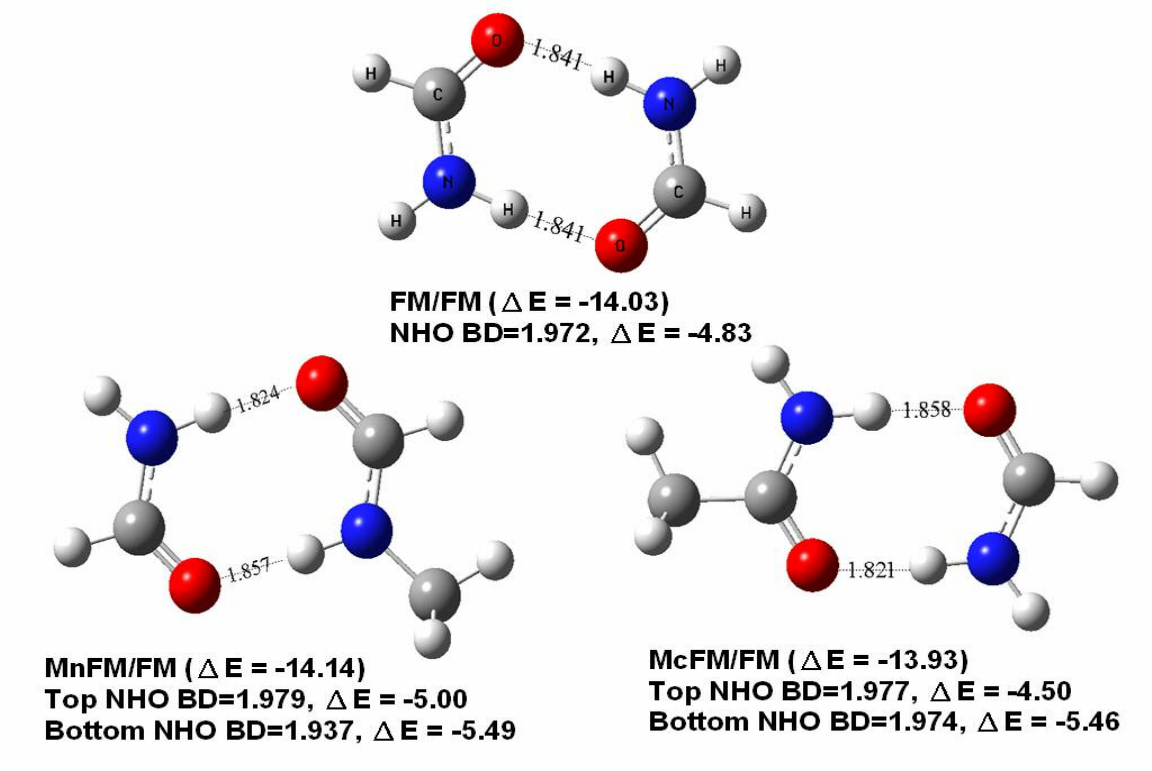

Figure 2-3. The geometric and energetic information of the FM/FM, $M_{(n)}$FM/FM and $M_{(c)}$FM/FM dimers**.**

Table 2-2. Interaction energies, enthalpies and the summary of the calculated H-bond distances and angles at the B3LYP/D95(d, p) computational levels of FM/FM, M(n)FM/FM and M(c)FM/FM dimers.[α]

SPECIES	ΔE	ΔH	N-H···O	N···O	degree	COOP(ΔE)
Amides						
FM/FM	-14.03	-12.12	1.841	2.869	173.6	-4.37
1-HB (N-H···O)	-4.83		1.972	2.971	163.6	
M(n)FM/FM	-14.14	-12.36	1.824/1.858	2.853/2.888	173.4/176.2	-3.65
1-HB (N-H···O) CH_3 on N	-5.00		1.979	2.988	167.4	
1-HB (N-H···O)	-5.49		1.937	2.938	163.4	
M(c)FM/FM	-13.93	-12.10	1.858/1.821	2.851/2.886	175.4/174.1	-3.97
1-HB (N-H···O) CH_3 on C=O	-5.46		1.974	2.977	167.2	
1-HB (N-H···O)	-4.50		1.977	2.989	170.2	

[α] Energies and enthalpies are in the unit of kcal/mol. COOP means "cooperativity". Bond distances are in angstrom and the angles are in degree.

2.3.7 H-bonds of formamide dimers substituted with two methyls

The detailed structures and single H-bonds of $M_{(n)}FM/M_{(n)}FM$, $M_{(c)}FM/M_{(c)}FM$, $M_{(N)}FM/M_{(c)}FM$ and DFM/FM dimers are illustrated in Figure 2-4. The geometric and energetic information of each dimer is listed in Table 2-3. In $M_{(n)}FM/M_{(n)}FM$ and $M_{(c)}FM/M_{(c)}FM$ dimers, I found the individual C-methyl substituted H-bond is stronger than that of N-methyl-substituted one by 0.09 kcal/mol (-5.17 ~ -5.08 kcal/mol). The cyclic $M_{(N)}FM/M_{(N)}FM$ dimer, shows the strongest H-bond cooperativity (-4.10 kcal/mol) and interaction energy (-14.26 kcal/mol) in this category.

The strongest single H-bond exists in DFM/FM dimer. This -5.70 kcal/mol H-bond interaction is associated with C-methyl substitution. The weakest single H-bond in this category also exists in DFM/FM dimer, which is -4.73 kcal/mol is associated with N-methyl substitution. In this dimer, the effect of methyl substitution is only concentrated on one monomer. In the $M_{(N)}FM/M_{(c)}FM$ dimer, the effect of one C-methyl and one N-methyl substitution on different monomers can be observed. In the $M_{(N)}FM/M_{(c)}FM$ and DFM/FM dimers, I found when methyls are substituted on different monomers, the dimer is more stable than those on the same monomer. I also found, although the sum of single H-bonds energies is more stable in the DFM/FM dimer, however, the $M_{(N)}FM/M_{(c)}FM$ dimer has more stable interaction energy. The strength of cooperativity plays a more important role than the strength of individual H-bond.

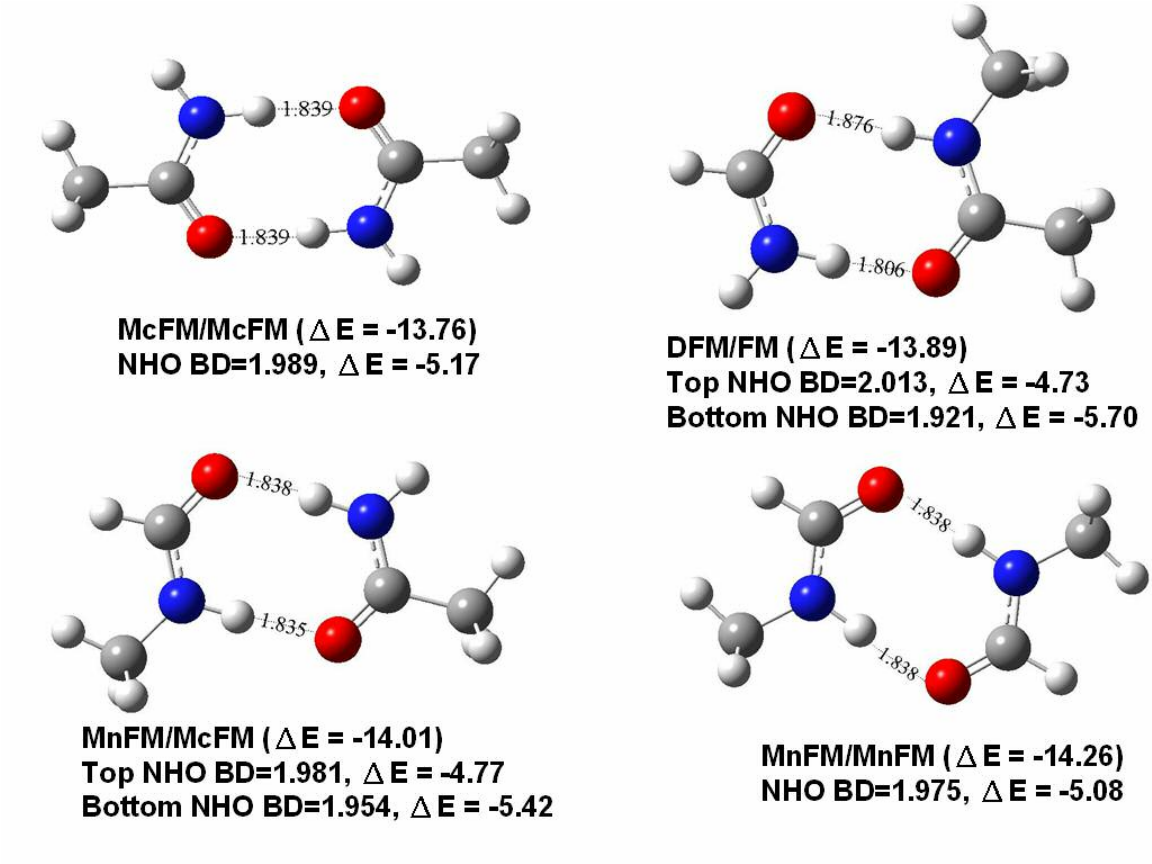

Figure 2-4. The geometric and energetic information of the $M_{(n)}FM/M_{(n)}FM$, $M_{(c)}FM/M_{(c)}FM$, $M_{(N)}FM/M_{(c)}FM$ and DFM/FM dimers.

Table 2-3. Interaction energies, enthalpies and the summary of the calculated H-Bond distances and angles at the B3LYP/D95(d, p) computational levels of M(n)FM/M(n)FM, M(c)FM/M(c)FM, M(N)FM/M(c)FM and DFM/FM dimers.[α]

SPECIES	ΔE	ΔH	N-H···O	N···O	degree	COOP (ΔE)
Amides						
M(c)FM/M(c)FM	-13.76	-12.00	1.839	2.869	175.9	-3.42
1-HB (N-H···O)	-5.17		1.989	2.991	165.8	
M(n)FM/M(n)FM	-14.26	-12.57	1.837	2.871	176.0	-4.10
1-HB (N-H···O)	-5.08		1.975	2.974	165.1	
M(n)FM/M(c)FM	-14.01	-12.27	1.838/1.835	2.868/2.868	175.2/176.6	-3.82
1-HB (N-H···O) CH_3 on C=O&N	-5.42		1.954	2.967	169.0	
1-HB (N-H···O)	-4.77		1.981	2.990	168.0	
DFM/FM	-13.89	-12.18	1.875/1.807	2.905/2.838	179.5/174.0	-3.46
1-HB (N-H···O) CH_3 on C=O	-5.70		1.921	2.940	170.0	
1-HB (N-H···O) CH_3 on N	-4.73		2.013	3.003	162.4	

[α] Energies and enthalpies are in the unit of kcal/mol. COOP means "cooperativity". Bond distances are in angstrom and the angles are in degree.

2.3.8 H-bonds of formamide dimers substituted with more than three methyls

The detailed structures and single H-bonds of DFM/$M_{(n)}$FM, DFM/$M_{(c)}$FM, and DFM/DFM dimers are illustrated in Figure 2-5. More than three methyl groups are added on each dimer. The geometric and energetic information of each dimer is listed in Table 2-4. In these dimers, under the influence of other methyl groups, I found the single C-methyl substituted H-bond is stronger than that of the N-methyl-substituted one by 0.89 kcal/mol (-5.71 ~ -4.82 kcal/mol). The DFM/$M_{(c)}$FM dimer shows the least H-bond cooperativity (only -2.92 kcal/mol), although individual H-bonds in this dimer are stronger. Because of this weak cooperativity, the interaction energy is only -13.66 kcal/mol, close to the least stable -13.62 kcal/mol of DFM/DFM dimer. This again indicates the strength of cooperativity is important than the sum of individual H-bonds, when considering H-bond interaction.

The strongest single H-bond in this category is the single C-methyl substituted H-bond in DFM/$M_{(c)}$FM dimer. This H-bond strength is -5.71 kcal/mol, which is close to similar H-bond (-5.70 kcal/mol) in DFM/FM dimer. The weakest single H-bond exists in DFM/DFM dimer. The strength of this one C- and one N-methyl substituted H-bond is -4.39 kcal/mol. This dimer has the strongest H-bond cooperativity (-4.84 kcal/mol) in all dimeric FM derivatives, however, the interaction energy -13.62 kcal/mol is also the least stable one in all dimeric FM derivatives. We can consider DFM/DFM dimer interaction energy as what we would observe in the real peptide nanotube, since FM must link to certain functional groups. The energy is slightly weaker than the FM/FM dimer by 0.41 kcal/mol. The cooperativity of all FM derivatives is -3.88 kcal/mol in average.

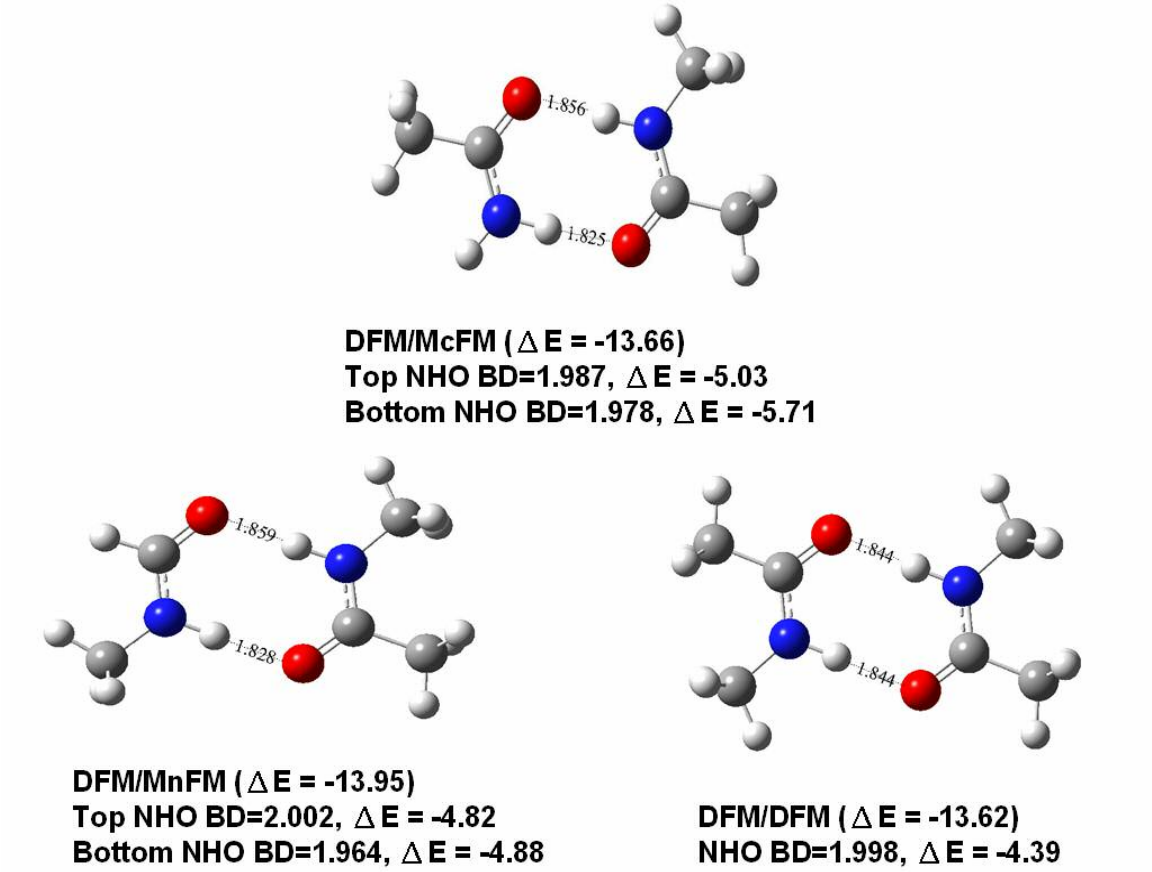

Figure 2-5 . The geometric and energetic information of the DFM/$M_{(n)}$FM, DFM/$M_{(c)}$FM, and DFM/DFM dimers.

Table 2-4. Interaction energies, enthalpies and the summary of the calculated H-Bond distances and angles at the B3LYP/D95(d,p) computational levels of DFM/M(n)FM, DFM/M(c)FM, and DFM/DFM dimers.[α]

SPECIES	ΔE	ΔH	N-H···O	N···O	degree	COOP (ΔE)
Amides						
DFM/M(n)FM	-13.95	-12.37	1.859/1.823	2.889/2.856	179.9/176.6	-4.25
1-HB (N-H···O) CH_3 on N	-4.88		1.964	2.988	176.3	
1-HB (N-H···O)	-4.82		2.002	2.989	161.4	
DFM/M(c)FM	-13.66	-12.02	1.858/1.826	2.887/2.856	179.8/175.8	-2.92
1-HB (N-H···O) CH_3 on C=O	-5.03		1.987	2.973	164.8	
1-HB (N-H···O)	-5.71		1.978	2.961	157.8	
DFM/DFM	-13.62	-12.07	1.844	2.874	179.8	-4.84
1-HB (N-H···O)	-4.39		1.998	2.987	161.9	

[α] Energies and enthalpies are in the unit of kcal/mol. COOP means "cooperativity". Bond distances are in angstrom and the angles are in degree.

2.3.9 H-bonds of formic dimers substituted with methyls

The interaction energies, enthalpies, bond distances, bond angles, and cooperativities of all possible formic/acetic acid (FA/FA, FA/AA, and AA/AA) dimers are tabulated in Table 2-5. The cyclic acetic acid (methylated formic acid) dimer is shown in Figure 2-6 with interactions enthalpies and energies of -15.26 and -16.56 kcal/mol, respectively. Luque et al. reported the interaction enthalpies of -14.7 ~ -16.9 kcal/mol and O···O distance of the single-bonded crystal structure is 2.680 Å.[119] Turi and Dannenberg reported the HF and MP2 studies of a cyclic acetic acid dimer, the interaction enthalpies are -15.0 and -11.2 kcal/mol, respectively.[38] They also summarized the enthalpies of cyclic carboxylic acids dimerization in the range between -13.8 to -17.0 kcal/mol. The interaction energy for a single H-bond is -5.64 kcal/mol, which is stronger than that of a FA dimer. Turi and Dannenberg also reported the HF and MP2 studies of the opened acetic acid dimer. The enthalpies of HF and MP2 methods are -4.40 and -4.80 kcal/mol, respectively.[38] The single H-bond in AA by DFT method is stronger than that by HF and MP2. The mixed dimer formic acid/acetic acid has an interaction enthalpy and energy of -16.58 and -15.24 kcal/mol, respectively. These energies are similar to those of an acetic acid dimer. However, the two O-H···O distances where the acetic acid is the acceptor is shorter (1.617 Å) and that where it is the donor, longer (1.660 Å) for the acetic or formic acid dimers. The H-bonding energies and O···H distances of the two H-bonds in Figure 2-6 are also quite different. The one with AA as the H-bond acceptor has the enthalpy of -6.22 kcal/mol and the bond distance of 1.778 Å. The other one has the enthalpy of -4.84 kcal/mol and the bond distance of 1.834Å. Thus, the effect of methyl substitution on formic acid enhances the H-bonding acceptor properties of the C=O,

while weakening the donor properties of the O-H. I noticed acetic acid to be a slightly more stable dimer (by 0.22kcal/ mol) than the formic acid one. The O-H···O bond distance in the formic acid dimer is longer than that in the formic acid one (1.636 vs. 1.629 Å). This indicates the stabilization and destabilization of structures might not directly reveal in the changing of H-bond distances and the cooperativity is more important than the sum of individual H-bond.

The strongest H-bond cooperativity was found in the FA/FA dimer. The cooperativities in FA/FA, FA/AA and AA/AA dimers do not show significant variances (-5.28 ~ -6.06 kcal/mol). The average cooperativity of the dimeric FA derivatives is -5.62 kcal/mol, which is stronger than that of the FM derivatives by 1.74 kcal/mol.

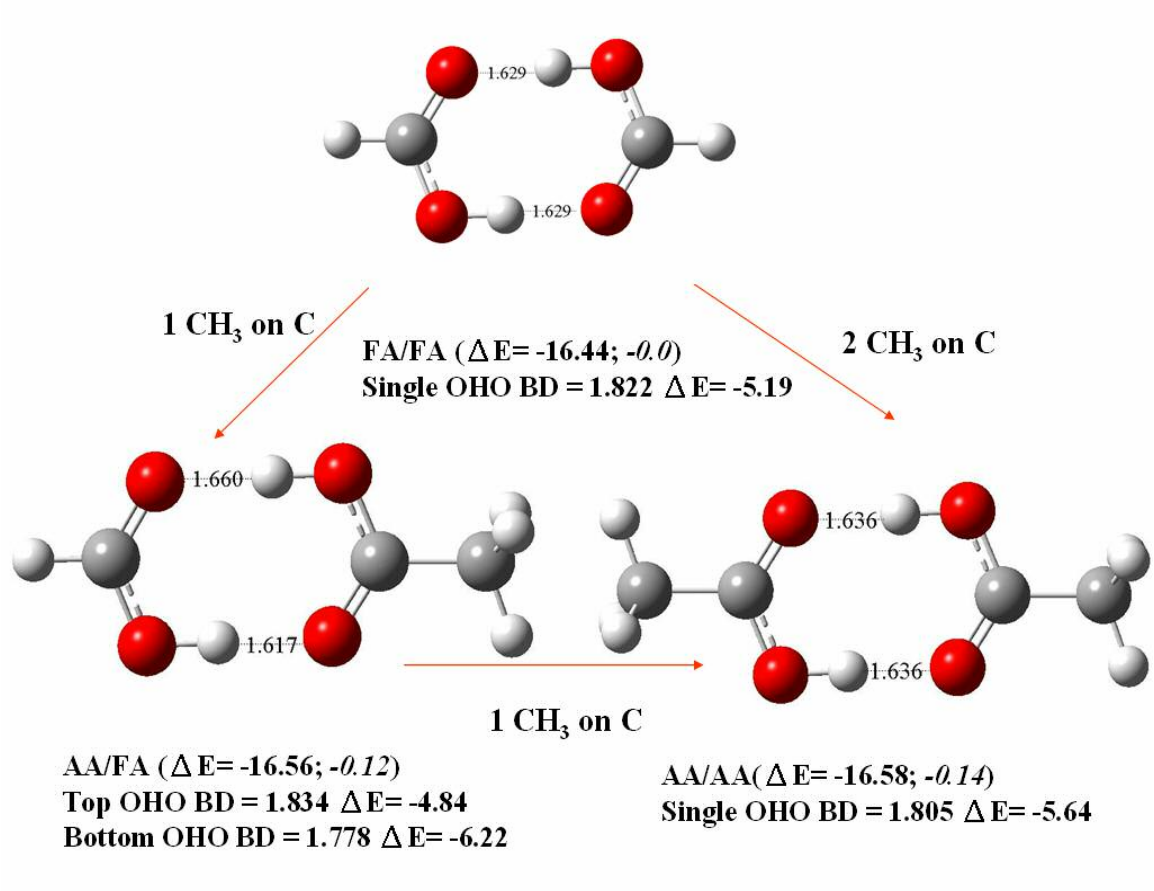

Figure 2-6. Interaction energies of formic acid dimers and their derivatives. Values in italic stand for the energy differenced (ΔΔE) between substituted dimers and formic acid dimer.

Table 2-5. Interaction energies, enthalpies and the summary of the calculated H-Bond distances and angles at the B3LYP/D95(d, p) computational levels of formic acid dimers and their derivatives.[α]

SPECIES	ΔE	ΔH	O-H···O	O···O	degree	COOP (ΔE)
Carboxylic Acids						
FA/FA	-16.44	-15.03	1.629	2.651	178.8	-6.06
1-HB						
(O-H···O)	-5.19		1.822	2.791	165.9	
FA/AA	-16.56	-15.24	1.617/1.660	2.630/2.666	179.8	-5.52
1-HB						
(O-H···O)						
CH_3 on C=O	-6.22		1.788	2.757	168.4	
1-HB						
(O-H···O)	-4.84		1.835	2.811	168.5	
AA/AA	-16.58	-15.26	1.635	2.644	179.0	-5.28
1-HB						
(O-H···O)	-5.64		1.805	2.781	168.1	

[α] Energies and enthalpies are in the unit of kcal/mol. COOP means “cooperativity”. Bond distances are in angstrom and the angles are in degree.

2.3.10 H-bonds of mixed dimers substituted with methyls

Figure 2-7 depicts the interaction energies of eight cyclic mixed dimers of formic acid and formamide. The most and least stable dimers in this category are DFM/FA (-0.74 kcal/mol) and AA/FM (+0.62 cal/mol) dimer, respectively. The AA/$M_{(n)}$FM and AA/$M_{(c)}$FM dimers have the same interaction energy, which indicates the effects of methyl substitution are reduced when AA is involved. It does not show significant differences of interaction energies of C- or N-methyl substitution, when they are substituted on the formamide. Either single C- or N-methyl substitution can stabilize the structure by 0.49 and 0.46 kcal/mol, respectively. What different from the previous homogenous dimers are C-methyl substitution on the formic acid to form acetic acid, significantly destabilize the interaction energy by 0.62 kcal/mol. By previous assumption, I can predict the most stable structure would be DFM/FA dimer, and the energy would be lowered by 0.95 kcal/mol. The calculated energy for that dimer is -0.74 kcal/mol. Significant deviation between predicted and calculated energies is also found in AA/DFM dimer, which indicates the interaction is not additive when DFM monomer is involved.

From the results in section 2.3.9, predicting the single C-methyl substituted AA/FM dimer is the least stable dimer is hard. In the AA/FM dimer (Figure 2-8), the N-H···O H-bond strength is increased by 0.33 kcal/mol while the addition of methyl on formic acid. Meanwhile, the other more stronger O-H···O H-bond in the dimer is weakened by 1.09 kcal/mol. The cooperativity is even stronger in this dimer than that of the FA/FM dimer, however, the interaction energy is still then destabilized.

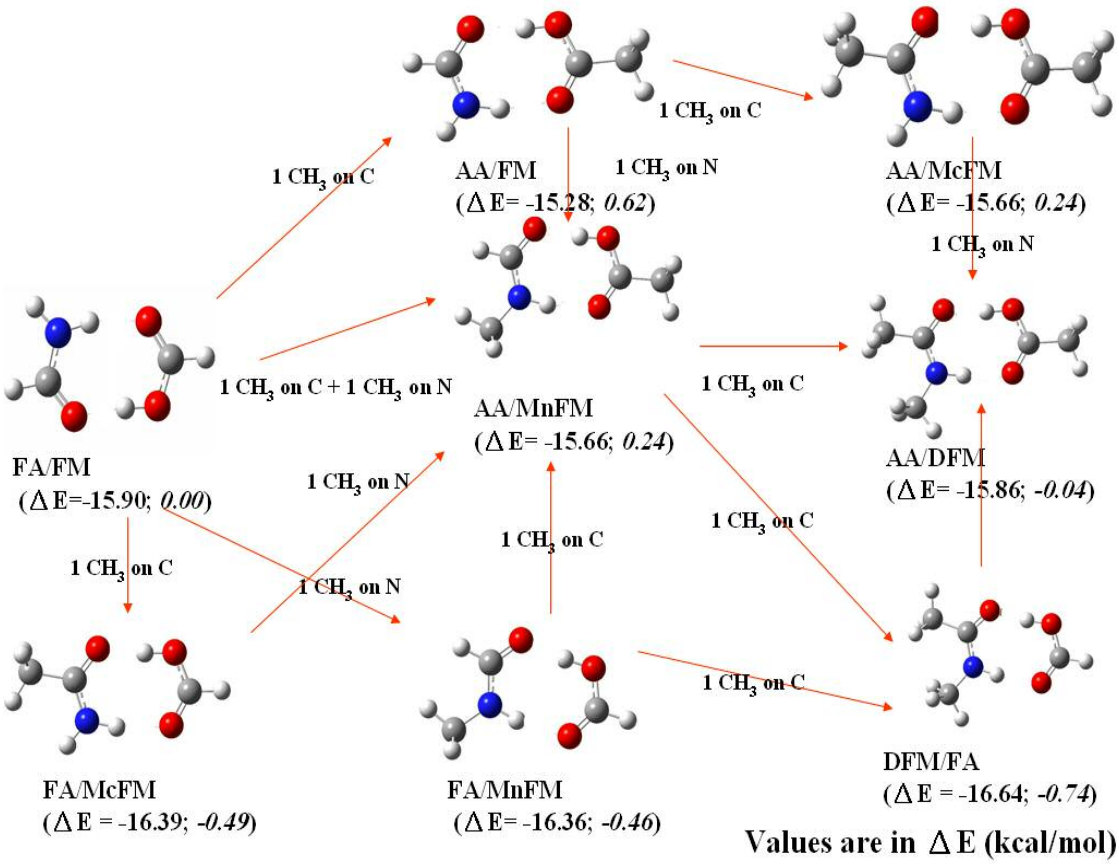

Figure 2-7. Interaction energies of FA/FM dimers and their derivatives. Values in italic stand for the energy differenced (ΔΔE) between substituted dimers and formic acid dimer.

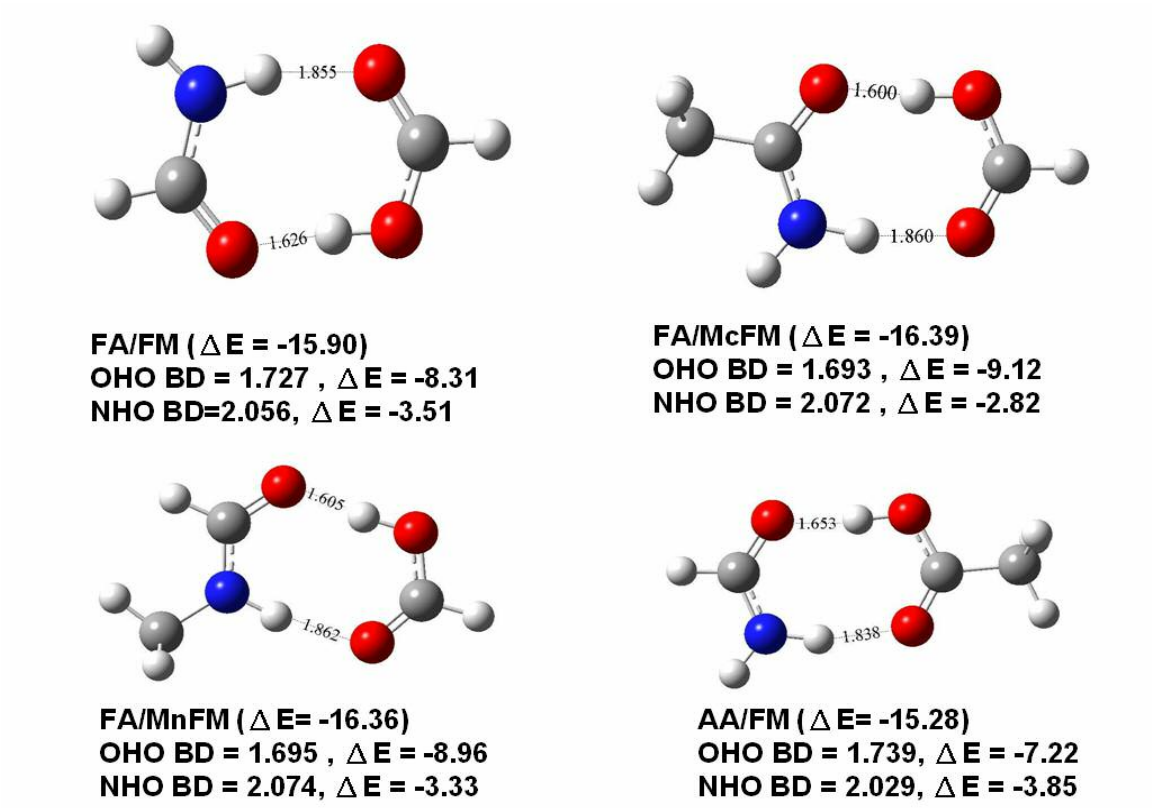

Figure 2-8. The geometric and energetic information of the FA/FM, FA/$M_{(c)}$FM, FA/$M_{(n)}$FM, and AA/FM dimers.

2.3.11 H-bonds of mixed dimers substituted with one methyl

The structures and single H-bonds of FA/FM, FA/$M_{(c)}$FM, FA/$M_{(n)}$FM, and AA/FM dimers are illustrated in Figure 2-8. One methyl group is added at various positions of each dimer. The interaction energies, enthalpies, bond distances, bond angles, and cooperativities of above dimers are listed in Table 2-6. The interaction energies of the FA/$M_{(c)}$FM and FA/$M_{(n)}$FM dimers are similar (the difference is only 0.03 kcal/mol). The results suggest the effects of the C-methyl and N-methyl substitutions are not significant in the mixed dimers.

The strongest cooperativity in this category occurs in FA/$M_{(c)}$FM dimer with the strength of -4.45 kcal/mol. In these four dimers, I found the cooperativity is increased (relative to -4.07 kcal/mol of the FA/FM dimer) while C-methyl substitution on either FA or FM. N-methyl substitution does not alter the strength of cooperativity (relative to the FA/FM dimer) of the FA/$M_{(n)}$FM dimer.

The strongest single N-H···O and O-H···O H-bonds both are associated with C-methyl substitution on FM and FA, respectively. The strongest single N-H···O H-bond is -3.85 kcal/mol in AA/FM dimer, and the weakest one is -2.82 kcal/mol in FA/$M_{(c)}$FM dimer. The strongest single O-H···O H-bond is -9.12 kcal/mol in FA/$M_{(c)}$FM dimer, and the weakest one is -7.22 kcal/mol in AA/FM dimer. The complementary combinations (the strongest O-H···O H-bond coexist with the weakest N-H···O H-bond, and vice versa) of N-H···O and O-H···O H-bond in the cyclic mixed dimer strongly support that the strength of H-bond in a rigid system is associated with each other and influenced by individual H-bond.

Table 2-6. Interaction energies, enthalpies and the summary of the calculated H-Bond distances and angles at the B3LYP/D95(d,p) computational levels of FA/FM, FA/$M_{(c)}$FM, FA/$M_{(n)}$FM, and AA/FM dimers.[α]

SPECIES	ΔE	ΔH	O-H···O	N-H···O	(OHO)	(NHO)	COOP (ΔE)
Carboxylic Acids/Amides							
FA/FM	-15.90	-14.27	1.626	1.855	175.4	165.3	-4.07
1-HB (O-H···O)	-8.31		1.727		170.2		
1-HB (N-H···O)	-3.52		2.056			176.7	
FA/M(n)FM	-16.36	-14.85	1.585	1.869	174.5	172.2	-4.07
1-HB (O-H···O)	-8.96		1.695		171.0		
1-HB (N-H···O)	-3.33		2.074			152.1	
FA/M(c)FM	-16.39	-14.88	1.600	1.861	174.7	167.4	-4.45
1-HB (O-H···O)	-9.12		1.693		171.6		
1-HB (N-H···O)	-2.82		2.072			167.6	
AA/FM	-15.28	-13.67	1.653	1.838	174.1	165.8	-4.21
1-HB (O-H···O)	-7.22		1.739		169.8		
1-HB (N-H···O)	-3.85		2.029			154.2	

[α] Energies and enthalpies are in the unit of kcal/mol. COOP means “cooperativity”. Bond distances are in angstrom and the angles are in degree.

2.3.12 H-bonds of mixed dimers substituted with two and more methyls

The energetic and of the DFM/FA, AA/M(c)FM, AA/M(n)FM, and AA/DFM dimers are illustrated in Figure 2-9. More than two methyl groups are added to each dimer. The energetic and geometric information of dimers are tabulated in Table 2-7. The most and the least stable dimers are the DFM/FA (-0.74 kcal/mol) and AA/M(n)FM (+0.24 kcal/mol) dimers, respectively. The strongest cooperativity with the value of -4.58 kcal/mol is found in the AA/M(n)FM dimer. The AA/M(c)FM dimer holds the weakest cooperativity of -3.82 kcal/mol.

The strongest single N-H···O and O-H···O H-bonds both are associated with C-methyl substitution on FM and FA, respectively. The strongest single N-H···O H-bond is -4.14 kcal/mol in AA/M(c)FM dimer, and the weakest one is -3.23 kcal/mol in DFM/FA dimer. The strongest single O-H···O H-bond is as high as -9.55 kcal/mol in DFM/FA dimer, and the weakest one is -7.70 kcal/mol in AA/M(c)FM dimer. The complementary N-H···O and O-H···O combination again indicates the strength of H-bond in a rigid system is related to each other.

The H-bonds are stronger in the mixed dimers than in the FA/FA and FM/FM dimers. The O-H···O H-bond is stronger than that of the FA/FA dimer by 2.87 kcal/mol (-8.34 vs. -5.16 kcal/mol), and N-H···O is weaker than that of the FM/FM dimer by 2.04 kcal/mol (-3.43 vs. -5.47 kcal/mol). That indicates the O-H···O is the more important

bonds in this system, any modification of this bond can significant change the interaction energy of this cyclic dimer. The average cooperativity of the mixed dimers is -4.20 kcal/mol. This is stronger than that of the dimeric FM derivatives but weaker than that of the dimeric FA derivatives.

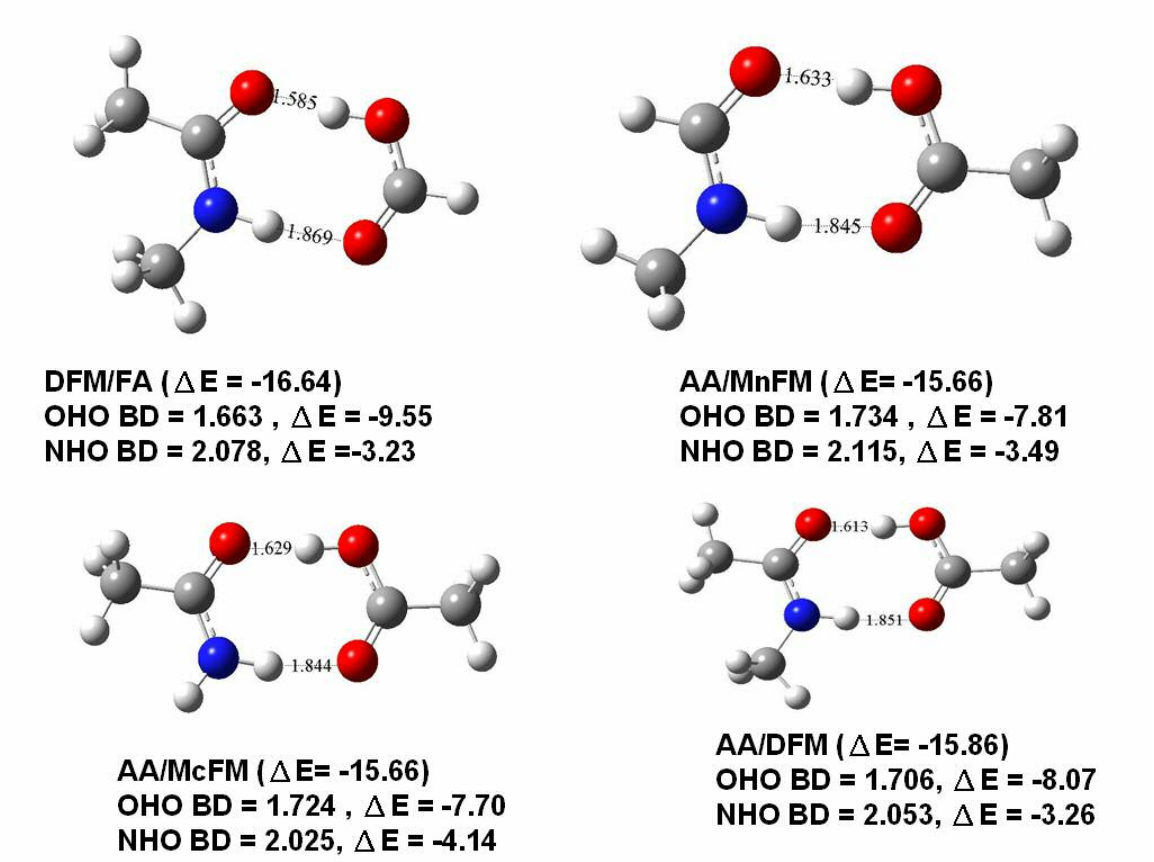

Figure 2-9. The geometric and energetic information of the DFM/FA, AA/$M_{(c)}$FM, AA/$M_{(n)}$FM, and AA/DFM dimers.

Table 2-7. Interaction energies, enthalpies and the summary of the calculated H-Bond distances and angles at the B3LYP/D95(d,p) computational levels of DFM/FA, AA/$M_{(c)}$FM, AA/$M_{(n)}$FM, and AA/DFM dimers.[α]

SPECIES	ΔE	ΔH	O-H···O	N-H···O	(OHO)	(NHO)	COOP (ΔE)
Carboxylic Acids/Amides							
FA/DFM	-16.64	-15.27	1.585	1.869	174.5	172.2	-3.86
1-HB (O-H···O)	-9.55		1.663		171.0		
1-HB (N-H···O)	-3.23		2.078			161.9	
AA/M(n)FM	-15.66	-14.18	1.633	1.845	174.3	168.4	-4.58
1-HB (O-H···O)	-7.81		1.734		170.2		
1-HB (N-H···O)	-3.27		2.031			168.8	
AA/M(c)FM	-15.66	-14.16	1.629	1.844	173.5	167.2	-3.82
1-HB (O-H···O)	-7.70		1.724		169.7		
1-HB (N-H···O)	-4.14		2.025			158.7	
AA/DFM	-15.86	-14.48	1.613	1.851	173.5	172.5	-4.53
1-HB (O-H···O)	-8.07		1.706		173.8		
1-HB (N-H···O)	-3.26		2.053			162.9	

[α] Energies and enthalpies are in the unit of kcal/mol. COOP means "cooperativity". Bond distances are in angstrom and the angles are in degree.

2.3.13 The analysis of individual N-H···O and O-H···O H-bonds

Figure 2-10 illustrates the relationship of interaction energies and bond distances of all single N-H···O and O-H···O H-bonds. From the high coefficient of determination (R^2 = 0.97), one can tell the energies and bond distances of single O-H···O H-bond show good linear relationship. This relationship of single N-H···O H-bonds is less linear (R^2 = 0.81) than that of O-H···O H-bond. To investigate the reasons for the less linear relationship of N-H···O H-bond, I categorize single N-H···O H-bonds into four different groups: Methyl on C=O (C-methyl substitution), methyl on N-H (N-methyl substitution), methyl on both (C- and N-methyl substitution) and no methyl (non-substitution). The linear relationship between energies and bond distances are shown in Figure 2-11. The values of coefficient of determination are increased to low as 0.93 (methyl on both) and high as 0.997 (no methyl). Better linear relationship in these groups indicates that the H-bond strength and bond distance are highly associated with the methyl substitution. However, without methyl substitution on FM, it shows the highest linear relationship between the energy and bond distance. The group of the "methyl on C=O" shows a more steep slope that indicates the interaction energy and bond distance are highly dependent than those in other groups. This means when the H-bond is increased, the more significant decrease of bond distance could be observed. That also supports the assumption that methyl on C=O alters the strength of H-bond more than methyl on N.

I also categorize single O-H···O H-bond into two groups as shown in Figure 2-12. The non-substituted single O-H···O H-bonds even show R^2 value is 1 (0.999, methylated one R^2 = 0.923) which shows great linear relationship. This also indicates the methyl substitution can reduce the linearity of not only single N-H···O but also O-H···O H-bond.

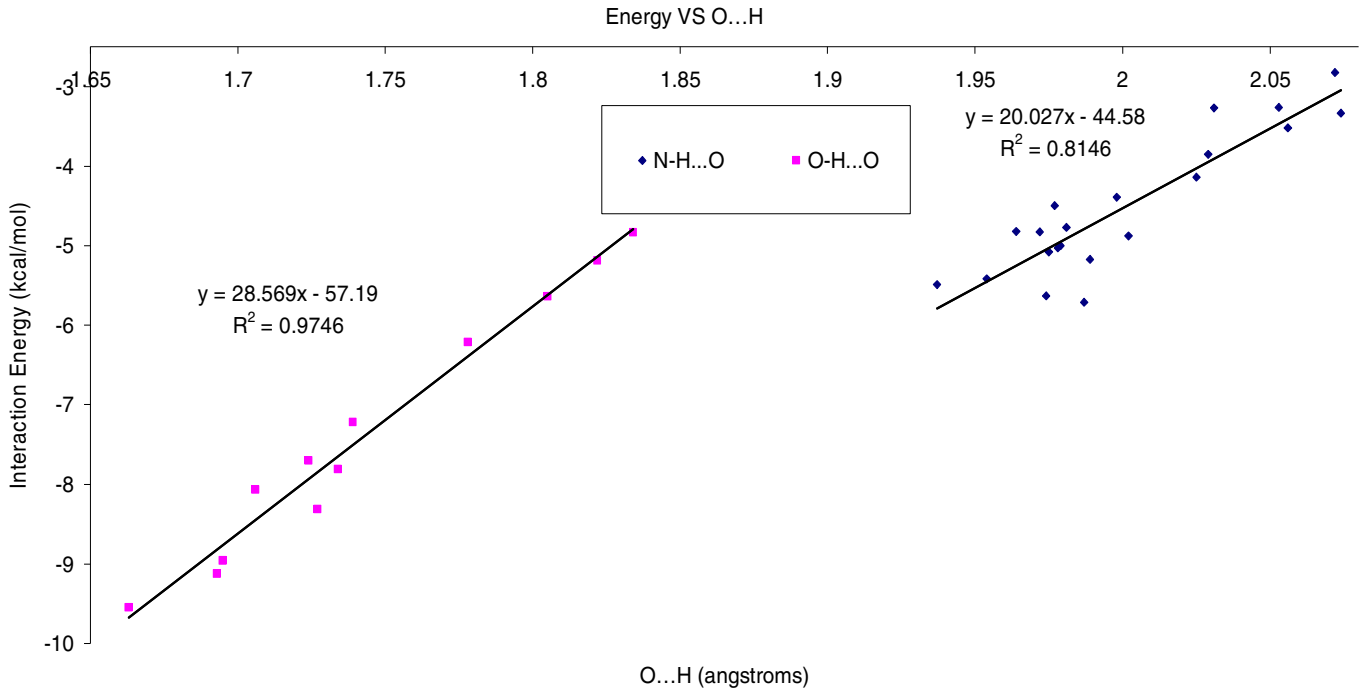

Figure 2-10. The relationship between interaction energies and bond distances of each single N-H···O and O-H···O H-bond.

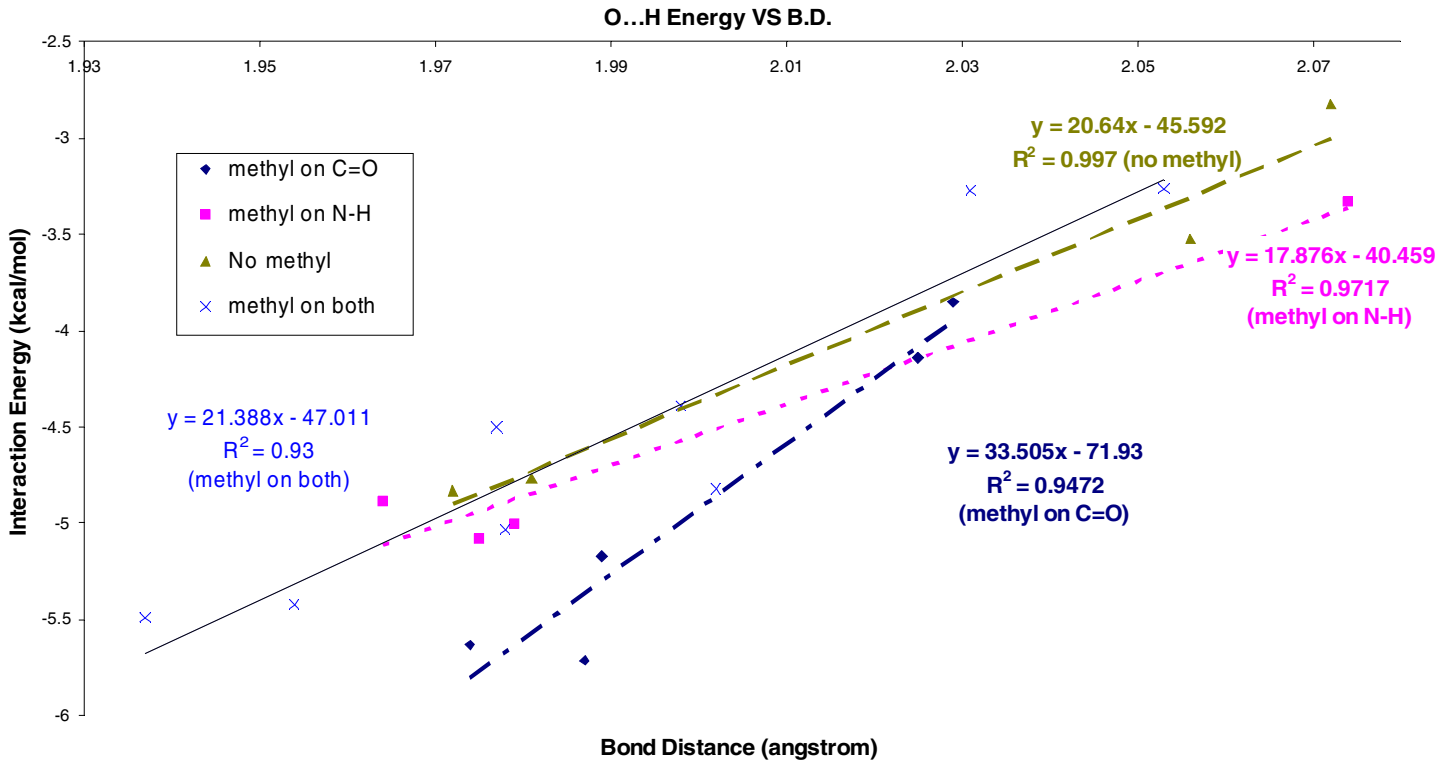

Figure 2-11. The relationship between interaction energies and bond distances of each single N-H···O.

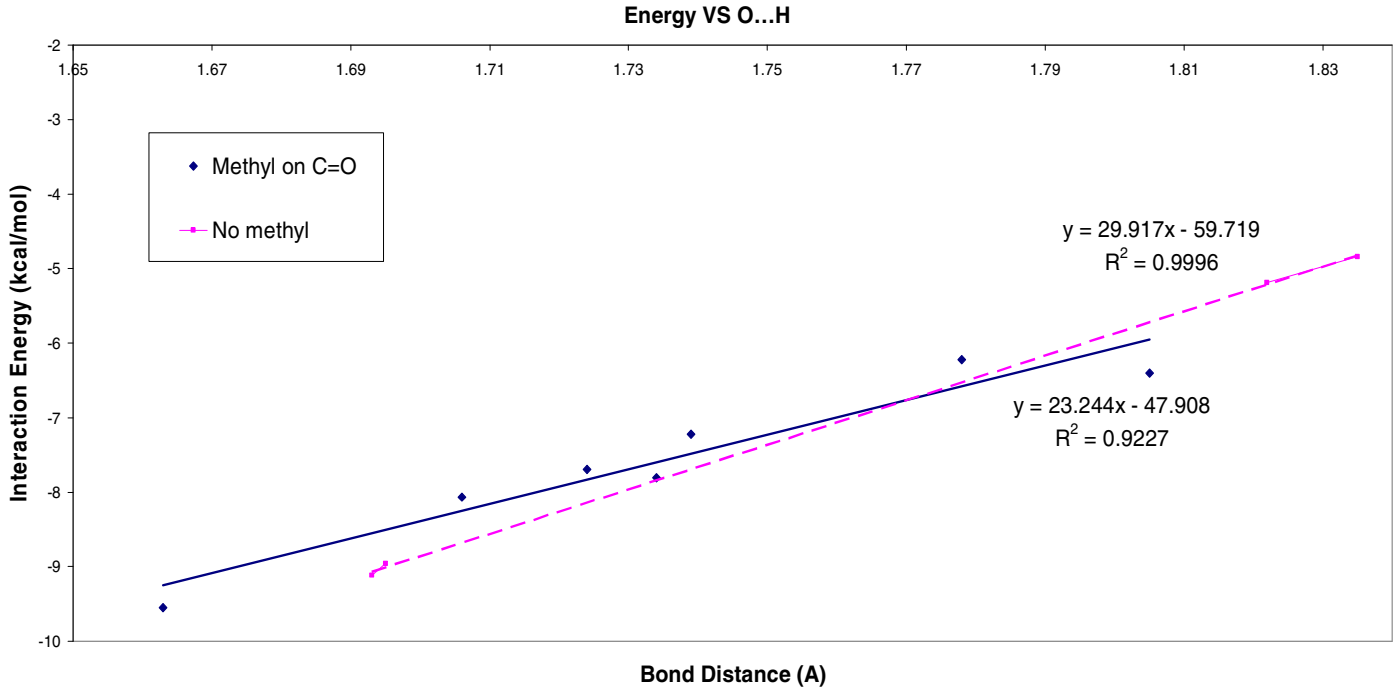

Figure 2-12. The relationship between interaction energies and bond distances of each single O-H···O H-bond.

2.4 Conclusions

The interaction energies and bond distances of non-substituted and substituted formic acid, formamide and the mixed dimers were investigated. The energy of the most stable cyclic formic acid dimer is -16.44 kcal/mol. It is followed by the formic acid - formamide mixed dimer (-15.90 kcal/mol). The cyclic formamide dimer is the least stable one (-14.03 kcal/mol) among them. The average interaction energy of single **O-H···O** H-bond is **-7.39** kcal/mol and of **N-H···O** H-bond is **-4.52 kcal/mol**. Regarding the strength of H-bond interaction, the cooperativity plays a more important role than the sum of single H-bonds. Other parameters such as H-bond combination and the geometry of the structures should also be considered.

While investigating the effect of alkylation, it is found that the most stable structures of substituted FM, FA and mixed dimers are $M_{(n)}FM/M_{(n)}FM$, AA/AA, and DFM/FA dimers, respectively. Those dimers are more stable than FM/FM dimer, FA/FA dimer and FA/FM dimer by -0.23, -0.14 and -0.74 kcal/mol, respectively. When methyls are substituted on all possible positions on dimers to mimic the real peptide monomer to form nanotube, the DFM/DFM dimer is only one that shows weaker interaction energy than that of the non-substituted dimer. It is destabilized by 0.41 kcal/mol than the FM/FM dimer. The AA/AA dimer is more stabilized than the FA/FA dimer by -0.14 kcal/mol, and the AA/DFM dimer shows almost no energy difference to the FA/FM dimer (-0.04 kcal/mol than FA/FM dimer).

In the nine methylated FM dimers, single N-methyl substitution could stabilize the dimer by 0.12 kcal/mol, whereas single C-methyl substitution destabilized the dimer by 0.10 kcal/mol. I noticed single C-methyl substitution on a FA to form an AA dimer would stabilize the structure by 0.12 kcal/mol. With the information above, I can then predict the difference in relative energy of a cyclic dimer compared to a FM

dimer. The most stable cyclic dimer structure is N-methyl substitution with FM dimer (stabilized by 0.23 kcal/mol). In the FA and FM mixed dimers, the O-H···O H-bond is strengthened while the N-H···O H-bond is weakened. In these mixed dimers, single methylation on a FA can destabilize the interaction energy by 0.62 kcal/mol.

In short, the effects of methyl substitution can be summarized as “it makes the adjacent C=O a stronger H-bond acceptor, but N-H or O-H a weaker H bond donor.”

CHAPTER 3– COOPERATIVE HYDROGEN BONDING: THE H-BOND INTERACTION OF DIGLYCINE WITH DIFFERENT SUBSTITUTUENTS

3.1 Introduction

Several recent reports of experimental[126-130]and theoretical studies[42,45,52,131-137] have both demonstrated the extensive H-bond cooperativity of chains of amidic H-bonds. However, only the many body effects modeling study of the stabilization energies of the complexes formed between formate or water and a linear array of n = 2-5 N-methylformamide (NMF) molecules by density functional theory (DFT), *ab initio* SCF and MP2, and SIBFA molecular mechanics computations shows the H-bond cooperativity.[138] Zhao and Wu carried out a study on little β-sheets of polyglycine models and concluded such cooperativity is mainly due to long-range electrostatic interactions and not to the resonance effect.[139]

In this chapter, I will examine the H-bonds in several fully optimized models of nylon, antiparallel – sheets, extended structures, carboxylic acid at the end structures to understand the cooperativity of the H-bonds in these structures and to elucidate the reasons of H-bonding energies between strands. It is of general interest because the amyloid diseases, such as Alzheimer's disease[140,141] and prion diseases, such as Bovine spongiform encephalopathy (BSE, the mad-cow disease) and human Creutzfeldt-Jakob disease (CJD)[142] are associated with the formation of β-sheet secondary structures that involves H-bond.

We shall consider different dimeric and tetrameric H-bonded sheets with diglycine residues and their derivatives, nylon-like structure with diglycine residues

and various sizes of alkyl group spacers, the extended sheet structures with the addition of the cis and trans terminal COOH, and the energetic effects of carboxylic acid groups at the end. All the sheet structures are constrained with the C_{2h} symmetry, unless noted elsewhere.

3.2 Calculation details

Density Functional Theory (DFT) calculations of B3LYP functional and D95(d, p) basis sets were performed by Gaussian 03[102] software. More about the computational details are described in section 2.2.. Due to the high cost of CP-OPT calculations, especially to large structures, single point counterpoise correction is performed. Several tetramers with the size exceeds the limitations of 32-bit Gaussian software, therefore the frequency analysis of those structures can not be performed. The CP corrected single point energies are utilized for energetic comparison.

3.3 Results and discussion

3.3.1 H-bonds of nylon-like dimers

To simplify the progress of the discussion, we first start with the simple nylon-like structures, and then deal with various larger sheet structures. The nylon-like structures are described as A-D-C-A-D. The letter "A" stands for the H-bond acceptor, "D" stands for the H-bond donor, and "C" means spacer, in this part of my study, "C" stands for methyl, ethyl, up to heptyl. The structures of various nylon-like dimers are illustrated in Figure 3-1. All dimeric structures contain two N-H···O H-bonds and the H-bonds are aligned anti-parallelly to each other. As shown in Table 3-1, the interaction enthalpies decrease when the larger spacers are inserted. The enthalpy decreases significantly (2.42 kcal/mol) when the spacer changes from methyl to ethyl. This is due to when the larger spacer exists between two amidic H-bonds, the *intra*strand C_5 interaction can not be developed. The trend of enthalpy decrements is smaller as the spacer is larger. This is explained by the pseudo dipole-dipole interaction in the following paragraphs.

The potential energy of dipole-dipole interaction (D-D interaction) can be described as $\boldsymbol{V = [(\mu_1)(\mu_2)/4\pi\varepsilon r^3][1-3\cos^2\theta]}$. V is the potential energy, μ is the dipole moment, ε is the vacuum permittivity, r is the distance between dipole moments, and θ is the angle between two dipole moments. To simply the calculation, the atomic units of Bohr radius (1 Bohr radius = 0.53 Å), Bohr-electron (1 Bohr-electron = 2.54 Debye) and energy (1 Hartree = 627.51 kcal/mol) were adopted in the calculation of dipole-dipole interaction.

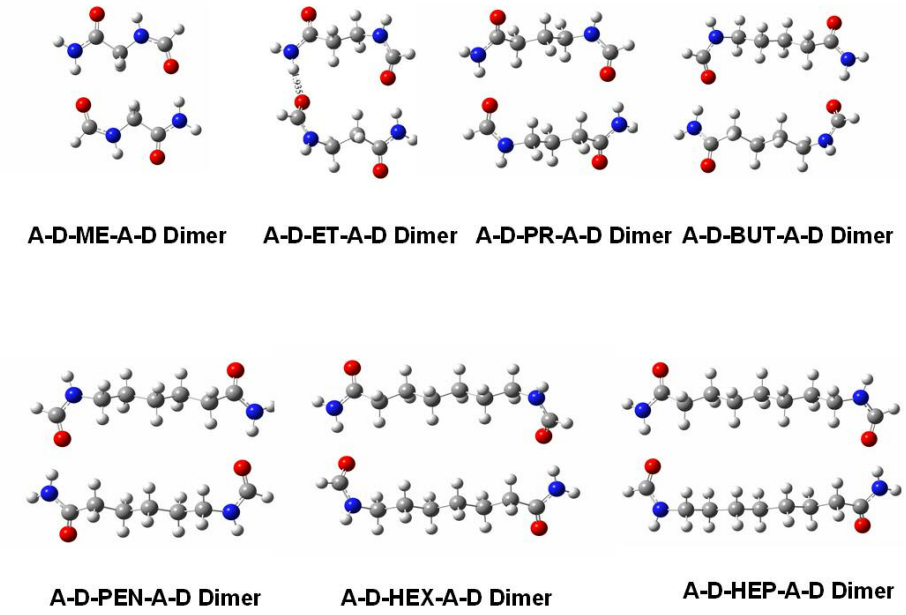

Figure 3-1. The structures of various nylon-like dimers.

How can we perform the calculation of pseudo D-D interaction when atomic units are adopted? Before we do any calculation, first we have to obtain the dipole moment of the half of the structure. Thus, the D-D interaction is considered as the interaction between two half structures. The second step is to convert the two dipole moments in the unit of Debye to the unit of Bohr-electron. This is done by dividing the value of dipole moment by 2.54. The third step is to convert the distance between two dipole moments from angstrom to Bohr radius, which can be done by dividing the value of estimated distance by 0.52. After steps above, the last step is to convert Hartree to kcal/mol. In the A-D-ME-A-D dimer, the dipole moment of half structure is 9.28 Debye, and the distance between two dipole moments is 5.14Å. The D-D interaction of A-D-ME-A-D is only -0.44 kcal/mol. Following the same procedures, the D-D interactions of A-D-ET-A-D, A-D-ME-A-D, A-D-PR-A-D, A-D-BUT-A-D, A-D-PEN-A-D, A-D-HEX-A-D and A-D-HEP-A-D are -0.35, -0.34, -0.12, -0.08, -0.05 and -0.04 kcal/mol, respectively. The D-D interaction decreases as the larger spacer is inserted into the monomer. This trend is similar to what can be observed in Table 3-1. The influence of the size of the spacer is also decreased when the spacer is larger.

Table 3-1. Interaction energies and enthalpies of observed nylon-like dimers structures. ME means methyl is the center molecule, ET means ethyl is the center molecule, PR means propyl is the center molecule, BUT means butyl is the center molecule, PEN means pentyl is the center molecule, HEX means hexyl is the center molecule, and HEP means heptyl is the center molecule.

Dimeric Structures	**ΔE (kcal/mol)**	**ΔH (kcal/mol)**
A-D-ME-A-D	-16.54	-14.02
A-D-ET-A-D	-13.70	-11.60
A-D-PR-A-D	-13.67	-11.46
A-D-BUT-A-D	-13.19	-11.04
A-D-PEN-A-D	-12.76	-10.53
A-D-HEX-A-D	-12.61	-10.33
A-D-HEP-A-D	-12.50	-10.29

3.3.2 The extended A-D-PR-A-D-PR-A-D-PR-A-D sheets

If we extend the A-D-PR-A-D monomer to form an A-D-PR-A-D-PR- A-D-PR-A-D monomer, it can form one small ring (SR) and one large ring (LR) dimers as shown in Figure 3-2. The interaction energies difference (**the single point counterpoise calculations of energy instead of enthalpy are performed because the 32-bit Gaussian software limitation of frequency calculation**) between SR and LR dimers is only by 0.52 kcal/mol (SR dimer dE = -10.94, and LR dimer dE = -10.42). The interaction energies of A-D-ME-A-D dimer are -16.54 kcal/mol (LR), and -6.54 kcal/mol (SR), respectively. The LR A-D-ME-A-D dimer possesses H-bond interaction that is stronger than the A-D-PR-A-D-PR-A-D-PR-A-D dimer because the strength of H-bond is increased by the *intra*strand C_5 coupling. The small energy difference between LR and SR A-D-PR-A-D-PR- A-D-PR-A-D dimer is due to the propyl group between H-bond donor and acceptor. The propyl avoids the formation of *intra*strand C_5 H-bond in the monomer, the interaction energy is then reduced. Several possible conformations of A-D-PR-A-D-PR- A-D-PR-A-D tetramer can be investigated which include the three LR, three SR, the one LR and two SR, the two LR and one SR, and the two LR and two SR. Up to now, only the tetramer with three LR has been optimized (as shown in Figure 3-3), the interaction energy is -34.09 kcal/mol. This three LR structure shows little cooperativity (2.83 kcal/mol). From the interaction energies obtained, we can predict that tetramer with two LR and two SR will be the structure with the strongest H-bond. This structure can also extend two-dimensionally, to form crystal structures with eight H-bonds.

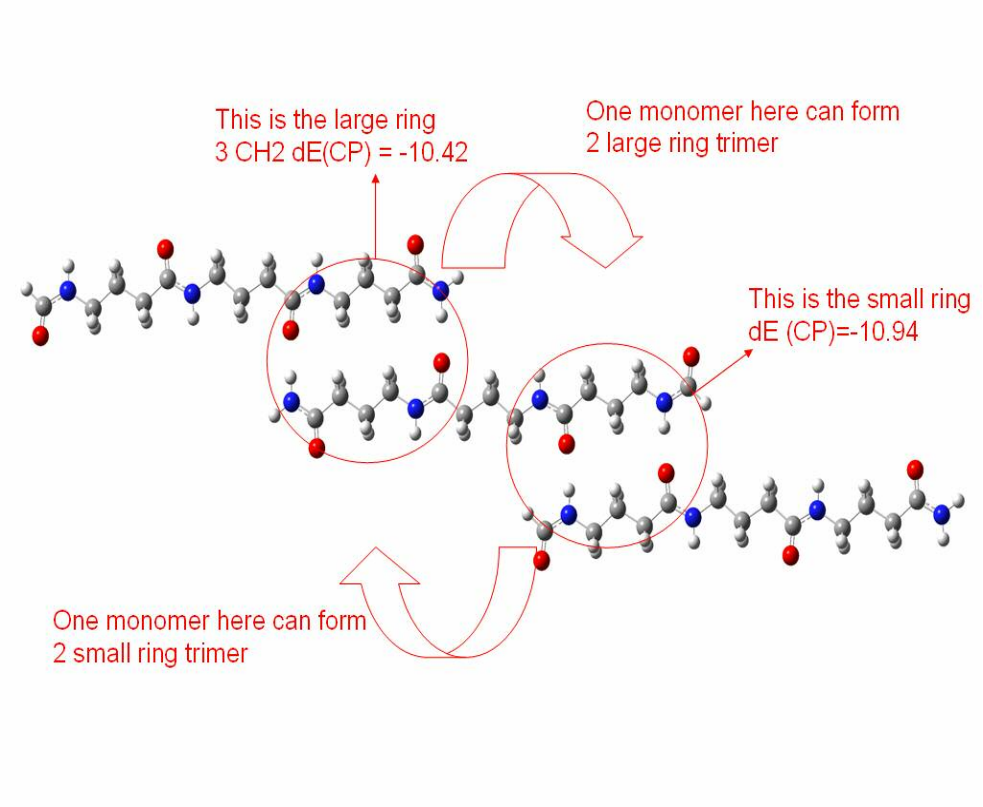

Figure 3-2. The A-D-PR-A-D-PR- A-D-PR-A-D extended structures.

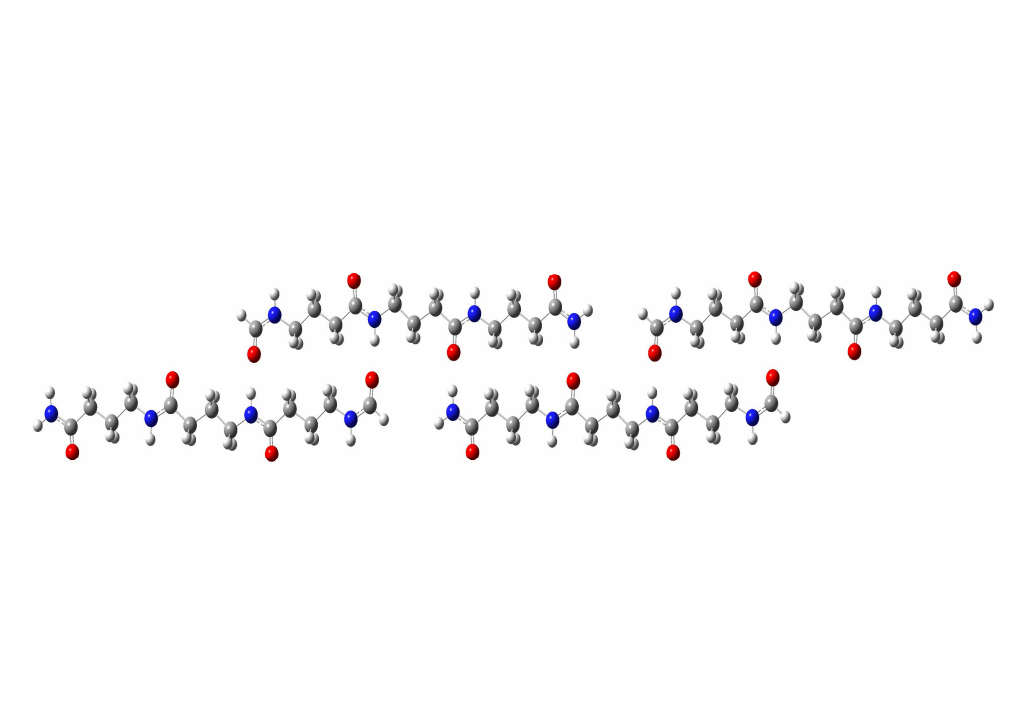

Figure 3-3. The extended LR A-D-PR-A-D-PR- A-D-PR-A-D tetramer. The interaction energy is -34.09 kcal/mol.

3.3.3 Diglycine plus the carboxylic acid (CA)

As we learned in Chapter 2, the O-H···O H-bond provides strong interactions than those of N-H···O H-bond. I then propose the insertion of a carboxylic acid (formic acid, FA is applied here) at the terminal of A-D-ME-A-D to develop FA-ME-A-D-ME-A-D (see Figure 3-4) as the representative portion of the reported peptide nanotube monomer bis (*N*-α-amido-glycylglycine)-1,7-heptane dicarboxylate.[18,143] This FA-ME-A-D-ME-A-D monomer includes the significant functional groups of half the bis (*N*-α-amido-glycylglycine)-1,7-heptane dicarboxylate monomer. This representative FA-ME-A-D-ME-A-D monomer was adopted to perform the energetic analysis because the smaller structure can save the computational power.

Several dimers can be built based upon this FA-ME-A-D-ME-A-D monomer. The 2FA-ME-A-D-ME-A-D1 and 2FA-ME-A-D-ME-A-D2 dimers form anti-parallel sheet structures and the 2FA-ME-A-D-ME-A-D3 and 2FA-ME-A-D-ME-A-D4 dimers form parallel sheet structures (see Figure 3-4). Each anti-parallel/parallel sheet structure can be distinguished from each other by the cis/trans FA at the terminal. When we only focus on the interaction energies of these dimer structures, the 2FA-ME-A-D-ME-A-D4 is the most stable structure with the H-bond interaction energy of -13.15 kcal/mol. However, this structure is not a good example of a two-stranded sheet for two reasons. First, the O-H···O H-bond at the end is not involved in the dimer, but in the weaker C-H···O H-bond. Second, two *intra*strand C_5 H-bonds and one C_7 H-bond occur in this dimer can reduce the H-bond interactions as the structures are extended vertically. Therefore, I decided to extend the 2FA-ME-A-D-ME-A-D2 dimer structure to a tetramer, because it satisfies both the structure stability (ΔE = -11.82 kcal/mol) and the ability to extend the sheet structure. As shown in Figure 3-5, the interaction energy of the tetramer is -34.13 kcal/mol, which is less

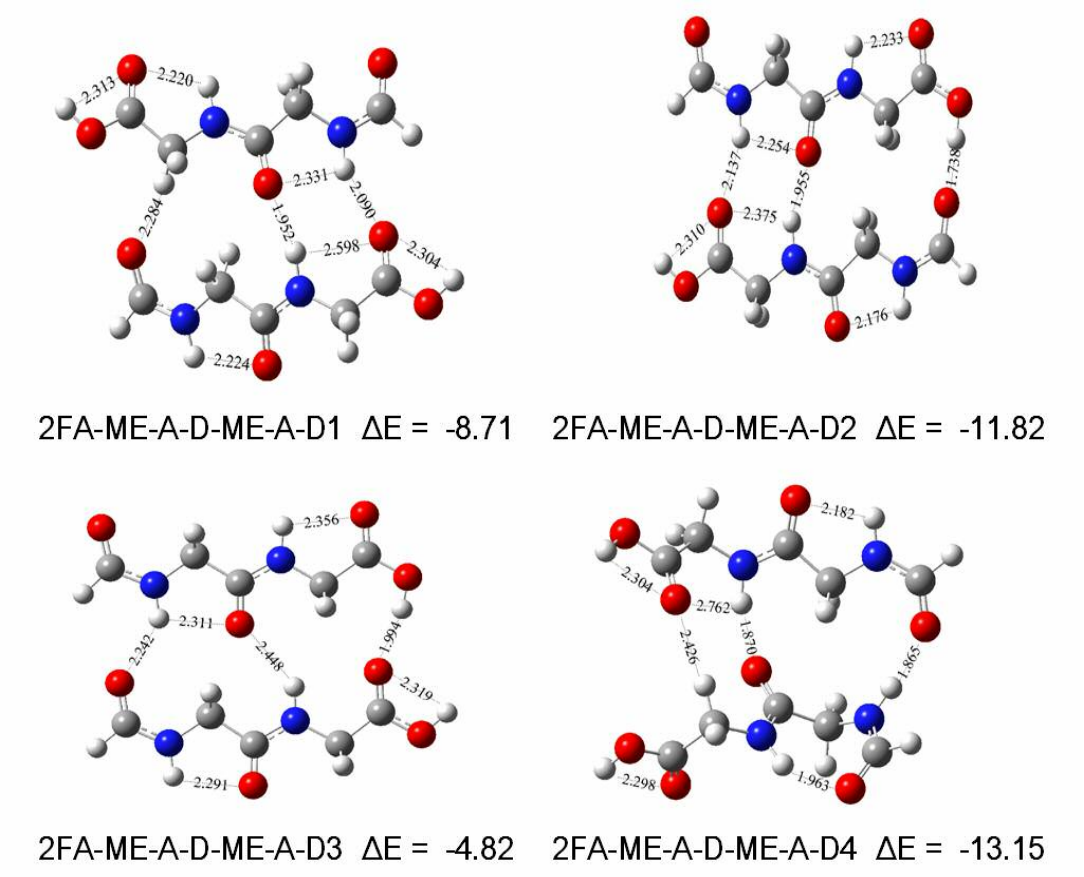

Figure 3-4. The extended FA-ME-A-D-ME-A-D dimers. The interaction energies are shown above.

than the value of –35.46 kcal/mol (three times larger than the value of -11.82). What happened to the cooperativity between strands?

When one looks at this four-stranded sheet, it shows two N-H···O and one O-H···O H-bonds between strands. The 2FA-ME-A-D-ME-A-D2 structure shows all those three bonds and its interaction energy has already been modified to illustrate the energy costs due to cis-trans transformation of formic acid. All the formic acids are in trans form in the tetramer. Although one O-H···O and two N-H···O H-bonds are formed, the energy lost in the cis-trans transformation diminishes the cooperativity. We can divide the tetramer into two parts, the top and the bottom two-stranded sheets. The interaction energy between the top and bottom sheet is -10.49 cal/mol. This energy might be attributed to the SR N-H···O H-bonds (-6.49 kcal/mol) and the single O-H···O H-bond (O-H··O -5.47 kcal/mol). The -1.47 kcal/mol energy shortage must be due to the cis-trans transformation and the energy needed to change the tetramer morphology.

Since the O-H···O H-bond is stronger than the N-H···O H-bond, is it possible to obtain more stable structures when CA reacts with each other as a cyclic dimer? As shown in Figure 3-6, the cyclic carboxylic acids (formic acid) at the end dimer possess interaction energy of -15.44 kcal/mol. This is even stronger than any other FA-ME-A-D-ME-A-D dimer with two N-H···O and one O-H···O H-bonds systems. This result indicates that the CA at the end is more appropriate to be utilized to extend the β-sheet structures horizontally. Shimizu et al.[3,25] suggested that in the formation of bis(*N*-α-amido-glycylglycine)-1,7-heptane dicarboxylate peptide nanotube, the monomers are connected sideways through the O-H···O H-bonds of cyclic CA dimer at the end.

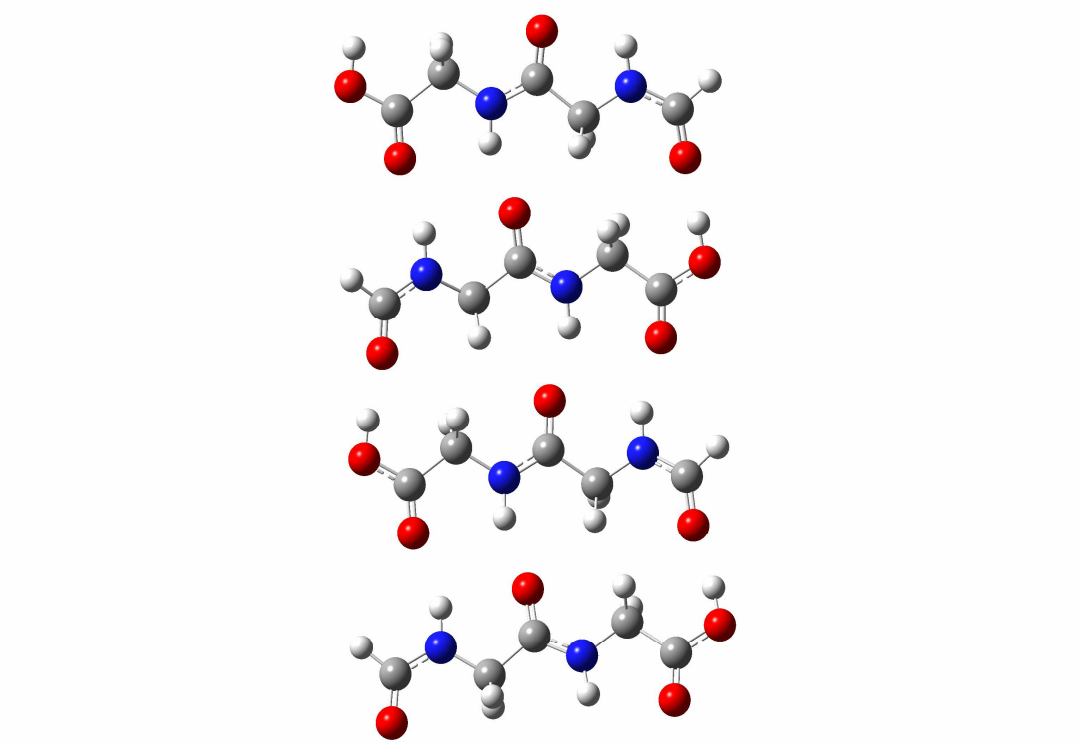

Figure 3-5. The 4FA-ME-A-D-ME-A-D2 tetramer. The interaction energy is -34.13 kcal/mol. The modified interaction energy for two-strand is -11.82 kcal/mol (relative to cis)**.** The N-H···O bond distances are 2.017, 1.907, 1.895, 1.932, 2.014 and 1.909 Å (top to down and left to right and, respectively); the O-H···O bond distances are 1.710, 1.718 and 1.725 Å (top to down, respectively). The C_5 H-bond distances are 2.205, 2.358, 2.371, 2.399, 2.408, 2.404, 2.306, and 2.249 Å (left to right and top to down, respectively).

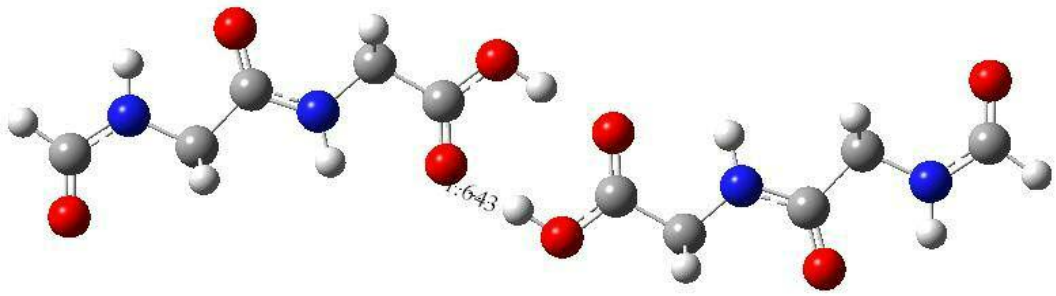

Figure 3-6. The two O-H···O H-bonds FA-ME-A-D-ME-A-D dimer. The interaction energy is -15.44 kcal/mol.

3.3.4 Extended diglycine plus carboxylic acid (CA)

Now we consider the "FA-ALK-A-D-ALK-A-D-ALK-FA" structure. The "ALK " stands for the alkyl groups in the monomer. This is important because we can then observe the cooperativity between strands and the extended directions. The structures are constrained to C_{2h} symmetry. Due to the size of the structures, only single point CP correction is applied here. Several LR and SR dimers are shown in Figure 3-7~8. In Figure 3-7, the FA-ME-A-D-ME-A-D-ME-FA SR dimer possesses the weakest interaction energy -3.39 kcal/mol, because the C_6 *intra*strand O-H···O H-bond weakens the adjacent *inter*strand N-H···O H-bonds. The FA-ET-A-D-ME-A-D-ET-FA dimer has an interaction energy of -10.22 kcal/mol, which is the middle of the three dimers. This energy is even weaker than that of the LR A-D-ME-A-D (-16.54 kcal/mol). Why a dimer structure with one LR and two O-H···O H-bonds like this, can only provide such a weak interaction? When cis-trans transformation is involved, the interaction energy is reduced. We even found that the N-H···O bond distances are shorter than the O-H···O ones, which is not common in H-bond interaction. This is because all structures are constrained to C_{2h} symmetry, so they are forced to be planar and the formic acid at the ends prefers to link sideways with other monomer. Regarding the effect of the carboxylic acid at the end, more discussion will be provided in later paragraphs. The FA-PR-A-D-ME-A-D-PR-FA dimer has the strongest H-bond interaction of -20.21 kcal/mol. This dimer possesses stronger H-bond interaction than the other two because no *intra*strand H-bond and no cis-trans transformation are involved.

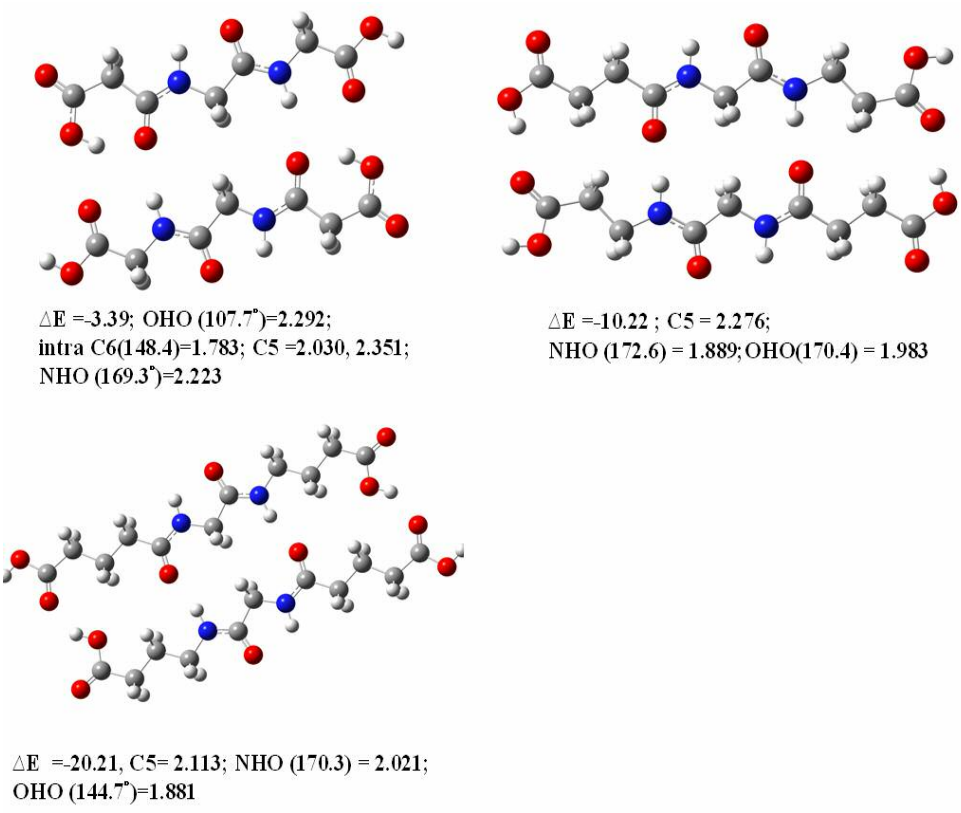

Figure 3-7. The LR FA-ME-A-D-ME-A-D-ME-FA, FA-ET-A-D-ME-A-D-ET-FA and FA-PR-A-D-ME-A-D-PR-FA dimers.

The SR FA-ME-A-D-ME-A-D-ME-FA, FA-ET-A-D-ME-A-D-ET-FA and FA-PR-A-D-ME-A-D-PR-FA dimers are shown in Figure 3-8. In these dimers, the H-bond interactions between strands are due to one SR A-D-ME-A-D (-6.49 kcal/mol) and two O-H···O H-bonds. However, the interaction energies are less than the value of -6.49 kcal/mol. The weaker interaction energy is due to the cis-trans transformation energy lost. The FA-PR-A-D-ME-A-D-PR-FA dimer, which is the one with the weakest interaction energy of -1.29 kcal/mol. One can also observe the O-H···O H-bond distances are even greater than 2 Å, which indicates the O-H···O H-bonds in such dimer only provide little to the interaction energy.

The dimers are kept planar with C_{2h} symmetry. The carboxylic acids at the ends are preferred to connect with other monomers horizontally rather than vertically. Therefore, I plan to examine the interaction energies and morphological differences when the dimers are not constrained to be planar structures. The non-planar LR and SR FA-ET-A-D-ME-A-D-ET-FA dimers are discussed here. As shown in Figure 3-9, both dimers are kept in C_i symmetry, and CA at the ends are not on the same plane with the rest of the structures. Both non-planar dimers show more negative interaction energies than that of the planar dimers. More surprising is the fact that the SR dimer possesses stronger interaction energy than that of the LR dimer. In the LR FA-ET-A-D-ME-A-D-ET-FA dimer, formic acid at the end has the tendency to stay out-of-plane. In this dimer, the O-H groups of formic acids share carbonyls on the LR dimer to form O-H···O H-bonds, thus weakens the LR N-H···O H-bonds. If we extend the structure vertically, these formic acid groups can link with other formic acid groups located above and below the LR plane to form a three-dimensional tetramers.

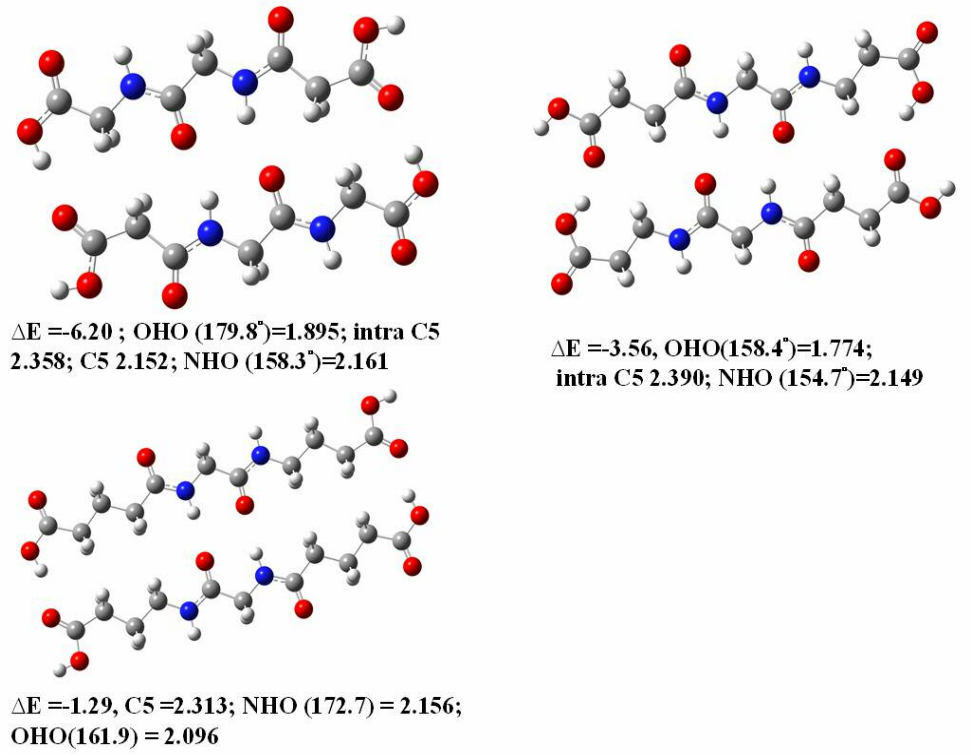

Figure 3-8. The SR FA-ME-A-D-ME-A-D-ME-FA, FA-ET-A-D-ME-A-D-ET-FA and FA-PR-A-D-ME-A-D-PR-FA dimers.

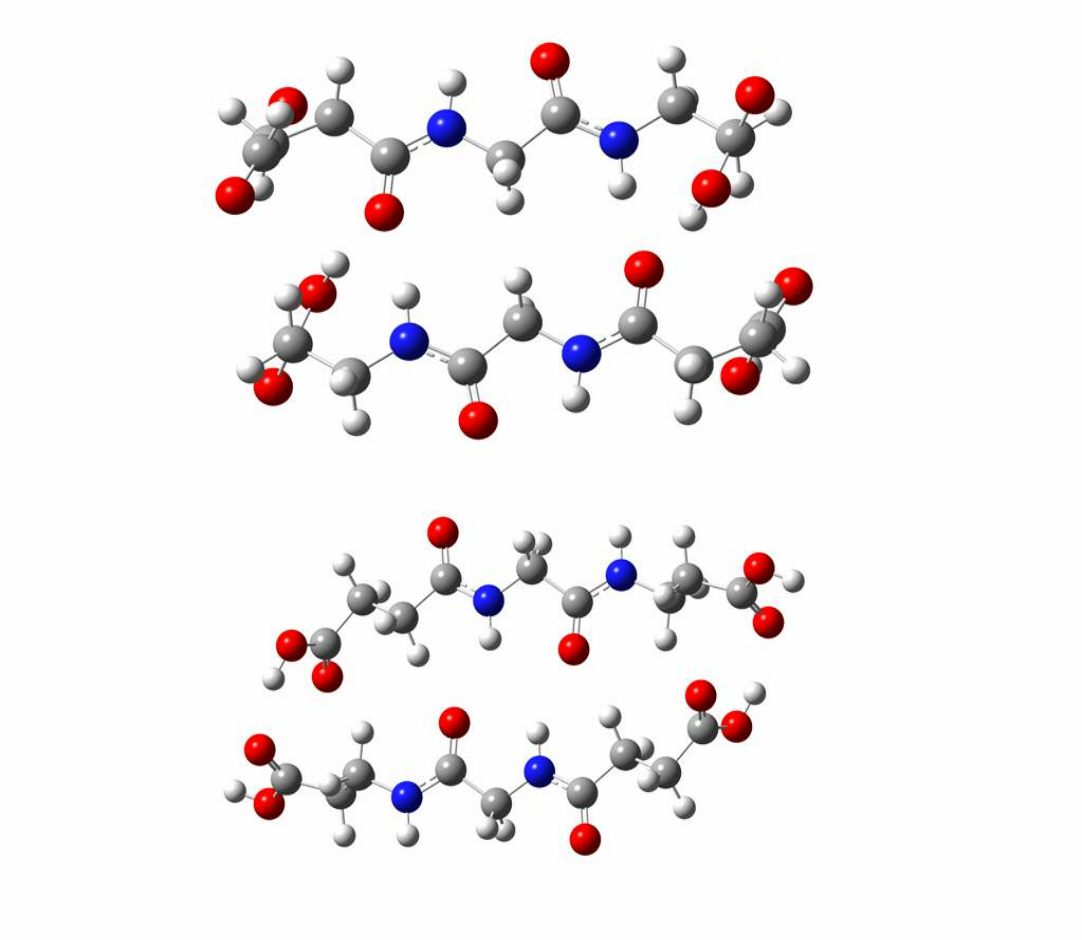

Figure 3-9. The non-planar LR and SR FA-ET-A-D-ME-A-D-ET-FA dimers. The LR dimer (top) ΔE = -15.84; C_5 = 2.108; NHO (166.4°) = 2.019; OHO (166.2°)=1.774. The SR dimer (bottom) ΔE = -21.52; C_5 = 2.223; NHO (168.5°) = 2.317(c); CHO (123.8°) = 2.426; OHO (174.6°) = 1.788.

Why the interaction energy of the SR FA-ET-A-D-ME-A-D-ET-FA dimer is stronger than that of the LR dimer? The formic acid group at the end also plays an important role here. The O-H···O bond distance is 1.788 Å and N-H···O bond distance is 2.317 Å. Which indicates the N-H···O H-bond contributes slightly to the interaction energy in this dimer. The O-H···O H-bond dominates the energy and the geometry. This also shows that the CA group at the end also contributes more interaction energy when it forms a cyclic dimer with another CA group and extends the structure sideway. If they are applied to extend a structure, they should link with the cis form group to avoid the energy deficiency due to the cis-trans transformation. More about the sideway-extended cyclic structures of CA groups will be discussed in the following section.

3.3.5 The carboxylic acid (CA) groups are connected horizontally

Figure 3-10 shows the dimeric, trimeric, and tetrameric CA structures. To mimic the CA group at the end of each monomer with possible extended functional groups, the acetic acid is adopted as the monomer to study. The methyl in acetic acid represents the possible donor and acceptor of H-bond.

The average O-H···O H-bonds in the dimer, trimer and tetramer are know to be -8.28, -7.17 and -7.45 kcal/mol, respectively. The interaction energy increases from -4.95 kcal/mol (dimer to trimer) to -8.26 (trimer to tetramer) as the structures grow. According to the interaction energy, one can tell that the more stable structure for the CA group is the planar sheet structure, not the circular trimer structure.

To examine if the CA groups at the end favors the sideway-linked tetramer, the energies of horizontally and vertically-extended LR FA-PR-A-D-ME-A-D-PR-FA tetramers are studied. The horizontally- and vertically- extended tetramers are shown in Figures 3-11 and 12. The horizontal-extended tetramer is more stable than the vertically-extended tetramer by only 3.36 kcal/mol. The result indicates that the horizontal-extended tetramer is slightly favored. The interaction energy of FA-PR-A-D-ME-A-D-PR-FA dimer is -20.21 kcal/mol, in its derivative horizontally-extended tetramer, the energy attributed from the center two O-H···O H-bonds is -18.44 kcal/mol. This is ever stronger than the interaction energy of an acetic acid dimer (-16.56 kcal/mol), which indicates the cooperativity exists in the cyclic tetramer.

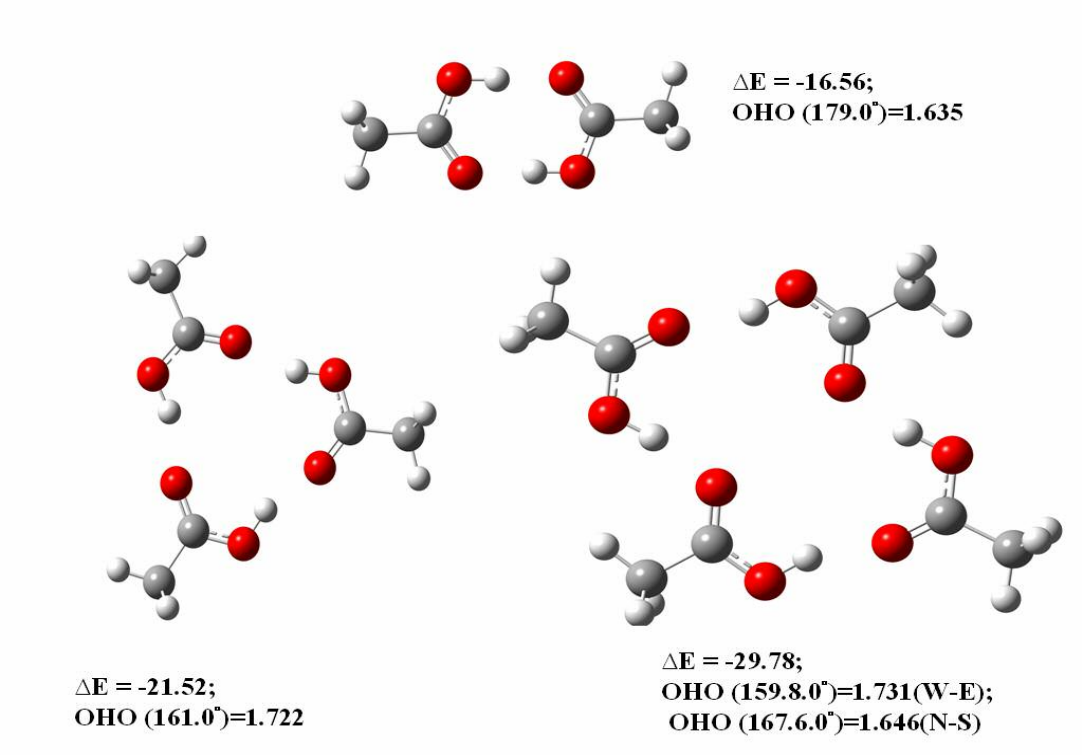

Figure 3-10 . The dimer, trimer, and tetramer of carboxylic acid group link.

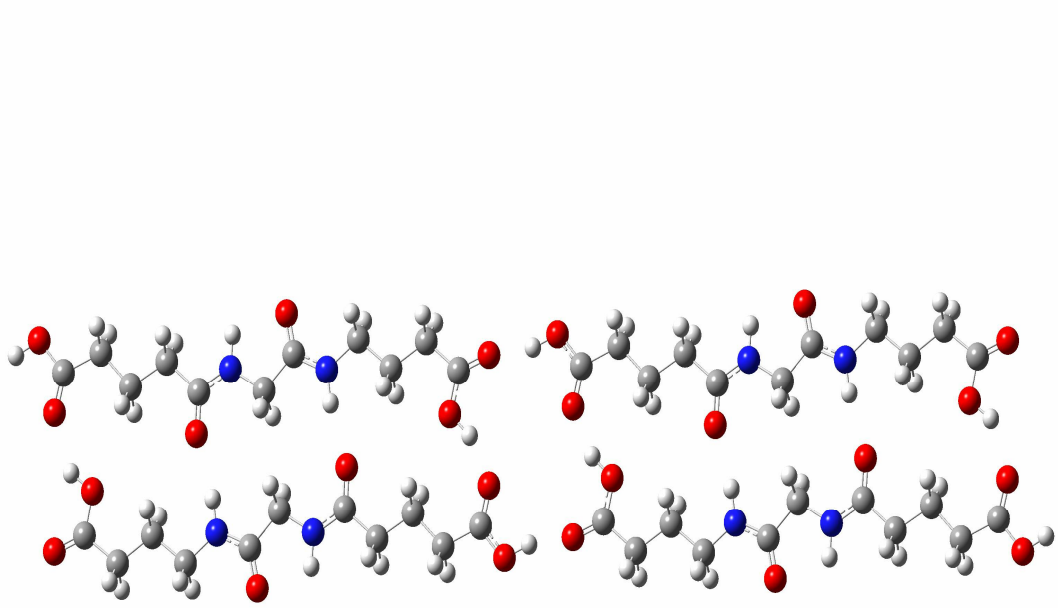

Figure 3-11. The horizontal LR FA-PR-A-D-ME-A-D-PR-FA tetramer. ΔE = -58.86 kcal/mol (dimer = -20.21); C5 = 2.115; NHO (170.2°)=1.997(center); NHO (170.9°)=2.034(side); OHO (163.8°)=1.668(C. W-E);OHO (156.0°)=1.670(C. N-S) ;OHO (144.8°)=1.884(side).

In the vertically-extended tetramer, the energy is only more unstable than that of the horizontally-extended tetramer by 3.36 kcal/mol. The interaction energy between the top and the bottom dimer in the vertically-extended tetramer is -15.08 kcal/mol. This energy is attributed to the contribution of two extra N-H···O H-bonds (SR A-D-ME-A-D) and two extra O-H···O H-bonds than two LR dimers. There are only two extra O-H···O H-bonds in the horizontally-extended tetramer than the two LR dimer structures. However, these two O-H···O H-bonds provide the interaction energy of -18.44 kcal/mol. As shown in Figure 3-12, cis-trans transformation occurs in the formation of the vertically-extended tetramer, even with more numbers of H-bonds, but this tetramer can not provide more stable interaction energy. No significant H-bond cooperativity seems to exist in this tetramer, and only a small amount of 2.88 kcal/mol cooperativity is observed in the horizontally-extended tetramer.

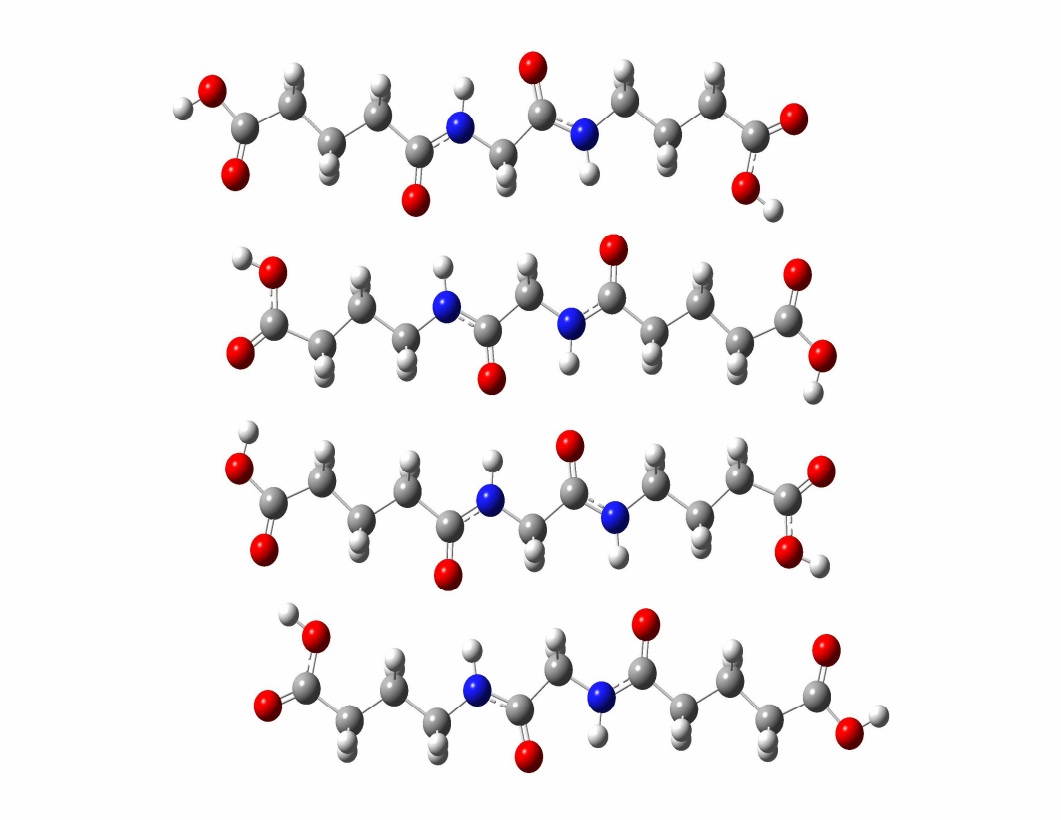

Figure 3-12. The vertiacl LR FA-PR-A-D-ME-A-D-PR-FA tetramer. The interaction energy is -55.50 kcal/mol.

3.4 Conclusions

H-bond cooperativity plays an important role in the formation of two-stranded and four-stranded sheet structures. The strength of the interaction can be reduced by inserting longer alkyl groups. This is because the dipole-dipole interaction is decreased as the distance of dipoles is increased. The diglycine structures can be extended both vertically and horizontally. Stronger cooperativity appears in the vertically-extended structures than in the horizontally-extended ones. The interaction can be increased by inserting carboxylic acid (CA) groups. These groups do not prefer planar structures, so the interaction energy is reduced. The stronger O-H···O of CA groups can form more stable structures. However, the CA cis-trans transformation energy deficiency must be considered, if we intend to design a structure that can be extended vertically. Which means that even with extra O-H···O H-bonds, the energy cost of transformation will reduce the interaction energy in the structure. Some vertically-extended structures with the extra H-bonds involved, but still offer less stable structures than the horizontally-extended structures. In addition, the CA groups at the end have the tendency to stay out of plane, therefore they have potential to form three-dimensional structures. This is because the dominated O-H···O H bonds are located at the end.

While designing more stable structures, the interaction is not the only factor. The geometry of the structure is important than the numbers of H-bonds can be formed in the structure. We also need to consider the possibility to expand the smaller structures, not only the strength of them. In the FA-ME-A-D-ME-A-D dimers, the most stable dimer is not a good structure to adopt to form a stable tetramer. This is because the *internal* C_6 H-bond that weakens the N-H···O H-bond between strands.

CHAPTER 4 —COOPERATIVE HYDROGEN BONDING: THE EXTENDED DIGLYCINE STRUCTURES WITH VARIOUS H-BOND DONOR-ACCEPTOR SEQUENCES

4.1 Introduction

Self-assembled peptide nanotubes have been extensively studied through experimental methods.[3,20,30,117,144-149] Since the structures are constructed by H-bonds, the stability and conformational features are important in designing better nanomaterials. Several theoretical studies have investigated the electronic properties of protein nanotubes[150-153], and stacking manner of cyclic peptide nanorings to form peptide nanotubes. [154,155] A study described the design of nanotubes from naturally occurring protein building blocks.[106] Little is known about H-bond cooperativity and interactions in the self-assembled peptide nanotubes.

An *ab initio* calculations of *β*-peptide strands to form various sizes of nanotubes has been recently reported.[58] It is the first report that attests that sheets of *β*-peptides have the tendency to exhibit nanotubular characteristics rather than two-dimensional planar sheets. The helical structure is similar to the structure of α-peptides. Lin et al. [156] also investigate the diglycine models of several *β*-peptide sheet structures through a quantum mechanical study. They suggested that large cooperativity could be found in sheet structures.

Since the *β*-peptides can form non-planar helical structures, methods to manipulate the H-bond strength and the conformation of such structures will be explored in this chapter. We will first present the influence of various H-bond donor and acceptor sequences and the insertion of several spacers, such as acetylene and

benzene. The DA-DA, DA-AD, and AD-DA sequence groups will be investigated. The conformational change resulting from the replacement of the donor and acceptor sequence and various spacers will also be considered.

The main goals of this study are to obtain energetic and structural characteristics of these structures and to provide theoretical results to the experimentalist to improve nanotechnology researches that involve self-assembled nanomaterials.

4.2 Calculation details

More about the computational details are described in section 2.2. Frequency calculations of the A-C3-D-Bz-A-C3-D, D-C3-A-Bz-D-C3-A, and D-C3-A-Bz-A-C3-D tetramers are not possible to perform due to the 32-bit limitations of Gaussian 03 software.

The “dipole moment alignment” in this chapter is referred to the pseudo-parallel or pseudo-anti-parallel alignment of dipole moments when the monomeric, dimeric, and tetrameric structures are divided into half from the center spacers. The calculation method of pseudo dipole-dipole interaction was described in section 3.3.1 in Chapter 3.

4.3 Results and discussion

4.3.1 Formamide (FM) with spacers

The formamide structure is described as D-A. As discussed in Chapter 2, the interaction enthalpy of the FM dimer is -12.12 kcal/mol and the N-H···O bond distance is 1.841 Å. The effects of polarizability can be investigated by inserting the easily polarizable molecules between H-bond donor and acceptor. This addition can create a loop to enhance the strength of H-bond within the dimer. We also try to manipulate the strength of H-bond in the system. The inserted molecule adopted here is acetylene, "**-C≡C-** , **C3**". It was referred as C3 because a triple bond forms between two carbon atoms. When one C3 between donor and acceptor as shown in Figure 4-1, the interaction enthalpy of the D-C3-A dimer increases 48% to -18.05 kcal/mol and the N-H···O distance is 1.744 Å. After adding the second acetylene (see Figure 4-2), the interaction enthalpy of the D-C3-C3-A dimer is slightly weaker than that of the D-C3-A dimer. The interaction enthalpy of the D-C3-C3-A dimer is -17.90 kcal/mol and the N-H···O distance is 1.746 Å. The weaker interaction is due to more atoms are involved in the polarizability process in the larger D-C3-C3-A dimer, thus weakening the polarizability effect that can enhance H-bond. In D-C3-A dimer, 12 atoms are involved in the polarizability. However, in the D-C3-C3-A dimer there are 16 atoms involved. The O atom of the D-C3-A dimer is more negative than that of the formamide dimer by -0.082 in charge, and the H atom of the same dimer is more positive by 0.055 in charge. The O atom of the D-C3-C3-A dimer is more negative than that of the formamide dimer by -0.083 in charge, and the H atom of the same dimer is more positive by 0.053 in charge.

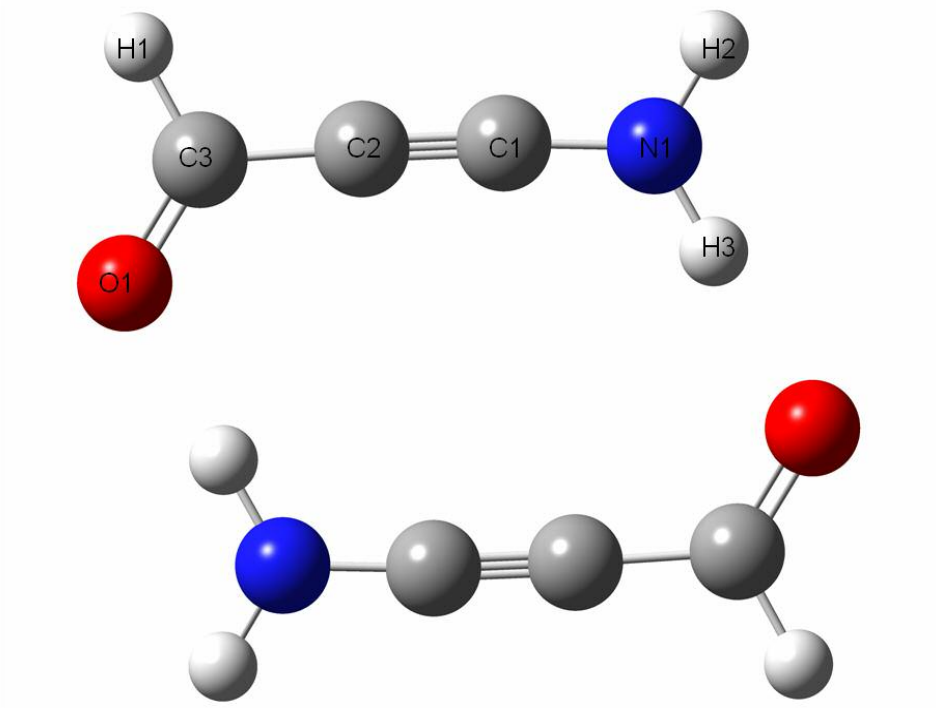

Figure 4-1. The A-C3-D dimer.

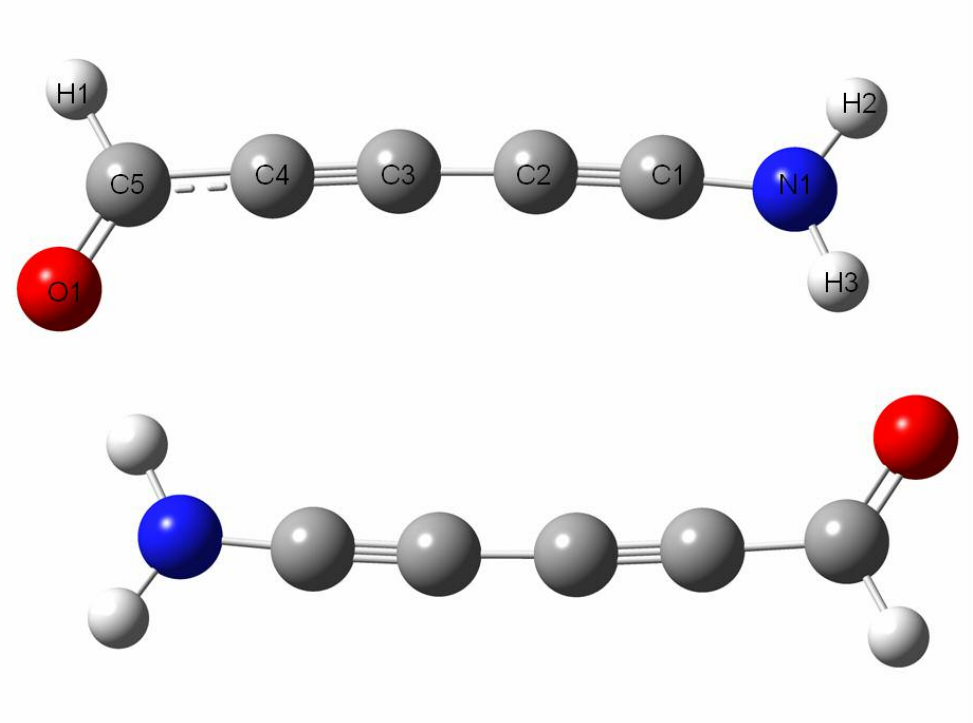

Figure 4-2. The A-C3-C3-D dimer.

4.3.2 Diglycine with spacer, the D-A-C3-D-A dimers

The diglycine molecule with one acetylene in the center can lead to various isomers. These isomers are the D-A-C3-D-A, D-A-C3-A-D and A-D-C3-D-A monomer. Several possible dimers include the small ring (SR), large ring (LR) structures, or small and large mixed ring (SL) could be constructed from the monomers above. The interaction enthalpy of the SR D-A-C3-D-A dimer (see Figure 4-3) is -21.98 kcal/mol. The enthalpies of the SR, LR, and SL dimers are even stronger than that of the previously described D-C3-A dimer. The D-A-C3-D-A dimer is even approximately 80% stronger than the formamide dimer. The interaction enthalpies of the LR (Figure 4-4) and SL (Figure 4-5) isomers are only -6.00 and -11.42 kcal/mol, respectively. The weaker interaction is because there are more atoms (14 and 16 atoms in the LR and SL dimers, respectively) in the loop, the influence of the polarizability is then reduced.

All the D-A-C3-D-A dimers are composed of two N-H···O H-bonds aligned in the opposite direction. The cis form D-A-C3-D-A dimer has the interaction enthalpy of only -9.42 kcal/mol is shown in Figure 4-6. The weak interaction is due to more atoms (14 atoms) are involved in the polarizability and the repulsion of the dipole-dipole interaction since the dipole moments are aligned in the same direction.

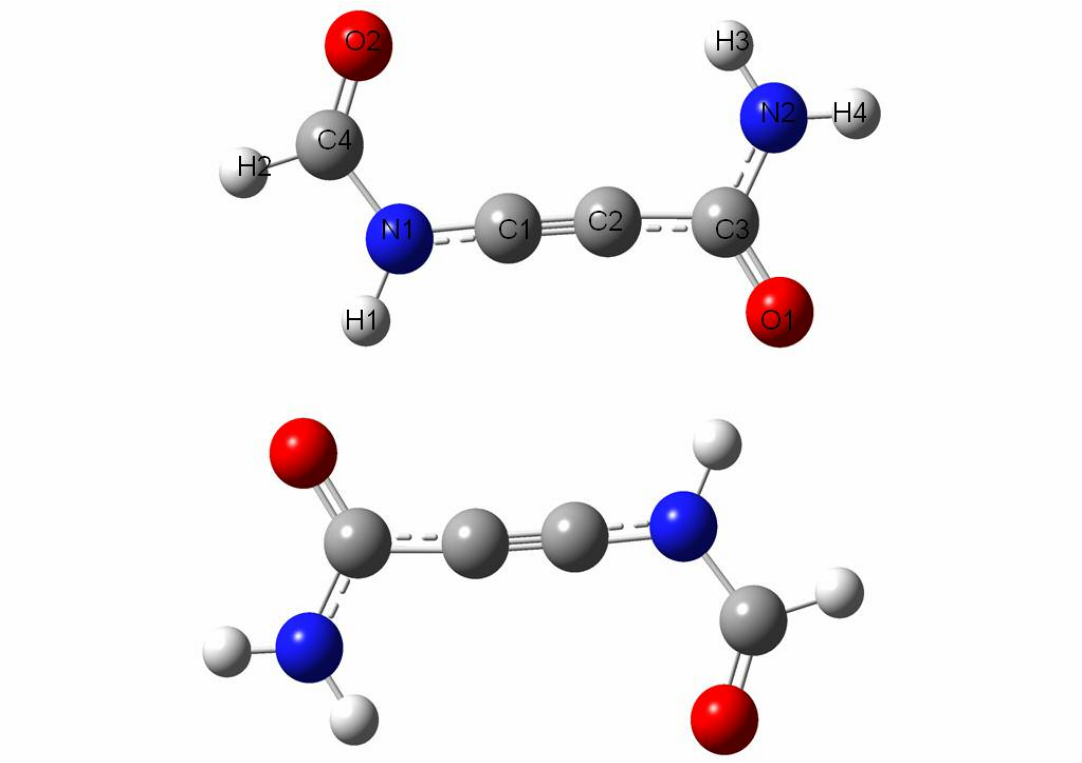

Figure 4-3. The SR D-A-C3-D-A dimer.

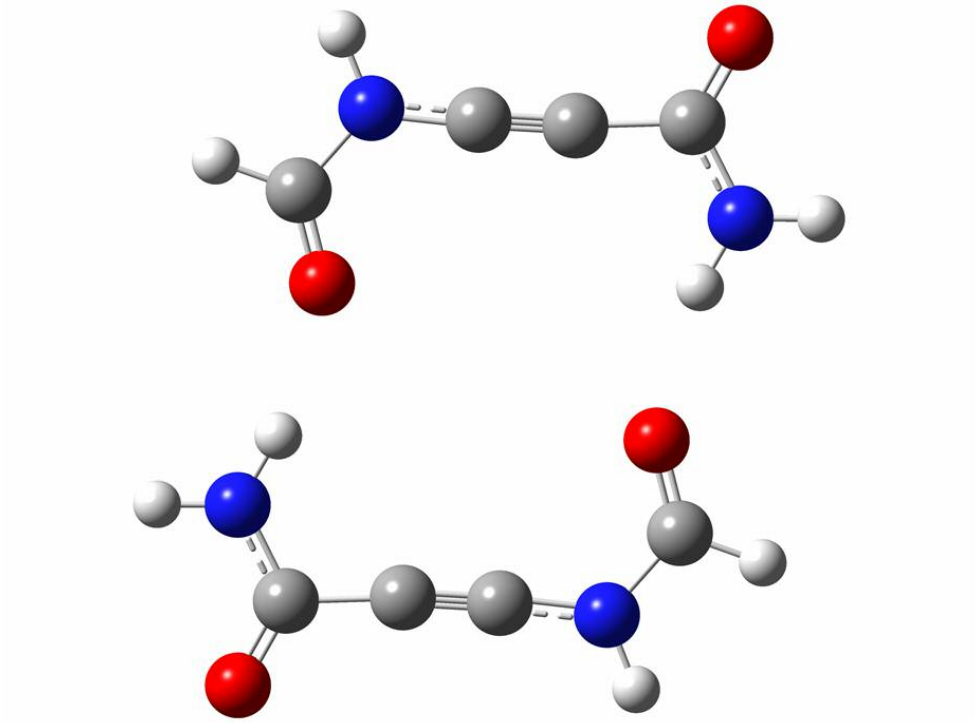

Figure 4-4. The LR D-A-C3-D-A dimer.

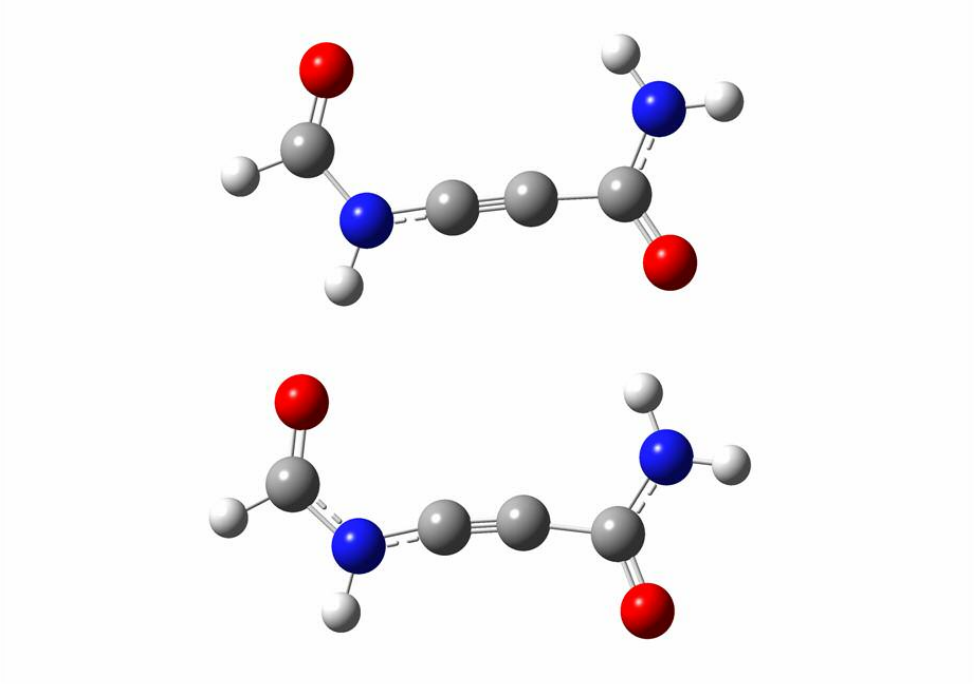

2gly2acSLCP ΔH(CP) = -11.42 kcal/mol
BD=1.839 (N-H…O=179.5); BD=1.973 (N-H…O=147.3)

Figure 4-5. The SL D-A-C3-D-A dimer.

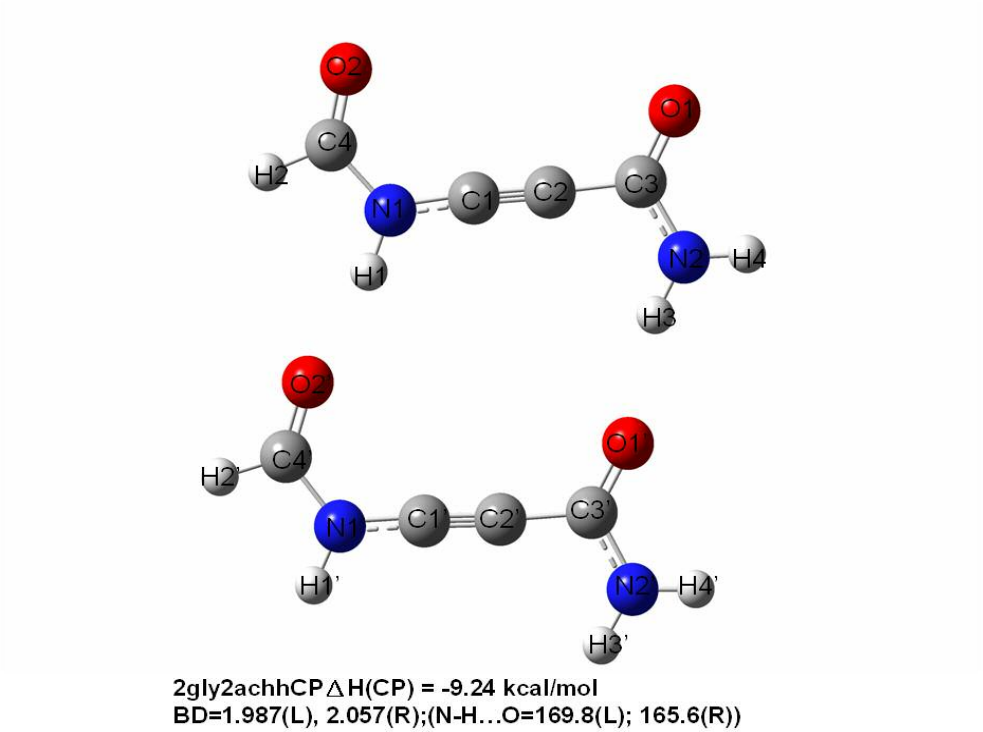

Figure 4-6. The cis D-A-C3-D-A dimer.

4.3.3 Diglycine with spacer, the D-A-C3-A-D dimers

There are two forms of D-A-C3-A-D dimers, the cis, and the trans isomers. Their structures are shown in Figures 4-7 and 8. The interaction enthalpies of those dimers are weaker than those of the D-A-C3-D-A dimers. The interaction enthalpies of cis and trans dimers are -7.48 and -11.82 kcal/mol, respectively. In this case, both dimers have 14 atoms involved in the polarizability, therefore the influence of different numbers of atoms can be ignored. This is because the atoms aligned in these dimers can not form the easily polarizable dimers that might enhance the strength of the H-bond. Unlike the planar D-A-C3-D-A dimers, these D-A-C3-A-D dimer structures are non-planar. This phenomenon provides the potential to develop helical structures, if we extend the structure to tetramers or larger structures. The longer trans structures have the potential to develop more stable structures. One can manipulate the conformation of the structures by changing the sequence of H-bond donor and acceptor. The cis dimer possesses weaker H-bond interaction than the trans dimer, since in the trans dimer the N-H···O H-bonds aligned in the opposite direction.

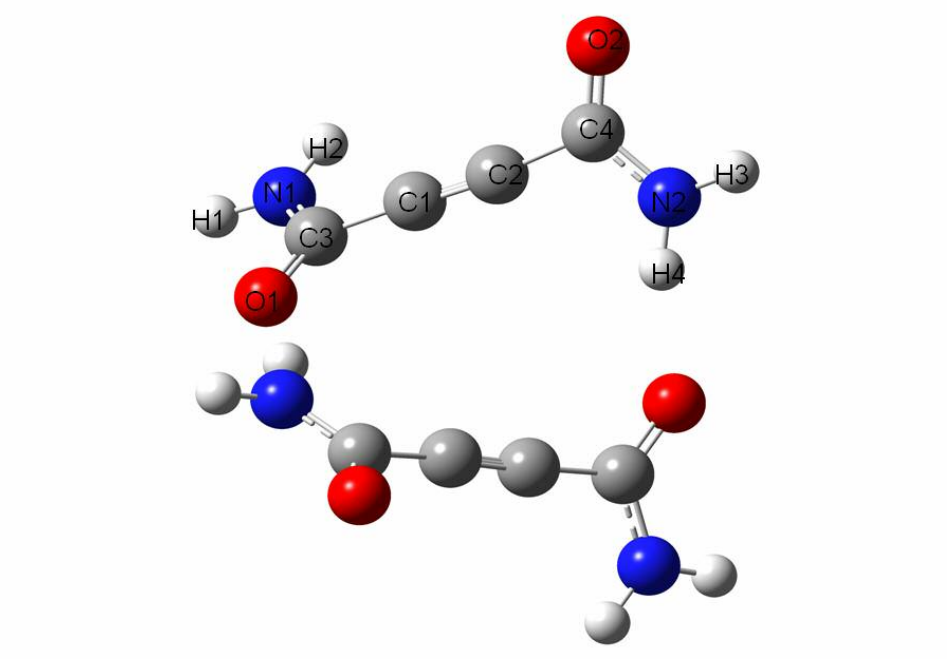

Non-planar: C2_2gly2acB_H1CP ΔH(CP) = -11.82 kcal/mol; BD=1.903;(N-H…O=169.3)
Planar: 2gly2acB_H1CP ΔH(CP) = -11.58 kcal/mol; BD=1.926;(N-H…O=157.0)1 imaginary freq -8.30

Figure 4-7. The trans D-A-C3-A-D dimer.

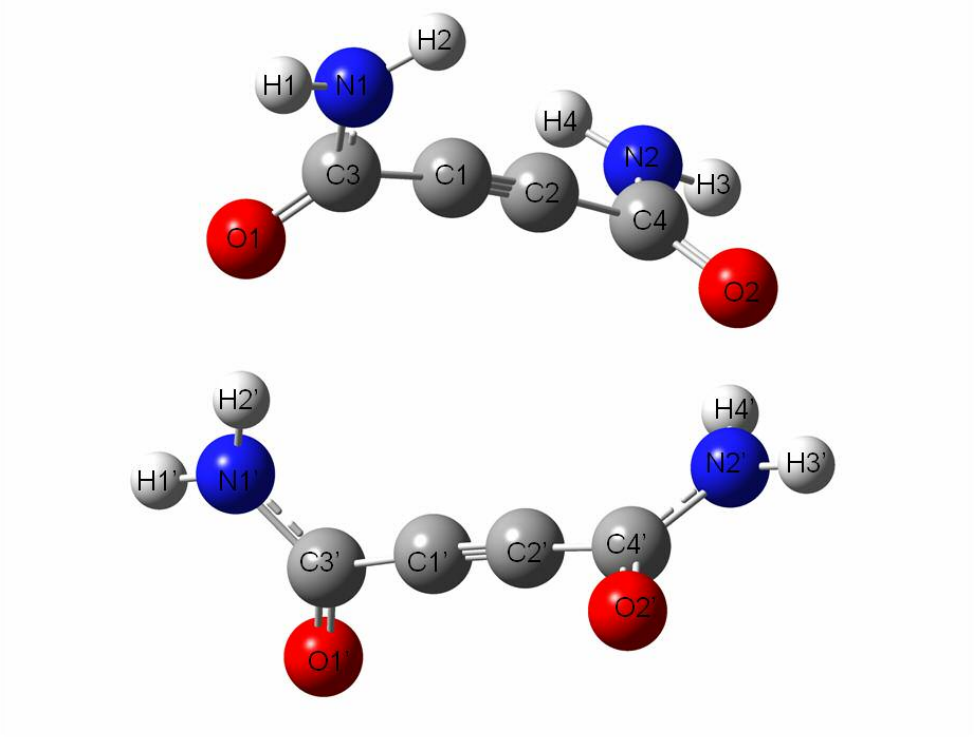

Non-planar: C2_2gly2acCCP ΔH(CP) = -7.48 kcal/mol; BD=2.008;(N-H…O=172.6)
Planar: ΔH(CP) = -5.54 kcal/mol; BD=2.102;(N-H…O=145.9) 2 imaginary freq -23.75, -13.97

Figure 4-8. The cis D-A-C3-A-D dimer.

4.3.4 Diglycine with spacers, the A-D-C3-D-A dimers

The cis and the trans A-D-C3-D-A dimers will be discussed here. These structures are shown in Figures 4-9 and 10. The interaction enthalpies of these dimers are weaker than those of the A-D-C3-D-A dimers. The interaction enthalpies of cis and trans dimers are -5.82 and -14.57 kcal/mol, respectively. The H-bond interaction of the cis dimer is weaker than that of the D-A-C3-A-D dimer, but the one corresponding to the trans A-D-C3-D-A dimer is stronger than that of the D-A-C3-A-D dimer. This is mainly due to the N-H···O H-bond geometry, but not to the polarizability. In this case, as in previous structures, the influence from different numbers of atoms involved should be ignored, because the charges of atoms do not follow the polarizability. Similar to the non-planar D-A-C3-A-D dimers, these A-D-C3-D-A dimers are also non-planar. This result can help one to develop extended helical structures, as the structures grow longer. The longer trans structures have the potential to develop the more stable structures. One can manipulate the conformation of the structures by changing the sequence of H-bond donor and acceptor. The cis dimer possesses H-bond interaction that is weaker than that of the trans dimer. This is because in the trans dimer, the N-H···O H bonds are aligned in the opposite direction. The interaction energies and enthalpies of the D-A-C3-D-A, D-A-C3-A-D, and A-D-C3-D-A dimers are tabulated in Table 4-1 in section 4.3.5.

The results above show that the interaction enthalpies of the D-A-C3-D-A, D-A-C3-A-D, and A-D-C3-D-A dimers can be controlled by various sequences of donor and acceptor and through the insertion of the easily polarizable spacers. In the SR D-A-C3-D-A dimer, the interaction enthalpy is the strongest among these dimers. This is because the dipole moments are aligned in the opposite direction and the charge of the atom can be polarized easily via acetylene spacers.

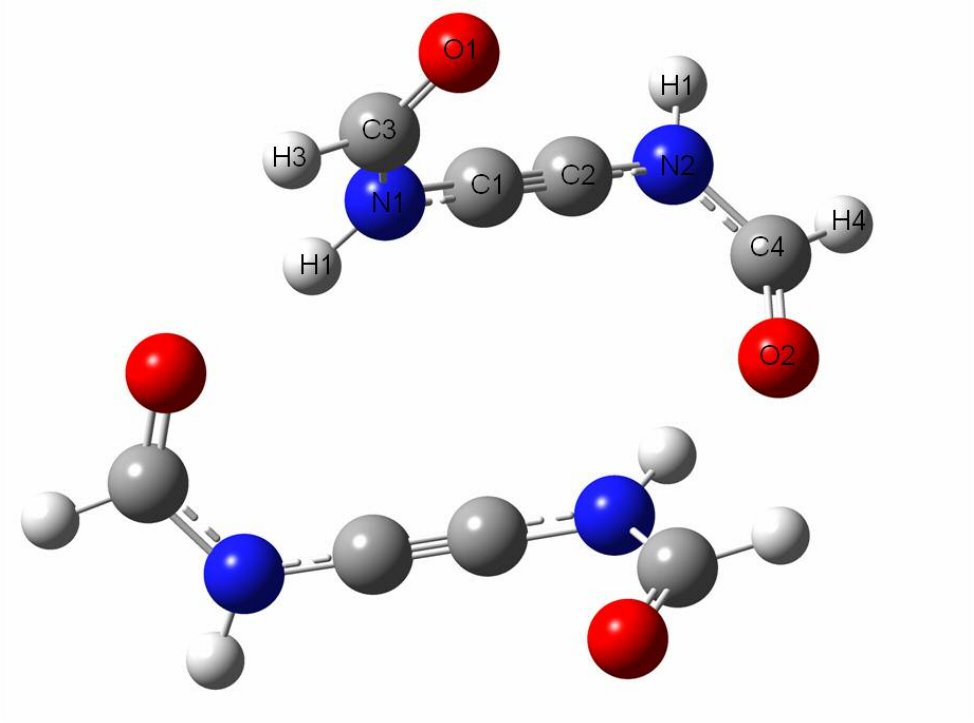

Non-planar:2gly2acDCP ΔH(CP) = -14.57 kcal/mol; BD=1.884;(N-H…O=158.9)
Planar:2gly2acDCP ΔH(CP) = -12.19 kcal/mol; BD=1.853;(N-H…O=158.9) 2 imaginary freq -42.79, -45.31

Figure 4-9. The trans A-D-C3-D-A dimer.

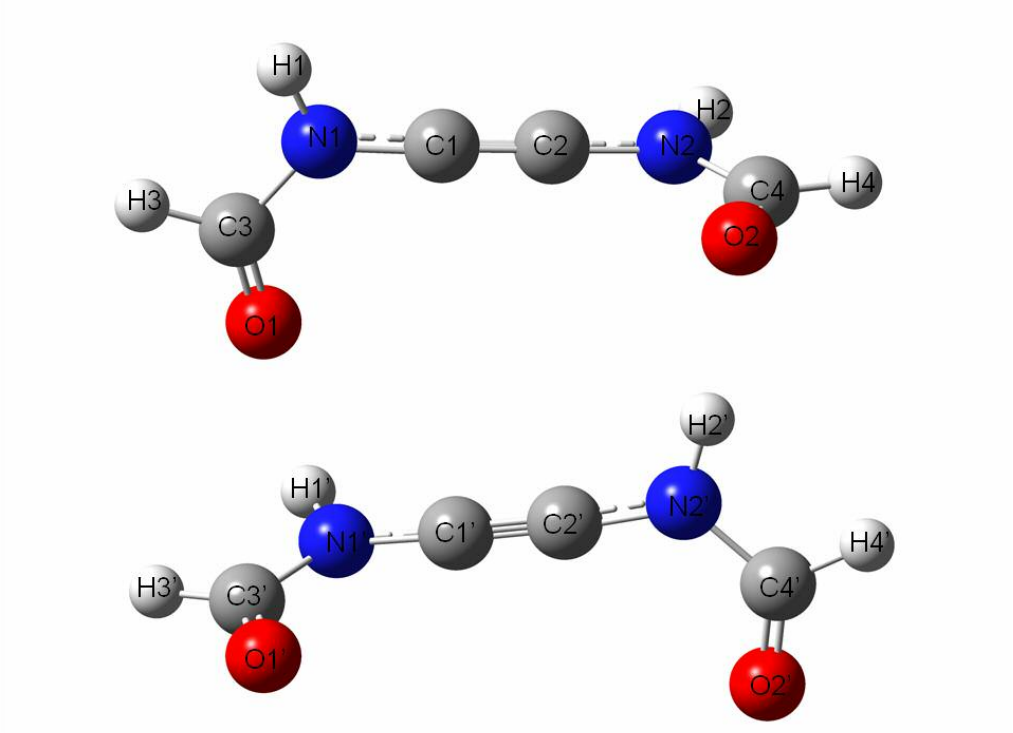

Non-planar: C2_ 2gly2acD2CP ΔH(CP) = -5.82 kcal/mol; BD=2.107;(N-H…O=148.0)
Planar: 2gly2acD2CP ΔH(CP) = -1.45 kcal/mol; BD=1.997;(N-H…O=161.3); 2 imaginary freq -78.98, - 26.03

Figure 4-10. The cis A-D-C3-D-A dimer.

4.3.5 Diglycine with a spacer, the D-A-C3-D-A, D-A-C3-A-D, and A-D-C3-D-A tetramers

The D-A-C3-D-A, D-A-C3-A-D, and A-D-C3-D-A tetramers will be shown in following sections. In the discussion of tetramers, no structures were constrained to be planar. These non-constrained structures will be in the following chapters while the more complicated structures are considered. The interaction energies, enthalpies and the H-bond cooperativity in enthalpy of all the dimers above are tabulated in Table 4-1.

Table 4-1. The interaction energies, enthalpies and the H-bond cooperativity of the D-A-C3-D-A, D-A-C3-A-D and A-D-C3-D-A dimers, and tetramers.

Structures	ΔE(kcal/mol)	ΔH(kcal/mol)	Cooperativity ΔH
Formamide Dimer	-14.03	-12.12	
D-C3-A dimer	-20.73	-18.05	
D-C3-C3-A dimer	-19.41	-17.90	
D-A-C3-D-A dimer(SR)	-23.47	-21.98	
D-A-C3-D-A dimer (LR)	-7.84	-6.00	
D-A-C3-D-A dimer (SL)	-13.29	-11.42	
D-A-C3-D-A dimer (trans)	-11.04	-9.24	
D-A-C3-D-A tetramer (cis)	-58.85	-54.17	-4.21
D-A-C3-D-A tetramer (trans)	-42.33	-36.61	-8.89
D-A-C3-A-D dimer (trans)	-13.58	-11.82	
D-A-C3-A-D dimer (cis)	-9.17	-7.48	
D-A-C3-A-D tetramer (cis)	-35.11	-29.87	-7.43
D-A-C3-A-D tetramer (trans)	-41.45	-37.77	-2.31
A-D-C3-D-A dimer (trans)	-16.39	-14.57	
A-D-C3-D-A dimer (cis)	-7.45	-5.82	
A-D-C3-D-A tetramer(cis)	-36.32	-30.98	-13.52
A-D-C3-D-A tetramer (trans)	-54.98	-49.59	-5.88

4.3.6 The D-A-C3-D-A tetramers

Several possible vertically-extended tetramers can be developed. I only describe the strongest H-bonded cis and trans tetramer as shown in Figures 4-11 and 12. The interaction enthalpies are -54.17 and -36.61 kcal/mol, respectively. Those tetramers are both planar structures. The stronger H-bond interaction is observed when the dipole moments of the tetramer are aligned in the opposite direction. In the trans tetramer (see Figure 4-11), although all dipole moments are aligned in the same direction, that does not mean stronger interaction can be observed. However, is the one with stronger H-bond cooperativity. The cooperativity of the trans tetramer is -8.89 kcal/mol, and that of the cis tetramer is -4.21 kcal/mol. The stronger cooperative effect of the trans tetramer than that of the cis tetramer might be due to all the dipole moments are aligned in the same direction. When this happens, the influence of the dipole moment can be accumulated constructively, the effect is then enhanced. The strongest interaction enthalpy of the tetramer here is the cis 2SR1LR tetramer and its structure is shown in Figure 4-12. I found the H-bonds in the center are weaker than those at the end. This is because in the tetramer, the center LR dimer provides weaker interaction. While building up vertically and horizontally-extended structures, the LR and SR interaction enthalpy difference must be taken into considerations. Therefore, more stable larger structures can be obtained. The LR and SR should be placed alternatively in the larger structures to obtain more stable structures.

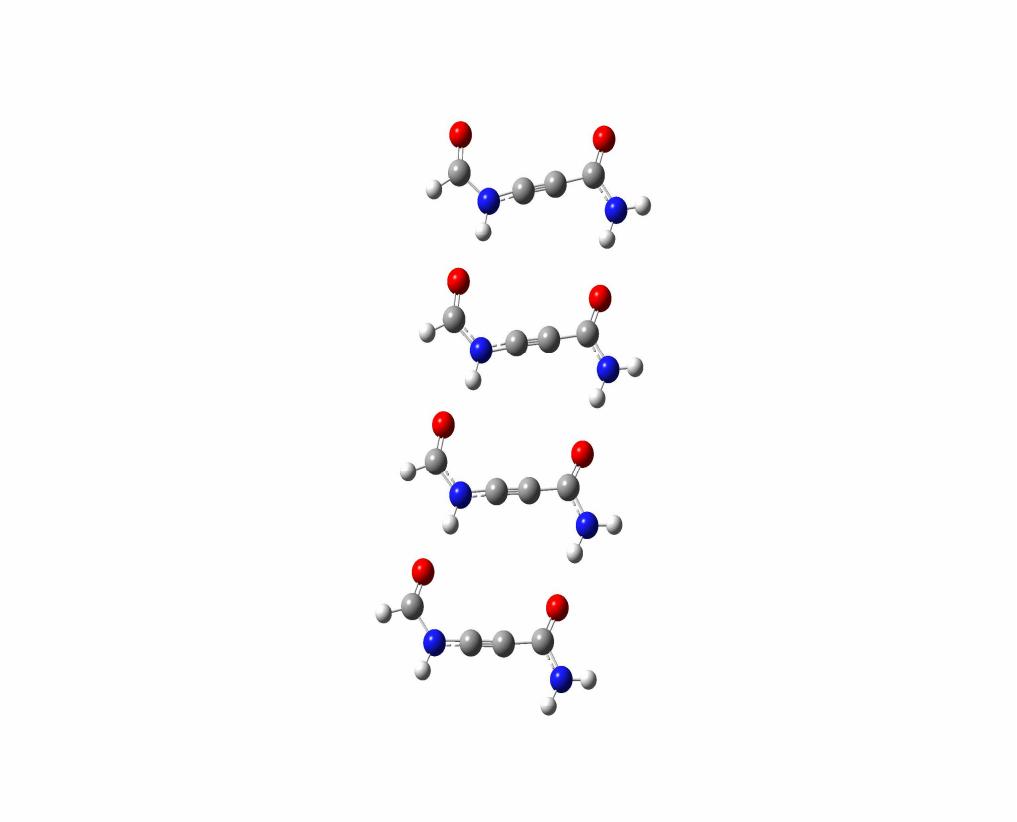

Figure 4-11. The trans D-A-C3-D-A tetramer. The ΔH is -36.61 and the dimeric ΔH is -9.24 kcal/mol. The N-H···O bond distances (top to down and left to right) are 1.921, 1.979, 1.886, 1.937, 1.914 and 1.976 Å.

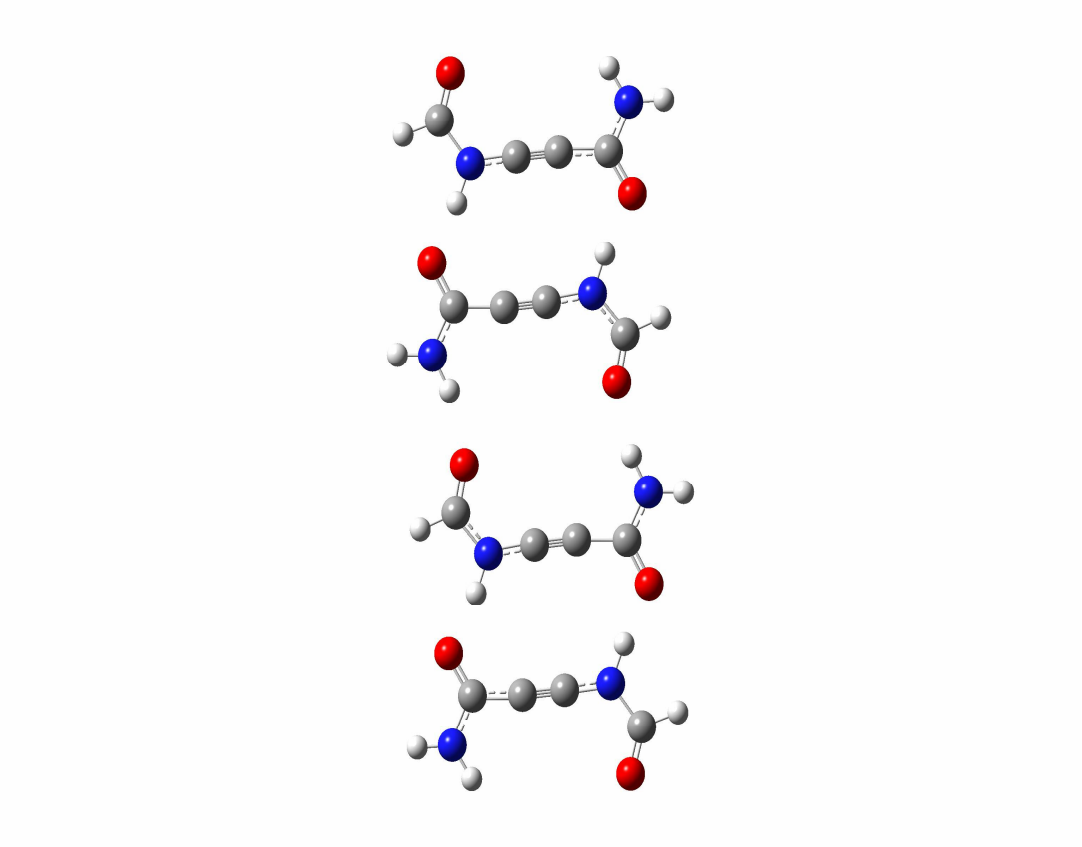

Figure 4-12. The cis D-A-C3-D-A tetramer. The ΔH is -54.17 and the SR dimeric ΔH is -21.98, and the LR dimeric ΔH is -6.00 kcal/mol. The N-H···O bond distances (top to down and left to right) are 1.689, 1.715 and 1.906 Å. Since the tetramer is symmetric (C_{2H}), the bond distances are paired.

4.3.7 The D-A-C3-A-D tetramers

The structures of both the cis and trans isomers are not planar but helical. As shown in Figure 4-13 and 14, the cis helical tetramer has a "dihedral angle" between both C=O in the range from 70 to 80° while dihedral angle for trans tetramer, is between 120~130°. The "dihedral angle" here refers to the angle between three successive chemical bond (O=C, -C-C≡C-C, and C=O) vectors. The interaction enthalpies of the cis and trans tetramer are -29.87 and -37.77 kcal/mol, respectively. The cis tetramer (see Figure 4-13), where all dipole moments are aligned in the same direction shows stronger H-bond cooperativity. However, this tetramer shows weaker H-bond interaction.

The cooperativity of the cis tetramer is -7.43 kcal/mol and that of the trans tetramer is -2.31 kcal/mol. The stronger cooperative effect of the cis tetramer might be due to that fact that all dipole moments are aligned in the same direction, so the influence can be accumulated constructively. The trans tetramer has stronger interaction enthalpy and the structure is shown in Figure 4-14. The stronger interaction is attributed to the fact that the dipole moments are aligned in the opposite direction. Thus, the dipole-dipole interaction of the anti-parallel alignment increases the overall interaction of the tetramer.

The geometries of these tetramers can be altered just by changing the sequence of H-bond donor and acceptor. The formation of helical structures is because both carbonyls are close to each other (5~6 Å), the repulsion between the electrons in O atom is significant. To reduce the repulsion, the non-linear helical structures are then formed.

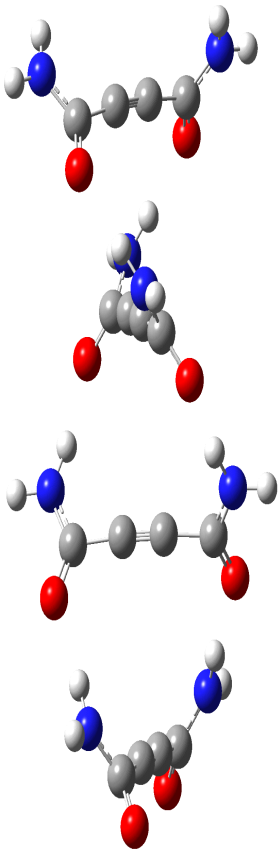

Figure 4-13. The cis D-A-C3-A-D tetramer. The ΔH is -29.87 and the dimeric ΔH is -7.48 kcal/mol. The N-H···O bond distances (top to down and left to right) are 1.937, 1.905 and 1.947 Å. Since the tetramer is symmetric (C2), the bond distances are paired.

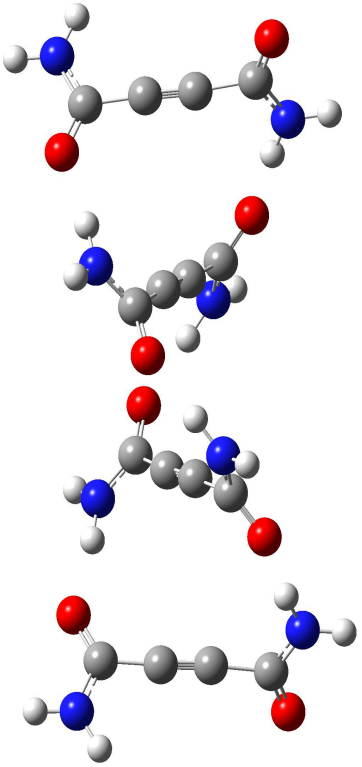

Figure 4-14. The trans D-A-C3-A-D tetramer. The ΔH is -37.33 and the dimeric ΔH is -11.82 kcal/mol. The N-H···O bond distances (top to down and left to right) are 1.914, 1.888 and 1.878 Å. Since the tetramer is symmetric (C_2), the bond distances are paired.

4.3.8 The A-D-C3-D-A tetramers

The cis and trans A-D-C3-D-A tetramers are also formed helical structures. As shown in Figures 4-15 and 16, the dihedral angles between both N-H (since N-H is attached adjacent to the spacer) of the cis helical tetramer fall in the range of -70 ~ -75° and those of the trans tetramer fall in the range of -105 ~ -115°. The interaction enthalpies of the cis and trans tetramers are -30.98 and -49.59 kcal/mol, respectively. As shown in Figure 4-15, all dipole moments of the cis tetramer are aligned in the same direction. This tetramer has stronger H-bond cooperativity, however, the enthalpy is weaker than that of the trans tetramer by -18.16 kcal/mol. The cooperativity of the cis tetramer is -13.52 and that of the trans tetramer is -2.31 kcal/mol. The stronger cooperative effect of the cis tetramer might be because all dipole moments are aligned in the same direction, so the influence can be accumulated constructively. The dihedral angle between N-H of the cis tetramer is also lessened by 10° (relative to the dimer), which indicates the contribution of the N-H···O H-bonds from extra monomer can reduce the dihedral angle. Thus, the strength of the H-bond is then increased. The trans tetramer is the one with stronger interaction enthalpy and the structure is shown in Figure 4-16. The stronger interaction results from the attraction between anti-parallelly aligned dipole moments. This alignment increases the H-bond interaction of the tetramer.

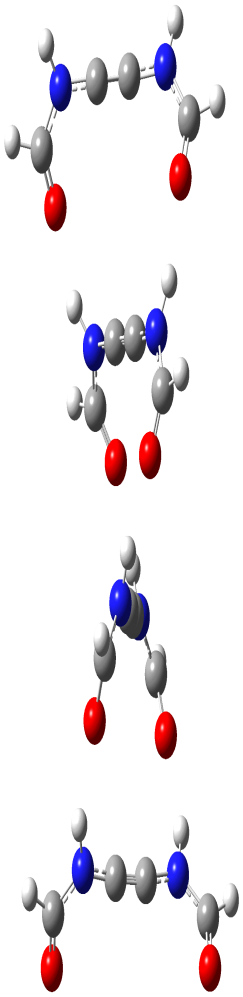

Figure 4-15. The cis A-D-C3-D-A tetramer. The ΔH is -30.98 and the dimeric ΔH is -5.82 kcal/mol. The N-H···O bond distances (top to down and left to right) are 1.927, 1.929 and 1.889 Å. Since the tetramer is symmetric (C_2), the bond distances are paired.

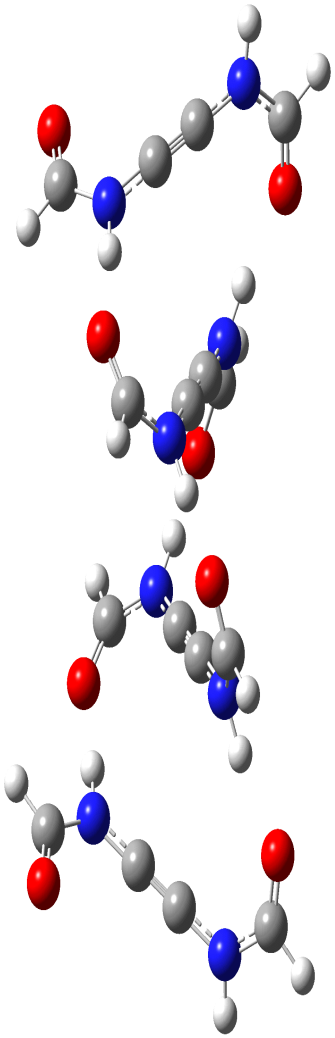

Figure 4-16. The trans A-D-C3-D-A tetramer. The ΔH is -49.59 and the dimeric ΔH is -14.57 kcal/mol. The N-H···O bond distances (top to down and left to right) are 1.843, 1.822 and 1.790 Å. Since the tetramer is symmetric (C_2), the bond distances are paired.

The trans D-A-C3-A-D monomer is the most stable monomer among the D-A-C3-D-A, D-A-C3-A-D and A-D-C3-D-A monomers. It is more stable than the D-A-C3-D-A and A-D-C3-D-A monomers by 9.46 and 22.30 kcal/mol.

The cis D-A-C3-D-A tetramer has the strongest H-bond interaction among all the tetramers. For the rest of the tetramers, the trans ones have stronger H-bond interactions than the cis ones. We can estimate the strength of the H-bond in the cis and trans forms by the alignment of dipole moments. If the dipole moments point to the same direction, their interactions are weaker (due to repulsion of dipole-dipole interaction) than those point to the opposite direction. This is due to the attractive dipole-dipole interactions when dipole moments are aligned in the opposite direction.

On the contrary, the strongest H-bonded tetramer does not show the strongest cooperative effect. The cis A-D-C3-D-A tetramer possesses the strongest cooperativity, although this tetramer is weaker than its trans isomer by -18.16 kcal/mol. When the dipole moments are aligned en route for the same direction, the H-bond cooperativity is enhanced. This is because when the structures are constructed in that way, the dipole moments can be increased as the structures expand.

4.3.9 The extended acetylene spacer tetramers

The D-C3-A-C3-D-C3-A, D-C3-A-C3-A-C3-D, and A-C3-D-C3-D-C3-A tetramers will be discussed in following sections. No tetramers are constrained to be planar. The H-bond interactions of more complicated structures with different spacers will be shown. All the interaction energies, enthalpies and the H-bond cooperativities in energy are shown in Table 4-2. The cooperativities in energy instead of in enthalpy are shown here because the energetic results here will be compared with the tetramers with Bz spacers in section 4.3.13. However, due to the 32-bit limitation of the software, frequency calculations of larger structures with Bz spacers are not possible to perform. To facilitate the discussion here, the cooperativities in energy are tabulated.

Table 4-2. The interaction energies, enthalpies, and cooperativities of the A-C3-D-C3-A-C3-D, A-C3-D-C3-D-C3-A, and D-C3-A-C3-A-C3-D, dimers, and tetramers.

Structures	ΔE(kcal/mol)	ΔH	Cooperativity ΔE
Extended Acetylene Center			
Dimer A-C3-D-C3-D-C3-A (Cis)	-13.72	-12.71	
Tetramer A-C3-D-C3-D-C3-A (Cis)	-47.87	-43.26	-6.71
Dimer A-C3-D-C3-D-C3-A (Trans)	-19.10	-17.57	
Tetramer A-C3-D-C3-D-C3-A (Trans)	-64.92	-60.77	-7.62
Dimer D-C3-A-C3-D-C3-A (Cis)	-17.48	-14.69	
Tetramer D-C3-A-C3-D-C3-A (Cis)	-55.95	-49.01	-3.51
Dimer D-C3-A-C3-D-C3-A (Trans)	-11.69	-10.10	
Tetramer D-C3-A-C3-D-C3-A (Trans)	-46.29	-40.36	-11.22
Dimer D-C3-A-C3-A-C3-D (Cis)	-12.30	-11.02	
Tetramer D-C3-A-C3-A-C3-D (Cis)	-43.41	-39.41	-6.51
Dimer D-C3-A-C3-A-C3-D (Trans)	-17.34	-16.16	
Tetramer D-C3-A-C3-A-C3-D (Trans)	-57.17	-53.49	-5.15

4.3.10 The A-C3-D-C3-D-C3-A tetramers

The A-C3-D-C3-D-C3-A tetramers are shown in Figures 4-17 and 18. The cis and trans tetramers are both non-planar helical structures, the trans tetramer can even form a caged-like structure. The dihedral angles of two N-H groups in the cis tetramer fall in the range of -75 ~ -105°. The dihedral angles of two N-H groups in the trans tetramer fall in the range of -80 ~ -95°. The interaction enthalpy of the trans tetramer (-60.77 kcal/mol) is stronger than that of the cis tetramer (-43.26 kcal/mol) by 17.51 kcal/mol. The trans tetramer is the strongest among A-C3-D-C3-D-C3-A, D-C3-A-C3-D-C3-A, and D-C3-A-C3-A-C3-D tetramers. The caged-like tetramer does not have extra N-H···O H-bonds (total six H-bonds), different from its cis isomer. The trans tetramer is also more cooperative in H-bond strength when both dimers are compared. The extraordinarily stronger H-bond interaction in trans tetramer might be because the N-H···O H-bonds are not aligned in the same direction, and the influence of some weak C-H···O H-bonds in the caged-like structure.

The H-bond cooperativity of cis tetramer in enthalpy is weaker than that of the trans tetramer (cis: -5.13 and trans: -8.06 kcal/mol), in contrast with the observation in previous section. However, the variance is not significant. This special situation results from non-linear combination of dipole moments in the more stable caged-like structure. The unique geometry of the structure plays a more important role than the alignment of the dipole moments in terms of interaction strength.

The significant conformation difference reveals that by the cis-trans structure transformation, we can obtain the desired structures, either helical or caged shape. When the easily polarizable acetylenes are inserted as spacers, the interaction enthalpies of both cis and trans dimers are stronger than those of the A-D-C3-D-A dimers. In this A-C3-D-C3-D-C3-A system, the center molecules can not enhance the polarizibility. However, the longer monomer provides more freedom to the tetramer and larger structures to form structures with more diverse geometries, such as caged, cubic, or twisted shapes.

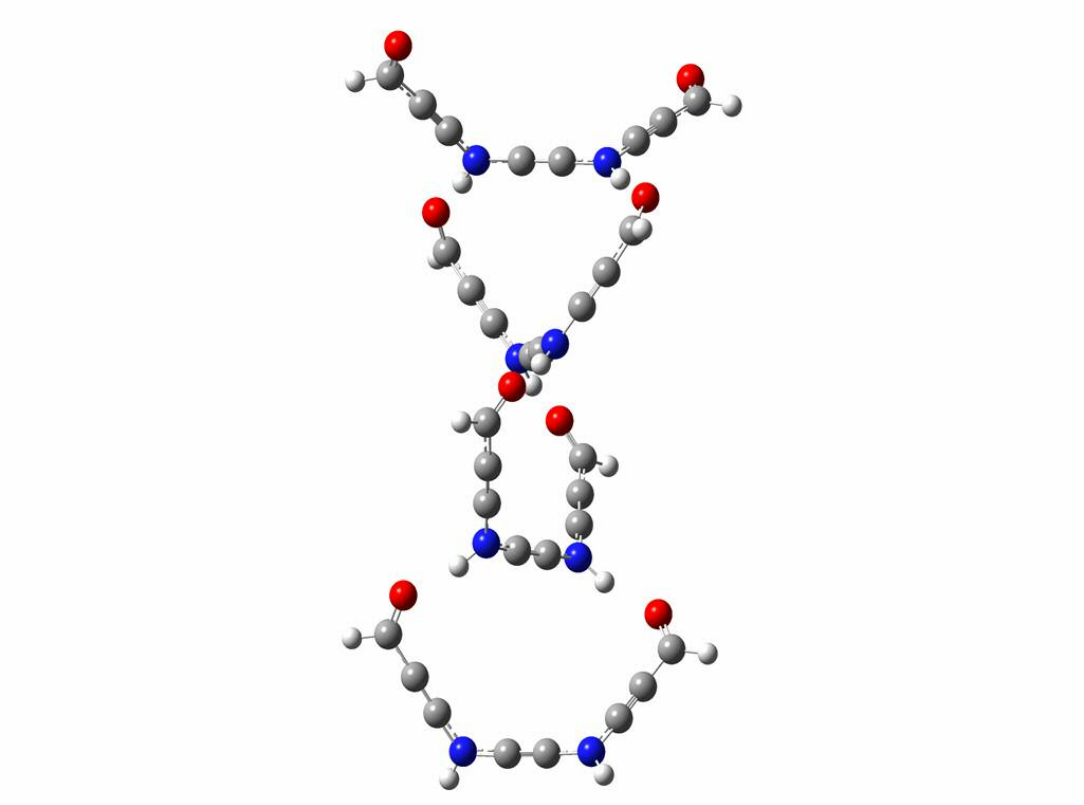

Figure 4-17. The trans A-D-C3-D-A tetramer. The ΔH is -49.59 and the dimeric ΔH is -14.57 kcal/mol. The N-H···O bond distances (top to down and left to right) are 1.843, 1.822 and 1.790 Å. Since the tetramer is symmetric (C_2), the bond distances are paired.

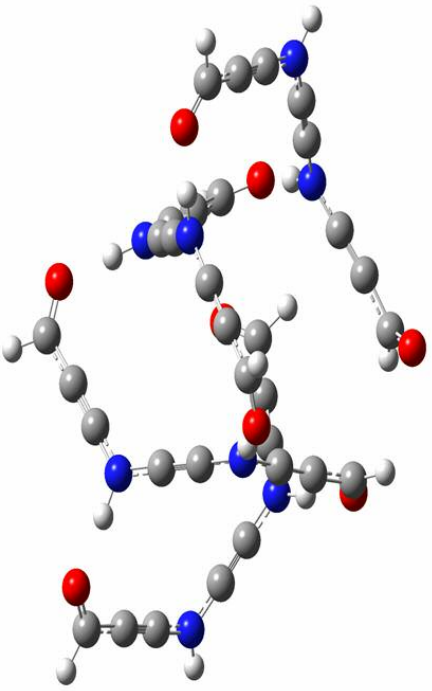

Figure 4-18. The trans A-C3-D-C3-D-C3-A tetramer. The ΔH is -60.77 and the dimeric ΔH is -17.59 kcal/mol. The N-H···O bond distances (top to down and left to right) are 1.746, 1.695, and 1.700 Å. Since the tetramer is symmetric (C2), the bond distances are paired.

4.3.11 The D-C3-A-C3-D-C3-A tetramers

The D-C3-A-C3-D-C3-A tetramers are shown in Figures 4-19 and 20. Both tetramers are planar structures. Although both tetramers were kept planar, it is observable that as the structure extended, the structures could be curved toward one direction. If enough monomers are linked, the structure can even form a ring. The curved structures result from not all the N-H···O H-bonds in tetramer are equivalent in strength. The N-H···O H-bond with -NH2 donor is slightly weaker than that with the N-H donor. In Figure 4-19, the bond distances of the H-bonds with NH2 donor are longer than those with N-H donor between 0.28 ~ 0.48 Å. The interaction enthalpy of the cis tetramer (-49.01 kcal/mol) is stronger than that of the trans tetramer (-40.36 kcal/mol) by -8.65 kcal/mol. This is the only cis tetramer that has stronger H-bond interaction than the trans isomer. This is due to this trans tetramer is the only tetramer that shows the dipole moments are aligned in the same direction. However, the cooperativity in the trans tetramer is more than twice stronger (cis: -4.94, trans: -10.06 kcal/mol) than that of the cis tetramer.

Besides the alignment of dipole moments, this system is also unique at the donor-acceptor sequence. The sequence follows the rules of polarizability (the positive and the negative charged atoms are next to each other). Since more atoms (18 atoms) are involved in the polarizability, thus the effect of polarizability is not as significant as that of the A-D-C3-A-D tetramer. Within the cis A-C3-D-C3-D-C3-A, D-C3-A-C3-D-C3-A, D-C3-A-C3-A-C3-D tetramers, the cis D-C3-A-C3-D-C3-A tetramer is the one with the strongest H-bond interaction. This is because the combined effects of the alignment of dipole moments and the polarizability.

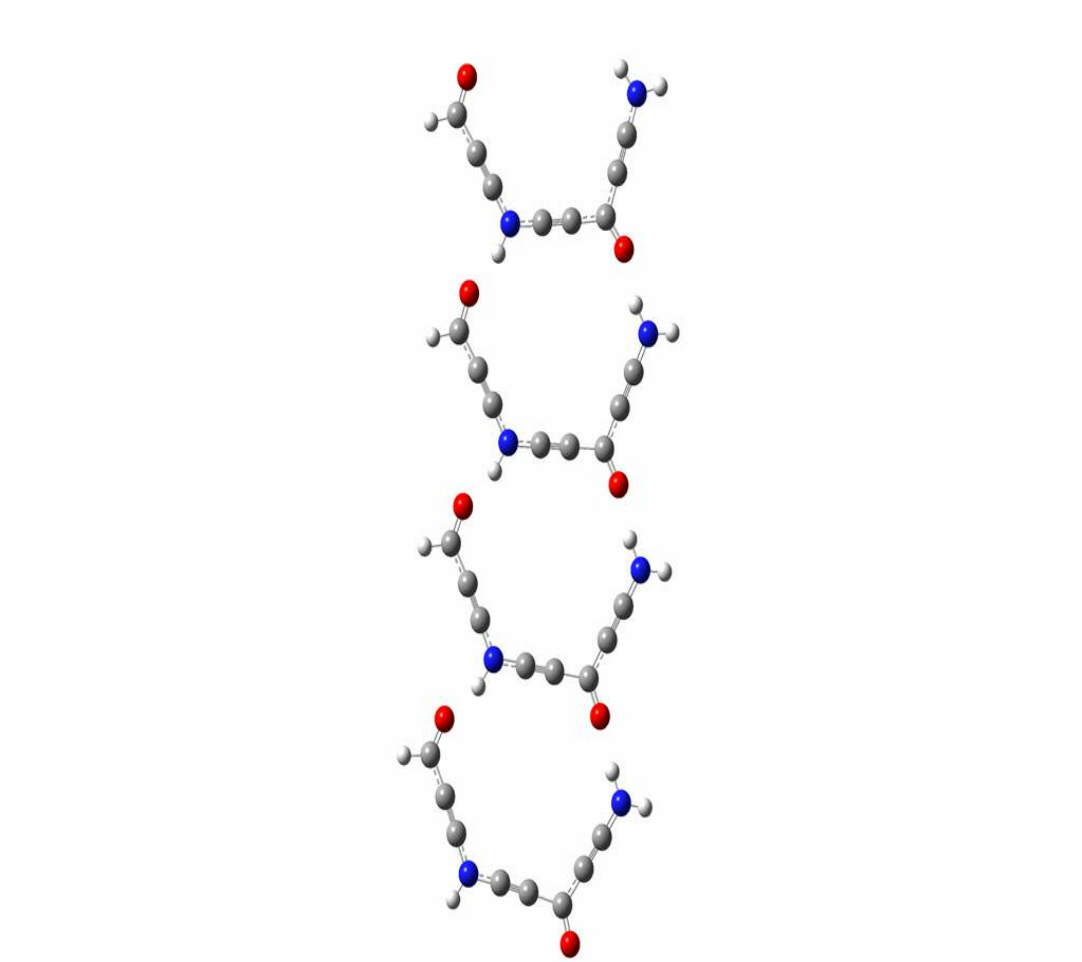

Figure 4-19. The cis D-C3-A-C3-D-C3-A tetramer. The ΔH is -49.01 and the dimeric ΔH is -14.69 kcal/mol. The N-H···O bond distances (top to down and left to right) are 1.764, 1.812, 1.754, 1.793, 1.789 and 1.817 Å.

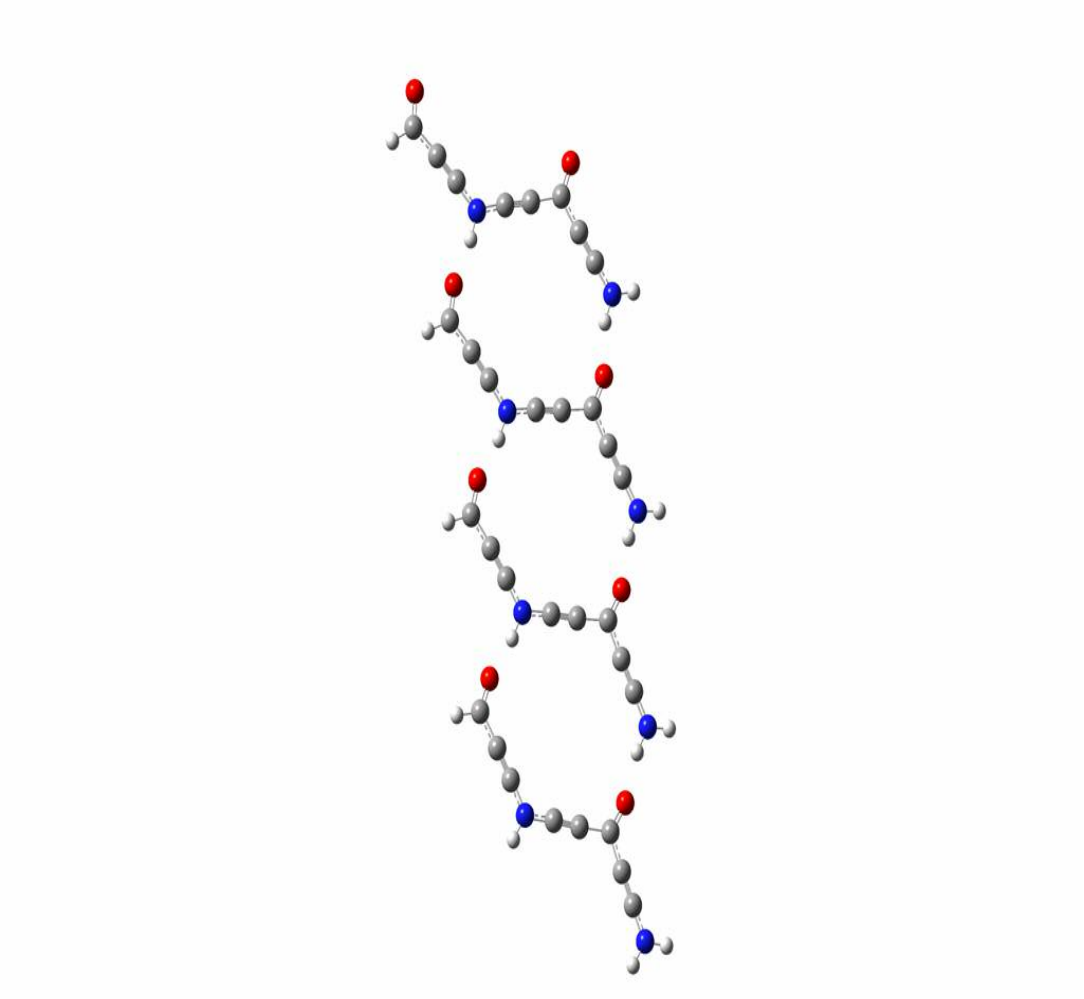

Figure 4-20. The trans D-C3-A-C3-D-C3-A tetramer. The ΔH is -40.36 and the dimeric ΔH is -10.10 kcal/mol. The N-H···O bond distances (top to down and left to right) are 1.829, 1.886, 1.791, 1.853, 1.820 and 1.889 Å.

4.3.12 The D-C3-A-C3-A-C3-D tetramers

Two forms of the D-C3-A-C3-A-C3-D tetramers are shown in Figures 4-21 and 22. Both the cis and trans tetramers are helical structures. The dihedral angles between C=O in both tetramers vary significantly. In the cis tetramer, the dihedral angles fell in the range between 24 (C=O top) to 108 ° (amide bottom). The dihedral angles of the trans tetramer are in the range from 105 to 110°. The smaller angle in the cis tetramer means the structure is more close to the planar structure. The interaction enthalpy of the trans tetramer (-53.49 kcal/mol) is stronger than that of the cis tetramer (-39.41 kcal/mol) by -14.08 kcal/mol. The stronger H-bond interaction in the trans tetramer is due to all of the N-H···O H-bonds of trans tetramer are not aligned in the same direction. The H-bond cooperativity of the trans tetramer in enthalpy is -6.35 kcal/mol and that of the cis tetramer is -5.01 kcal/mol. The cis tetramer shows slightly stronger cooperativity than trans tetramer. This is the only system that agrees with the stronger cooperativity of the cis tetramer in the diglycine with only one spacer, which refers to the D-A-C3-A-D tetramer, et cetera.

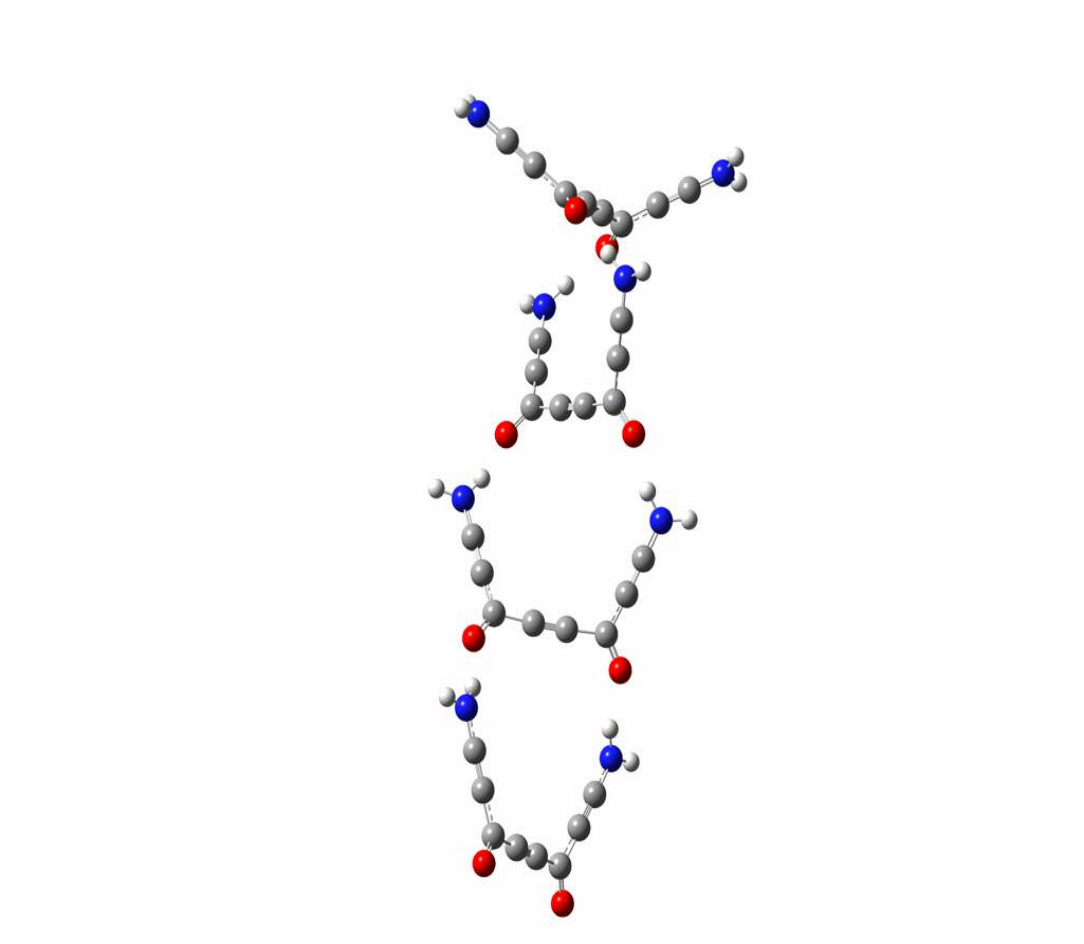

Figure 4-21. The cis D-C3-A-C3-A-C3-D tetramer. The ΔH is -39.41 and the dimeric ΔH is -11.02 kcal/mol. The N-H···O bond distances (top to down and left to right) are 1.868, 1.858, and 1.904 Å. Since the tetramer is symmetric (C2), the bond distances are paired.

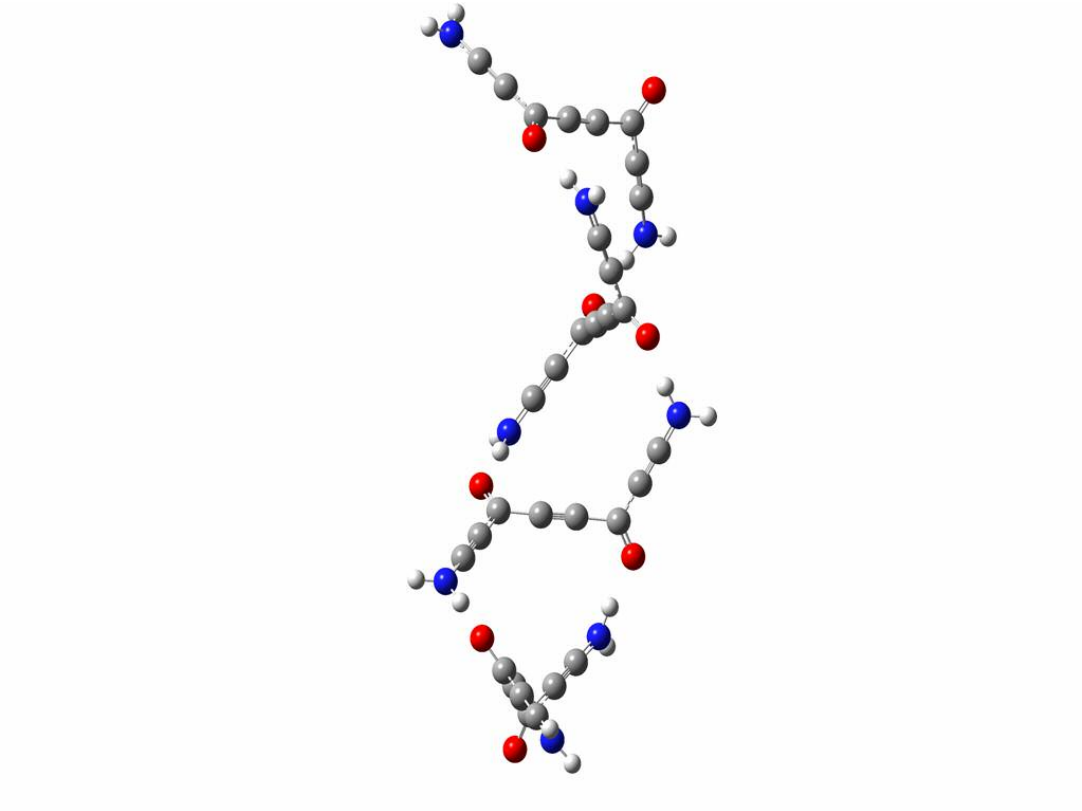

Figure 4-22. The trans D-C3-A-C3-A-C3-D tetramer. The ΔH is -53.49 and the dimeric ΔH is -16.16 kcal/mol. The N-H···O bond distances (top to down and left to right) are 1.795, 1.758, and 1.794 Å. Since the tetramer is symmetric (C_2), the bond distances are paired.

The trans D-C3-A-C3-A-C3-D monomer is more stable than the D-C3-A-C3-D-C3-A and A-C3-D-C3-D-C3-A monomer by -11.90 and -27.44 kcal/mol.

The cis D-C3-A-C3-A-C3-D tetramer holds the weakest interaction enthalpy among all the tetramers. The trans D-C3-A-C3-A-C3-D tetramer is the middle among all trans tetramers, and it was kept as the non-planar, helical structure. The caged-like trans A-C3-D-C3-D-C3-A tetramer holds the strongest H-bond interaction among all the tetramers. Regarding others tetramers, most trans ones have stronger H-bond interactions than the cis ones. The only exception is the cis D-C3-A-C3-A-C3-D tetramer, which has all the dipole moments are aligned in the opposite direction. We can estimate the strength of the H-bond in the cis and trans forms by looking at the directions of dipole moment alignment.

On the contrary, the strongest H-bonded tetramer does not show the strongest cooperative effect. The trans D-C3-A-C3-A-C3-D tetramer possesses the strongest cooperativity, although this tetramer is weaker than its trans isomer by -8.65 kcal/mol. When the dipole moments are aligned in the same direction, the H-bond cooperativity is enhanced because the dipole moment can be accumulated as the structures expended.

4.3.13 Benzene as the center molecule

We replace the center spacer as benzene (Bz) to form D-C3-A-Bz-D-C3-A, D-C3-A-Bz-D-C3-A, and D-C3-A-Bz-A-C3-D monomer to observe the geometry changes with this larger center spacer. Due to the large size of the tetramer, it reaches the limit of 32-bit Gaussian 03 software. In following sections, only the interaction energies instead of enthalpies are discussed in later paragraphs. The interaction energies, enthalpies, and H-bond cooperativity (in energy) of all the three spacers (three C3) tetramers are listed in Table 4-3.

Table 4-3. The interaction energies, enthalpies, and cooperativities in energy of the A-C3-D-Bz-A-C3-D, D-C3-A-Bz-D-C3-A, and D-C3-A-Bz-A-C3-D dimers and tetramers.

Structures	**ΔE(kcal/mol)**	**ΔH**	**Cooperativity ΔE**
Benzene Center			
Dimer A-C3-D-Bz-D-C3-A (Cis)	-11.09	-9.98	
Tetramer A-C3-D-Bz-D-C3-A (Cis)	-68.92	N/A	N/A (8-HB)
Dimer A-C3-D-Bz-D-C3-A (Trans)	-16.72	-14.85	
Tetramer A-C3-D-Bz-D-C3-A (Trans)	-44.57	N/A	5.59
Dimer D-C3-A-Bz-D-C3-A (Cis)	-16.31	-14.77	
Tetramer D-C3-A-Bz-D-C3-A (Cis)	-54.72	N/A	-5.79
Dimer D-C3-A-Bz-D-C3-A (Trans)	-12.76	-11.16	
Tetramer D-C3-A-Bz-D-C3-A (Trans)	-40.53	N/A	-2.25
Dimer D-C3-A-Bz-A-C3-D (Cis)	-12.51	-11.06	
Tetramer D-C3-A-Bz-A-C3-D (Cis)	-26.88	N/A	10.65
Dimer D-C3-A-Bz-A-C3-D (Trans)	-15.57	-14.22	
Tetramer D-C3-A-Bz-A-C3-D (Trans)	-50.74	N/A	-4.03

4.3.14 The A-C3-D-Bz-D-C3-A tetramers

The A-C3-D-Bz-D-C3-A tetramers are shown in Figures 4-23 and 24. The cis tetramer forms a cuboids-like structure and the trans tetramer forms an irregular non-planar structure. The interaction energy of the cis tetramer (-68.92 kcal/mol) is lower than that of the trans tetramer by -24.35 kcal/mol. The extraordinary H-bond interaction energy is not only due to the H-bond cooperativity but also due to the eight H-bonds instead of the normal six H-bonds in the tetramer. Besides, the weaker H-bond interaction in the trans tetramer is due to the trans-cis transformation at the end of the tetramer, the out-of-plane benzene position, and the interstrand benzene-benzene C-H repulsion. I also found no cooperativity in this tetramer. Actually, the cooperativity of the trans tetramer in energy is +5.59 kcal/mol, which is not attractive but repulsive.

Without looking at the structures, I originally predicted the trans tetramer would hold stronger interaction energy because dipole moments are aligned in opposite direction. This prediction fails because there are eight H-bonds in this cuboids shape tetramer. This indicates when the structures are more complex, one should consider not only the dipole moment alignment, but more factors. Those factors include the geometry of the structures such as extra H-bonds from a non-linear structure, and so on.

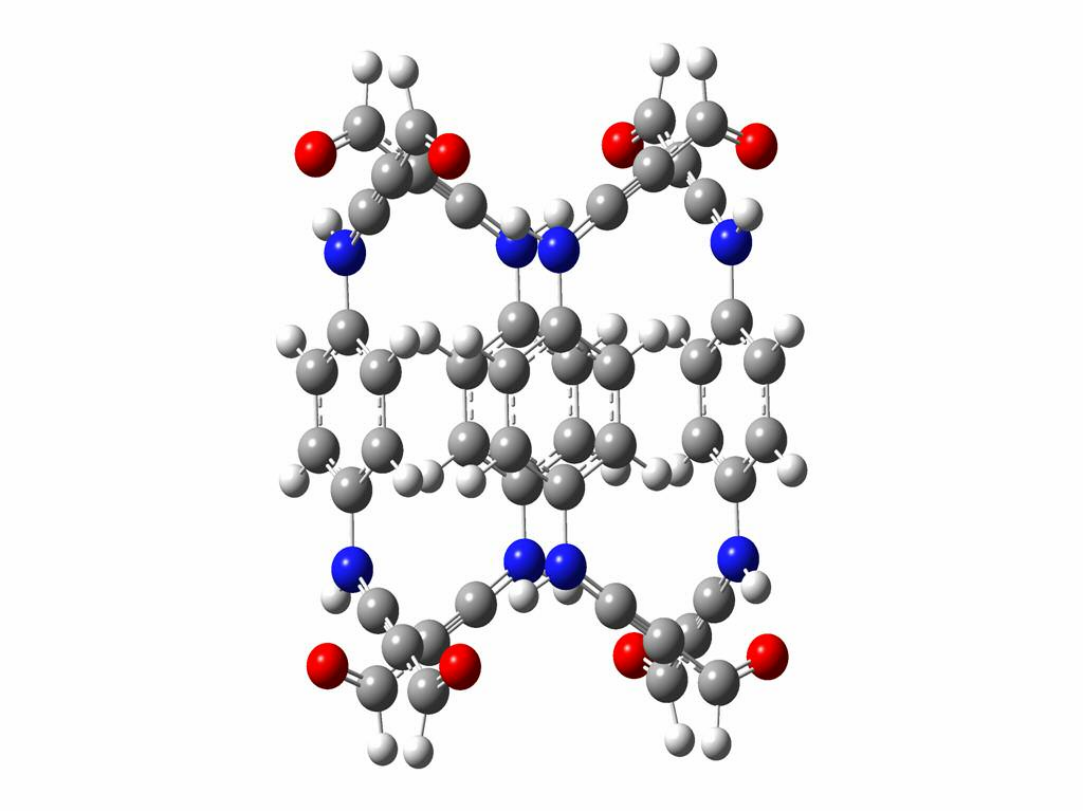

Figure 4-23. The cis A-C3-D-Bz-D-C3-A tetramer. The ΔE is -68.92 (8 H-bonds) and the dimeric ΔE is -11.09 kcal/mol. All of the N-H···O H-bond distance is 1.789 Å. Since the tetramer is symmetric (C_{4H}), the bond distances are paired.

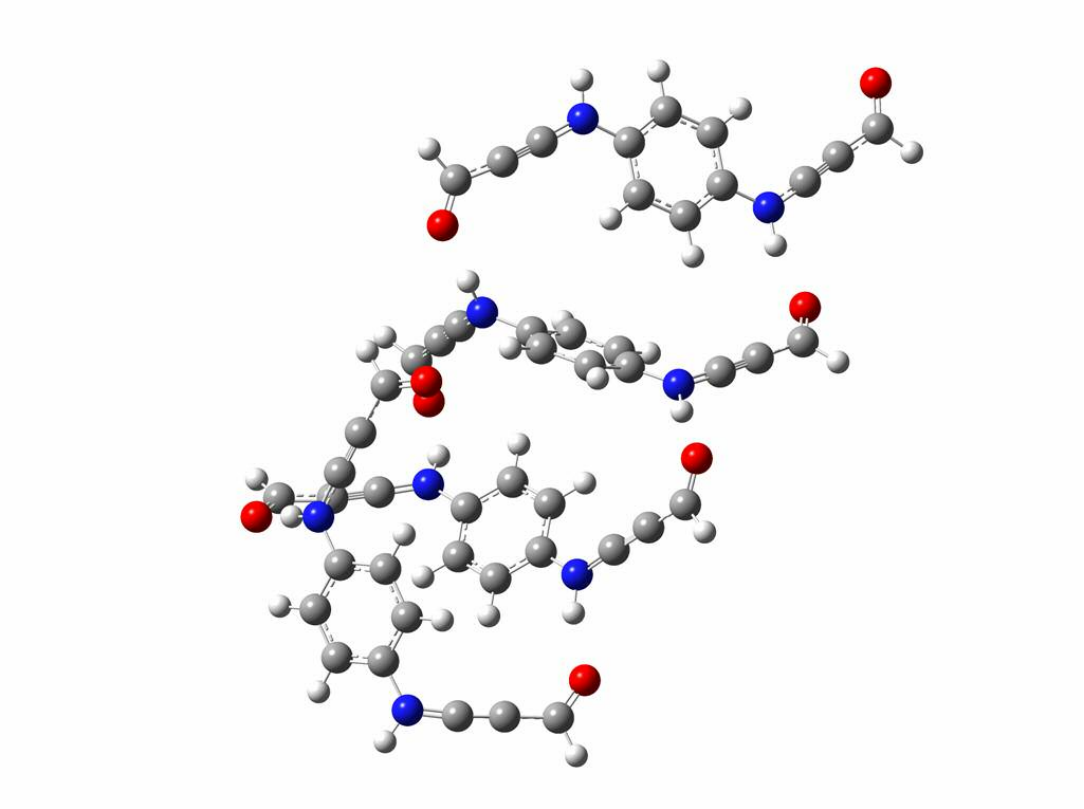

Figure 4-24. The trans A-C3-D-Bz-D-C3-A tetramer. The ΔE is -44.57 and the dimeric ΔE is -16.72 kcal/mol. The N-H···O bond distances (top to down and left to right) are 1.773, 1.831, 1.825, 1.731, 1.800 and 1.851 Å.

4.3.15 The D-C3-A-Bz-D-C3-A tetramers

The D-C3-A-Bz-D-C3-A tetramers are shown in Figures 4-25 and 26. The cis tetramer forms a semi-sphere structure and the trans tetramer can form an irregular structure. The interaction energy of the cis tetramer (-54.72 kcal/mol) is stronger than that of the trans tetramer (-40.53 kcal/mol) by -14.19 kcal/mol.The semi-sphere cis tetramer can form a circle when it reacts with another tetramer. In the trans tetramer, the benzene ring of the second monomer (from the top) and the third one are almost perpendicular to each other. The trans monomer at the end could also be transferred to the cis form, which develops the irregular structure.

The H-bond cooperativity in the cis tetramer is stronger than that in the trans tetramer in energy by -3.54 kcal/mol (cis: -5.79 and trans: -2.25 kcal/mol). The dipole moments in the cis tetramer are aligned in the opposite direction, which does not agree with the constructive accumulation of dipole moment elucidation. The stronger cooperativity is found in the tetramer with stronger H-bond interaction.

The H-bond interaction energies can be predicted by the dipole moments alignment in these tetramers, when no extra H-bonds and other effects are involved. In the cis tetramer, because the dipole moments are aligned in the opposite direction, leads to the stronger H-bond interaction. The tetramer has the dipole moments are aligned in the same direction, can be expected to have weaker H-bond interaction. The DFT calculated results show that the cis tetramer has stronger H-bond interaction than that of the trans one, which agrees with the assumption.

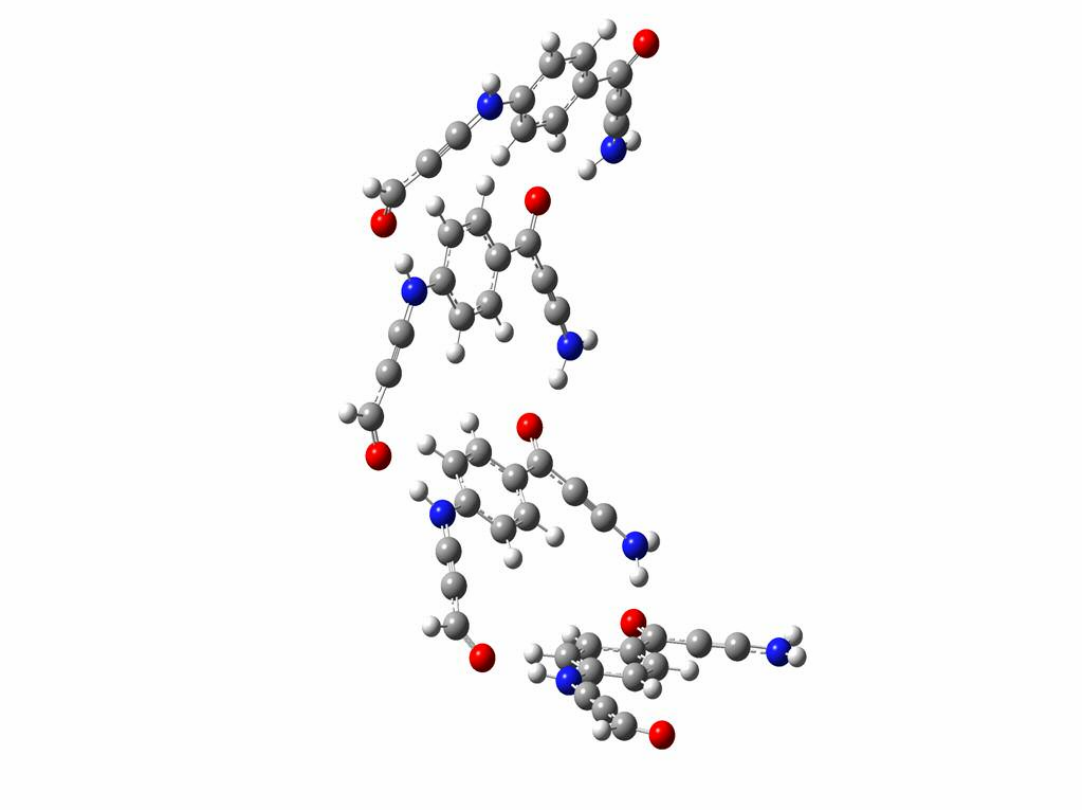

Figure 4-25. The cis D-C3-A-Bz-D-C3-A tetramer. The ΔE is -54.72 and the dimericΔE is -16.31 kcal/mol. The N-H···O bond distances (top to down and left to right) are 1.812, 1.823, 1.781, 1.781, 1.813 and 1.805 Å.

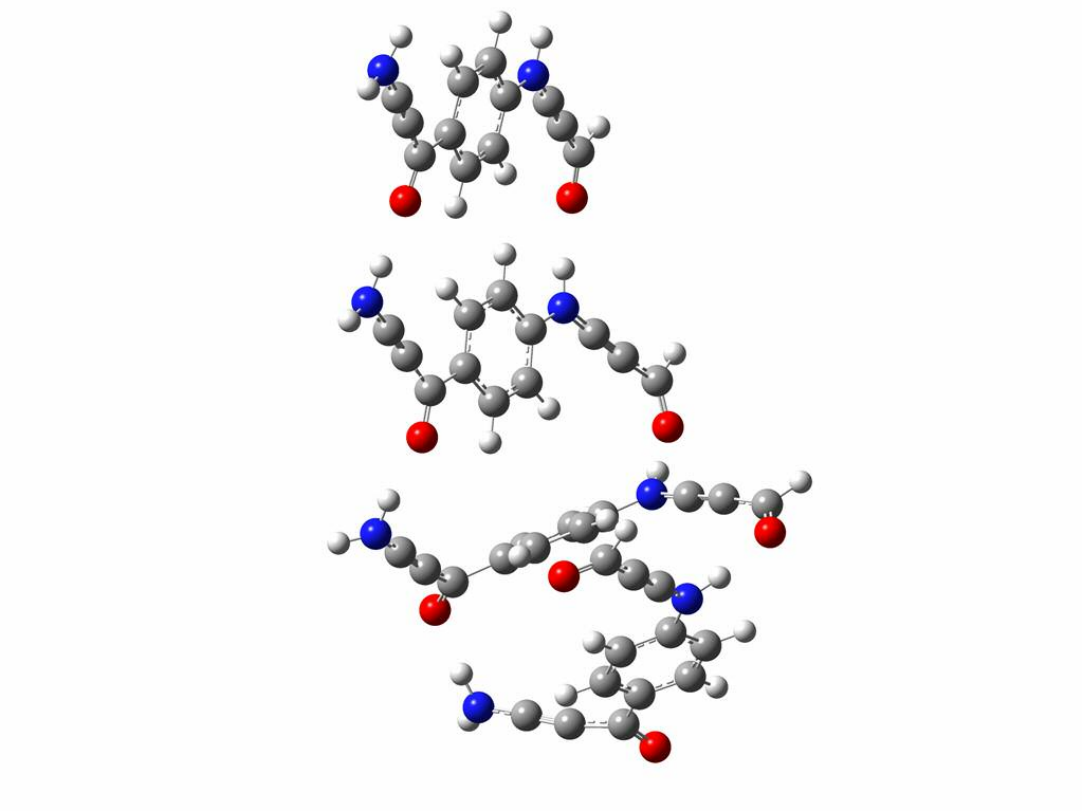

Figure 4-26. The trans D-C3-A-Bz-D-C3-A tetramer. The ΔE is -40.53 and the dimeric ΔE is -12.76 kcal/mol. The N-H···O bond distances (top to down and left to right) are 1.896, 1.883, 1.880, 1.796, 1.908 and 1.845 Å.

4.3.16 The D-C3-A-Bz-A-C3-D tetramers

The D-C3-A-Bz-A-C3-D tetramers are shown in Figures 4-27 and 28. Both of the cis and trans tetramers can form the regular structures. The cis tetramer is a helical structure, and the trans tetramer is close to planar structure. Several dihedral angles between two C=O groups are about -120°, except the bottom monomer, the dihedral angle is -167°. The center benzene ring and the shoulders (D-C3-A) form dihedral angles between -170 ~ -177°, which is very close to a planar structure. The interaction energy of the cis tetramer (-26.88 kcal/mol) is weaker than that of the trans tetramer (-50.74 kcal/mol) by -23.86 kcal/mol. Why the helical cis tetramer is not an energy-favored structure? Because the benzene rings in the tetramer tend be parallel to each other. Thus, the dihedral angle between the benzene ring and the shoulders is about -150°. In the cis dimer, the dihedral angle is close to -180°. In order to maintain the helical structure with a non-planar dihedral angle, it will cost some energy; therefore, the energy is then reduced. The trans tetramer with dipole moments in the opposite direction can be expected to provide stronger H-bond interaction. This result agrees with this prediction.

The H-bond cooperativity in the cis tetramer is stronger than that in the trans tetramer in energy by -14.68 kcal/mol (cis: +10.65 and trans: -4.03 kcal/mol). The dipole moment alignment fails to explain the H-bond interaction here because of the energy lost in geometric transformation. However, in this system the structure with stronger H-bond cooperativity shows stronger H-bond interaction.

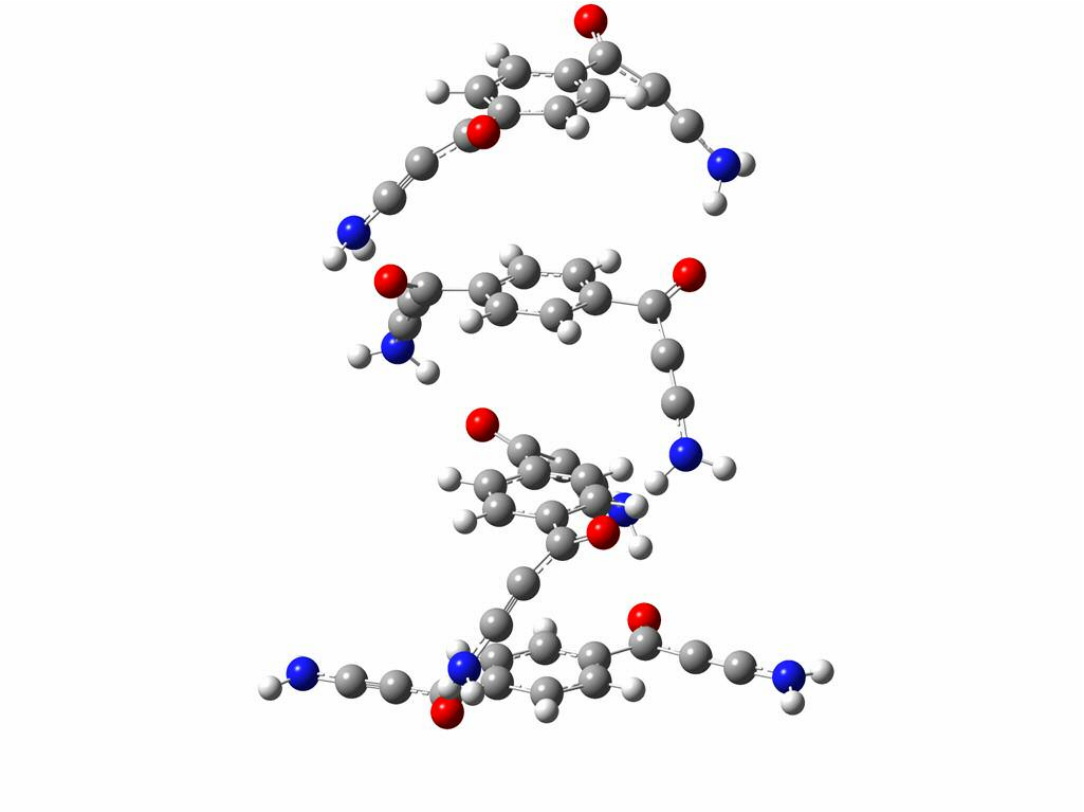

Figure 4-27. The cis D-C3-A-Bz-A-C3-D tetramer. The ΔE is -26.88 and the dimericΔE is -12.51 kcal/mol. The N-H···O bond distances (top to down and left to right) are 1.926, 1.905 and 1.961 Å. Since the tetramer is symmetric (C_2), the bond distances are paired.

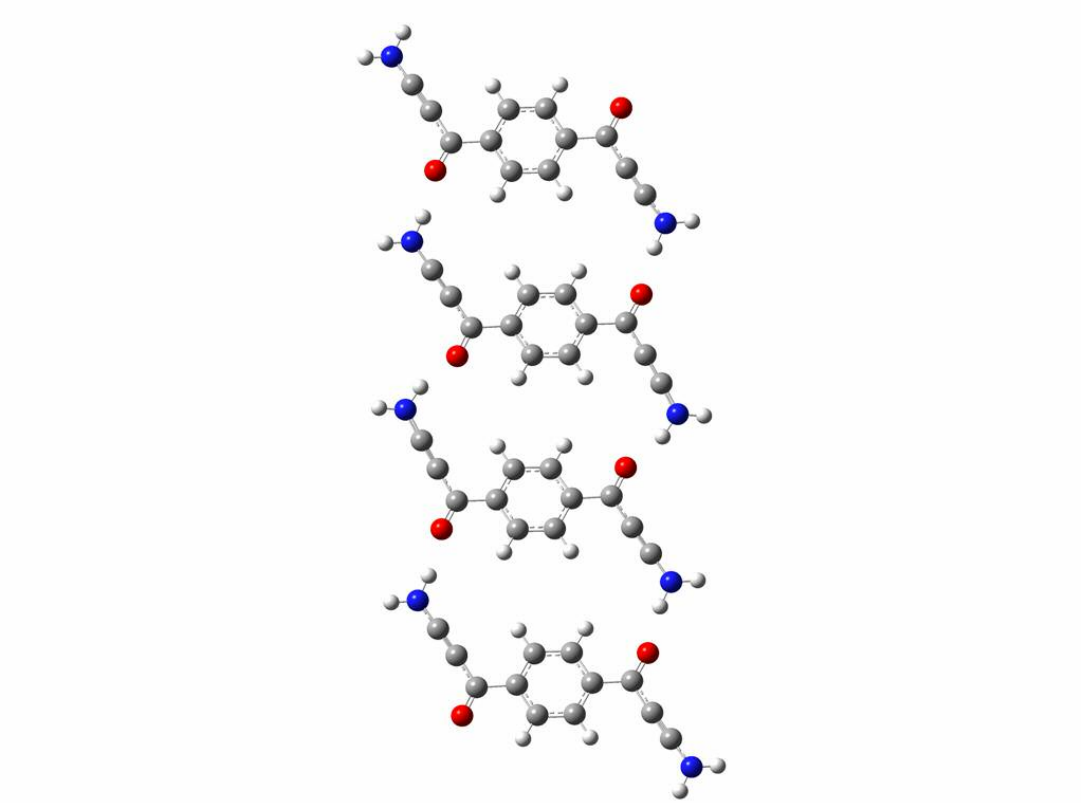

Figure 4-28. The trans D-C3-A-Bz-A-C3-D tetramer. The ΔE is -50.74 and the dimeric ΔE is -15.57 kcal/mol. The N-H···O bond distances (top to down and left to right) are 1.830, 1.834 and 1.808 Å. Since the tetramer is symmetric (C_I), the bond distances are paired.

The trans D-C3-A-Bz-A-C3-D monomer is more stable than the D-C3-A-Bz-D-C3-A and A-C3-D-Bz-D-C3-A monomers by -7.92 and -18.01 kcal/mol, correspondingly.

The cis D-C3-A-Bz-A-C3-D tetramer has the weakest interaction energy among all tetramers. The cis A-C3-D-Bz-D-C3-A tetramer is the strongest H-bonded tetramer, with the cuboids-like structure. This cis tetramer has eight H-bonds that contribute the strongest H-bond interaction than other tetramers.

Most cis tetramers have stronger H-bond interactions than the trans ones. The only exception is the cis D-C3-A-Bz-A-C3-D tetramer, which has the energy lost due to the transformation. The H-bond strength in the cis and trans forms by looking at the directions of dipole moment alignment. The opposite direction alignment ones beat the same direction ones.

In these tetramers, the geometries again play more important roles than the dipole moments alignment in terms of interaction energy prediction.

4.3.17 Summary

Three categories were discussed, the AD-DA, DA-DA, and DA-AD sequence groups. The interaction energies and cooperativities of all the tetramers are tabulated in Table 4-4. Non-linear relationship in interaction energy is obtained in the diglycine with spacers, extended diglycine with spacers, and the extended diglycine with benzene spacer tetramers. It also shows non-linear relationship in the H-bond cooperativity in various types of extended structures. The tetramers in the DA-DA sequence group show a small variation range of interaction energy (less than 5 kcal/mol), which indicates that various spacers do not influence the H-bond interaction in that sequence. Interaction energies in the same donor and acceptor sequence can be increased or decreased by more than 20 kcal/mol in the tetramers when the different spacers are inserted.

The A-C3-D-Bz-D-C3-A tetramer possesses the strongest H-bond interaction. However, it is due to eight H-bonds. The tetramers with six H-bonds, the A-C3-D-C3-D-C3-A tetramer has the strongest H-bond interaction. The D-C3-A-Bz-A-C3-D has the weakest H-bond interaction.

Table 4-4. The interaction energies and cooperativities of various donor-acceptor sequences.

Tetrameric Structures	ΔE (kcal/mol)	Cooperativity ΔE
AD-DA		
A-D-C3-D-A (Cis)	-36.32	-13.97
A-C3-D-C3-D-C3-A (Cis)	-47.87	-6.71
A-C3-D-Bz-D-C3-A (Cis)	-68.92	N/A (8-HB)
A-D-C3-D-A (Trans)	-54.98	-5.81
A-C3-D-C3-D-C3-A (Trans)	-64.92	-7.62
A-C3-D-Bz-D-C3-A (Trans)	-44.57	5.59
DA-DA		
D-A-C3-D-A (Cis)	-58.85	-4.07
D-C3-A-C3-D-C3-A (Cis)	-55.95	-3.51
D-C3-A-Bz-D-C3-A (Cis)	-54.72	-5.79
D-A-C3-D-A (Trans)	-42.33	-9.21
D-C3-A-C3-D-C3-A (Trans)	-46.29	-11.22
D-C3-A-Bz-D-C3-A (Trans)	-40.53	-2.25
DA-AD		
D-A-C3-A-D (Cis)	-35.11	-7.60
D-C3-A-C3-A-C3-D (Cis)	-43.41	-6.51
D-C3-A-Bz-A-C3-D (Cis)	-26.88	10.65
D-A-C3-A-D (Trans)	-41.45	-1.71
D-C3-A-C3-A-C3-D (Trans)	-57.17	-5.15
D-C3-A-Bz-A-C3-D (Trans)	-50.74	-4.03

4.4 Conclusions

There are several approaches to manipulate H-bond interactions. The study of the variation of H-bond cooperativity under various H-bond donor and acceptor sequences and spacers in glycine and diglycine can provide information to design smarter nanotube materials. By inserting the easily polarizable acetylene in the center between H-bond donor and acceptor, a cyclic dimer with two N-H···O H-bonds, can provide interaction enthalpy up to -21.98 kcal/mol. The possible geometry and the possibility of various combinations, for example large ring and small ring structure, must be considered in order to obtain the most stable structure. In most regular structures (planar, helical, or cubic ones), the H-bond strength can be predicted by checking the dipole moments alignment in the structure. If the dipole moments are aligned in the same direction, the H-bond interaction will be weaker than those aligned in the opposite direction.

The DA-DA sequence group can form planar or semi-sphere structures and the DA-AD and AD-DA sequence groups can form helical or caged-like structures. The strongest tetramer in diglycine with one spacer, diglycine with three spacers, and diglycine with three spacer and benzene as center molecule are the cis D-A-C3-D-A, the cis D-C3-A-C3-D-C3-A and the cis A-C3-D-Bz-D-C3-A tetramers, respectively.

The H-bond cooperativity is stronger when the dipole moments are aligned in the same direction. The stronger H-bond interaction might not always be the one with stronger H-bond cooperativity. The geometry of the structure is the key role in the determination of H-bond strength and cooperativity, especially when the structure is inserted with a larger spacer. In the DA-DA sequence group, different spacers will not influence the H-bond cooperativity and the interaction significantly.

CHAPTER 5 —A DFT MOLECULAR ORBITAL STUDY OF COOPERATIVE 4-PYRIDONE H-BONDS WITH EXTRAORDINARY STABILITY

5.1 Introduction

This chapter is based on the paper we published at *Journal of the American Chemical Society*.[45] Amidic (N-H···O=C) hydrogen bonds play an important role in both biochemical and synthetic self-assembling systems. Simple amide H-bonds contribute to the determination of the relative stabilities of peptide secondary structures. For example, the unusually significant (up to 200%) cooperative interactions of chains of amidic H-bonds[52] contribute enormously to the stability of α-helices.[137] The more complex patterns of H-bonds in the nucleic acid base pairs generally occur as pairs or triads of cyclic H-bonds; however, amidic (N-H···O=C) subunits are always present in the cyclic systems. The self-assembly of nylons follows the pattern of peptides, while that of cyanuric acid/melamine[157] or those formed from structures containing 2-pyridone[158] units resemble that of the nucleic acid bases.

The ΔH_{inter} of the cyclic 2-pyridone dimer[159] exceeds that of formamide by about 50% (-18 vs. -12 kcal/mol), while that of a large ring diglycine dimer exceeds that of the isomeric small ring (see Figure 5-1) by about 9 kcal/mol.[160] Why do the stabilizations associated with amidic H-bonds differ so much? I have suggested that the enhanced stability of the large ring structure of Figure 5-1 is due to the coupling of the C=O and N-

H involved in the H-bonds through a C_5 *intra*strand H-bonding interaction that affects the H-bonding groups at the termini of the strands. One could imagine 2-pyridone as a formamide whose N-H and C=O are coupled via a -C=C-C=C- π-system in addition to the direct bond between them. As such π-systems can easily be polarized; one might reasonably expect the increased polarizability to enhance the H-bonding interactions.

I present density functional molecular orbital calculations of chains of 4-pyridone. These chains illustrate how coupling of the N-H and C=O of an amide through the easily polarizable π-system (-C=C-) together with cooperative H-bonding typical of amides, can combine to produce extraordinarily strong H-bonds between neutral molecules, with stabilization enthalpies as large as 23 kcal/mol. Besides the chains of 4-pyridone, the chains of 4-hydroxypyridine and 1,3-cyclohexanedione and some unique structures will also be discussed in this chapter.

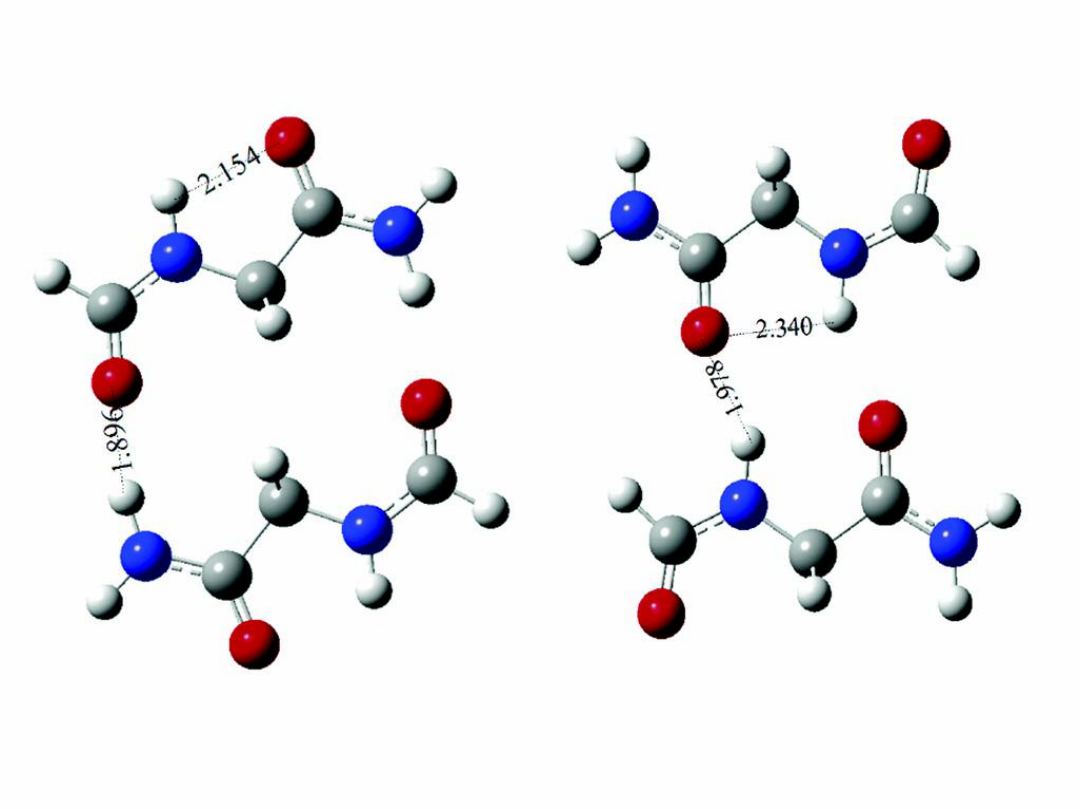

Figure 5-1. Large (left) and small (right) ring H-bonding dimers of a model diglycine. The enthalpies of interaction are -12.99 and -4.85 kcal/mol, respectively.

5.2 Calculation details

The DFT computational details are described in Chapter 1 and in section 2.2. Calculations of planar chains containing up to five monomers of 4-pyridone were completely optimized on the counterpoise (CP)-corrected energy surface[82] as were the vibrational frequencies needed to obtain the enthalpies at 298 K using the GAUSSIAN 03 suite of programs.[102] In the study of H-bonding in formamides by Kobko and Dannenberg,[52] they found both the CP and vibrational corrections to be relatively constant upon addition of another monomer to the chain. We simply used these constants to correct the energies for chains containing more than five monomers. The geometric parameters plotted in the figures come from the normal (not CP-corrected) optimizations.

5.3 Results and discussion

5.3.1 Chains of 4-pyridone

In the structure of 4-pyridone, the direct link between the NH and C=O of formamide is removed and replaced by two parallel -C=C- ethylenic π-systems. The molecule has C_{2v} symmetry, as do all planar H-bond chains formed from this monomeric unit. Unlike its isomer, 2-pyridone, which is virtually isoenergetic with its tautomer, 2-hydroxypyridine, we calculated 4-pyridone to be 2.37 kcal/mol less stable than 4-hydroxypyridine. Nevertheless, the crystallographic evidences show that the 4-pyridone molecules do exist in salt and hydrate.[44,161] The energetic analysis of more complicated polycyclic aromatic hydrocarbons (PAHs) with a set of NH and C=O separated by ethylenic π-system was calculated to investigate the practicability of designing stronger amidic H-bonds by including more ethylenic π-systems in a monomer. The PAHs studied are naphthalene (2-rings), phenanthrene (3-rings), anthracene (3-rings), and pyrene (4-rings), and I noticed the enol tautomer of each PAH is more stable than the keto one as the size of the ring is increased. The energetic variations between keto-enol automats of naphthalene, phenanthrene, anthracene, and pyrene are -12.02, -17.46, -22.13 and -23.18 kcal/mol in enthalpy, respectively. The significant more energetic stable enol tautomer suggests the idea of applying larger aromatic rings in the monomer to increase increasing amidic H-bond (N-H···O=C) is not feasible, since the keto form monomer is energetic unstable by double-digit.

The ΔH_{inter} values for each H-bond in chains of 4-pyridones (illustrated in Figure 5-2) containing from 2 to 10 monomeric units are compared with those previously reported[1] for chains of formamides and shown in Figure 5-3, while the H-bond distances for each H-bond are shown in Figure 5-4. We obtain each of the H-bonding enthalpies for a chain of N monomers from the simple expression $\Delta H_{inter} = \Delta H_N - \Delta H_M - \Delta H_{N-M} - C_1 - C_2$, where M and $N - M$ are the number of monomers in each fragment after rupture of the H-bond, and C_1 and C_2 are the constants used to correct each H-bond for CP and vibrations.

The enthalpy of interaction for the H-bonded dimer of 4-pyridone is -9.90 kcal/mol, which is more than twice that of the analogous formamide dimer and more than half the H-bond enthalpy that we calculate for the 2-pyridone cyclic dimer (which has two, presumably cooperative, H-bonds) using the same methods. Inspection of Figure 5-3 and Table 5-1 shows that the strongest H-bond (that nearest to the center of the decamer) has an enthalpy of interaction of -22.2 kcal/mol. Since the H-bonding enthalpies have clearly not yet reached their asymptotic limit, we expect even stronger H-bonds near the middle of longer chains of approximately 23 kcal/mol. This interaction for only one amidic H-bond between neutral species is greater than that for the entire interaction in the cyclic 2-pyridone dimer (which has two amidic H-bonds). Furthermore, the extent of the cooperativity in the chains of 4-pyridones is significantly greater in magnitude than that for formamide chains (~13.3 vs. ~8.5 kcal/mol), although it is somewhat less in terms of percent of the dimeric interaction.

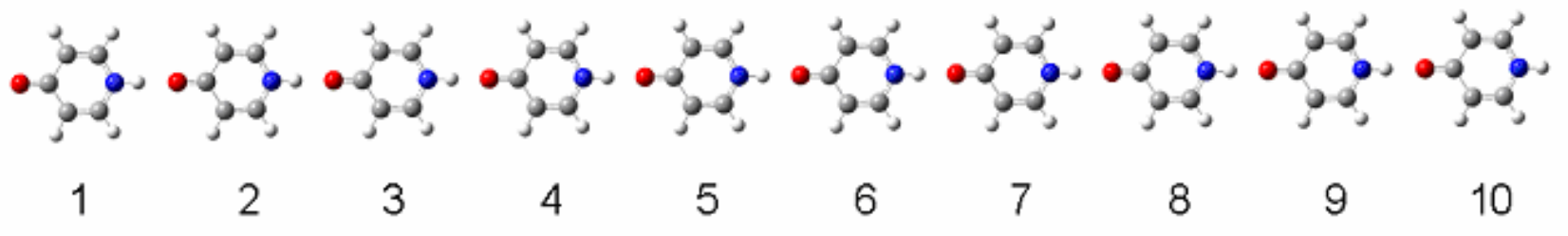

Figure 5-2. H-bonding chain of 4-pyridones.

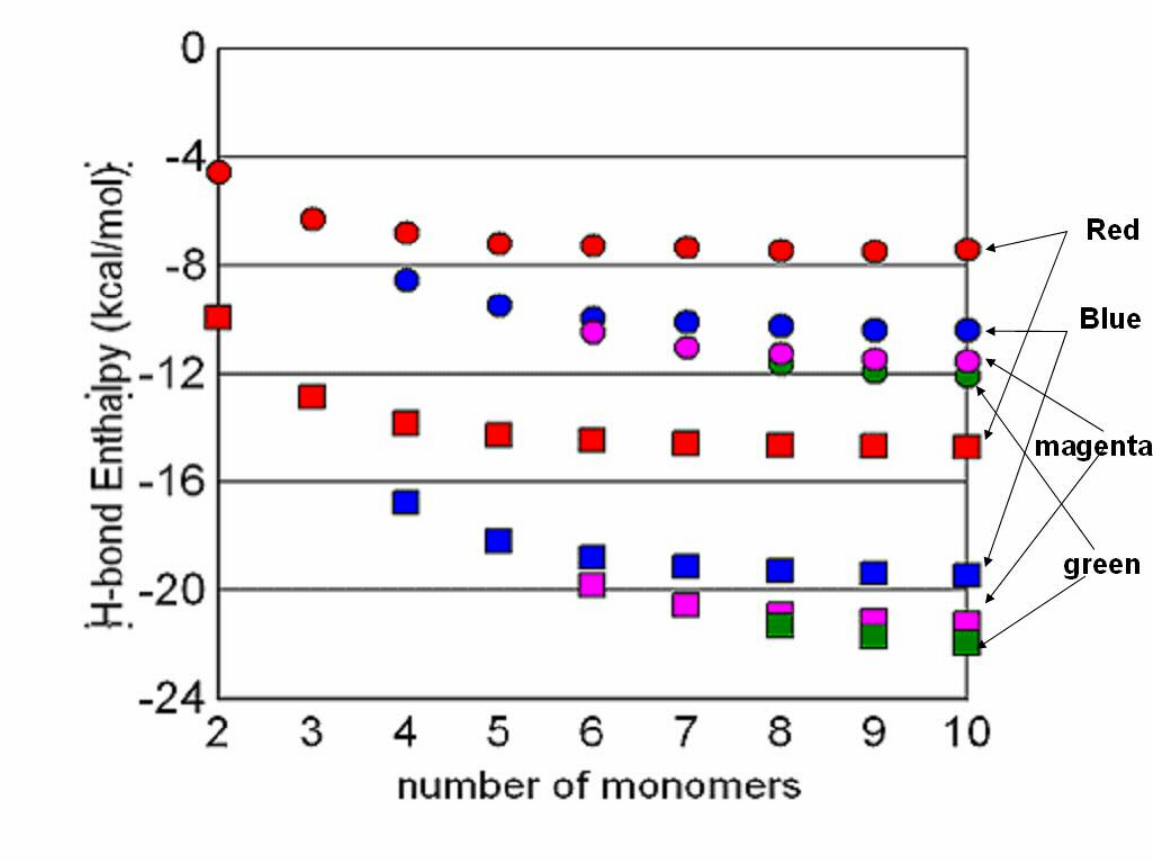

Figure 5-3. H-bond interaction energies by H-bond type. Circles denote formamide and squares 4-pyridone chains. Red symbols denote type 1 (terminal), blue denote type 2 (second from end), magenta type 3 (third from end), and green type 4 (fourth from end) H-bonds.

Table 5-1. H-bond enthalpies (kcal/mol) as a function of the number of monomers in the 4-pyridone chains and the H-bond type. H-bond type 1 is the terminal H-bond, type 2 is adjacent to the terminal, type 3 is third from terminal, etc.

monomer	**1**	**2**	**3**	**4**	**5**
2	-9.90				
3	-12.83				
4	-13.83	-16.75			
5	-14.25	-18.17			
6	-14.45	-18.79	-19.79		
7	-14.55	-19.10	-20.52		
8	-14.62	-19.27	-20.89	-21.31	
9	-14.66	-19.37	-21.10	-21.72	
10	-14.68	-19.44	-21.23	-21.96	-22.16

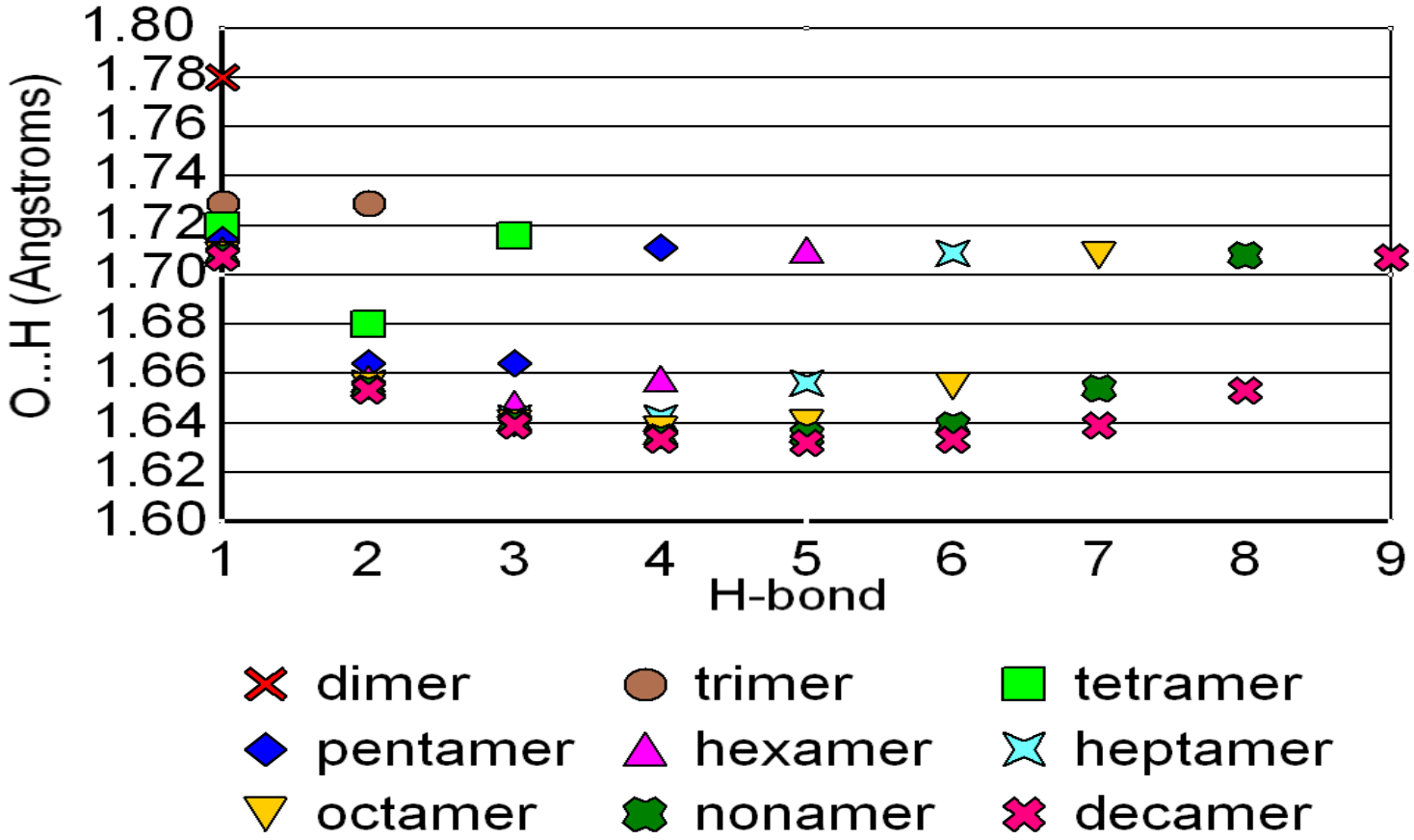

Figure 5-4. H-bond lengths (on surface uncorrected for CP) as a function of H-bond in 4-pyridone H-bonding chains.

Putting these results in perspective, we see that the (deceptively) simple N-H···O=C H-bond can have interaction energies in neutral systems that vary from about -2 kcal/mol (one H-bond, or half the total interaction in the small ring dimer of a diglycine model[160]) to about -23 kcal/mol. Perhaps examples of even stronger N-H···O=C interactions can be found using more efficient coupling than that described here. Clearly controlling the extent of intramolecular coupling between the N-H and C=O of H-bonded molecules can become a key tool for modulating the energies of H-bonds for improved control of self-assembled systems. In retrospect, nature seems to have used similar tools to design different kinds of self-assembled biomaterials, such as proteins.

The large cooperative interactions between the 4-pyridones might be due to some combination of polarization, mutual polarization, and covalent interactions (charge transfer). As in the previously reported formamide chains, the cooperativity far exceeds that predicted by electrostatic interactions (which should be largely due to the sum over all dipole-dipole interactions). Figure 5-5 illustrates the change in dipole moments upon addition of a 4-pyridone molecule to the growing chain. This value should be constant for electrostatic interactions between the monomers. Instead, the asymptotic value exceeds 12 D, more than 70% more than the dipole moment of monomeric 4-pyridone. Gilli has discussed the importance of resonance-assisted H-bonds (RAHBs), which have proved to be important to the stability of many crystal structures, including enaminones,[162] related to 4-pyridone. We studied the interaction enthalpies of 1, 3-cyclohexanedione (CHD) chains as an example of RAHB (see Figure 5-6). The CHD interaction enthalpies are expected to be stronger than the 4-pyridone due to the usually stronger O-H···O H-bond is

presented in the CHD chains. However, what we have observed is not the case (see Table 5-2).

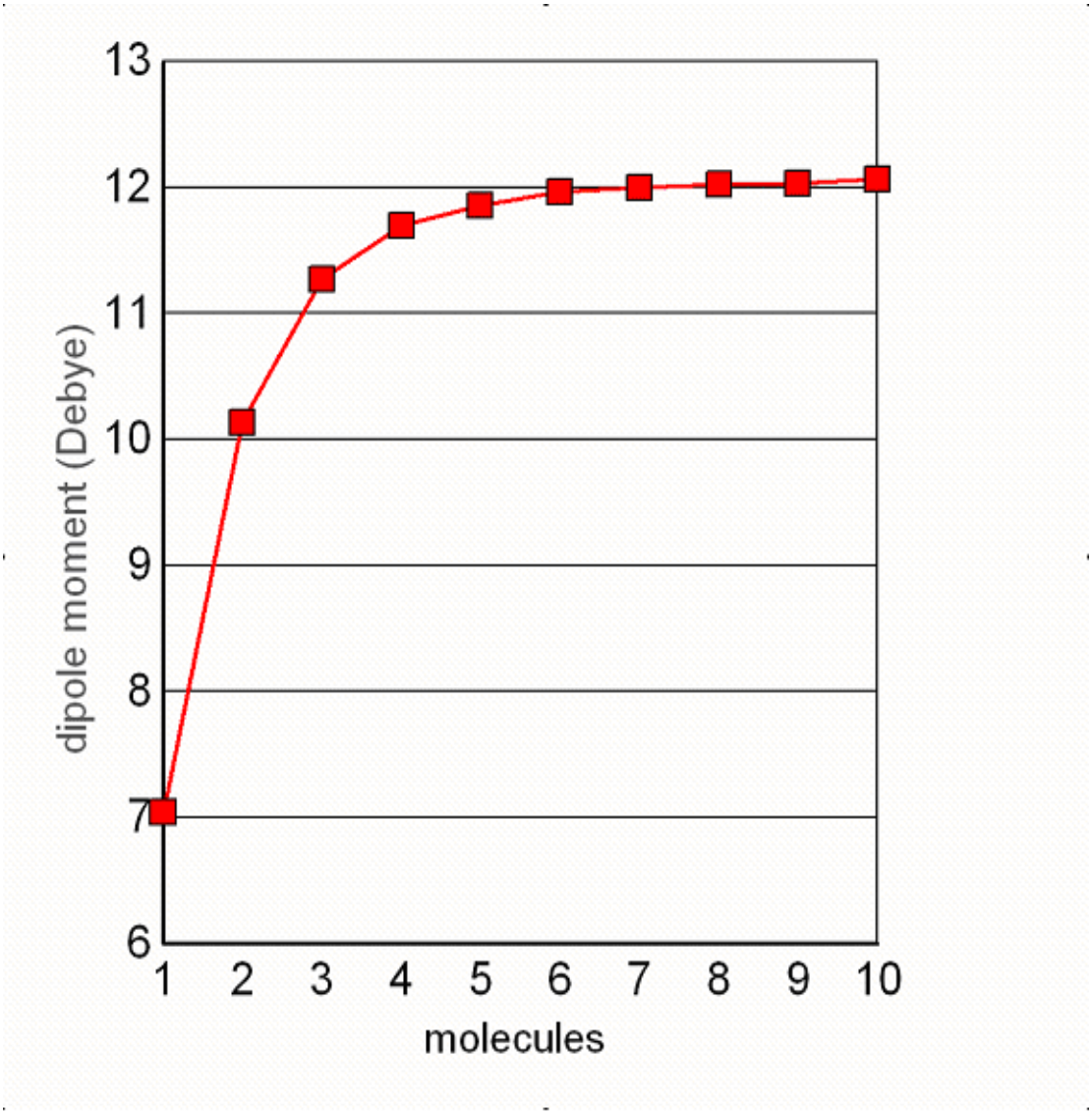

Figure 5-5. Change in dipole moments upon addition of a 4-pyridone molecule to the H-bonding chain.

The H-bonds in the 4-pyridone decamer between either monomer 1~2 (CHD ΔH = -9.75 and 4-pyridone ΔH = -9.90 kcal/mol) or monomer 5~6 (CHD ΔH = -21.29 and 4-pyridone ΔH = -22.16 k cal/mol) are both slightly stronger than those in the CHD chains. This indicates the N-H···O H-bond in 4-pyridone system is even stronger than the RAHB. To evaluate the importance of covalent interactions (which we expected to be primarily between the π-orbitals) between the 4-pyridone units, we rotated the planes of adjacent molecules so that they became perpendicular to each other (thus eliminating π-overlap between them) both in the dimer and about the central H-bond of the decamer. Neither the change in the H-bond energy of the dimer (0.23 kcal/mol) nor the change in the central H-bond in the decamer (0.66 kcal/mol) is appreciable upon destroying the overlap in this manner. We must conclude that whatever covalent stabilization might exist between the monomers cannot be primarily within the π-system.

Figure 5-6. H-bonding chain of 1, 3-cyclohexanediones**.**

Table 5-2. H-bond enthalpies (kcal/mol) as a function of the number of monomers in the 1, 3-cyclohexanedione chains and the H-bond type. H-bond type 1 is the terminal H-bond, type 2 is adjacent to the terminal, type 3 is third from terminal, etc.

monomer	**1**	**2**	**3**	**4**	**5**
2	-9.75				
3	-12.11				
4	-13.13	-15.54			
5	-13.55	-16.98			
6	-13.78	-17.62	-18.64		
7	-13.90	-17.98	-19.41		
8	-13.97	-18.18	-19.84	-20.26	
9	-13.97	-18.24	-20.03	-20.68	
10	-14.06	-18.33	-20.19	-20.96	-21.19

5.3.2 Chains of 4-hydroxypyridone

The H-bond strength of the tautomer of 4-pyridone, 4-hydroxypyridine (4-HyP), is of the interest, since 4-HyP is only more stable than 4-pyridone by 2.37 kcal/mol. The ΔH_{inter} values for each H-bond in chains of 4-HyP (illustrated in Figure 5-7) contain 2 to 10 monomeric units. The H-bond interaction energies by H-bond type of 4-hydroxypyridine is shown in Figure 5-8. The H-bond distances for each H-bond are shown in Figure 5-9. The 4-HyP chains are connected through O-H···N H-bonds, due to the geometric nature of 4-HyP, the chains are not linear as the previous discussed chains of 4-pyridone and CHD. These non-linear chains provide more opportunities to form 2-D, 3-D or even cyclic structures. More about the cyclic structures will be discussed in section 5.3.3.

The interaction enthalpy of H-bond in 4-HyP dimer is -8.72 kcal/mol, which is weaker than that of 4-pyridone (-9.90 kcal/mol) and of CHD dimer (-9.75 kcal/mol). However, it is close to twice that of the formamide dimer. The strongest H-bond, which is nearest to the center of the decamer, has the interaction enthalpy of -17.15 kcal/mol. The energetic and geometric information of chains of 4-HyP is shown in Figure 5-8 and Table 5-3. This H-bond is only about 5 kcal/mol weaker than that of 4-pyridone. The strong H-bonds between the terminal and the center of the decamer again demonstrate the potentials to construct crystals and nanostructures by 4-HyP monomers. The extent of the H-bond cooperativity in these non-linear chains of 4-HyP is also very strong, which indicates the factors to cause these unexpected H-bonds only exist inside the monomer, not with the surrounding neighbors.

Figure 5-10 illustrates the change in dipole moments upon the addition of 4-pyridone, CHD and 4-HyP molecule. The dipole moment changes of 4-pyridone and CHD show similar trends. Both increments are greater than the dipole moment of each monomer (12 D of 4-pyridone and 5.97 D of CHD). However, the patterns of dipole moment changes in CHD and 4-HyP are very similar. The increments are greater when even numbers of CHD and 4-HyP chains are formed. The increments are smaller when odd numbers of CHD and 4-HyP chains are formed. The alternative increment of dipole moment is due to the non-linear CHD and 4-HyP chains. However, from Figure 5-6 and 5-7, one can easily tell the CHD chains are more linear than those of 4-Hyp. This explains why the incremental trend of CHD dipole moment is similar to that of 4-pyridone. When another monomer is added, the accumulated dipole moment is not aligned toward similar direction, before the addition. Nevertheless, when a dimer is added, the accumulated dipole moment has more potential to be aligned toward similar direction, before the addition.

As discussed in section 5.3.1., the interactions between monomers are not electrostatic interaction in 4-pyridone. The situations are also true in the chains of CHD and 4-HyP, because no additive dipole moment changes are observed there. Factors other than electrostatic contribute to this extraordinary H-bond phenomenon.

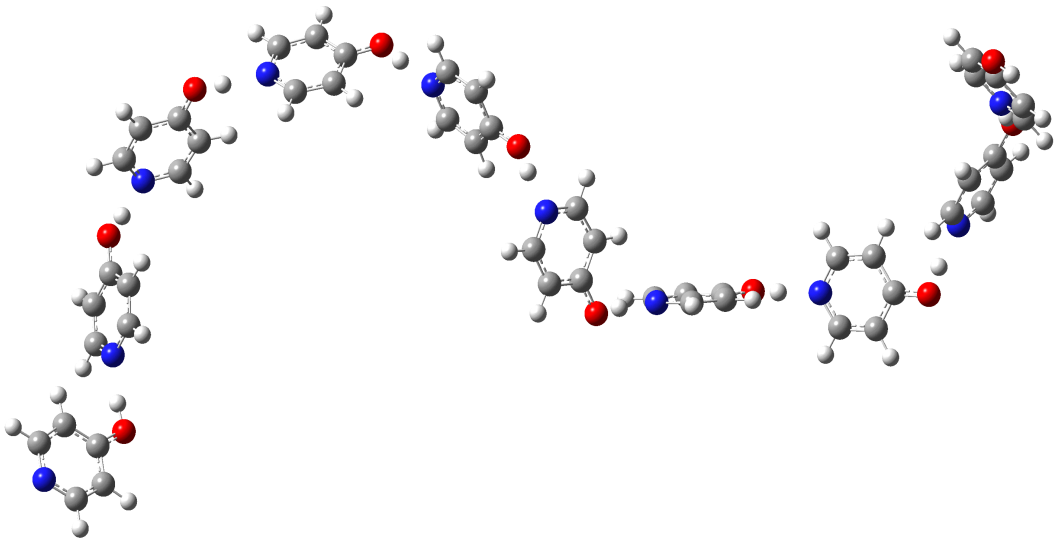

Figure 5-7. H-bonding chain of 4-hydroxypyridine.

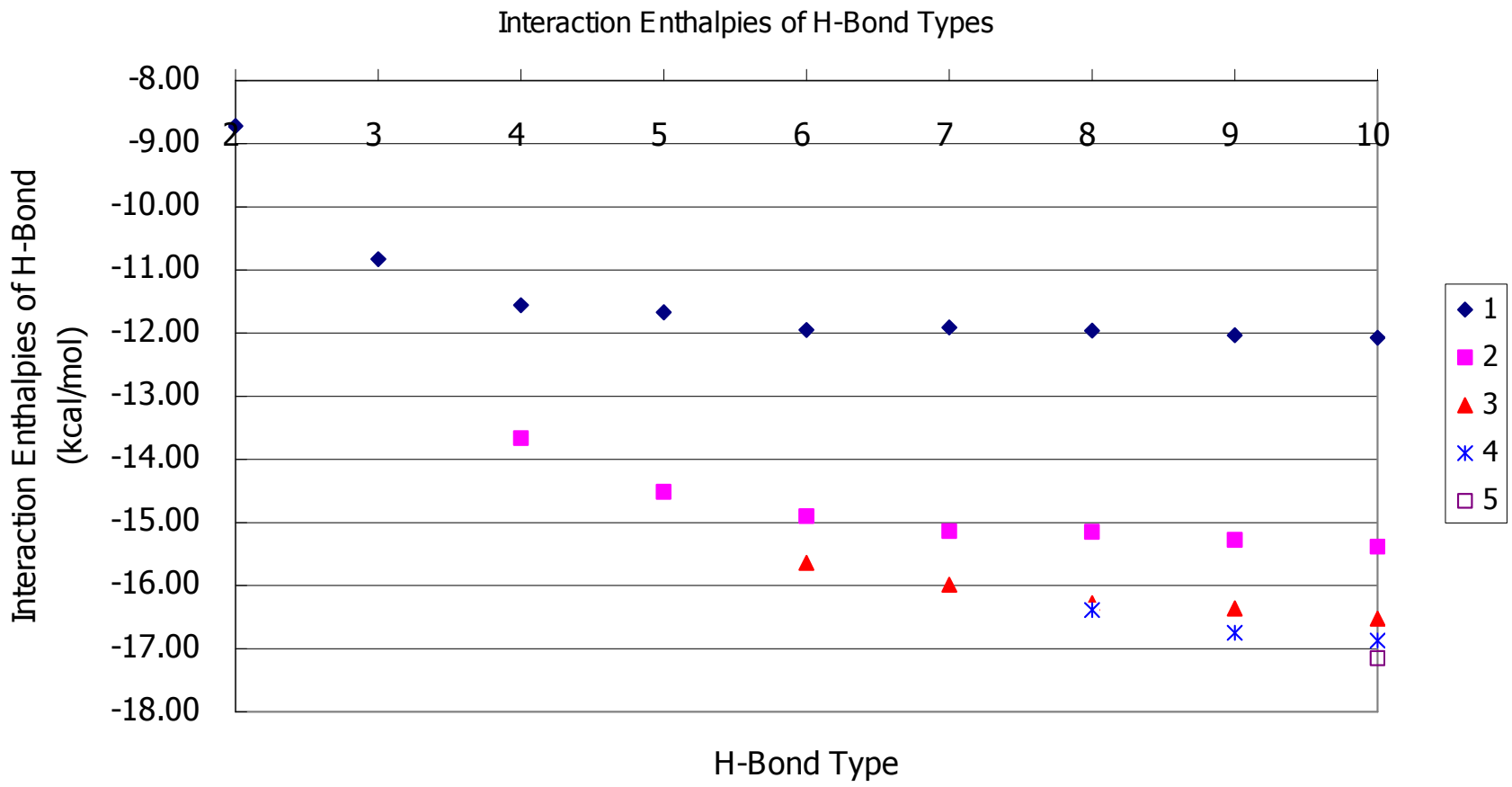

Figure 5-8. H-bond interaction energies by H-bond type of 4-hydroxypyridine.

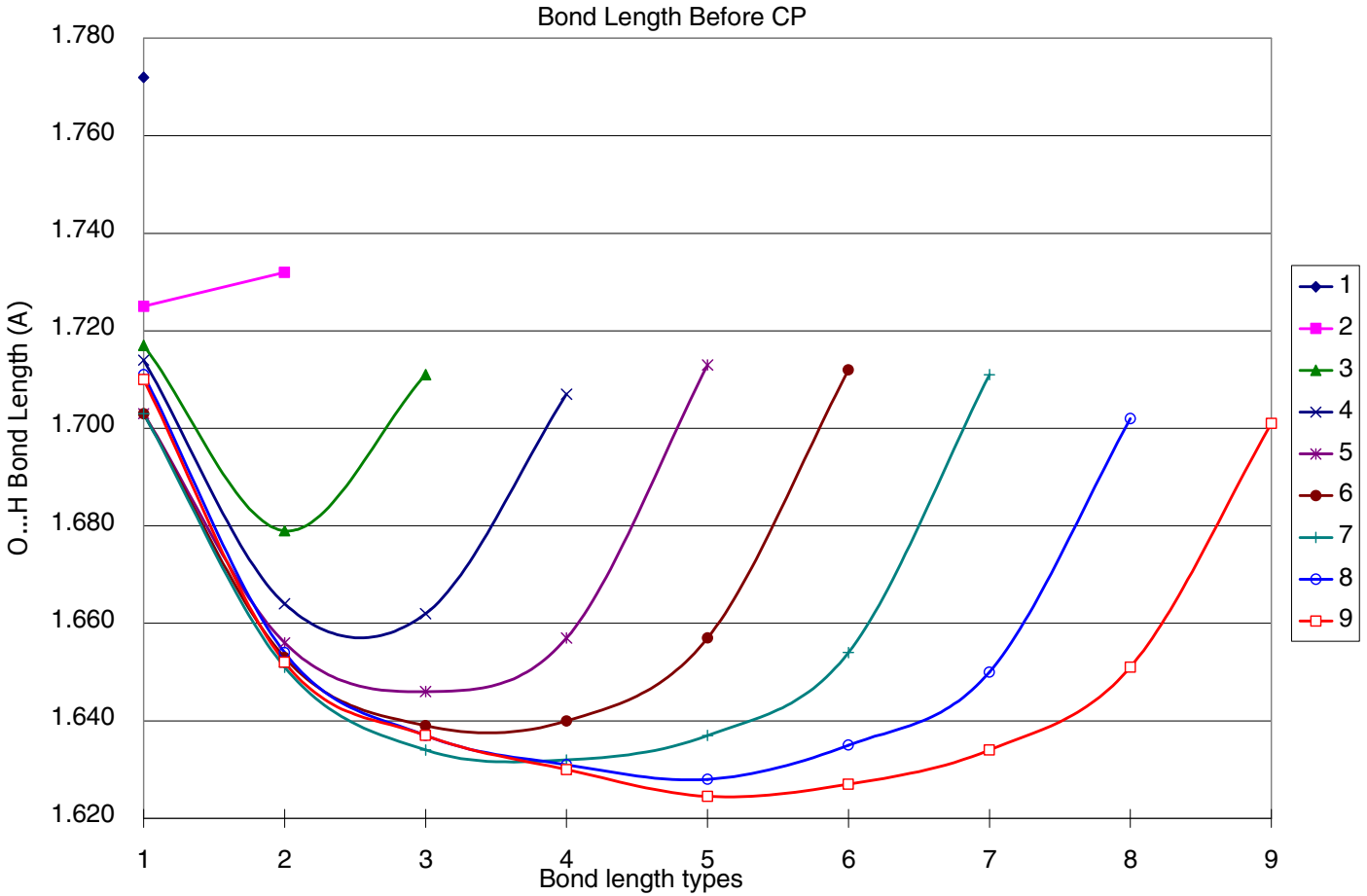

Figure 5-9. H-bond lengths (on surface uncorrected for CP) as a function of H-bond in 4-hydroxypyridine H-bonding chains.

Table 5-3. H-bond enthalpies (kcal/mol) as a function of the number of monomers in the 4-hydroxypyridine chains and the H-bond type. H-bond type 1 is the terminal H-bond, type 2 is adjacent to the terminal, type 3 is third from terminal, etc.

monomer	**1**	**2**	**3**	**4**	**5**
2	-8.72				
3	-10.83				
4	-11.56	-13.66			
5	-11.67	-14.51			
6	-11.95	-14.90	-15.64		
7	-11.91	-15.14	-15.99		
8	-11.96	-15.15	-16.28	-16.39	
9	-12.03	-15.28	-16.36	-16.75	
10	-12.07	-15.38	-16.52	-16.87	-17.15

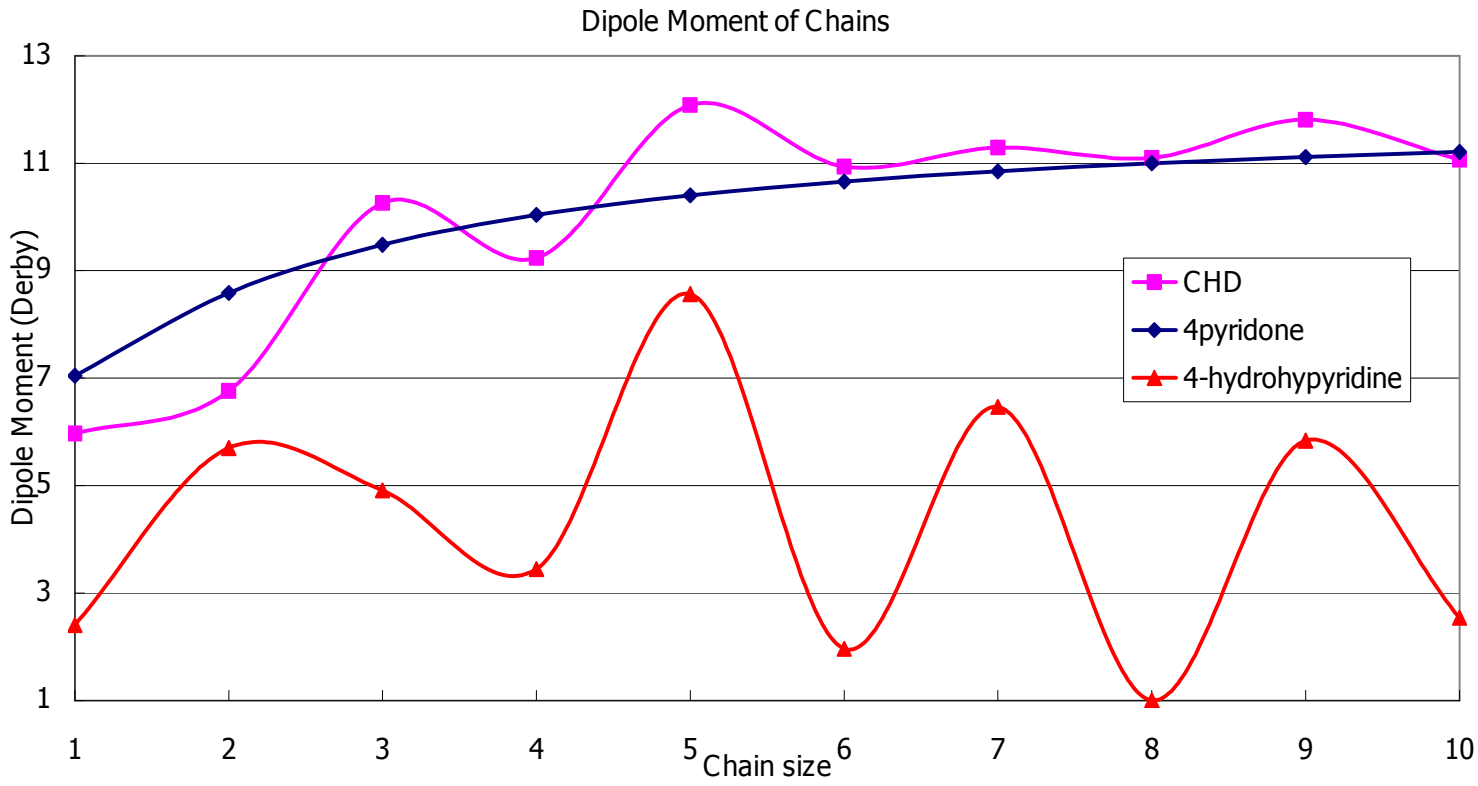

Figure 5-10. Change in dipole moments upon addition of 4-pyridone, CHD and 4-hydroxypyridine molecules to the H-bonding chain.

5.3.3 Cyclic octamers of 4-pyridone and 4-hydroxypyridone

Two cyclic structures will be discussed in this section, the cyclic 4-pyridone and 4-hydroxypyridine octamers are shown in Figure 5-11 and 5-12. These structures can form S_8 symmetry. While comparing with the corresponding linear octamers, both cyclic octamers are significantly stronger than the linear ones by about -20 kcal/mol. This is because the cyclic octamers can form one extra H-bond than the linear octamers. Therefore, the extra stabilization enthalpy is not only from the cyclic structure but also from the extra H-bond.

The cyclic 4-pyridone octamer (-111.60 kcal/mol) is more stable than the 4-hydroxypyridine (-95.16 kcal/mol) one by 16.50 kcal/mol in enthalpy. When symmetric structure is considered, all the H-bonds in the cyclic structure are equivalent. The interaction enthalpy of each H-bond should be the average of the overall interaction enthalpy. Therefore, the interaction enthalpies of each N-H···O and O-H···N H-bond are -13.96 and -11.90 kcal/mol, respectively. The 2.06 kcal/mol enthalpy difference is greater than the H-bond difference between a 4-pyridone and a 4-Hyp dimer (-1.15 kcal/mol). Either the N-H···O or O-H···N H-bond is stronger than that in the corresponding dimer. This indicates the cyclic structures can enhance the H-bond strength. Both N-H···O and O-H···N H-bonds are also weaker than the strongest center H-bonds in the octamer that clearly suggests, the influence of the H-bond enhancement in the center of the linear chain is greater than that in the cyclic chain.

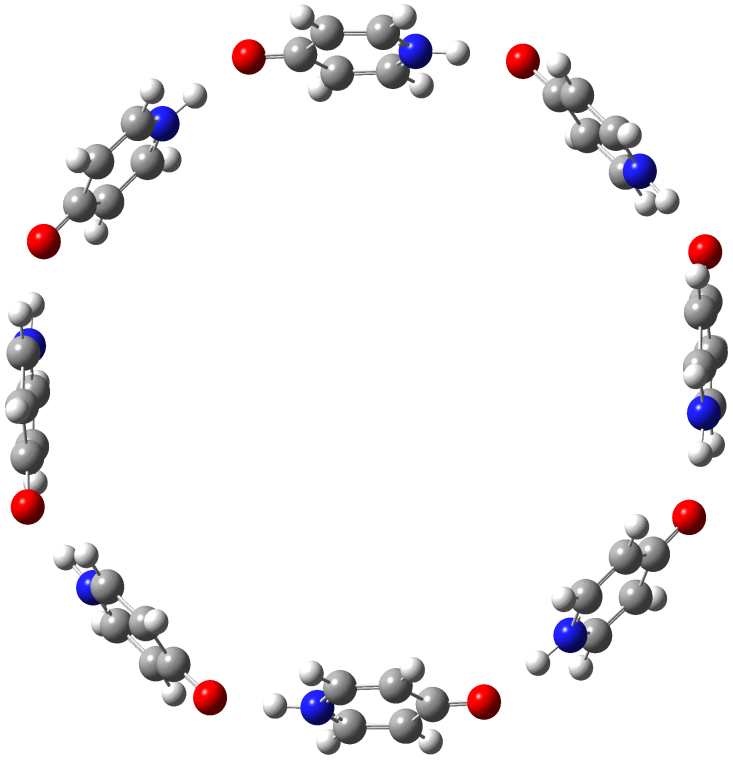

Figure 5-11. Cyclic 4-pyridone octamer.

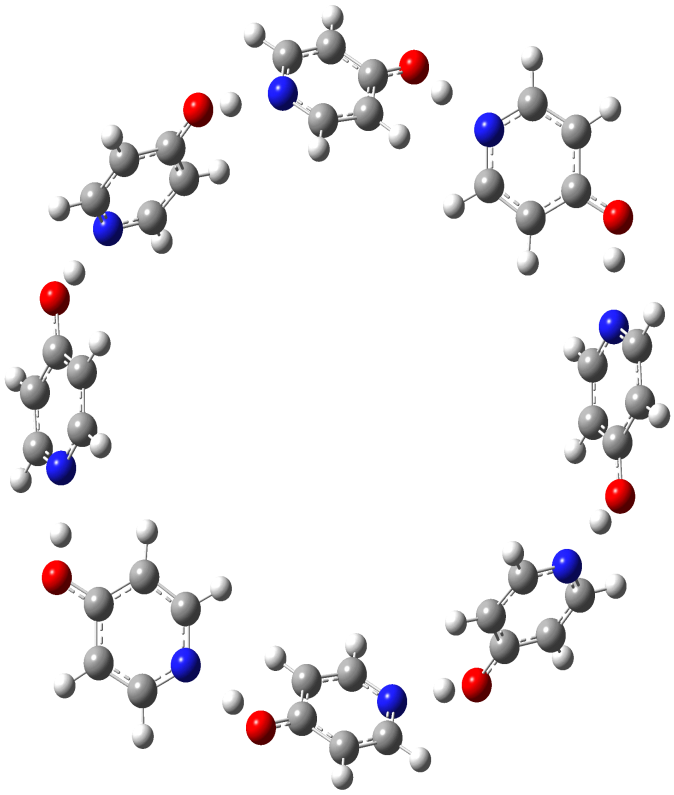

Figure 5-12. Cyclic 4-hydroxypyridine octamer.

5.4 Conclusion

The N-H···O H-bonding enthalpy between 4-pyridones connected in a chain of H-bonds can achieve as strong as 23 kcal/mol for the most central H-bonds, while that between dimeric 4-pyridones is 9.90 kcal/mol based upon DFT calculations of the counterpoise-corrected potential energy surfaces. This H-bond is stronger than the O-H···O of 1,3-cyclohexanedione and the O-H···N of the 4-pyridone tautomer, 4-hydroxypyridine. That the range of enthalpies for N-H···O H-bonds can vary from as little as 2 to as much 23 kcal/mol depends primarily upon the polarizability of whatever internally connects the N-H and C=O within the H-bonded molecule, which are two parallel -C=C- entities in 4-pyridone. As such π-systems can easily be polarized; one might reasonably expect the increased polarizability to enhance the H-bonding interactions. However, this does not mean the amidic H-bond can be increased with larger ring PAHs. The energetic difference between tautomers must be considered.

The cyclic 4-pyridone structure provides significant stronger H-bond interaction than its cyclic tautomer, although the energetic difference between single N-H···O and O-H···N H-bond is about 2 kcal/mol in cyclic structure.

The importance of the covalent/charge-transfer interactions between π-systems of adjacent 4-pyridones is reduced. If covalent interaction exists, it must not mainly be in the π-system. This is also supported in the chains of 1,3-cyclohexanedione and 4-hydroxypyridine. We conclude that the main contributions to the cooperativity in these systems must be some combination of polarization and mutual polarization. However, resonance *within the π-systems* certainly must contribute to the large polarizability of 4-pyridone.

CHAPTER 6 – THROUGH HYDROGEN BOND VIBRATIONAL COUPLING IN HYDROGEN-BONDED CHAINS OF 4-PYRIDONES WITH IMPLICATIONS FOR PEPTIDE AMIDE I ABSORPTIONS: DENSITY FUNCTIONAL THEORY COMPARED WITH TRANSITION DIPOLE COUPLING

6.1 Introduction

Nature has made extensive use of the N-H···O=C H-bonding motif in various guises to form self-assembled biomaterials. She has used a paradigm of multiple complementary H-bonding arrays in nucleic acids where the specific base pairs are complementary in their H-bonding donors/acceptors and in size (only one purine plus one pyrimidine can fit across the backbones) to form stable structures. This paradigm has been successfully applied to many self-assembling systems (I cite only a small selection of representative reports).[163-166] She has used a different paradigm in the self-assembly of proteins. Unlike the nucleic acids, which allow relatively little structural variation, proteins can form an almost limitless number of stable structures. If all the N-H···O=C H-bonds were energetically equivalent, then the peptide's structures would be dictated entirely by other factors, such as steric, hydrophobic, covalent (sulfur bridges) or electrostatic (between ionized side chains and/or other ions) effects. However, this particular kind of H-bond can have an unusually wide range of energies depending upon its environment as it is subject to enormous

amounts of cooperative interactions. The remarkable N-H···O=C H-bond can achieve enthalpies of association from about 2 kcal/mol (in one of the dimers of a diglycine)[160] to 23 kcal/mol in the centermost H-bonds of chains of 4-pyridones.[45] Cooperative H-bond interaction plays an important role in modulating the magnitude of the H-bonding interactions.[167] Coupling between the C=O's in proteins and peptides results in the amide I infrared absorption often used to characterize these molecules. The coupling involved in the amide I band can occur by through-space transition dipole coupling (TDC) or by coupling of the C=O's mediated by H-bonds. The TDC method of calculating the coupling between C=O's in peptides was introduced by Krimm.[101] The coupling between the oscillators is based upon the electrostatic interactions between the oscillating dipoles. As dipole-dipole interactions are electrostatic in nature, the mechanism of TDC depends upon the predominance of electrostatics in determining the interaction between the coupled entities. The failure of electrostatic interactions to predict the cooperativity of H-bonds in peptides [52,134,137,168] and in molecular crystals[40,131,169,170] has long been established. The importance of vibrational coupling of C=O's through the H-bonds in H-bonding formamide chains[100] dimers and trimers of N-methylformamide,[171] and in infinite α-helices have been mentioned in the literature.[172] However, many reports continue to ignore this important effect. In this chapter, I use H-bonded chains of 4-pyridones which I discuss in Chapter 5 to demonstrate the importance of coupling C=O's through H-bonds. Chains of 4-pyridones (see Figure 5-2 in Chapter 5) provide the strongest single N-H···O=C H-bonds between neutral species of which we are aware.[45] Thus, the effect of C=O coupling through H-bonds should be magnified in 4-pyridone H-bonded chains relative to peptides, rendering the demonstration of this effect more evident. In contrast, larger distance between C=O's will reduce the

magnitude of the TDC from that expected from peptides. Both the monomers and the chains attain structures with C_{2v} symmetry. Thus, the co-linear C=O's have their individual transition dipoles aligned with each other and with the transition dipoles of the amide I vibrations of the aggregates.

The amide-II (C-N-H stretch/bend) and amide-A (N-H stretch) bands also provide structurally useful information on peptide structure. There is no vibration truly equivalent to the amide II band for H-bonded chains of 4-pyridones. However, the N-H stretching couple quite strongly. We will also discuss these vibrations below.

6.2 Calculation details

All DFT B3LYP functional with D95 (d,p) calculations reported here are as described in section 5.2. The geometries of the 4-pyridone chains were completely optimized within the constraint that they maintain a plane and an axis of symmetry. The vibrational frequencies used the harmonic approximation. Through space dipole-dipole coupling (TDC) interactions are presented for comparison with the DFT results. These have been calculated from the Cartesian coordinates of only the carbons and oxygens of the C=O's taken from the same optimized geometries used for the DFT calculations. We used a program developed by Diem[173] for this purpose which incorporates procedures he described earlier. The transition dipoles are co-linear with the C=O bonds because of the symmetry of the H-bonded chains. The vibrational 'frequencies' are reported as wavenumbers in cm^{-1} which are more appropriately $1/\lambda$ than ν, (c/λ). While I strongly believe the practice of scaling frequencies to be unfavorable to the spirit of *ab initio* calculations, we realize that scaling makes the computed vibrations more easily comparable to those obtained experimentally by biochemists and spectroscopists. Therefore, I have applied a scaling factor of 0.965. This has been previously found to be suitable for B3LYP/D95(d,p) and similar DFT calculations.[174,175] The original calculated frequencies can be obtained by dividing the scaled values by this factor.

I used ^{14}C substitution of the structures to decouple vibrational modes selectively. Substitution of four ^{14}C's in the two C=C bonds of each pyridone was used to decouple these stretching modes from those of the C=O to remove any ambiguity about which modes of the pyridones coupled in the aggregates. I (separately) decoupled individual C=O's in the nonamer to obtain the stretching modes of individual C=O's within the aggregate to illustrate the relationship between the C=O bond length variation and the C=O frequencies.

6.3 Results and discussion

6.3.1 H-bonded 4-pyridone chains

Figure 6-1 depicts the C=O stretching region of the IR spectra for 4-pyridone and aggregates containing from two to nine monomers. The upper part shows the spectra of the unsubstituted aggregates, while the lower part illustrates the spectra of the tetra-^{14}C substituted aggregates. The ^{14}C substitutions clearly remove the coupling observed in the upper spectra. We shall refer to the decoupled spectra in the lower part of the figure for the remaining discussion. The most intense absorption for all aggregates involves synchronous stretching of all C=O's. This absorption both increases in intensity and becomes more red shifted as the aggregate becomes larger. The extents of these changes exceed the qualitatively similar changes previously reported for H-bonded chains of formamides[100], as might be expected from the larger H-bonding energies reported for the pyridone[45] rather than formamide[52] H-bonded chains.

The most intense, lowest energy and, therefore, most red shifted C=O vibration for each chain involves the synchronous symmetric stretches of each C=O. The vibrational wavefunction for this mode would have no nodes. The next higher in energy belongs to the couple mode where half of the C=O's on one end of the pyridone chain stretch synchronously in phase with each other, but out of phase with the other half. The vibrational wavefunction for this mode would have a node near the center of the chain. Thus, this mode should have little intensity. The third lowest energy mode should have two nodes. This mode should have more intensity than the second lowest, but less than the lowest mode. Continuing in this manner, most of the intensity should be due to the odd-numbered modes (counting from the lowest) and the intensity should fall off in these modes as the energy increases. Careful inspection

of the figure reveals that a weak shoulder slightly blue-shifted from the most intense absorption appears for $N = 3$ or more. The chain of three is the smallest that can have two nodes in the vibrational wavefunction. This shoulder increases in intensity and becomes more red shifted as N increases from three to nine in a manner similar to the most intense peak.

When I investigated the top panel of Figure 6-1 closely, I found two major amide I absorption peaks; one of the higher intensity at a lower frequency; and another of lower intensity at higher frequency. The high intensity, lower frequency peak is due to the symmetric motion of carbonyls between monomers associated with the -C=C- *π-system* rocking within the monomer. The lower intensity, high frequency peak is due to the symmetric motion of carbonyls between monomers associated with the -C=C- *π-system* scissoring within the monomer. As shown in Figure 6-1, it is worth noting that the most intense absorption frequencies are shifted as the H-bonded chains are increased in length. In this monomer, the intensity of the lower frequency is almost zero, as the chain lengths increase the frequencies become more red shifted and their intensities increased markedly. As the chain is lengthened, the intensity grows from 1538 km/mol for the dimer to 5849 km/mol for the nonamer. When N is less than 7, the most intense peak is still the one at higher frequency but the intensity is roughly close to the most red shifted one. The lower frequency absorption becomes the one with the strongest intensity and the most red shifted when N is greater than 7. The more intense C=O stretching frequency of a 4-pyridone dimer is at 1645 cm^{-1} (see Figure 6-1). As the chain becomes longer to $N = 9$, the lowest frequency vibration decreases to 1578 cm^{-1}. In comparison to formamide chains[100], the C=O stretching frequencies are more red shifted in 4-pyridone chains. The lowest frequency C=O stretch of formamide decreases by 40 cm^{-1} on going from the dimer to the decamer

chain (53 cm^{-1} from the monomer). As shown in Figure 6-1, the lowest frequency C=O stretch in the 4-pyridone chains decreases by 69 cm^{-1} on going from the dimer to the nonamer (88 cm^{-1} from the monomer). Because the previous mentioned intensity changes in 4-pyridone chains, the C=O frequency shifts in 4-pyridone from the corresponding motion will be 34 cm^{-1} on going from dimer to nonamer (40 cm^{-1} from the monomer). The observed frequency red shifts from the corresponding modes in the monomer and dimer reflect the cooperative stabilization of the H-bonds, which causes the N-H and C=O bonds to elongate with increasing chain size (see Table 6-1). On the contrary, the C-N bond lengths decrease with increasing chain size. The effects are greater near the center and near the terminals of the chains. This observation reflects the polarization of the *π-system* of the 4-pyridones associated with the H-bonding cooperativity. As the C=O and N-H bonds lengthen, the *π-character* increases, whereas the C-N bonds shorten as they obtain more *π-character*. These 4-pyridione chains not only illustrate good examples of how the coupling of carbonyls leads to the red shift of frequency, but also of how the H-bonding formation can change the strength of the intensity.

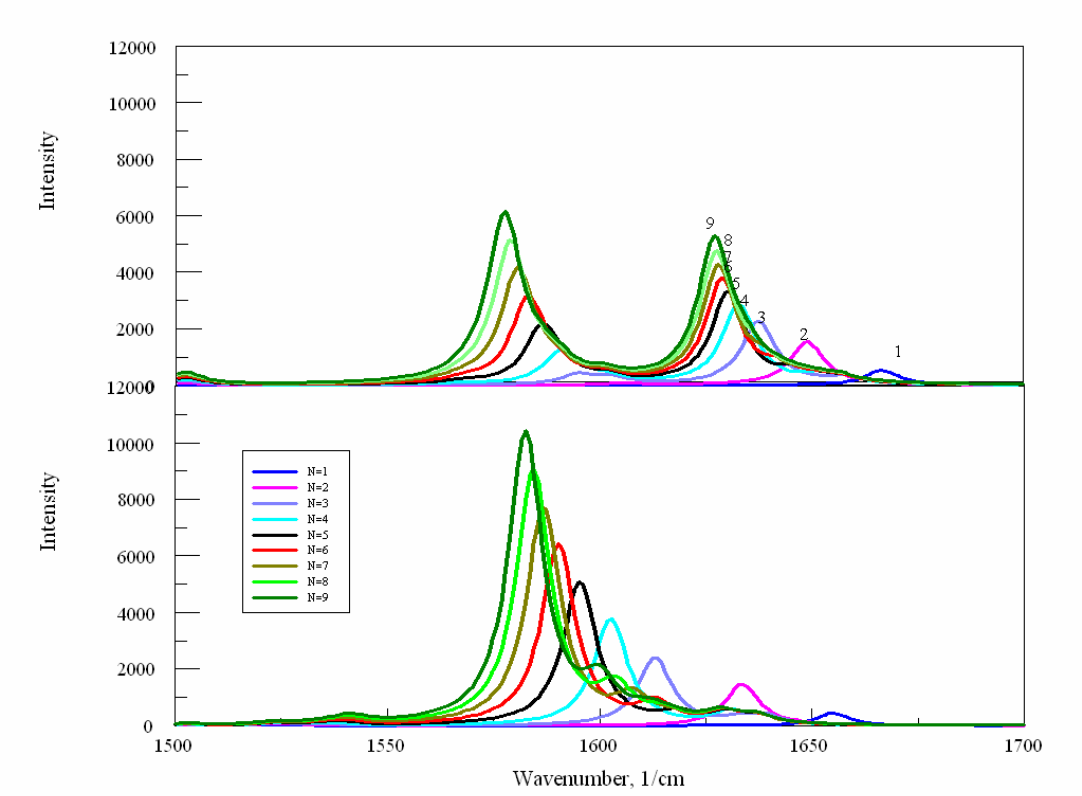

Figure 6-1. The C=O region of the IR spectrum for (4-pyridone)$_N$. The lower panel shows the spectrum when all C=C's are substituted with ^{14}C.

Table 6-1. Variation of bond lengths (Å) for 4-pyridone monomer, dimer and decamer*

Bond	Monomer	Dimer	Decamer
C=O	1.239	1.246	1.258
N-H	1.010	1.022	1.038
C-N	1.376	1.370	1.361
C=C	1.363	1.366	1.372
O…H		1.780	1.632

* The bond lengths for the dimer are to those most involved in the H-bond, for the decamer, for those most involved in the central H-bond.

Figure 6-2 depicts the N-H stretching region of the same 4-pyridone chains. The upper part shows this region for the isotopically unsubstituted molecules. The red shifts for the larger chains move the most intense N-H stretch into the region of the spectrum where C-H stretches might be expected. The lower part of the figure shows the same region for chains where all the C-H's have been replaced with C-D's to shift these vibrations out of the range of the IR spectrum covered in the figure. The observation that no substantial differences can be found between the two demonstrates that all the C-H vibrations are too weak to substantially alter the appearance of the N-H stretching absorptions. The approximately 500 cm^{-1} red shifts of the most prominent N-H stretch from that of the monomer and approximately 300 cm^{-1} from the H-bonded N-H in the dimer are much larger than those normally expected for H-bonded N-H's. The intensity of the strongest absorption for $N = 9$ approaches 2000 times that for the monomer.

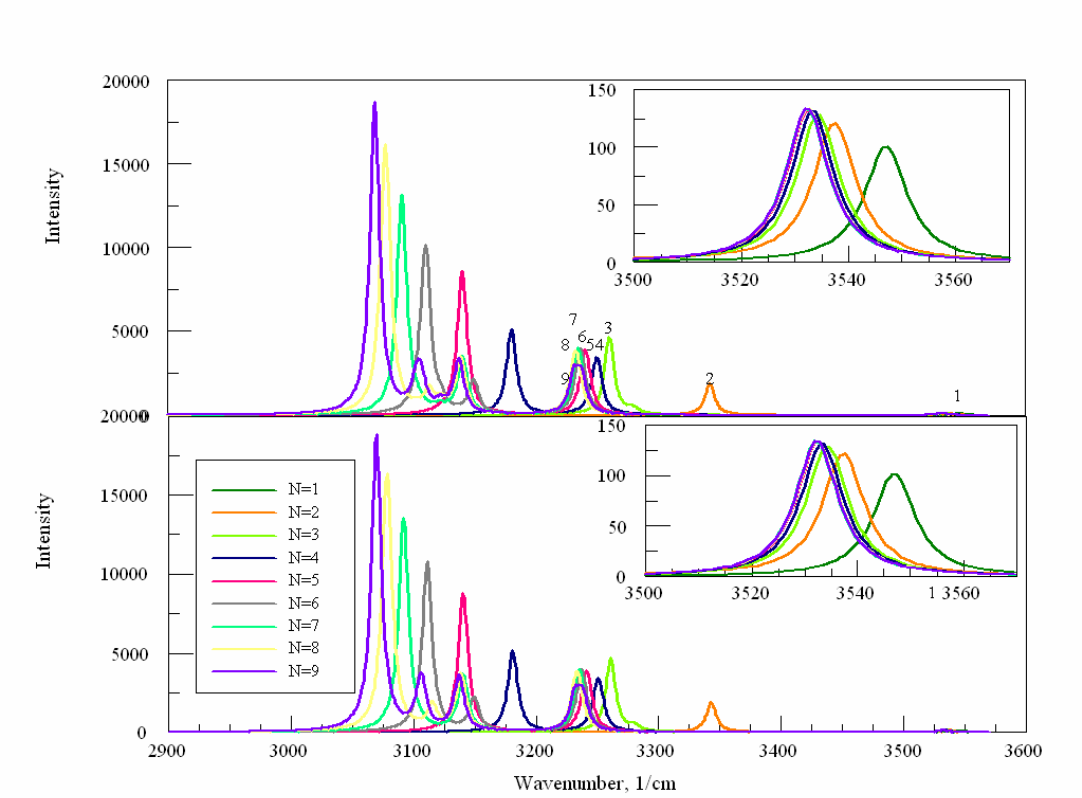

Figure 6-2. N-H stretching region of $(4\text{-pyridone})_N$. The lower panel shows the results for the chains where all four carbons in the C=C bonds are substituted with ^{14}C. The inset expands the part of the spectrum near 3500 cm-1. The intensities are in km/mol.

While the absorption spectra of the chains in the C=O and N-H regions have much in common (increasing red shift and intensity as the chain increases in length) several features distinguish then from one another. Most notably, the terminal N-H does not participate in an H-bond. It is largely unaffected by the growth of the H-bonded chain. It exhibits small red shifts that stop increasing when N exceeds 5. It shows only a modest increase in intensity that also stops when N reaches 5. Thus, the coupling really involves the N-1 N-H's that participate in the H-bonds. The most intense and red shifted N-H stretch is for the completely symmetric stretch of the 8 H-bonded N-H for N = 9. In addition to this strong absorption, three others can be seen which correspond to the other vibrational wavefunctions that have an even number of nodes. Note that the least red shifted of these coincides with absorptions from those chains with N = 5 or more. Thus this absorption appears to have reached its limiting value, N = 5. The next least red shifted of the absorptions for N = 9 coincides with absorptions for N = 7 or more, suggesting that this absorption reaches its limiting value for N = 7. The two most red shifted absorptions for N = 9 do not coincide with others, suggesting that these have not yet reached limiting values. Thus, the red shifts larger than 500 cm^{-1} and the intensities higher than 2000 times that of the monomer might be expected for longer chains.

I repeated the vibrational coupling calculations using the TDC method. We set the reference frequency for these calculations to the scaled frequency of the 4-pyridone monomer (substituted with four ^{14}C's in the C=C bonds) as calculated by DFT (1655 cm^{-1}) so that the shifts calculated by the two methods could be compared. Figure 6-3 shows the individual C=O absorptions that comprise the amide-I band of $(4\text{-pyridone})_9$ as calculated by DFT (upper part) and TDC (lower part). Figure 6-4 depicts all the absorptions of the amide-I region for each H-bonded chain.

In $(4\text{-pyridone})_9$, the C=O's are so extensively coupled that one cannot assign a unique stretching frequency to each one. Nevertheless, each C=O is in a unique environment due to its position in the H-bonded chain. As expected from previous reports, [39,40,45,52,100,134,137,160] the H-bonding increases the C=O bond length. Those H-bonds nearest the center of the H-bonded chains, which participate in the strongest H-bonds, have the longest C=O bonds. Since the C=O stretching frequency depends upon the strength of the bond, and since the bond length is generally a good indicator of C=O bond strength, one might expect the different C=O's in $(4\text{-pyridone})_9$ to have different stretching frequencies were they not coupled. In order to probe these uncoupled C=O stretching, we decoupled individual C=O's in $(4\text{-pyridone})_9$ by substituting one ^{14}C=O at a time for each of the nine unique 4-pyridones in the chain. Figure 6-5 shows the variation of the frequencies of the ^{14}C=O substituted 4-pyridones as a function of their position in the chain. Since the ^{14}C=O frequencies are necessarily red shifted from the ^{12}C=O frequencies, they are plotted as the shift from the frequency of the ^{14}C=O substituted monomer. Red shifts occur for all nine positions, even for the terminal 4-pyridone that does not form an H-bond with its C=O. The largest red shifts occur in the more central monomers of $(4\text{-pyridone})_9$.

Figure 6-6 shows the $^{14}C=O$ frequencies plotted against the C=O bond lengths. The linear plot resembles those previously reported for formamide chains.[100] These data show the C=O bond lengthening upon H-bonding to be a major contributor to the red shifts of the C=O band of the $(4\text{-pyridone})_N$ chains.

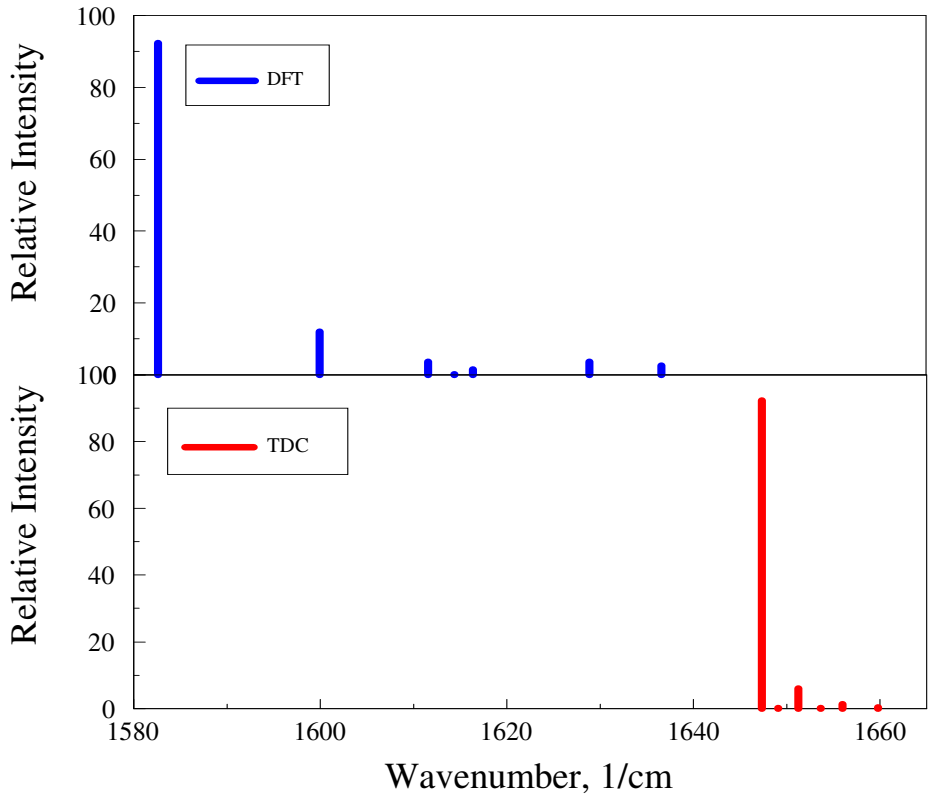

Figure 6-3. Individual C=O absorptions for (4-pyridone)$_9$ as calculated by DFT (above) and TDC (below). The DFT calculations refer to the H-bonded chain with ^{14}C=O's (to remove the coupling with the C=C's). The TDC frequencies are adjusted to match the scaled C=O stretching frequency of the monomeric 4-pyridone as calculated using DFT.

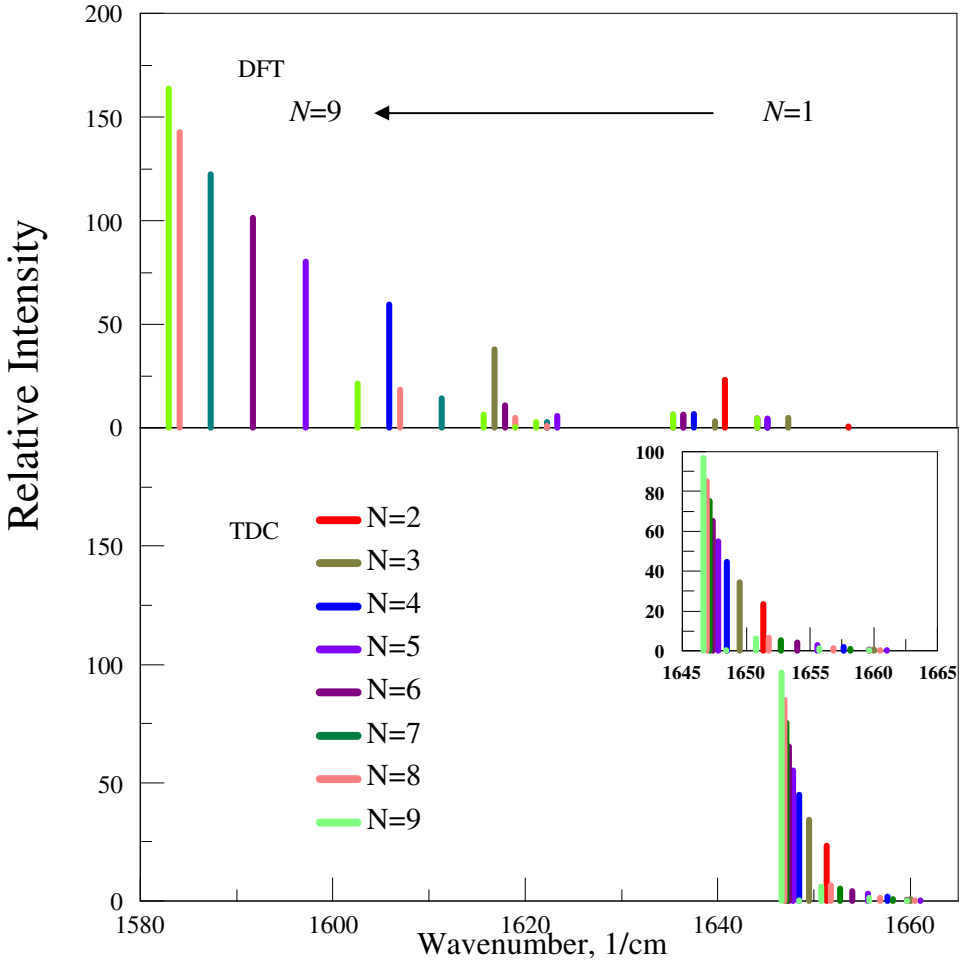

Figure 6-4. The individual C=O absorptions for (4-pyridone)$_N$ with four ^{14}C's as calculated by DFT (upper panel) and TDC (lower panel). The relative intensities are scaled to keep the intensity for N = 2 the same for both methods. The inset in the lower panel magnifies the scale.

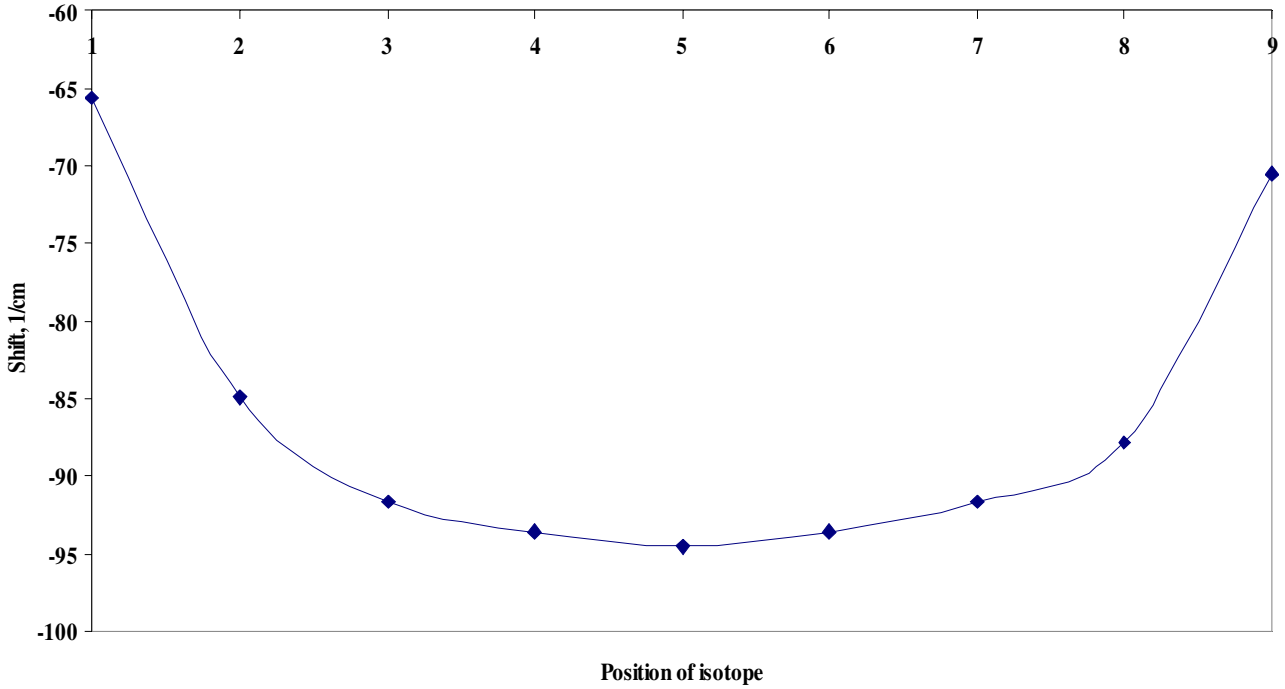

Figure 6-5. Shifts of the frequencies of the $^{14}C=O$'s the individually 14C -substituted 4-pyridones in $(4\text{-pyridone})_9$. The X-axis denotes which of the 4-pyridones contains the $^{14}C=O$.

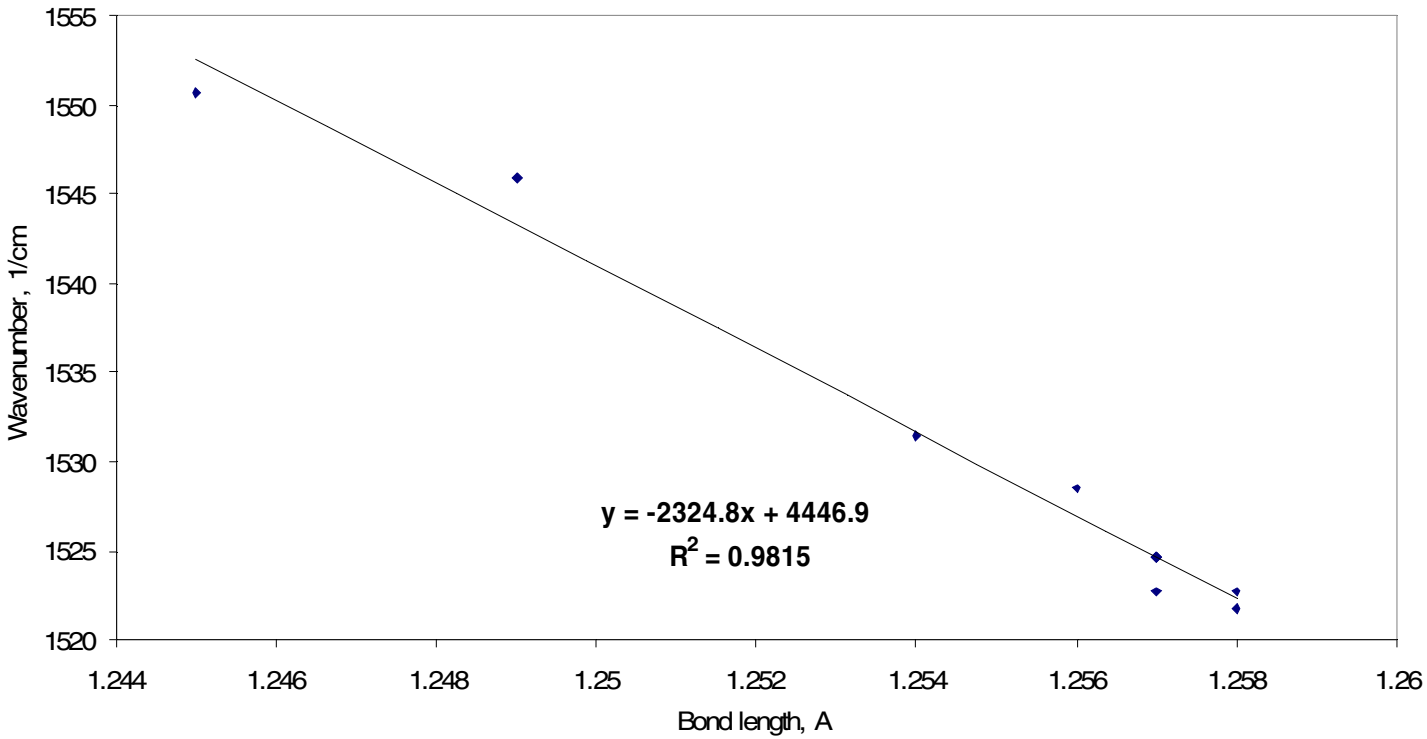

Figure 6-6. The frequency of the individually ^{14}C=O substituted 4-pyridones in $(4\text{-pyridone})_9$ plotted against the C=O bond length.

6.3.2 Amplitudes of the C=O stretches

More information of the C=O coupled vibration is described in this section. Here I introduced the amplitude analysis related to C=O coupling. The amplitudes were determined by the changes of relative displacements of the C and O atoms in individual C=O bonds. Figures 6-7 ~ 24 illustrate the amplitudes of the C=O stretching for each normal 4-pyridone (non-isotopic substitution) in a chain of nonamer. The scaled frequencies are described in each caption. The unscaled frequencies are illustrated in each figure. The lowest vibration (1578 cm^{-1}) is composed of a linear combination of C=O stretches that all are symmetric in phase. It is shown in Figure 6-24 that it has the highest intensity. The second lowest frequency has half the C=O groups stretches in one direction and the other half stretches n opposite direction (see Figure 6-23). The intensity should be zero because the chain is symmetric. The linear combinations of amplitudes of the individual C=O stretches for the lowest frequencies represent the lowest wave function for the coupled C=O's.[100] In these figures each of the coupled vibrations are shown. It can be observed that the lowest frequency has no nodes, the second lowest one has two modes, and the third lowest one has three nodes. Patterns like this might continue, as the chains are getting larger. However, the reality is usually more than what we expect. The central H-bonds became dramatically stronger than the terminal ones as the chain numbers increase (see chapter 5). Consequently, the coupling between the central and terminal C=O stretching reduces with larger chain length. Therefore, the higher frequency C=O stretches become localized at terminal of the longer chains.

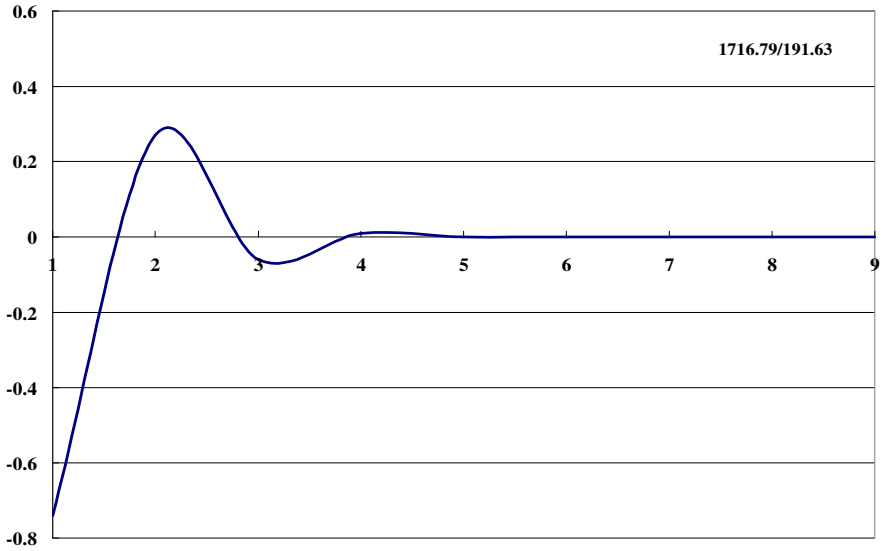

Figure 6-7. Amplitude at 1656 cm^{-1} for each 4-pyridone in the coupled C=O stretching (Amide I) ; see Chapter 5 for numbering.

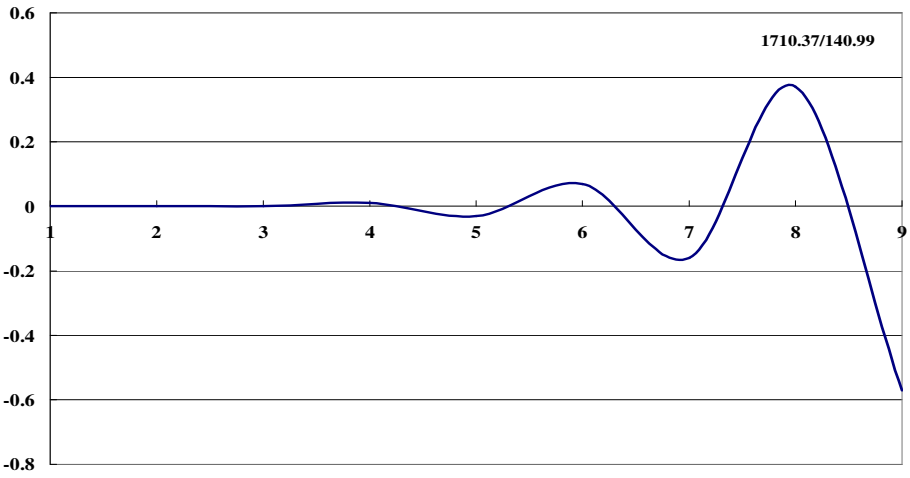

Figure 6-8. Amplitude at 1650 cm^{-1} for each 4-pyridone in the coupled C=O stretching (Amide I).

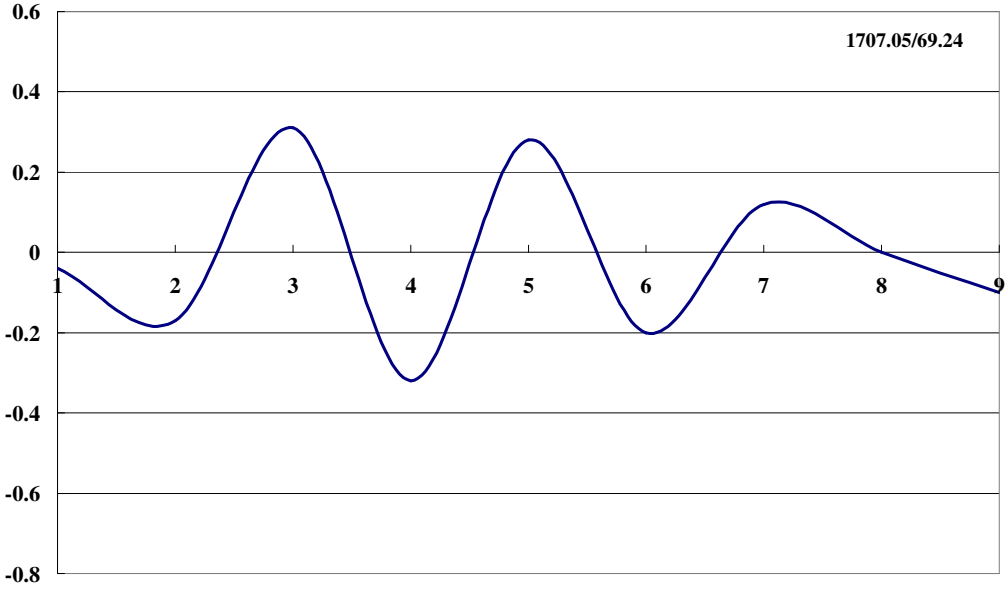

Figure 6-9. Amplitude at 1647 cm^{-1} for each 4-pyridone in the coupled C=O stretching (Amide I).

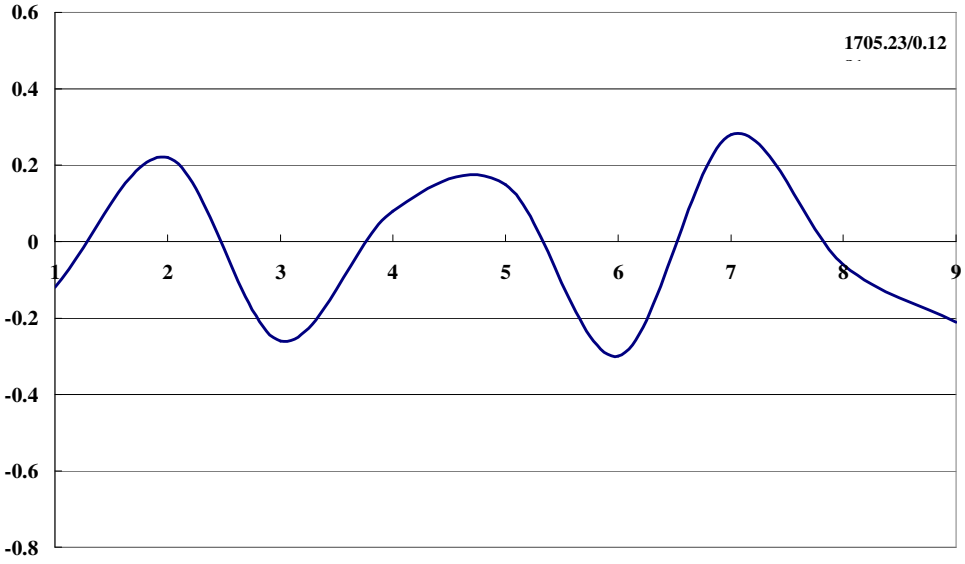

Figure 6-10. Amplitude at 1645 cm^{-1} for each 4-pyridone in the coupled C=O stretching (Amide I) .

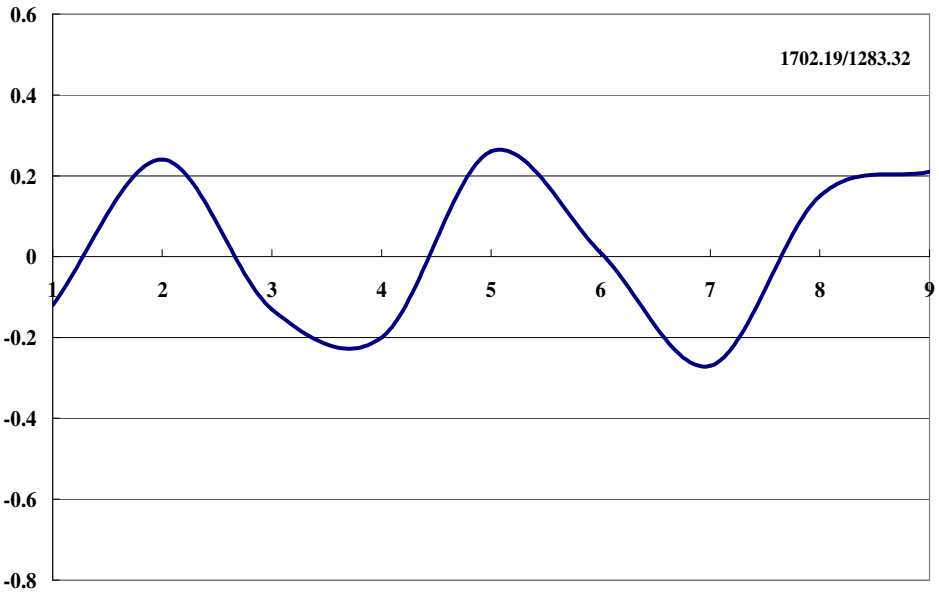

Figure 6-11. Amplitude at 1642 cm^{-1} for each 4-pyridone in the coupled C=O stretching (Amide I).

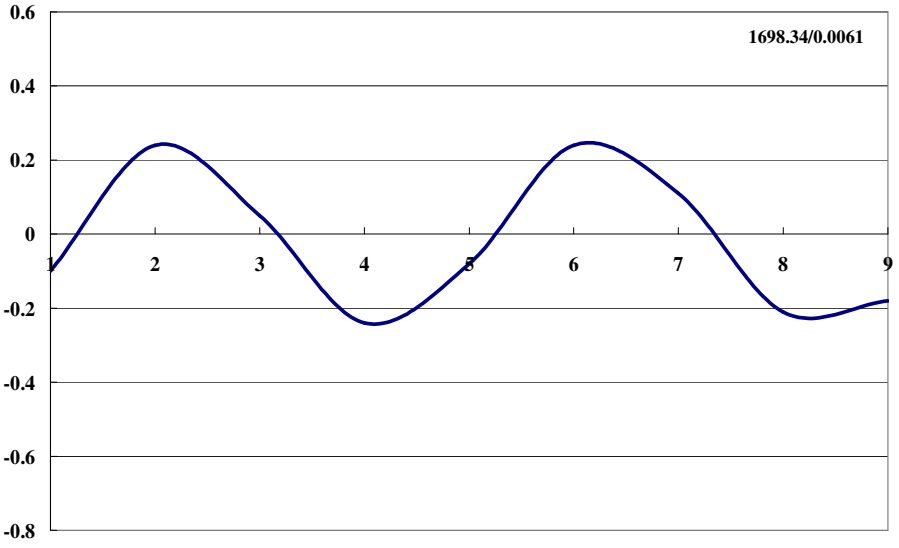

Figure 6-12. Amplitude at 1639 cm^{-1} for each 4-pyridone in the coupled C=O stretching (Amide I).

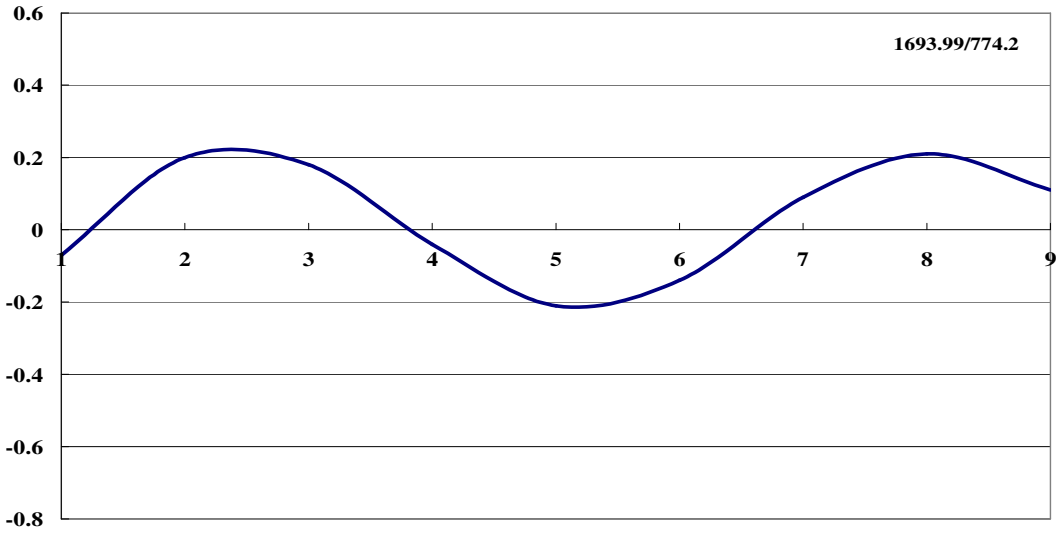

Figure 6-13. Amplitude at 1634 cm^{-1} for each 4-pyridone in the coupled C=O stretching (Amide I).

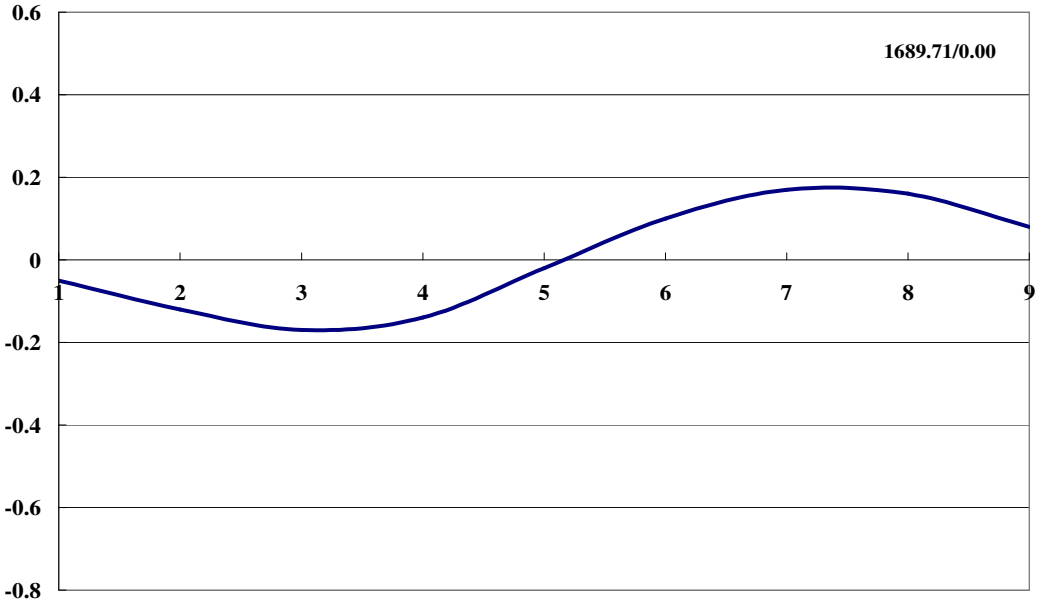

Figure 6-14. Amplitude at 1630 cm^{-1} for each 4-pyridone in the coupled C=O stretching (Amide I).

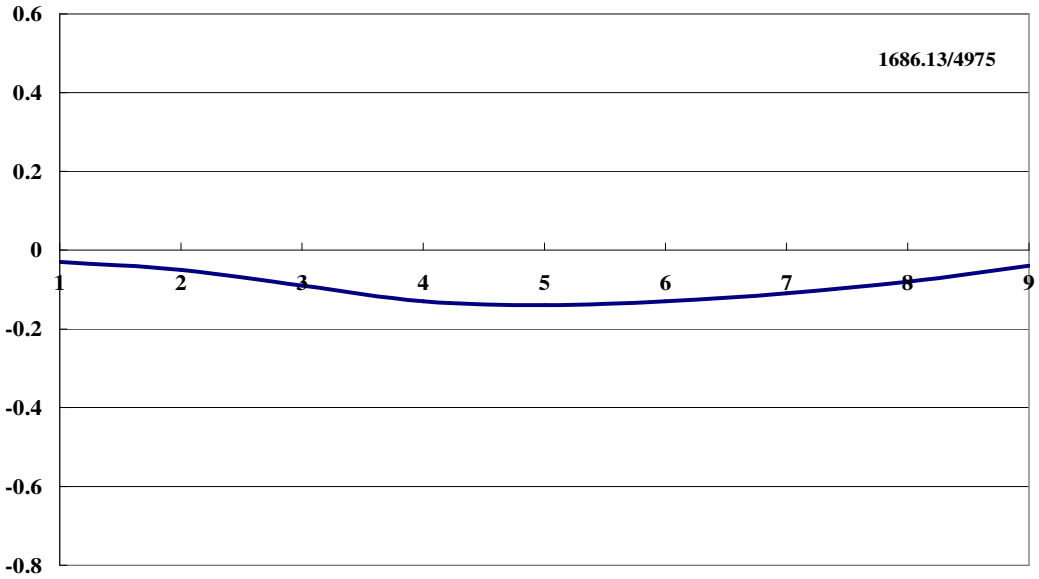

Figure 6-15. Amplitude at 1627 cm^{-1} for each 4-pyridone in the coupled C=O stretching (Amide I).

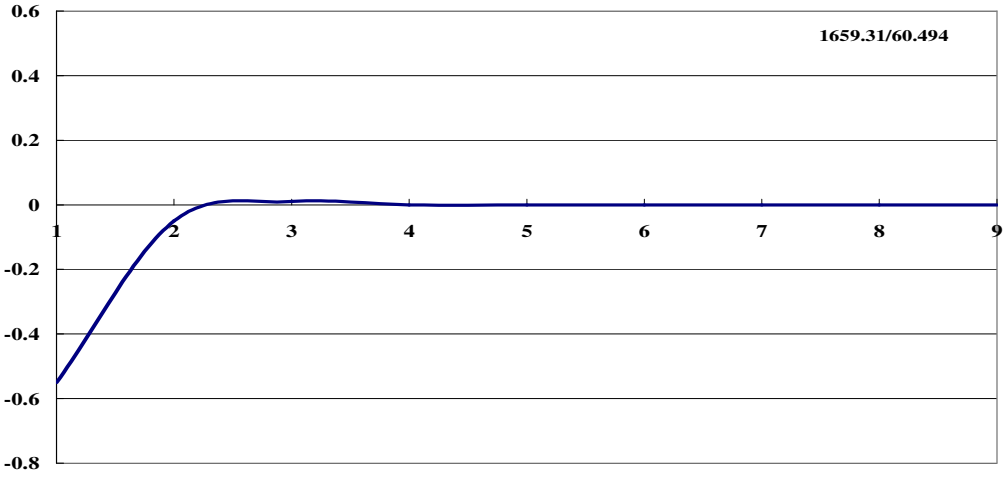

Figure 6-16. Amplitude at 1601 cm^{-1} for each 4-pyridone in the coupled C=O stretching (Amide I).

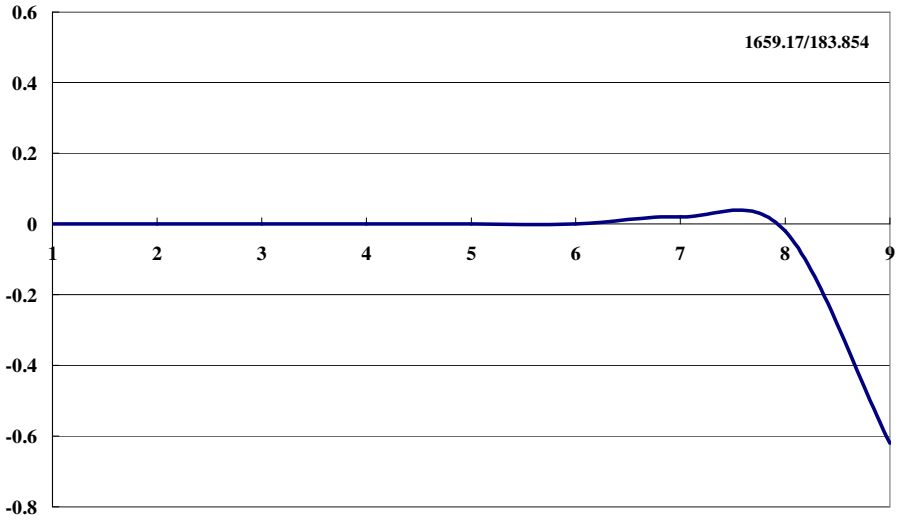

Figure 6-17. Amplitude at 1600 cm^{-1} for each 4-pyridone in the coupled C=O stretching (Amide I).

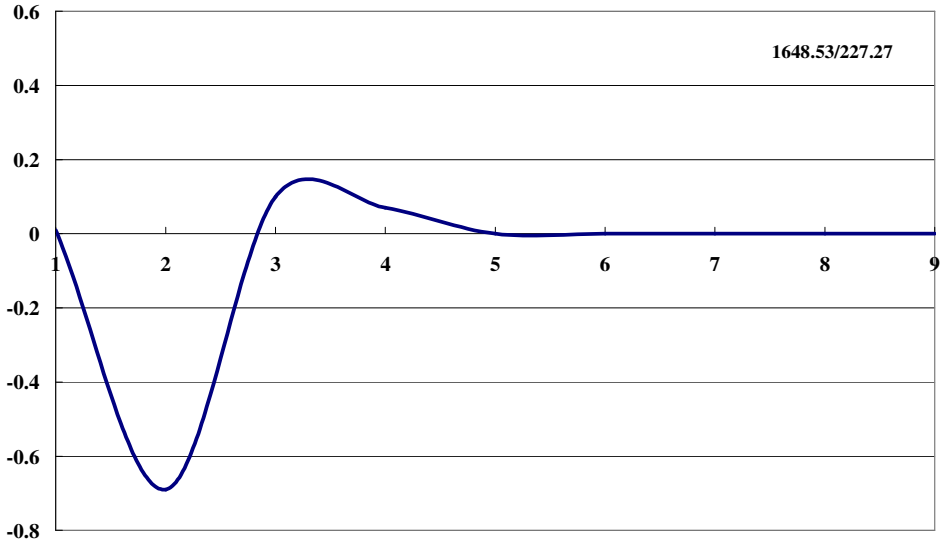

Figure 6-18. Amplitude at 1591 cm^{-1} for each 4-pyridone in the coupled C=O stretching (Amide I).

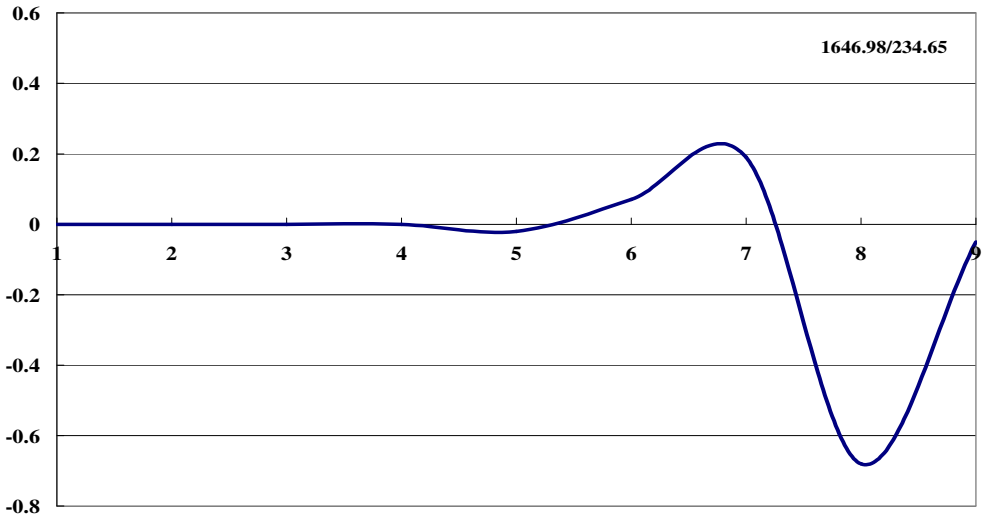

Figure 6-19. Amplitude at 1589 cm^{-1} for each 4-pyridone in the coupled C=O stretching (Amide I).

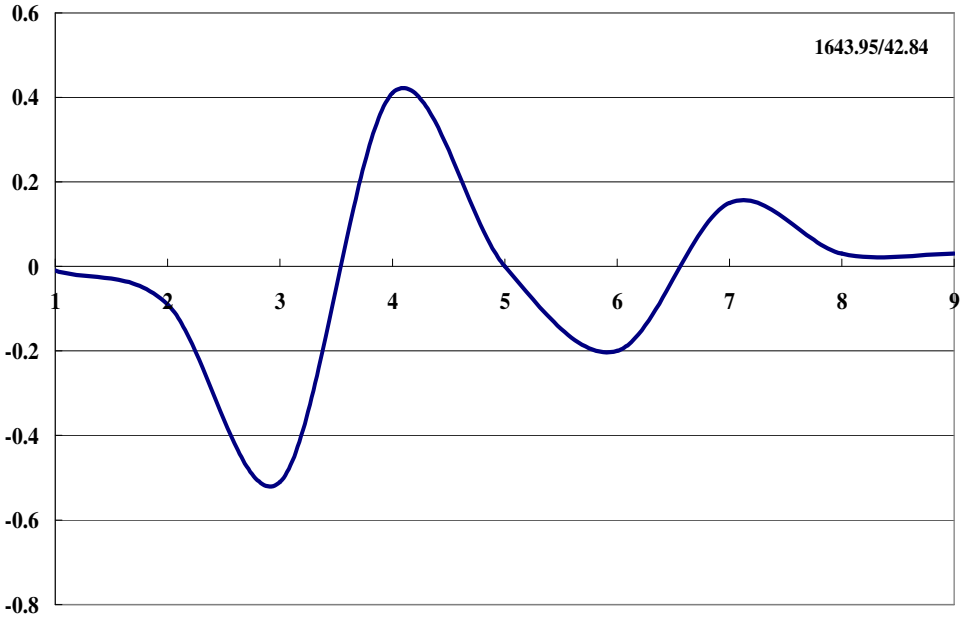

Figure 6-20. Amplitude at 1586 cm^{-1} for each 4-pyridone in the coupled C=O stretching (Amide I).

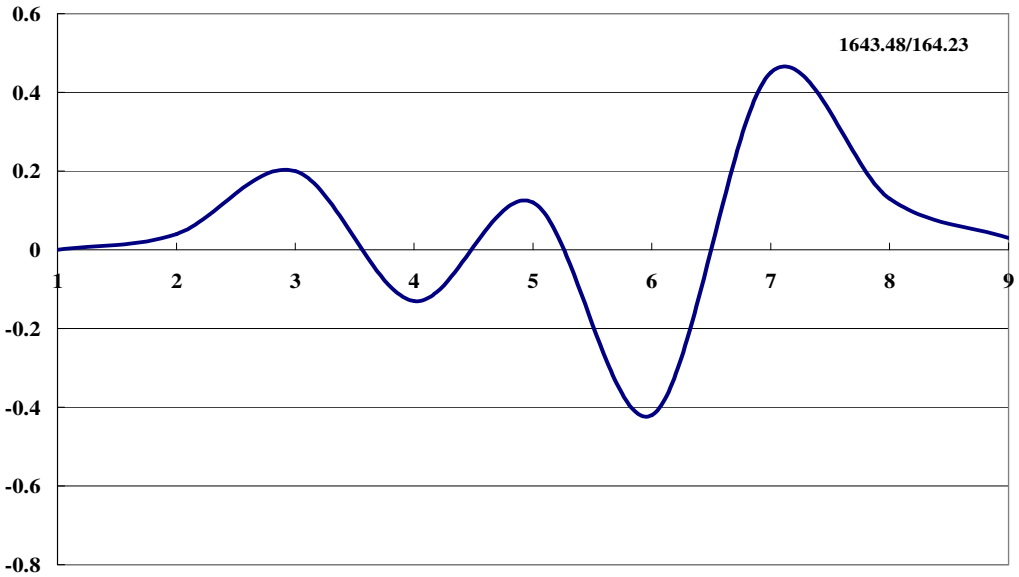

Figure 6-21. Amplitude at 1586 cm^{-1} for each 4-pyridone in the coupled C=O stretching (Amide I).

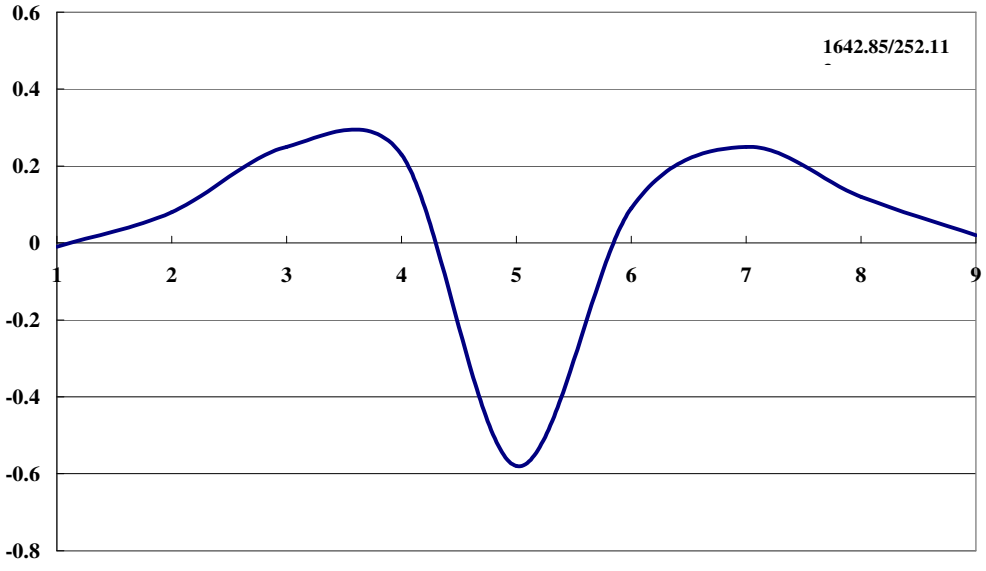

Figure 6-22. Amplitude at 1585 cm^{-1} for each 4-pyridone in the coupled C=O stretching (Amide I).

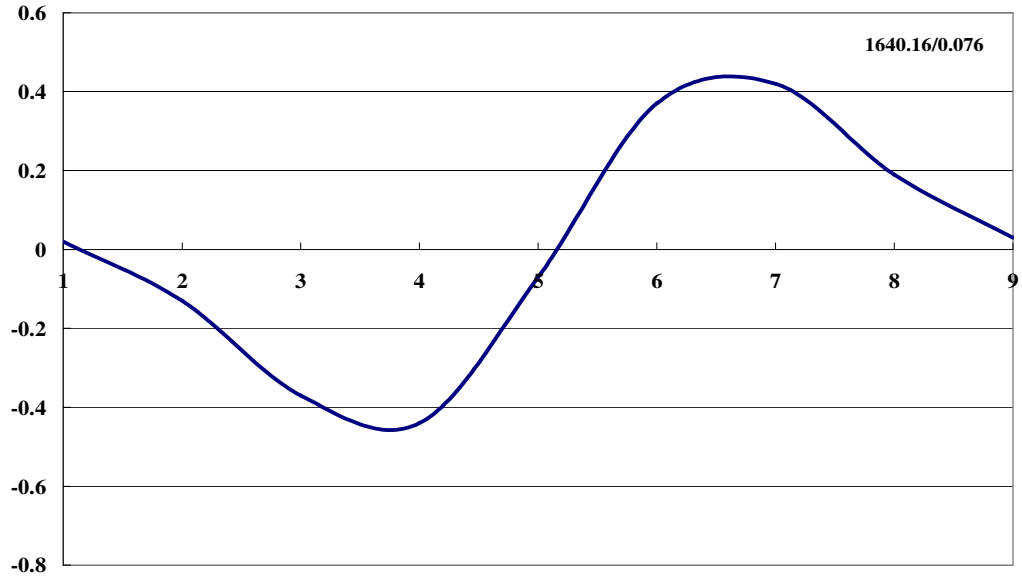

Figure 6-23. Amplitude at 1583 cm^{-1} for each 4-pyridone in the coupled C=O stretching (Amide I).

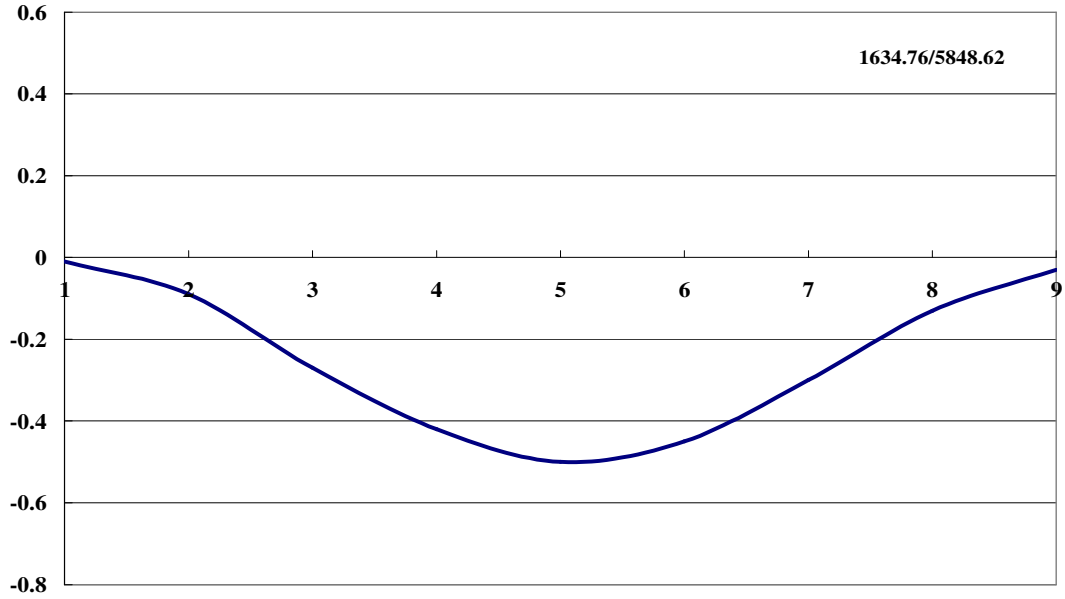

Figure 6-24. Amplitude at 1578 cm^{-1} for each 4-pyridone in the coupled C=O stretching (Amide I).

6.3.3 Comparison of DFT with TDC

The observed couplings of the C=O stretching in the 4-pyridone chains differs from the expectations of TDC in several aspects:

a) The distance dependence of dipole-dipole coupling causes the interaction to vary as the inverse cube of the distance between the dipoles. Since the interaction C=O dipoles are more distant from each other in the 4-pyridone chains than in the previously reported[100] formamide chains, TDC predicts less coupling for the 4-pyridones than for the formamides, contrary to our observations.

b) TDC coupling predicts the center of the set of coupled absorptions to remain at the frequency of the single uncoupled oscillator (assuming they are equivalent, as is the case here). However, both the 4-pyridone and formamide chains show extensive red shifts of the center of the absorptions. In fact *all* of the absorption frequencies are red shifted from that of the monomer. TDC cannot account for these shifts.

c) The C=O bond lengths in the individual molecules within both the 4-pyridone and formamide chains vary with position and lengths of the chains. No mechanism exists for this geometry change in simple dipole-dipole coupling. Furthermore, the decoupled ^{14}C=O's frequencies correlate with the C=O bond lengths, for which TDC does not account.

d) The relative intensities of the coupled C=O absorptions are not properly predicted by TDC. In particular, the most intense (and most red shifted) absorption increases in relative intensity as the H-bonded chain grows in length much more rapidly than predicted by TDC for both the 4-pyridone and formamide chains.

On the other hand, these observations can be easily explained assuming the coupling occurs though the H-bonds:

a) The coupling depends upon the strength of the H-bonds rather than the distance between the C=O's, as observed.

b and c) The C=O's become more red shifted as the H-bonded chain grows because the growing strength of the cooperative H-bonding interactions shorten the O···H distances while lengthening (and weakening) the C=O bonds.

d) Since the dipole moments of the 4-pyridone H-bonded chains increase much more rapidly than predicted by electrostatic interactions (i.e., vector addition of the dipole moments isolated of the individual 4-pyridones) due to the polarization that complements the H-bonding,[45] the transition dipoles (which determine the intensities of the individual absorptions - not to be confused with TDC) of the chains follow a similar trend.

6.3.4 Implications for peptides and proteins

While some reports of *ab initio* and DFT based vibrational analyses for some small peptides (too small to contain extensive cooperative H-bonded chains) have been reported,[176-186] biochemical vibrational spectroscopists have generally modeled the amide I band using through space dipole coupling of the relevant C=O's, often referred to as transition dipole coupling (TDC), either alone or in combination with other methods,[187] although several criticisms of TDC have appeared.[188-190] One very recent report calculates the coupling in the α-helical conformation of trialanine.[186] However, this conformation was not fully optimized as it is not even a local minimum,[137] and is too small for cooperative H-bonding. We shall describe our DFT based vibrational analyses of α-helical and β-sheet peptides elsewhere.

Electrostatic interactions between oscillators (or molecules) do not allow for reorganization of charge or for reorganization of molecular interactions. Thus, the dipole moment of an ensemble of molecules or oscillating dipoles that interact purely by electrostatics would be the vector sum of the individual dipole moments. This is a reasonable approximation for many molecular situations including many peptides where extensive H-bonding is not important, such as individual β-strands and most small peptides. However, this approximation clearly breaks down where extended cooperative H-bonding becomes cooperative. For example, the dipole moments of H-bonded chains of acetic acid,[170] enols of 1,3-diones,[169] 4-pyridones,[45] formamides,[52] urea,[40] and α-helical peptides[137] all increase more than expected from the vector sums of their components as the chains grow. The reorganization of charge in response to an electric field is due to polarization, which is distinctly different as it is not static but is responsive to the magnitude of an applied electric field. More precisely, while the dipole moment is $d\mathrm{E}/d\mathrm{F}$, the polarizability is $d^2\mathrm{E}/d\mathrm{F}^2$ where E is the energy and F

is the electric field. Unfortunately, many reports in the literature do not make the distinction between purely electrostatic interactions and those significantly due to polarizablity. When the electron density of a molecule becomes significantly polarized, the molecular geometry will necessarily relax to accommodate the change. In the chains of 4-pyridones considered in this paper, part of the geometry relaxation involves the lengthening of the C=O bonds. The effect of the lengthening of these C=O bonds can be observed in the correlation of the frequencies of the individually ^{14}C=O substituted pyridone monomers within the (4-pyridone)$_9$ H-bonded chain. Similar effects have been observed for H-bonding formamide chains,[100] α-helical and β-sheet peptides.[191] Hydrogen-bonding clearly is not always an entirely electrostatic interaction. Rather, it generally involves both polarization and covalent interactions.[192] For example, the observation that trans-hydrogen-bond scalar ^{13}C-^{15}N J-couplings can be measured indicates that spin information can be transferred across H-bonds. This cannot be accomplished through purely electrostatic interactions. Furthermore, the magnitude of these J-couplings is influenced by the existence of other H-bonds within a H-bonded chain as predicated by DFT calculations[193] and observed by experiments. Gilli has shown that H-bonds can be stabilized by resonance[162] to form what he calls resonance assisted H-bonds (RAHB's). Perhaps the clearest example of this phenomenon occurs in crystals of the enol of 1,3-cylcohexanedione,[162] in which the oxygens of two adjacent atoms are only 2.56 Angstroms apart.[194] The cyclic enol of acetylacetone provides another example. Here there is some controversy both in the theoretical [195-198] and experimental[199-201]literature as to whether the cyclic H-bond is truly symmetrical or slightly unsymmetrical. Even in the simple case of water dimer, electrostatic interactions provide only a fraction of the stabilizing interaction that decreases as the H-bond

becomes shorter. The implications for the interpretation of the amide I bands of peptides are evident, if not entirely new[202]. Where chains of cooperative H-bonds are prevalent, the coupling of C=O's through the H-bonds should predominate over TDC. Through H-bond coupling modifies the local geometries of the C=O's, thereby explaining the red shifts of the amide I bands in α-helices and β-sheets (as well as the blue-shifts if the amide II bands, not discussed here). In fact, H-bonding aggregation of simple amides in solution has long been known to give rise to similar red shifts.[203] This suggestion agrees with the experimental observations that the amide I bands of α-helices (which contain three chains of highly cooperative amide H-bonds10) are more red shifted that those of unfolded peptide motifs, while those of *β*-sheets (which contain stronger and shorter[111,204]H-bonds than the helices) are even more red shifted.

6.4 Conclusions

In the analysis of amide I and amide A frequencies, I found longer H-bonded chains can produce lower frequency, more intense amide I and amide A vibration peaks. When larger H-bonded chains are present, the intensities of these red shifted frequencies could dominate the spectra. The ^{14}C substitution at the C=C bonds decoupled the red shifts and the intensities of the amide I but not those of the amide A. The ^{14}C substitution at the carbon of C=O confines the vibrations to either side of the position of substitution that effectively restricts the level of delocalization and lowering the intensity of the vibration.

The coupling of both the amide I and amide A bands of H-bonded chains of 4-pyridones proceeds primarily by means of "through H-bond coupling". These results, together with those already reported for formamide chains, suggest that those similar coupling mechanisms for the amide I bands of those domains of proteins and peptides that contain significant N-H···O=C cooperative H-bonded chains. The extensive polarizations caused by cooperative H-bonded chains induce geometric perturbations of the individual 4-pyridone monomers (particularly C=O bond-lengthening) that directly explain the large red shifts of the amide I bands, similar to those observed in α-helices and β-sheets of proteins and peptides.

CHAPTER 7 – AMIDE I VIBRATIONAL FREQUENCIES OF THE HELICAL STRUCTURES WITH VARIOUS H-BOND DONOR-ACCEPTOR SEQUENCES

7.1 Introduction

It is well known that the vibrational spectrum is a powerful tool to study peptide structures, especially the secondary structures. The coupling of the frequencies and intensities of the amidic C=O stretching modes of amide I infrared absorption has been considered for this purpose.[205-208] Both the intensities and frequency shifts are sensitive to the coupling of carbonyl stretch resulting from the interaction between amidic carbonyls, either through space, hydrogen bonds, through covalent bonds, or the combination of these. A model was used by spectroscopists to assume the through bond or through space dipole-dipole coupling to be prevailing[209-211]. However, several reports have found errors within this model.[190,212,213] A recent report[191] compares the C=O stretching vibrational frequencies with through space dipole coupling (transition dipole coupling, TDC) and found the inadequacy of the TDC calculations for analyzing amide I couplings. The C=O vibrational stretching modes H-bonded chains of 4-pyridones[45] (see Chapter 6) and formamides[100] couple significantly through H-bonds than through space were also reported. These results are consistent with experimental and theoretical studies by Fillaux [203]and Torii [171].

The Amide I vibrations in models of chains of 4-pyridones were discussed in Chapter 6. In this chapter, the Amide I vibrations of several proposed structures will be

described. Those designed structures include various combinations of donor-acceptor sequence. How the frequencies and intensities of the Amide I are influenced by the addition of various spacers and the extension to form through H-bond couplings can also be observed and discussed here.

7.2 Calculation details

The calculation details are described in Chapter 1 and section 2.2. Through space dipole-dipole coupling (TDC) model analysis is not considered here because it fails to explain C=O coupling, as presented in Chapter 6 and a recent report.[191] The calculated frequencies values in this chapter are original and not modified with scaling factor 0.965.

Due to the limitation of Gaussian 03 reversion C.02 software limitation, the aim to obtain enthalpies of D-C3-A-Bz-A-C3-D, D-C3-A-Bz-D-C3-A, and A-C3-D-Bz-D-C3-A were unsuccessful. I will discuss the representative D-C3-A-C3-A-C3-D, D-C3-A-C3-D-C3-A, A-C3-D-C3-D-C3-A tetramers, since they have spacers located at both the center and the sides of the monomer.

7.3 Results and discussion

Several new structures with various donor-acceptor sequences and inserted spacer combinations will be discussed here. The interaction energies of those structures are discussed in Chapter 4. Besides the one donor-acceptor pair such as formamide and 4-pyridone, the designed structures with two pairs of donor-acceptor sequences are also illustrated in Figure 7-1. All the geometries of the structures here were discussed in the previous chapters. The "**D**" represents the H-bond donor, NH or NH_2, and the "**A**" means H-bond acceptor, **C=O**. For simplicity, the "spacer" acetylene is shortened as "**C3**" which means **C≡C**, and benzene is abbreviated as "**Bz**". Three structures illustrated in Figure 7-1 can be divided into three categories. In the first category, two pairs of donor-acceptor with one spacer in the center, those structures include D-A-C3-A-D, D-A-C3-D-A, and A-D-C3-D-A. In the second category, instead of inserting just one spacer, the C3 spacers are inserted between each donor and acceptor (three spacers overall). Those structures include D-C3-A-C3-A-C3-D, D-C3-A-C3-D-C3-A, and A-C3-D-C3-D-C3-A. The last category is similar to the second category. The only difference is the center spacer is replaced as Bz. Those structures include D-C3-A-Bz-A-C3-D, D-C3-A-Bz-D-C3-A, and A-C3-D-Bz-D-C3-A. The dimer structures and selected tetrameric structures will also be discussed here. Due to software limitations, the enthalpy calculations of category 3 (D-C3-A-Bz-A-C3-D, etc.) tetrameric structures are not feasible. In order to obtain the maximum degree of freedom and the minimum, the structures were not constrained to be symmetric.

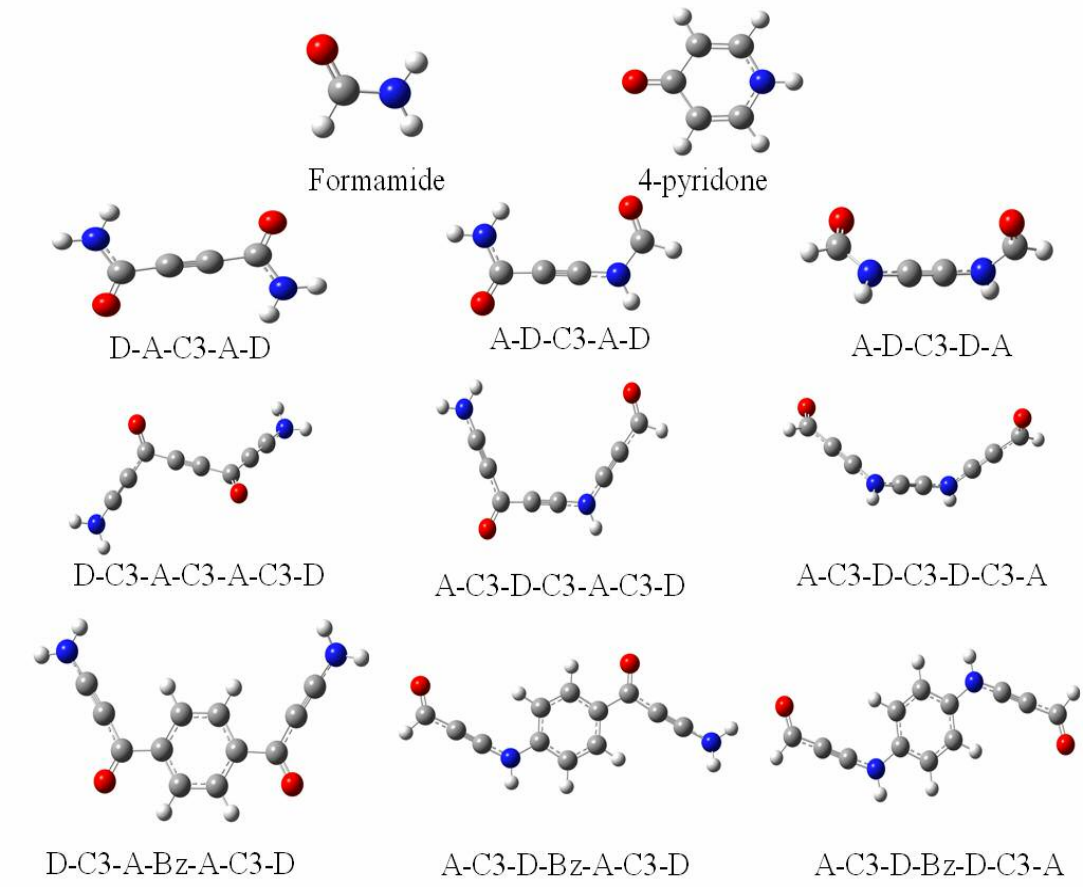

Figure 7-1. Illustration of newly designed structures with various donor-acceptor position sequences.

7.3.1 Monomers

Let us begin with the vibrations of all monomers. The intensities of calculated frequencies using the DFT method are shown in Figures 7-2~5. Generally speaking, the carbonyl shows more intense absorptions and lower frequency when the asymmetric stretch occurs. The symmetric stretches of both carbonyls possess higher frequency and a lower intensity. However, this is not always the case. When the H-bond acceptors, C=O, are attached next to the spacer (D-A-C3-A-D, D-C3-A-C3-A-C3-D, and D-C3-A-Bz-A-C3-D), the lowest frequency is the one with symmetric stretches of both C=O groups. Regarding the intensity, the lowest frequency does not show the most intense peak. In one extreme case, the D-C3-A-Bz-A-C3-D, the lowest frequency of symmetric stretch provides the most intense peak. This might be due to the motion of carbonyl is conjugated with the -C=C- π-system in the center spacer, benzene. The frequency difference is less than 3 cm^{-1}. In the D-A-C3-A-D monomer, the symmetric stretch has almost zero-intensity. Some missing C=O absorptions associated with zero-intensity are also noted in the figures.

The A-D-C3-A-D and its derivative monomers (A-C3-D-C3-A-C3-D, and A-C3-D-Bz-A-C3-D) show two observable peaks. One can easily see that the two carbonyl stretches are separated nearly 50 cm^{-1}. The absorptions peaks show the lower absorption peaks have higher intensity. However, the most intense peak of A-C3-D-Bz-A-C3-D monomer is the one with the second lowest frequency. In addition, the separation of two carbonyl stretches is shortened nearly 30 cm^{-1}. This might be due to the conjugation with rigid benzene spacers.

The A-D-C3-D-A, A-C3-D-C3-D-C3-A, and A-C3-D-Bz-D-C3-A) monomers show two observable absorptions (the A-C3-D-Bz-D-C3-A monomer is an exception). The most intense peak is found at the lowest frequency (asymmetric stretch), and the second lowest frequency (symmetric stretch) has the intensity about 60% of the most intense peak. With the spacers are inserted, the frequency difference between the two carbonyls is shortened (from about 10 to 3 cm^{-1}). In the A-C3-D-Bz-D-C3-A monomer, the lowest frequency still corresponds to the higher intensity peak, but the intensity of the second lowest frequency is almost zero. This is due to the most stable geometry is changed to a planar structure, when the benzene spacer is inserted. This planar structure with two equivalent C=O group point toward different directions, thus the changes in dipole moment is reduced when vibrates.

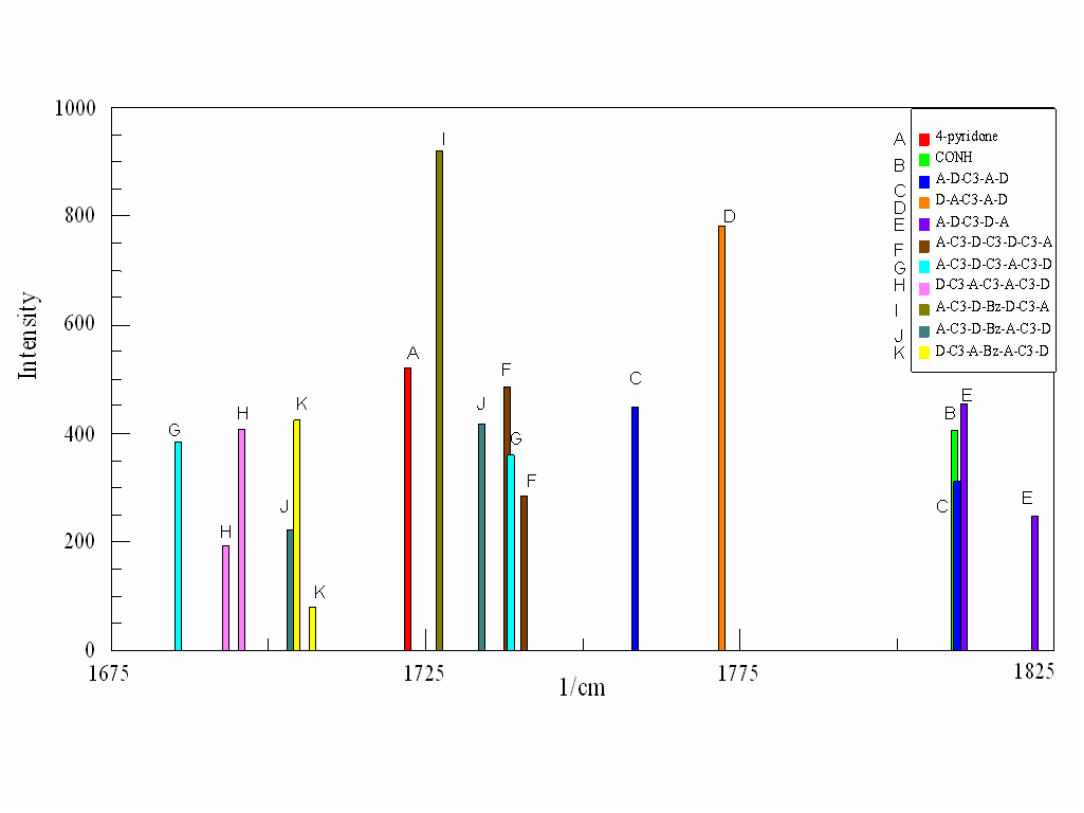

Figure 7-2. The C=O absorptions of newly designed monomers with various donor-acceptor position sequences.

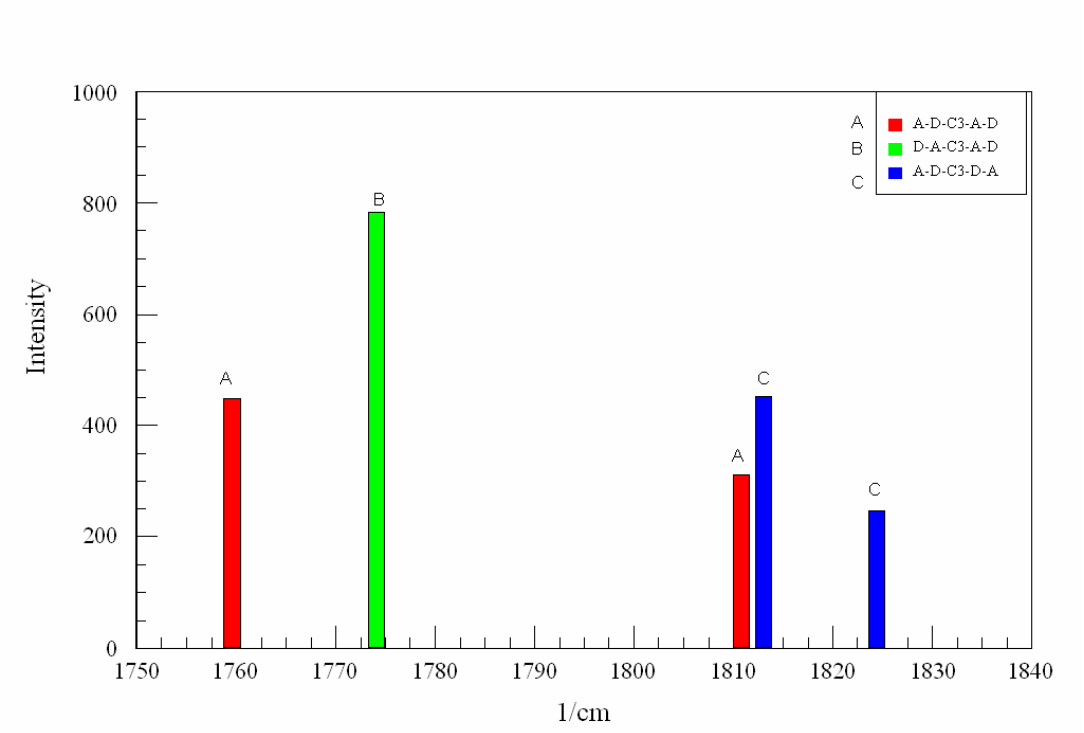

Figure 7-3. The C=O absorptions of D-A-C3-A-D, D-A-C3-D-A, A-D-C3-D-A (category 1) with various donor-acceptor position sequences. The zero-intensity C=O absorption of D-A-C3-A-D locates at 1668 cm^{-1}.

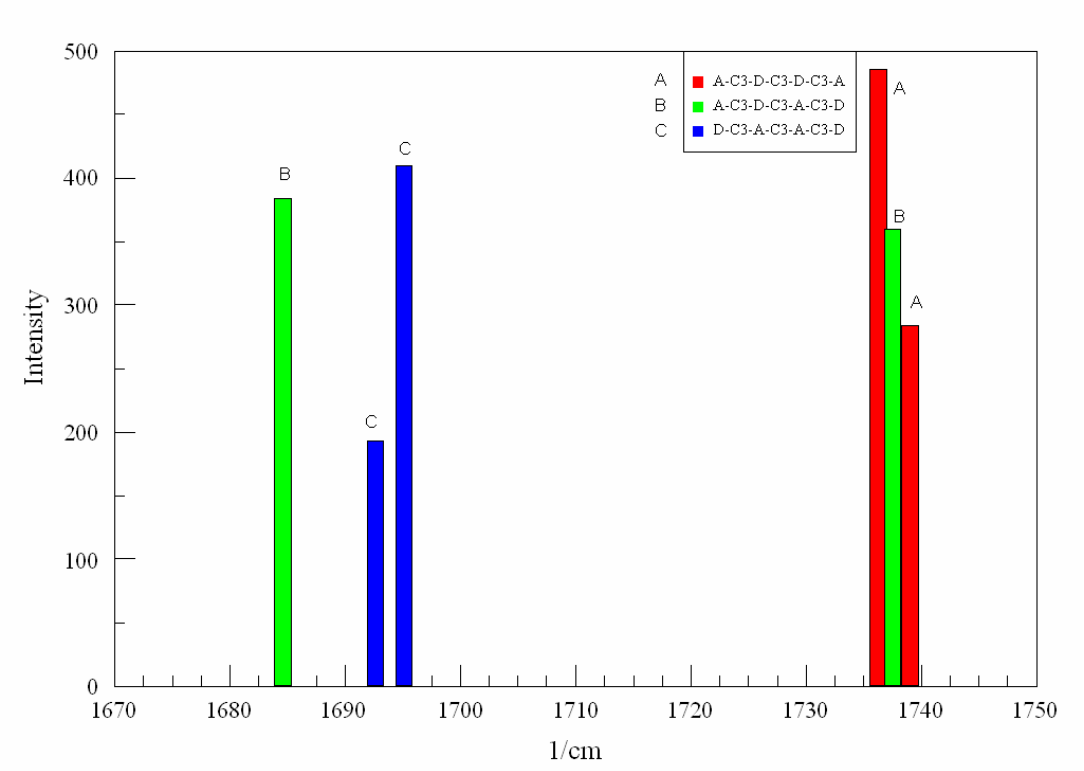

Figure 7-4. The C=O absorptions of D-C3-A-C3-A-C3-D, D-C3-A-C3-D-C3-A, A-C3-D-C3-D-C3-A (category 2) with various donor-acceptor position sequences.

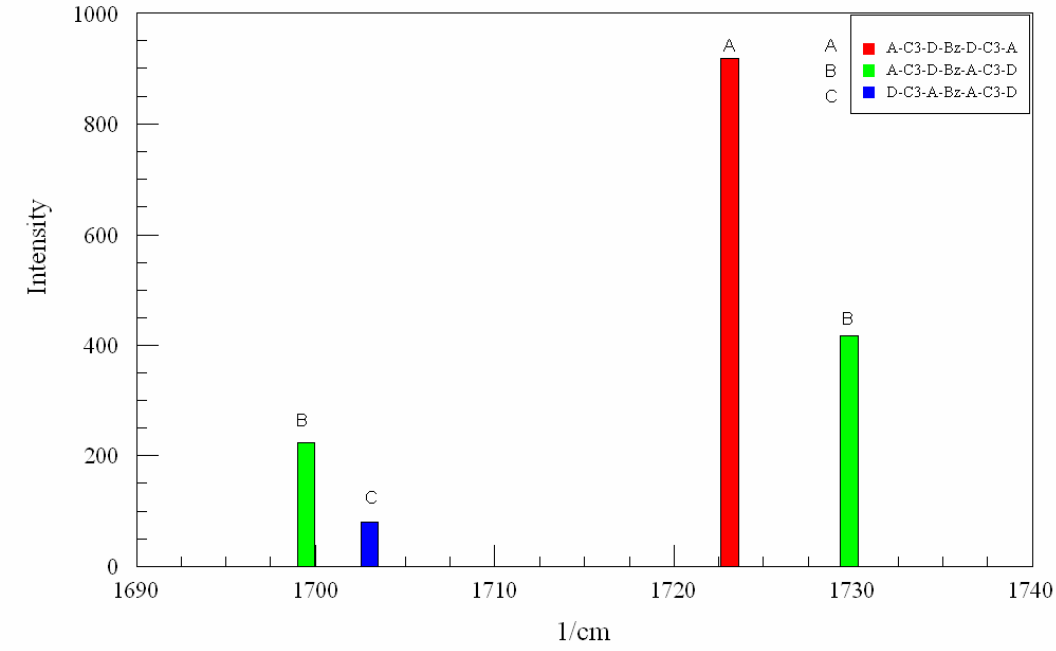

Figure 7-5. The C=O absorptions of D-C3-A-Bz-A-C3-D, D-C3-A-Bz-D-C3-A, A-C3-D-Bz-D-C3-A (category 3) with various donor-acceptor position sequences**.** A C=O absorption of A-C3-D-Bz-D-C3-A with intensity = 0 locates at 1726 cm^{-1} and D-C3-A-Bz-A-C3-D Intensity = 81 at 1702 cm^{-1}.

7.3.2 The A-D-C3-A-D dimers

Each monomer discussed previously can form more than two different dimers. Those dimers can be planar β-sheets or twisted α-helices. Figure 7-6 illustrates the C=O absorptions of A-D-C3-A-D dimers including the small ring dimer (S), the large ring dimer, the large ring and one small ring mixed dimer (SL), and the trans dimer (Trans refers the position of $-NH_2$ in the head to head dimer). The corresponding structures have been shown in the previous chapter. The most red-shifted peaks are H-bonded to C=O with higher intensity. Four absorption peaks can be observed with some exceptions. In the small ring and trans dimers, the carbonyls are aligned anti-parallelly to each other thus reducing the changes of dipole moment. Therefore, intensities of the two intermolecular symmetry modes are zero. A pattern is shown in the four observable peaks of the SL dimer. Within these four peaks, the most (1724 cm^{-1}, 749 km/mol) and second most (1789 cm^{-1}, 742 km/mol) intense peaks are associated with H-bonded inter strand symmetric C=O stretch modes. The other two peaks with weaker intensities are the inter strand asymmetric peaks. The trans dimer absorption peaks also possess similar patterns. However, the most intense peaks are found when the C=O are located at the end with only one side linked to H atoms.

The most red-shifted is the small ring dimer, which also contains the strongest H-bond (ΔH = -21.98 kcal/mol) interaction. The second most red-shifted one is the SL dimer (ΔH = -11.42), the third most red-shifted one is the Trans dimer (ΔH = -9.24), and the least red-shifted one is the LR dimer (ΔH = -6.00). The stronger the H-bond interaction is, the more red-shifted it is.

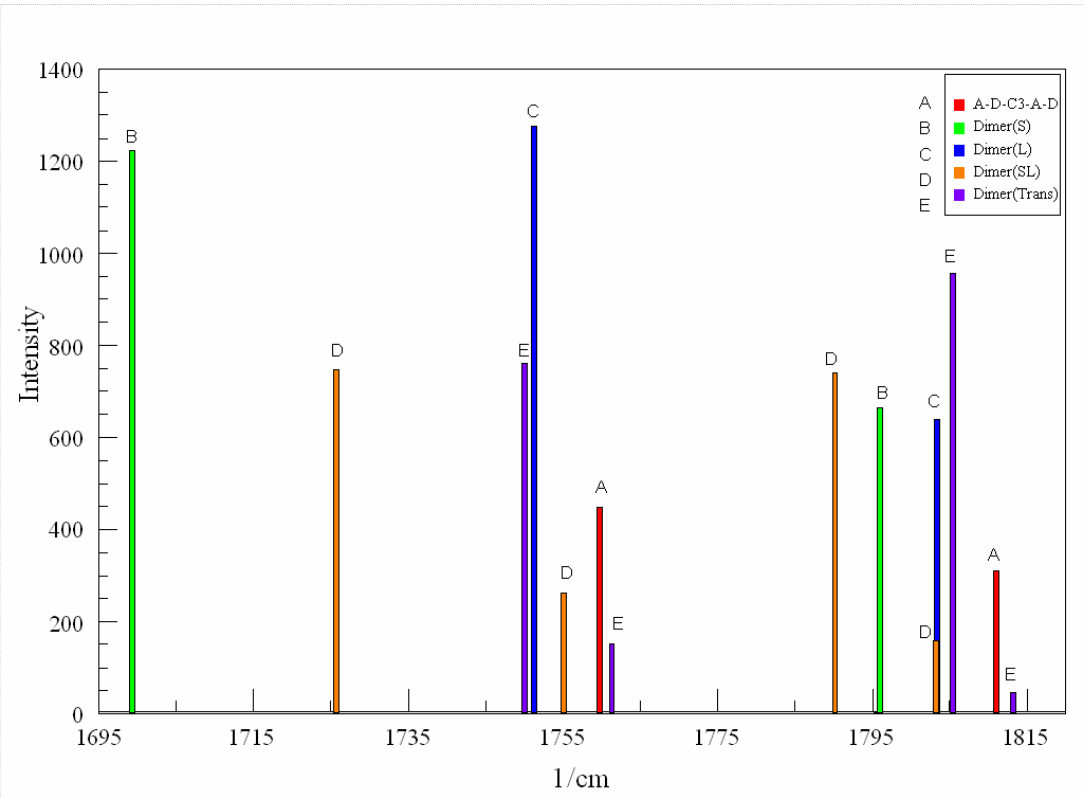

Figure 7-6. The C=O absorptions of A-D-C3-A-D dimers. A-D-C3-A-D monomer shown as red lines, small ring dimer (S) shown as green lines, large ring dimer shown as blue lines, mixed dimer (SL) shown as orange lines, and the trans dimer shown as purple lines.

7.3.3 The D-A-C3-A-D dimers

Figure 7-7 illustrates the C=O absorptions of the D-A-C3-A-D dimers including the trans (Trans) and cis (Cis) dimers (trans refers to the two carbonyls are parallel to each other and point toward opposite directions). The corresponding structures were shown in Chapter 4. The monomer shows one observable peak, due to the other absorption with asymmetric C=O stretch. Both dimers show four observable peaks, with different patterns. The most intense absorptions are not the most red-shifted frequencies but the second lowest frequencies. In the trans dimer the most intense absorption is the inter and *intra*strand asymmetric C=O stretch and of the cis dimer, the most intense absorption is the inter strand symmetric and *intra*strand asymmetric C=O stretch. The pattern of intensity of the two higher frequencies is different between the cis and trans dimer. In the trans dimer the third lowest frequency is the one with the most intense peak, but in the cis dimer, the most intense peak is located at the second lowest frequency. The more intense intensities in those two frequencies are both asymmetric C=O stretches between strands. It shows symmetric *intra*strand motion within the trans dimer, but the *intra*strand motion is asymmetric in the cis dimer.

The most red-shifted C=O stretch comes from the trans dimer with stronger H-bond interaction (Trans ΔH = -11.82; Cis ΔH = -7.48). This correlates well with stronger H-bond interaction with more red-shifted condition in A-D-C3-A-D dimers.

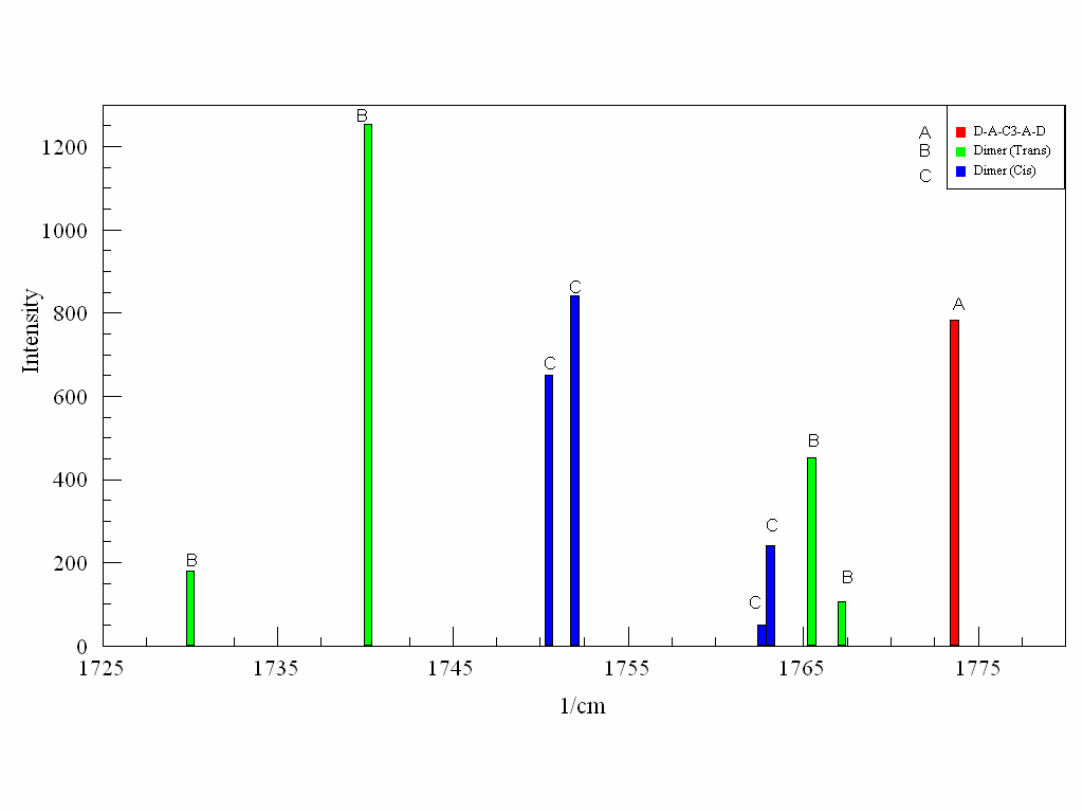

Figure 7-7. The C=O absorptions of D-A-C3-A-D dimers. The D-A-C3-A-D monomer shown as red lines, the trans dimer (Trans) shown as green lines, and the cis dimer (Cis) shown as blue lines.

7.3.4 The A-D-C3-D-A dimers

Figure 7-8 illustrates the C=O absorptions of the A-D-C3-D-A dimers including the trans (Trans) and cis (Cis) dimers (trans refers to the two carbonyls are parallel to each other and point toward opposite directions). Both dimers show four observable peaks with different patterns. The most intense absorption peaks are those of the C=O's associated with H-bonding. The trans dimer has one very intense absorption peak, along with another lower and two very low peaks. The cis dimer shows a pattern of a strong peak, two lower absorptions with one stronger than the other by roughly 150 km/mol, and a very weak peak. The most intense absorption in the cis dimer is the *inter* and *intra*strand symmetric motion. However, the most intense absorption in the tran dimer is the both *inter* and *intra*strand asymmetric motion. The lower frequencies of the cis and the trans dimers correspond to the antisymetric motion between strands and symmetric motion within a strand.

The most red-shifted C=O stretch comes from the trans dimer with the stronger H-bond interaction (Trans: ΔH = -14.57; Cis: ΔH = -5.82) in the dimeric isomers. This correlates well with stronger H-bond interaction with more red-shifted condition in A-D-C3-A-D and D-A-C3-A-D dimers.

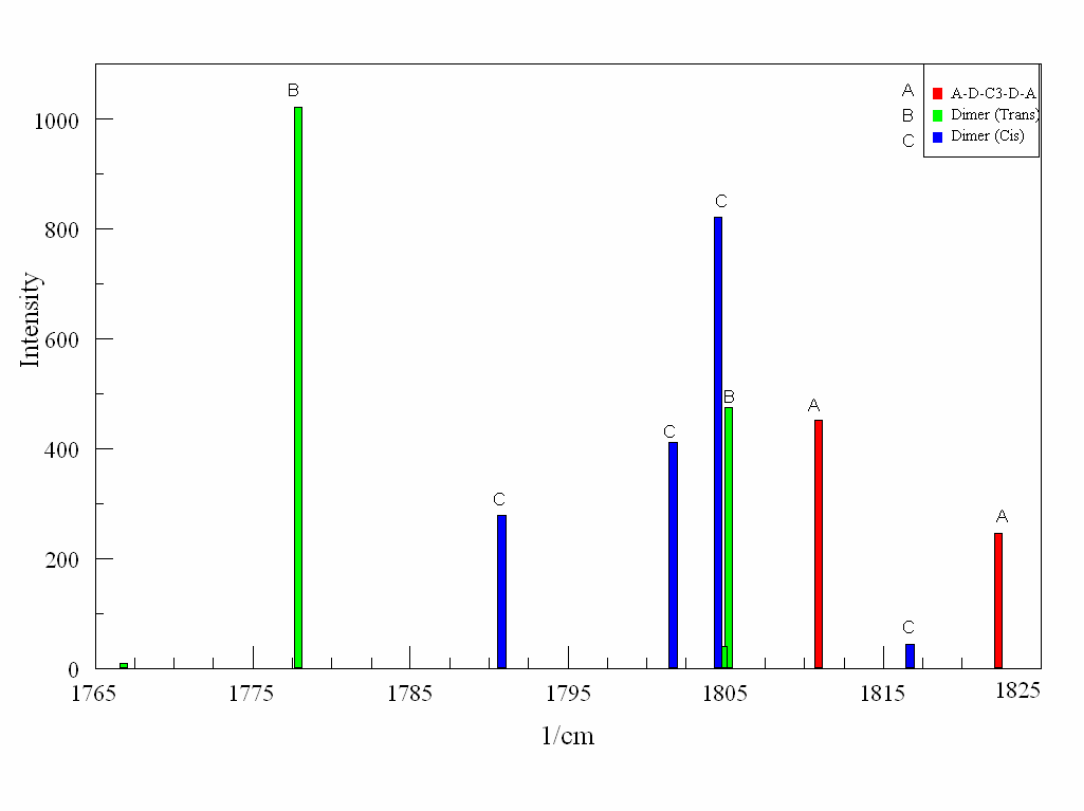

Figure 7-8. The C=O absorptions of A-D-C3-D-A dimers. The A-D-C3-D-A monomer shown as red lines, the trans dimer (Trans) shown as green lines, and the cis dimer (Cis) shown as blue lines.

7.3.5 The A-C3-D-C3-A-C3-D dimers

Figure 7-9 illustrates the C=O absorptions of the A-C3-D-C3-A-C3-D dimers including the trans (Trans) and cis (Cis) dimers. Both dimers show four observable peaks with similar patterns. The four absorption peaks in the trans dimer are separated into lower and higher frequency groups. There is a difference less than 10 cm^{-1} between the lower and higher frequency groups. The four peaks in the cis dimer are more separated than those in the trans dimer. The lowest frequencies are the most red-shifted due to H-bonding, but those frequencies do not correspond to the most intense absorption. The lowest frequency in the cis dimer is the one with *inter* and *intra*strand C=O symmetric motions. In the trans dimer, the lowest frequency is the one with *inter* strand C=O symmetric and *intra*strand asymmetric motion. The most intense absorption peaks are those corresponding to the C=O's associated with H-bonding. Two higher intensity and two lower intensity peaks are observed in both dimers. The most intense absorption in the trans dimer is the one with the *inter* and *intra*strand C=O symmetric motion. In the cis dimer, the highest intensity is the one with *inter* strand C=O symmetric and *intra*strand asymmetric motion.

The cis dimer (Cis) is the one with stronger H-bond interaction (Trans ΔH = -10.10; Cis ΔH = -14.69) in the dimeric isomers. This dimer also shows more red-shifted C=O frequencies than the trans dimer.

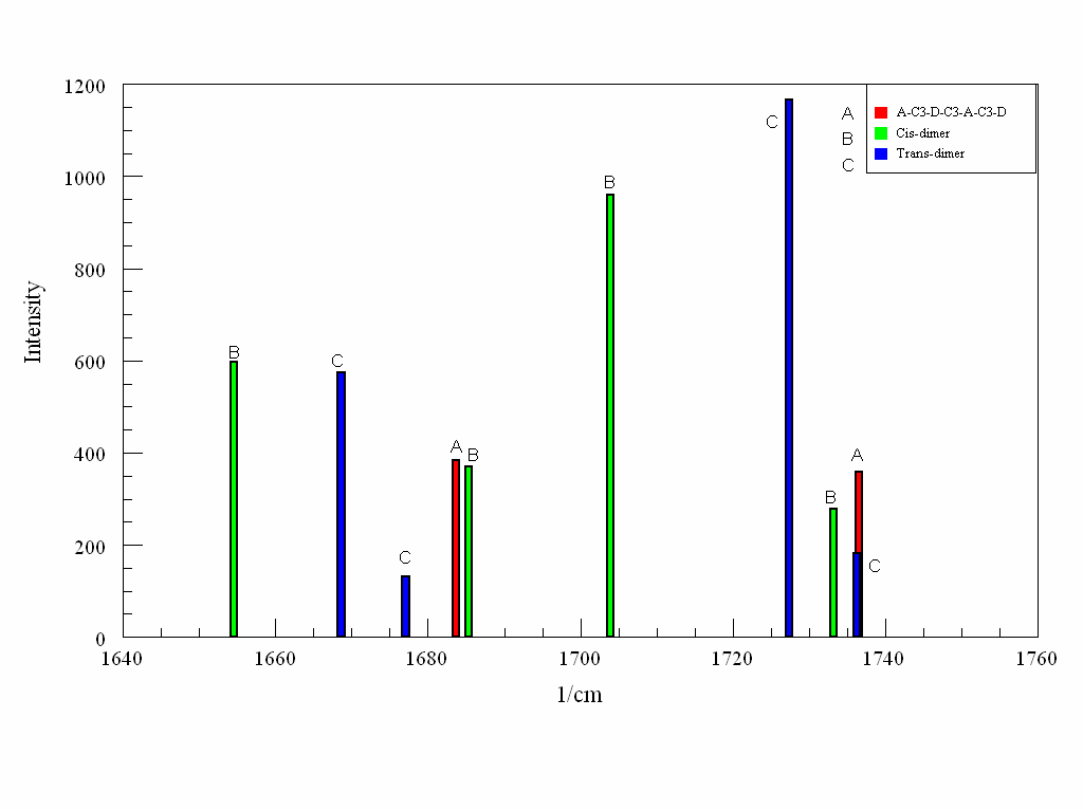

Figure 7-9. The C=O absorptions of A-C3-D-C3-A-C3-D dimers. The A-C3-D-C3-A-C3-D monomer shown as red lines, the cis dimer (Cis) shown as green lines, and the trans dimer (Trans) shown as blue lines.

7.3.6 The D-C3-A-C3-A-C3-D dimers

Figure 7-10 exhibits the C=O absorptions of D-C3-A-C3-A-C3-D dimers including the trans (Trans) and cis (Cis) dimers. While the trans dimer shows four observable peaks, the cis dimer has only two. It should be noted that the optimized cis dimer geometry with four H-bonds was used, not the usual geometry with two H-bonds. The intensities in the cis dimer are much weaker than those in the trans dimer due to its association with $-NH_2$ in H-bonds. The spectra are more complicated and should not be considered as a normal dimer structure with 2 H-bonds. In the trans dimer, the most intense absorption peak is not the one with the lowest frequency rather than the highest intensity peak is the H-bonded to both the *inter* and *intra*strand asymmetric C=O stretch. The lowest frequency in the trans dimer is the one corresponding to the *inter* strand C=O asymmetric and *intra*strand symmetric motions.

In these dimers, the trans dimer is the one with stronger H-bond interaction (Cis ΔH = -11.02; Trans ΔH = -16.16). This dimer also shows more red-shifted C=O frequencies.

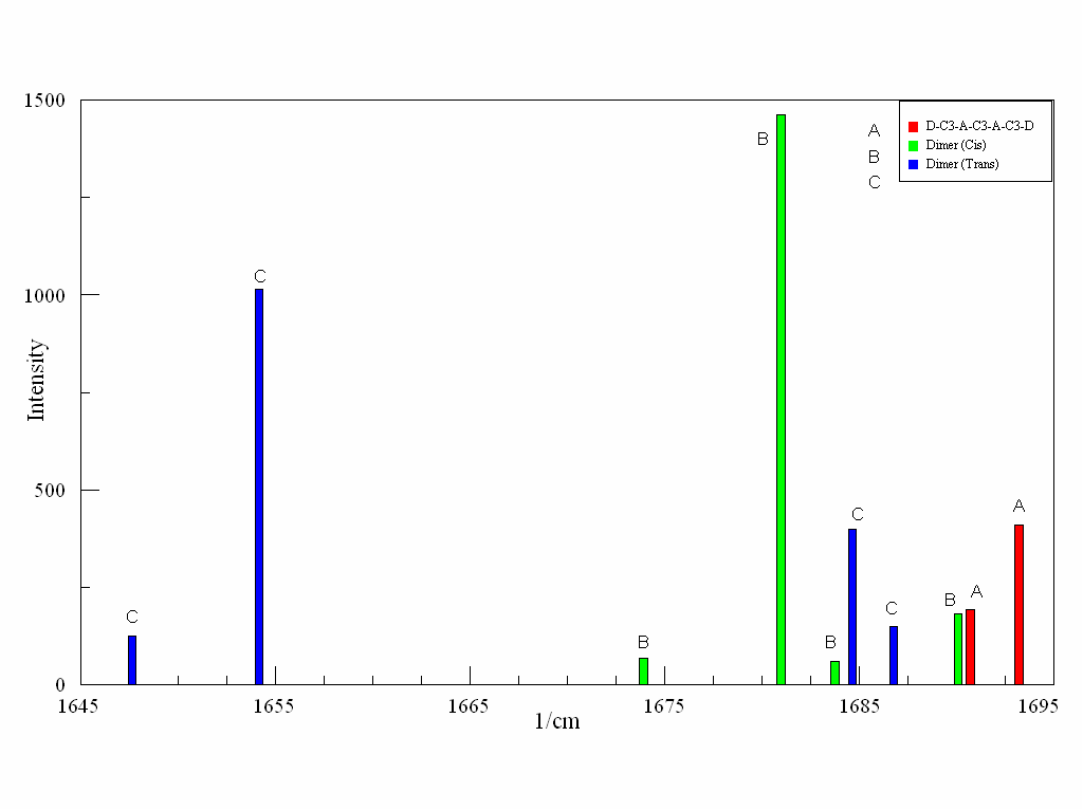

Figure 7-10. The C=O absorptions of D-C3-A-C3-A-C3-D dimers. The D-C3-A-C3-A-C3-D monomer shown as red lines, the cis dimer (Cis) shown as green lines, and the trans dimer (Trans) shown as blue lines.

7.3.7 The A-C3-D-C3-D-C3-A dimers

Figure 7-11 illustrates the C=O absorptions of A-C3-D-C3-D-C3-A dimers including the trans (Trans) and cis (Cis) dimers. Both dimers show four observable peaks, and similar patterns are observed with some exceptions. They have two higher intensity peaks and two lower intensity peaks, but with a different order of the two higher frequencies. In the trans dimer, the more intense peak among the two higher frequency absorptions is the one with *inter*strand symmetric and *intra*strand asymmetric motion. In the cis dimer, the more intense peak is the one with *inter*strand asymmetric and *intra*strand asymmetric motion. The most intense peaks for both dimers are the second most red-shifted peaks. In the cis dimer, the most intense peak is the H-bonded one with *inter*strand symmetric and *intra*strand asymmetric motion. In the trans dimer, the most intense peak is the H-bonded one with *inter* and *intra*strand asymmetric motion.

Unlike the monomer, the lowest C=O frequency (asymmetric motion) is the one with the second lowest intensity. In these tetramers, the most intense peaks are both at the second lowest frequencies. In the trans dimer, the intensity of the most red-shifted peak is even the weakest among the four observable peaks. The second and third most red-shifted peaks are separated more in the trans dimer than the cis dimer. In the trans dimer, they are separated nearly 40 cm^{-1}. However, in the cis dimer, they are separated only nearly 20 cm^{-1}.

In these dimers, the trans dimer is the one with the stronger H-bond interaction (Cis ΔH = -12.71; Trans ΔH = -17.57). Again it is the one with more red-shifted C=O stretching mode.

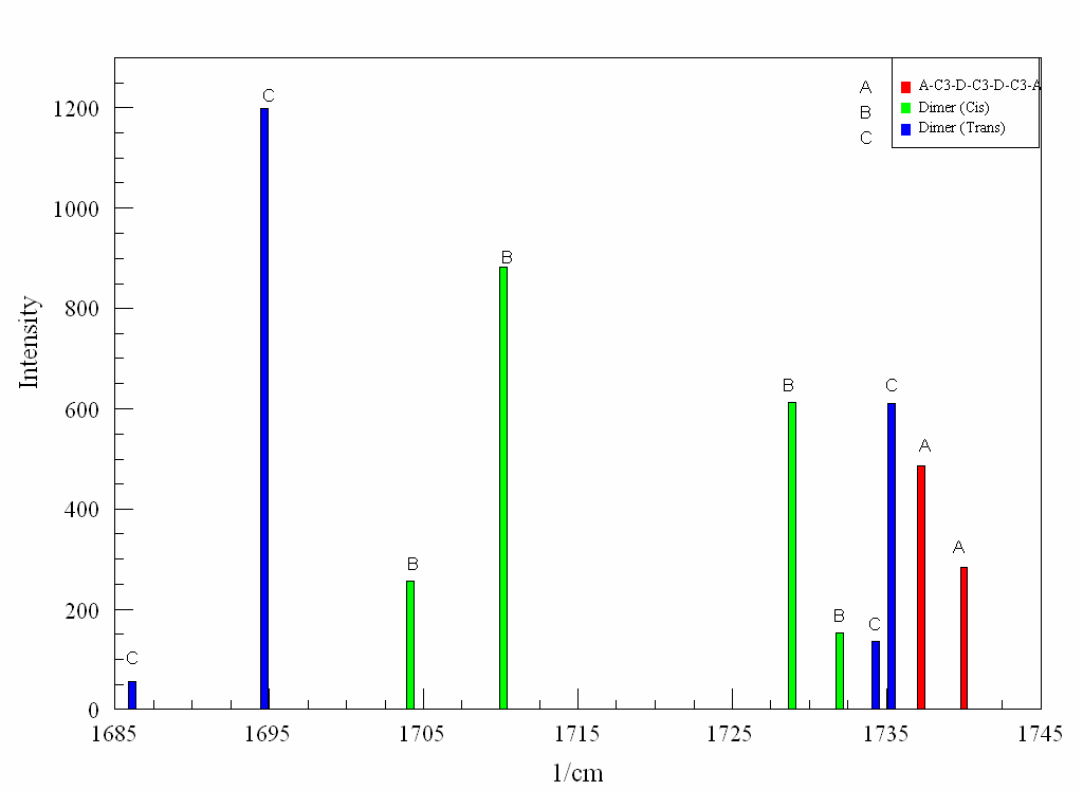

Figure 7-11. The C=O absorptions of A-C3-D-C3-D-C3-A dimers. The A-C3-D-C3-D-C3-A monomer shown as red lines, the cis dimer (Cis) shown as green lines, and the trans dimer (Trans) shown as blue lines.

7.3.8 The D-C3-A-Bz-A-C3-D dimers

Figure 7-12 illustrates the C=O absorptions of D-C3-A-Bz-A-C3-D dimers including the trans (Trans) and cis (Cis) dimers. The cis dimer has four observable peaks, while the trans dimer only has two observable peaks. The most red-shifted peaks of both dimers are again those with the highest intensities. In the cis dimer, the most intense peak is the H-bonded with *inter* and *intra*strand symmetric motions. In the trans dimer, the most intense peak is the H-bonded with *inter* and *intra*strand asymmetric motions. Compared with the D-C3-A-C3-A-C3-D dimers in Figure 7-10, the most intense peaks in these dimers are not the most red-shifted but those with the second lowest frequencies. The most and the second most intense peaks are more separated in the D-C3-A-Bz-A-C3-D dimers than those in the D-C3-A-C3-A-C3-D dimers. The lowest frequencies of the D-C3-A-Bz-A-C3-D dimers are lower than those of the D-C3-A-C3-A-C3-D dimers. This different behavior might be due to the influence associated with the -C=C- stretching of the benzene ring.

In these dimers, the trans dimer has stronger H-bond interaction (Cis ΔH = -11.06; Trans ΔH = -14.22). This also shows more red-shifted C=O frequencies.

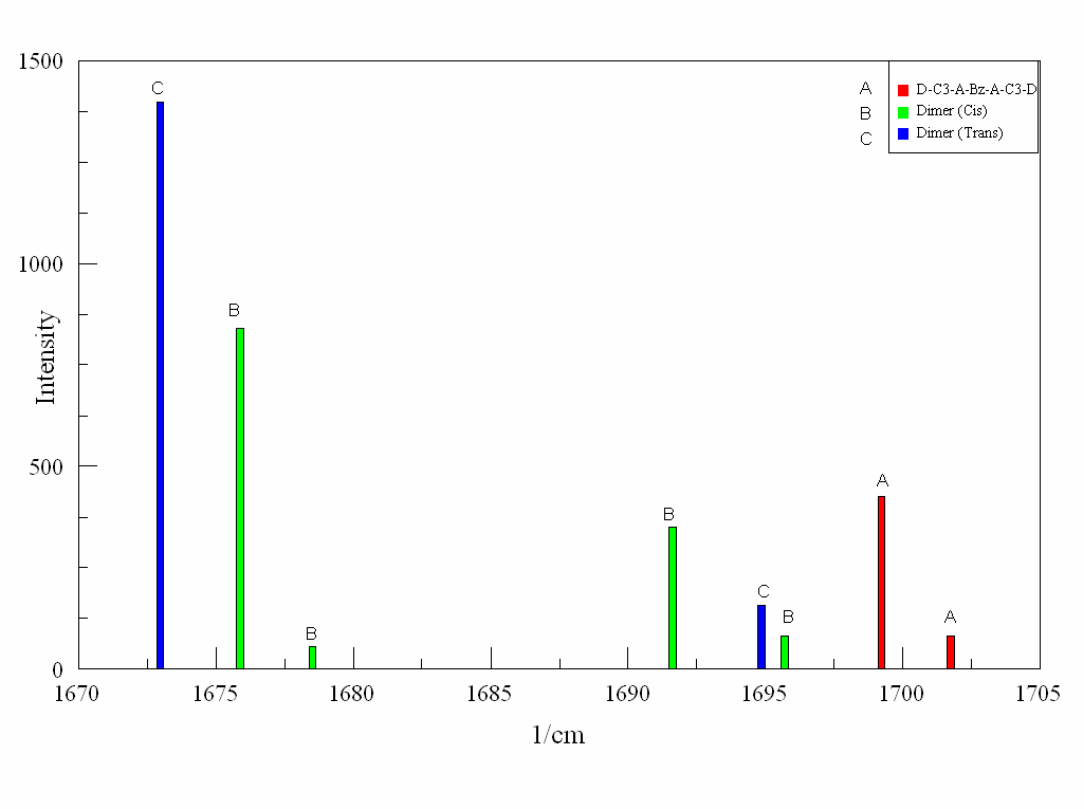

Figure 7-12. The C=O absorptions of D-C3-A-Bz-A-C3-D dimers. The D-C3-A-Bz-A-C3-D monomer shown as red lines, the cis dimer (Cis) shown as green lines, and the trans dimer (Trans) shown as blue lines.

7.3.9 The A-C3-D-Bz-D-C3-A Dimers

Figure 7-13 illustrates the C=O absorptions of the A-C3-D-Bz-D-C3-A dimers including the trans (Trans) and cis (Cis) dimers. The patterns of the dimers are similar to the A-C3-D-Bz-D-C3-A dimers with the most intense peaks not being the lowest but the second lowest frequency. The cis dimer has four observable peaks with the trans dimer only having two observable peaks. The most red-shifted peaks of both dimers are not those with the highest intensities rather than those with the second lowest frequencies. In the cis dimer, the most intense peak is the H-bonded one with *inter* and *intra*strand symmetric motions. In the trans dimer, the most intense peak is the H-bonded *inter* and *intra*strand asymmetric motion. The second most intense peak in the trans dimer is the *inter* asymmetric and intra symmetric motion. The second most intense peak is the *inter* and intra symmetric motion. Compared with the A-C3-D-C3-D-C3-A structures in Figure 7-11, the monomer of A-C3-D-C3-D-C3-A has two peaks but the A-C3-D-Bz-D-C3-A monomer only has one peak because the insertion of benzene rings leads to a planar structure as the most stable A-C3-D-Bz-D-C3-A monomer. When the C=O's in the planar structure are aligned toward different directions with and the symmetric motion, the observed intensity is zero.

In these dimers, the trans dimer is the one with stronger H-bond interaction (Cis ΔH = -9.98; Trans ΔH = -14.85). It also shows more red-shifted C=O stretching mode. The trans dimer has two zero-intensity peaks at 1693 and 1674 cm^{-1}.

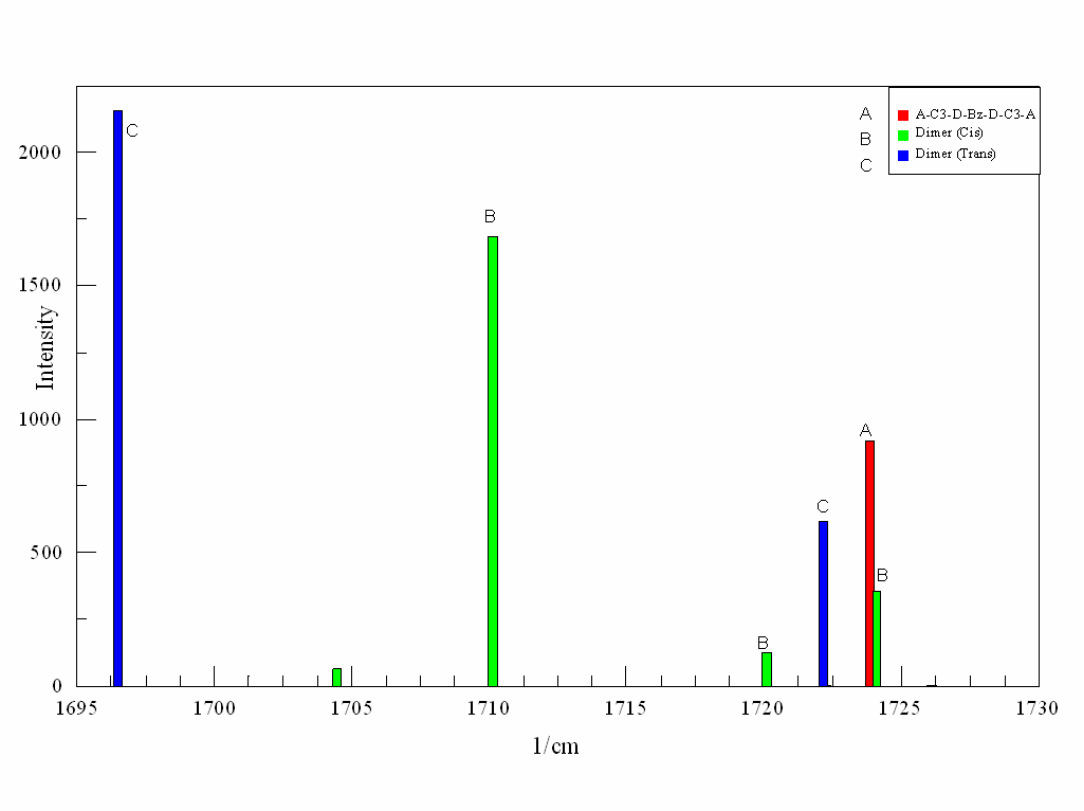

Figure 7-13. The C=O absorptions of A-C3-D-Bz-D-C3-A dimers. The A-C3-D-Bz-D-C3-A monomer shown as red lines, the cis dimer (Cis) shown as green lines, and the trans dimer (Trans) shown as blue lines. The trans dimer with two zero-intensity peaks at 1693 and 1674 cm^{-1}.

7.3.10 The A-C3-D-Bz-A-C3-D dimers

Figure 7-14 illustrates the C=O absorptions of A-C3-D-Bz-A-C3-D dimers including the trans (Trans) and cis (Cis) dimers. The patterns of these dimers are neither similar to each other nor to their A-C3-D-C3-A-C3-D derivatives. The most intense peaks are not the lowest but the second lowest frequency in the cis, and the third lowest frequency in the trans. Both dimers have four observable peaks. The most red-shifted peaks of both dimers correspond to the second highest intensities. In the cis dimer, the most intense peak is the H-bonded with *inter* and *intra*strand symmetric motions. In the trans dimer, the most intense peak is the H-bonded one with *inter* and *intra*strand symmetric motions. The monomers of the cis dimer are perpendicular to each other, which shows a significant C=O absorptions relative to the planar A-C3-D-C3-A-C3-D. The second most intense peak in the trans dimer has *inter* asymmetric and intra symmetric motion. The second most intense peak has *inter* and intra symmetric motion. Compared with the A-C3-D-C3-A-C3-D structures in Figure 7-9, the monomer of A-C3-D-Bz-A-C3-D is more red-shifted than the A-C3-D-C3-D-C3-A monomer. The most intense peak in the trans dimer of A-C3-D-C3-D-C3-A is the one with the third lowest frequencies. This is also the same in the A-C3-D-Bz-A-C3-D trans dimer. The cis structures absorption peaks difference of A-C3-D-C3-D-C3-A and A-C3-D-Bz-A-C3-D dimers is due to the planar (A-C3-D-C3-D-C3-A) and perpendicular (A-C3-D-Bz-A-C3-D) geometry changes. The cis dimer is the one with stronger H-bond interaction (Cis ΔH = -14.77; Trans ΔH = -11.16) and the more red-shifted C=O stretching mode.

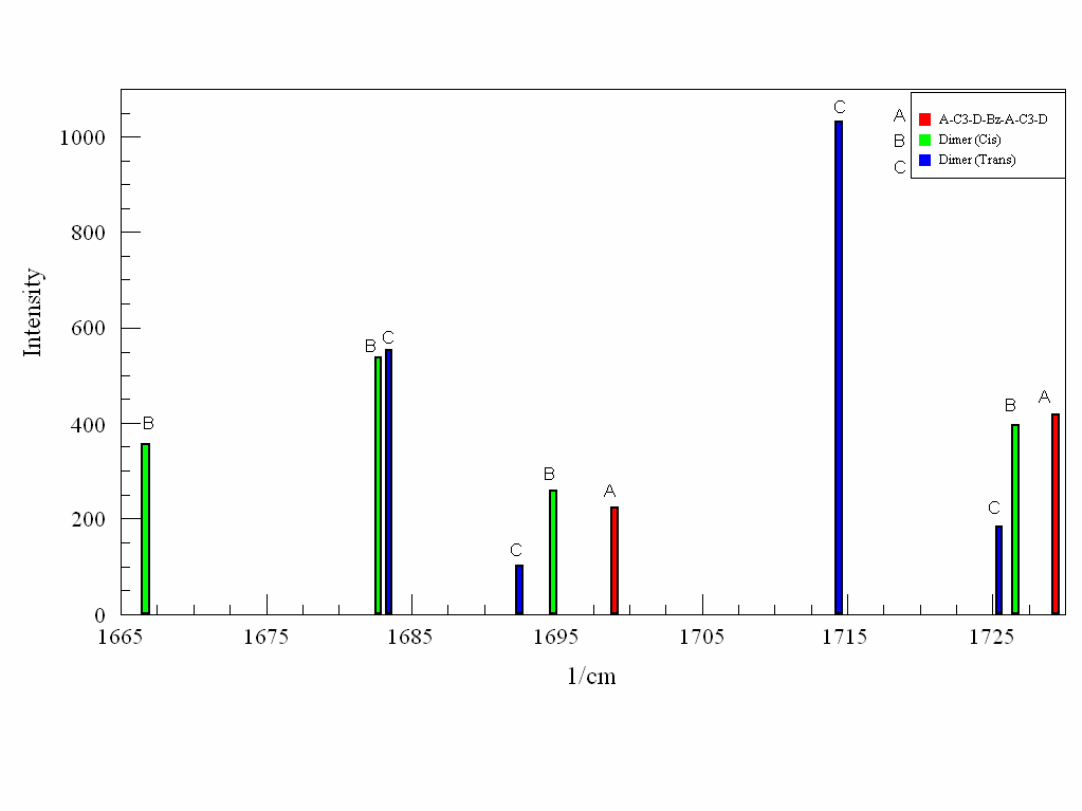

Figure 7-14. The C=O absorptions of A-C3-D-Bz-A-C3-D dimers. The A-C3-D-Bz-A-C3-D monomer shown as red lines, the cis dimer (Cis) shown as green lines, and the trans dimer (Trans) shown as blue lines.

7.3.11 The tetramers

Due to the limitation of the 32-bit Gaussian 03 software, the frequency calculations for all the tetramers are not achievable. I only discuss the representative D-C3-A-C3-A-C3-D, D-C3-A-C3-D-C3-A, A-C3-D-C3-D-C3-A tetramers in this section. Those tetramers are chosen because they are the tetrameric structures with both donor-acceptor combinations and the spacers in each monomer that the results of frequency analysis are available. The geometric and energetic analysis of these structures were discussed and depicted in Chapter 4.

7.3.12 The D-C3-A-C3-A-C3-D tetramers

Figure 7-15 depicts the C=O absorptions of the D-C3-A-C3-A-C3-D tetramers including the trans (Trans) and cis (Cis) tetramers. Both tetramers show more than eight C=O stretching absorptions, the extra numbers of absorptions come from the C=O stretching absorption peaks associated with the N-H_2 scissoring about 1600 ~ 1700 cm^{-1}. Separating completely the pure C=O stretching mode and the combination with N-H_2 scissoring absorptions is difficult. One can predict how many absorption peaks will be available in these two tetramers. Since there are eight N-H_2 scissoring and eight C=O stretching modes in the tetramers, therefore 16 possible C=O modes can be expected. The 1618 cm^{-1} absorption in the cis tetramer is due to the non H-bonded N-H_2 scissoring mode. Regarding the red-shift of C=O stretching, one should not consider this peak, since no H- bond is involved in this frequency. In Figure 7-15, the trans tetramer has stronger H-bond interaction (Cis ΔH = -39.41; Trans ΔH = -53.49) and more red-shifted C=O stretching mode. Because both tetramers are not planar but helical-like, the most intense C=O stretching absorption in the cis tetramer corresponds to the one when all C=O stretch symmetrically (1659 cm^{-1}). The most intense C=O stretching absorption in trans tetramer is the one corresponding to an asymmetric C=O stretching mode at 1630 cm^{-1}.

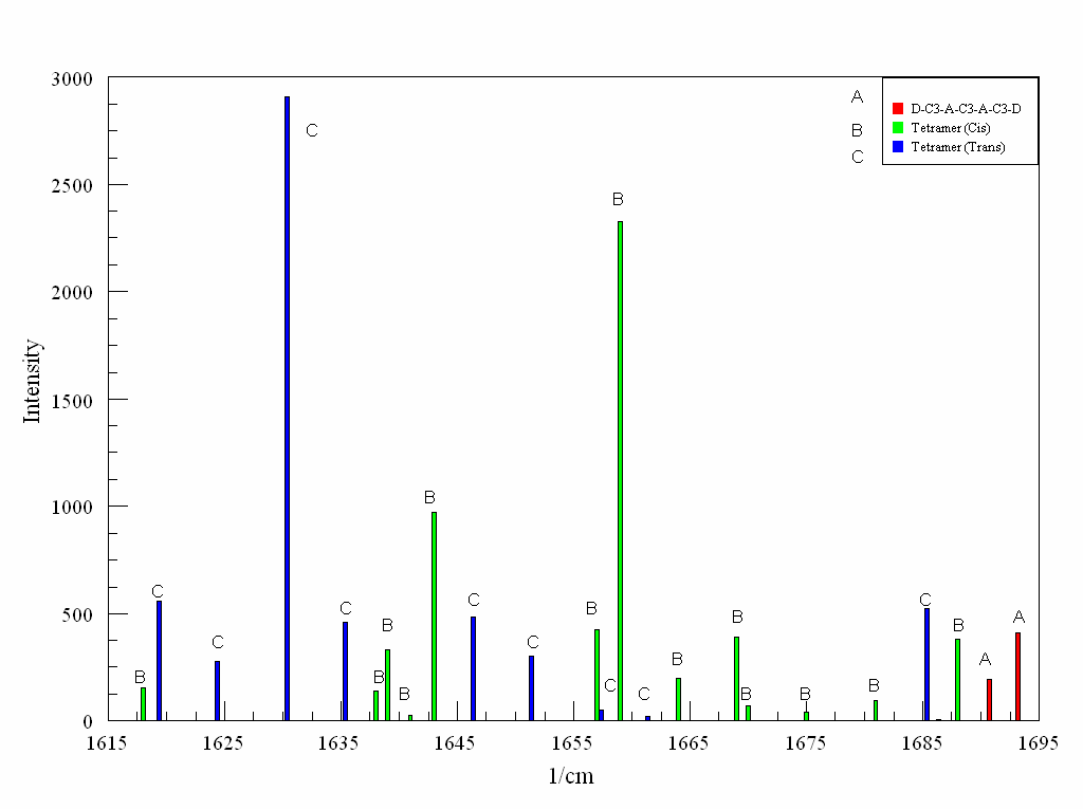

Figure 7-15. The C=O absorptions of D-C3-A-C3-A-C3-D tetramer. The D-C3-A-C3-A-C3-D monomer shown as red lines, the cis dimer (Cis) shown as green lines, and the trans dimer (Trans) shown as blue lines. The arrow shows non H-bonded NH_2 scissoring mode in the cis tetramer.

7.3.13 The A-C3-D-C3-D-C3-A tetramers

Figure 7-16 depicts the C=O absorptions of A-C3-D-C3-D-C3-A tetramers including the trans (Trans) and cis (Cis) tetramers. Both tetramers show eight C=O stretching absorptions. This is not similar to the previously described structures where the C=O stretching is conjugated with N-H_2 scissoring. This is due to no available N-H_2 scissoring mode is in the monomer. The cis tetramer shows helical structure, and the caged-like trans structure. The most intense C=O stretching absorption in the cis tetramer corresponds to the one when all C=O groups have symmetric stretching (1688 cm^{-1}). The most intense C=O stretching absorption in trans tetramer is the one with an asymmetric C=O stretching mode at 1685 cm^{-1}. Because the trans tetramer is a non-planar caged-like structure, each C=O shows similar intensity. The most intense C=O absorption in the cis tetramer is about 3.5 times higher than that in the trans tetramer, because the helical structure can provide better C=O's alignment that can increase the intensity.

As shown in Figure 7-15, the trans tetramer has stronger H-bond interaction (Cis ΔH = -43.26; Trans ΔH = -60.77) and is the one with more red-shifted C=O stretching mode. However, the intensity is much weaker to those in the cis one.

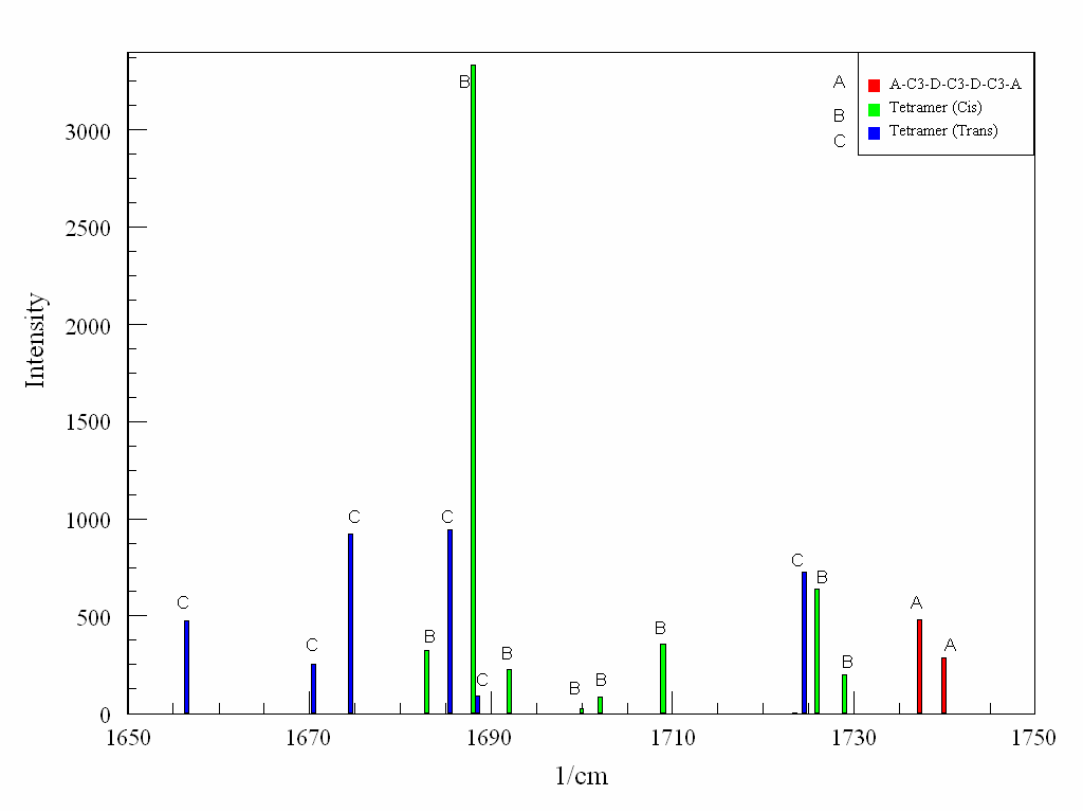

Figure 7-16. The C=O absorptions of A-C3-D-C3-D-C3-A tetramer. The A-C3-D-C3-D-C3-A monomer shown as red lines, the cis dimer (Cis) shown as green lines, and the trans dimer (Trans) shown as blue lines.

7.3.14 The A-C3-D-C3-A-C3-D tetramers

Figure 7-17 depicts the C=O absorptions of the A-C3-D-C3-A-C3-D tetramers including the trans (Trans) and cis (Cis) tetramers. Both tetramers show more than eight C=O stretching absorptions peaks. The extra numbers of absorptions come from the C=O stretching associated with the N-H_2 scissoring around 1600~1700 cm^{-1}. The number of peaks can be predicted in these two tetramers. Since there are four N-H_2 scissoring and eight C=O stretching modes, we can expect 12 peaks in those tetramers. It is shown in Figure 7-17.

Both tetramers are planar. The most intense C=O stretching absorption in the cis tetramer corresponds to the C=O symmetric stretching at 1689 cm^{-1} where the C=O interacts with N-H (not associated with N-H_2 scissoring). The second most intense C=O symmetric stretching associated with N-H_2 scissoring.

The most intense C=O stretching absorption in trans tetramer is the one with asymmetric C=O stretching mode at 1704 cm^{-1} with C=O interact with N-H (not associated with N-H_2 scissoring). This peak is about 1.5 times stronger than the most intense peak in the cis tetramer.

A shown in Figure 7-17, the cis tetramer has the stronger H-bond interaction (Cis ΔH = -49.01; Trans ΔH = -40.36) in the tetrameric isomers. This is also the one with more red-shifted C=O stretching mode. This indicates that the stronger H-bond can provide the stronger C=O coupling.

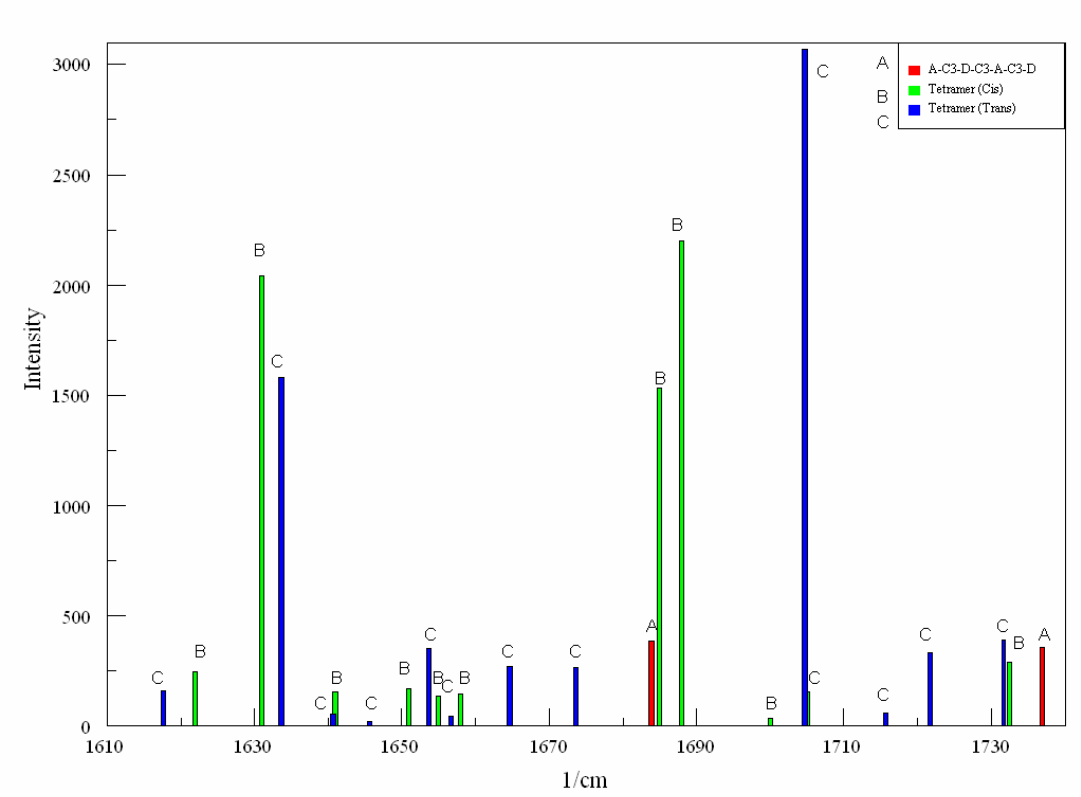

Figure 7-17. The C=O absorptions of A-C3-D-C3-A-C3-D tetramer. The A-C3-D-C3-A-C3-D monomer shown as red lines, the cis dimer (Cis) shown as green lines, and the trans dimer (Trans) shown as blue lines.

7.4 Conclusions

Various donor-acceptor sequenced structures have been investigated. Frequency analysis of C=O clear shows the geometric information of the structures. The monomeric, dimeric, and tetrameric structures can be distinguished from each other by frequency calculations. Not all of the most red-shifted C=O absorptions are the most intense. It depends on the alignment of C=O and the stretching movements. The donor-acceptor sequence in the monomer and polymers can be observed each from the C=O absorption peaks. Some peaks might be missing that is because the symmetric vibration of C=O in opposite directions that minimize the intensity.

The cis-trans isomers of the dimers and tetramers exhibit significant spectroscopic variations. The trans isomers show more intense peaks than the cis ones because the linear combination of C=O stretches that are all in the phase. It is also observed in the cis-trans isomers, the isomers have stronger H-bond interaction can more red-shifted frequency in amide I region. When the structure is getting larger (from dimer to tetramer), certain N-H bending might interfere with the C=O stretching to cause extra C=O absorption peaks. This could occur in the A-D-Center-A-D and D-A-Center-A-D structures due to the non-H-bonded N-H groups exist in the structure. The phenomenon can not be observed in the A-D-Center-D-A structures, since all N-H groups are involved in the H-bond interaction.

BIBLIOGRAPHY

(1) Lehn, J. M. *Science* **2002**, *295*, 2400-3.

(2) Guo, Y.; Yui, H.; Minamikawa, H.; Yang, B.; Masuda, M.; Ito, K.; Shimizu, T. *Chemistry of Materials*, ACS ASAP.

(3) Shimizu, T.; Masuda, M.; Minamikawa, H. *Chemical Reviews (Washington, DC, United States)* **2005**, *105*, 1401-1443.

(4) Macdonald, J. C.; Whitesides, G. M. *Chemical Reviews* **1994**, *94*, 2383-2420.

(5) Baldini, L.; Sansone, F.; Massera, C.; Casnati, A.; Ugozzoli, F.; Ungaro, R. *Inorganica Chimica Acta* **2007**, *360*, 970-980.

(6) Grosshans, P.; Jouaiti, A.; Bulach, V.; Planeix, J.-M.; Hosseini, M. W.; Nicoud, J.-F. *CrystEngComm* **2003**, *5*, 414-416.

(7) Felix, O.; Hosseini, M. W.; De Cian, A. *Solid State Sciences* **2001**, *3*, 789-793.

(8) Hosseini, M. W. *Acc Chem Res* **2005**, *38*, 313-23.

(9) Sijbesma, R. P.; Meijer, E. W. *Chemical Communications* **2003**, 5-16.

(10) Nguyen, T.-Q.; Martel, R.; Bushey, M.; Avouris, P.; Carlsen, A.; Nuckolls, C.; Brus, L. *Physical Chemistry Chemical Physics* **2007**, *9*, 1515-1532.

(11) Prins, L. J.; Reinhoudt, D. N.; Timmerman, P. *Angewandte Chemie-International Edition* **2001**, *40*, 2383-2426.

(12) De Santis, P.; Morosetti, S.; Rizzo, R. *Macromolecules* **1974**, *7*, 52-8.

(13) Ghadiri, M. R.; Granja, J. R.; Milligan, R. A.; McRee, D. E.; Khazanovich, N. *Nature* **1994**, *372*, 709-709.

(14) Ghadiri, M. R.; Granja, J. R.; Milligan, R. A.; McRee, D. E.; Khazanovich, N. *Nature* **1993**, *366*, 324-327.

(15) Fernandez-Lopez, S.; Kim, H. S.; Choi, E. C.; Delgado, M.; Granja, J. R.; Khasanov, A.; Kraehenbuehl, K.; Long, G.; Weinberger, D. A.; Wilcoxen, K. M.; Ghadiri, M. R. *Nature* **2001**, *412*, 452-5.

(16) Ghadiri, M. R.; Granja, J. R.; Buehler, L. K. *Nature FIELD Full Journal Title:Nature* **1994**, *369*, 301-4.

(17) Motesharei, K.; Ghadiri, M. R. *Journal of the American Chemical Society* **1997**, *119*, 11306-11312.

(18) Matsui, H.; Gologan, B. *Journal of Physical Chemistry B* **2000**, *104*, 3383-3386.

(19) Matsui, H.; Gologan, B.; Schaffer, H.; Adar, F.; Seconi, D.; Phanstiel, O. *Langmuir* **2000**, *16*, 3148-3153.

(20) Matsui, H.; Gologan, B.; Pan, S.; Douberly, G. E. *European Physical Journal D* **2001**, *16*, 403-406.

(21) Djalali, R.; Chen, Y. F.; Matsui, H. *Abstracts of Papers of the American Chemical Society* **2003**, *226*, U714-U714.

(22) Djalali, R.; Chen, Y.; Matsui, H. *Journal of the American Chemical Society* **2002**, *124*, 13660-13661.

(23) Yu, L.; Banerjee, I. A.; Shima, M.; Rajan, K.; Matsui, H. *Advanced Materials (Weinheim, Germany)* **2004**, *16*, 709-712.

(24) Chen, Y.-f.; Banerjee, I. A.; Yu, L.; Djalali, R.; Matsui, H. *Langmuir* **2004**, *20*, 8409-8413.

(25) Kogiso, M.; Ohnishi, S.; Yase, K.; Masuda, M.; Shimizu, T. *Langmuir* **1998**, *14*, 4978-4986.

(26) Reches, M.; Gazit, E. *Current Nanoscience* **2006**, *2*, 105-111.

(27) Silva, G. A.; Czeisler, C.; Niece, K. L.; Beniash, E.; Harrington, D. A.; Kessler, J. A.; Stupp, S. I. *Science* **2004**, *303*, 1352-1355.

(28) Vauthey, S.; Santoso, S.; Gong, H.; Watson, N.; Zhang, S. *Proc Natl Acad Sci U S A* **2002**, *99*, 5355-60.

(29) Reches, M.; Gazit, E. *Israel Journal of Chemistry* **2005**, *45*, 363-371.

(30) Yemini, M.; Reches, M.; Rishpon, J.; Gazit, E. *Nano Letters* **2005**, *5*, 183-186.

(31) Reches, M.; Gazit, E. *Science* **2003**, *300*, 625-7.

(32) Reches, M.; Gazit, E. *Nano Letters* **2004**, *4*, 581-585.

(33) Jeffrey, G. A. *An introduction to hydrogen bonding*; Oxford University Press: New York, 1997.

(34) Aakeroy, C. B.; Seddon, K. R. *Chemical Society Reviews* **1993**, *22*, 397-407.

(35) Desiraju, G. R. *Accounts of Chemical Research* **1991**, *24*, 290-296.

(36) Parthasarathi, R.; Subramanian, V.; Sathyamurthy, N. *Journal of Physical Chemistry A* **2006**, *110*, 3349-3351.

(37) Turi, L.; Dannenberg, J. J. *Journal of the American Chemical Society* **1994**, *116*, 8714-8721.

(38) Turi, L.; Dannenberg, J. J. *Journal of Physical Chemistry* **1993**, *97*, 12197-12204.

(39) Kobko, N.; Paraskevas, L.; del Rio, E.; Dannenberg, J. J. *Journal of the American Chemical Society* **2001**, *123*, 4348-4349.

(40) Masunov, A.; Dannenberg, J. J. *Journal of Physical Chemistry B* **2000**, *104*, 806-810.

(41) Turi, L.; Dannenberg, J. J. *Journal of Physical Chemistry* **1996**, *100*, 9638-9648.

(42) Turi, L.; Dannenberg, J. J. *Chemistry of Materials* **1994**, *6*, 1313-1316.

(43) Turi, L.; Dannenberg, J. J. *Molecular Crystals and Liquid Crystals* **1992**, *219*, 63-69.

(44) Jones, P. G. *Acta Crystallographica, Section C: Crystal Structure Communications* **2001**, *C57*, 880-882.

(45) Chen, Y. F.; Dannenberg, J. J. *Journal of the American Chemical Society* **2006**, *128*, 8100-8101.

(46) Alvarez-Rua, C.; Garcia-Granda, S.; Goswani, S.; Mukherjee, R.; Dey, S.; Claramunt, R. M.; Santa Maria, M. D.; Rozas, I.; Jagerovic, N.; Alkorta, I.; Elguero, J. *New Journal of Chemistry* **2004**, *28*, 700-707.

(47) Gilli, P.; Bertolasi, V.; Pretto, L.; Antonov, L.; Gilli, G. *Journal of the American Chemical Society* **2005**, *127*, 4943-4953.

(48) Gilli, P.; Bertolasi, V.; Pretto, L.; Lycka, A.; Gilli, G. *Journal of the American Chemical Society* **2002**, *124*, 13554-13567.

(49) Gilli, P.; Bertolasi, V.; Ferretti, V.; Gilli, G. *Journal of the American Chemical Society* **2000**, *122*, 10405-10417.

(50) Gilli, G.; Gilli, P. *Journal of Molecular Structure* **2000**, *552*, 1-15.

(51) Dykstra, C. E. *Chemical Reviews (Washington, DC, United States)* **1993**, *93*, 2339-53.

(52) Kobko, N.; Dannenberg, J. J. *Journal of Physical Chemistry A* **2003**, *107*, 10389-10395.

(53) (a)Alivisatos, A. P. J., K. P.; Peng, X.; Wilson, T. E.; Loweth, C. J.; Bruchez, M. P., Jr.; Schultz, P. G. Nature 1996, 382, 609.(b) Jenekhe, S. A.; Chen, X. L. Science 1999, 283, 372.(c). Ghadiri, M. R.; Granja, J. R.; Milligan, R. A.; McRee, D. E.; Khazanovich, N. Nature 1993, 366, 324.(d)Fuhrhop, J.-H.; Helfrich, W. Chem. Rev. 1993, 93, 1565.(e)Barklis, E.; McDermott, J.; Wilkens, S.; Fuller, S.; Thompson, D. J. Biol. Chem. 1998, 273, 7177.(f) Chen, Y.-f.; Banerjee, I. A.; Yu, L.; Djalali, R.; Matsui, H.; Langmuir 2004; 20 8409.

(54) (a)Lehn, J. M. S. C. C. a. P. V. W., Germany, 1995.(b) Atwood, J. L.; Lehn, J. M.; Davis, J. E. D.; MacNicol, D. D.; Vogtle, F. Comprehensive Supramolecular Chemistry; Pergamon: New York, 1996.

(55) (a)Douberly, G. J. P., S.; Walters, D.; Matsui, H. J. Phys. Chem. B 2001, 105, 7612.(b) Matsui, H.; Porrata, P.; Douberly, G. E. J. Nano Lett. 2001, 1, 461.(c) Djalali, R.; Chen, Y.-f.; Matsui, H. J. Am. Chem. Soc. 2002, 124, 13660.(d) DeLongchamp, D.; Hammond, P. T. Adv. Mater. 2001, 13, 1455. (e)Matsui, H.; MacCuspie, R. Nano Lett. 2001, 1, 671.(f) Matsui, H.; Gologan, B.; ; J. Phys. Chem. B. 2000; 104 3383. (g) Kogiso, M. M., M.; Shimizu, T. Supramol. Chem 1998, 9, 183.

(56) (a) Zhong, Z. H. W., D. L.; Cui, Y.; Bockrath, M. W.; Lieber, C. M. Science 2003, 302, 1377. (b) Chen, R. J.; Bangsaruntip, S.; Drouvalakis, K. A.; Kam, N. W. S.; Shim, M.; Li, Y. M.; Kim, W.; Utz, P. J.; Dai, H. J. Proc. Natl. Acad. Sci. U.S.A. 2003, 100, 4984. (c) Fennimore, A. M.; Yuzvinsky, T. D.; Han, W. Q.; Fuhrer, M. S.; Cumings, J.; Zettl, A. Nature 2003, 424, 408.

(57) (a)Wieczorek, R. D., J. J. J. Am. Chem. Soc. 2003, 125, 8124.(b)Wieczorek, R.; Dannenberg, J. J. J. Am. Chem. Soc. 2003, 125, 14065.(c) Kobko, N.; Dannenberg, J. J. J. Phys. Chem. A 2003, 107, 10389.(d) Kobko, N.; Dannenberg, J. J. J. Phys. Chem. A 2003, 107, 6688.(e) Ireta, J.; Neugebauer, J.; Scheffler, M.; Rojo, A.; Galvan, M. J.Phys. Chem. B 2003, 107, 1432.(f) Wu, Y.-D.; Zhao, Y.-L. J. Am. Chem. Soc. 2001, 123, 5313.(g) Topol, I. A.; Burt, S. K.; Deretey, E.; Tang, T.-H.; Perczel, A.; Rashin, A.; Csizmadia, I. G. J. Am. Chem. Soc. 2001, 123, 6054. (h) Guo, H.; Gresh, N.; Roques, B. P.; Salahub, D. R. J. Phys. Chem. B 2000, 104, 9746.(i) Lin, J.-Q.; Luo, S.-W.; Wu, Y. D. J. Comput. Chem. 2002, 23, 1551.(j)Wieczorek, R.; Dannenberg, J. J. Submitted for publication.(k) Salvador, P.; Kobko, N.; Wieczorek, R.; Dannenberg, J. J. J. Am.Chem. Soc., submitted. (l)Viswanathan,R.; Asensio, A.; Dannenberg, J. J. J.Phys. Chem, accepted.

(58) Beke, T.; Csizmadia, I. G.; Perczel, A. *Journal of the American Chemical Society* **2006**, *128*, 5158-5167.

(59) (a) Kenward, M. W., M. D. J. Chem. Phys. 2002, 116, 3455. (b) Lopez, C. F.; Moore, P. B.; Shelley, J. C.; Shelley, M. Y.; Klein, M. L. Comput. Phys. Commun. 2002, 147, 1. (c) Tsonchev, S.; Troisi, A.; Schatz, G. C.; Ratner, M. A.; Nano Lett.; 2004; 4; 427.

(60) Gennes, P. G. d.; Prost, J. *The physics of liquid crystals*; 2nd ed.; Clarendon Press ;

Oxford University Press: Oxford

New York, 1993.

(61) Dannenberg, J. J. *Theochem* **1997**, *401*, 279-286.

(62) Keinan, S.; Ratner, M. A.; Marks, T. J. *Chemical Physics Letters* **2004**, *392*, 291-296.

(63) Muller-Dethlefs, K.; Hobza, P. *Chem Rev* **2000**, *100*, 143-68.

(64) Perrin, C. L.; Nielson, J. B. *Annu Rev Phys Chem* **1997**, *48*, 511-44.

(65) Steiner, T. *Angewandte Chemie-International Edition* **2002**, *41*, 48-76.

(66) Steiner, T.; Desiraju, G. R. *Chemical Communications* **1998**, 891-892.

(67) Novoa, J. J.; Lafuente, P.; Mota, F. *Chemical Physics Letters* **1998**, *290*, 519-525.

(68) Del Bene, J. E.; Jordan, M. J. T. *Theochem* **2001**, *573*, 11-23.

(69) Ireta, J.; Neugebauer, J.; Scheffler, M. *Journal of Physical Chemistry A* **2004**, *108*, 5692-5698.

(70) Cramer, C. J. *Essentials of computational chemistry : theories and models*; 2nd ed.; Wiley: Chichester, West Sussex, England ; Hoboken, NJ, 2004.

(71) Kohn, W.; Sham, L. J. *Physical Review* **1965**, *137*, 1697-705.

(72) Becke, A. D. *Journal of Chemical Physics* **1993**, *98*, 1372-7.

(73) Rappe, A. K.; Bernstein, E. R. *Journal of Physical Chemistry A* **2000**, *104*, 6117-6128.

(74) Had*zi, D. *Theoretical treatments of hydrogen bonding*; John Wiley Sons: Chichester ; New York, 1997.

(75) McLean, A. D.; Liu, B. *Journal of Chemical Physics* **1973**, *58*, 1066-78.

(76) van Duijneveldt, F. B.; van Duijneveldt-van de Rijdt, J. G. C. M.; van Lenthe, J. H. *Chemical Reviews (Washington, DC, United States)* **1994**, *94*, 1873-85.

(77) Boys, S. F.; Bernardi, F. *Molecular Physics* **2002**, *100*, 65-73.

(78) Simon, S.; Duran, M.; Dannenberg, J. J. *Journal of Chemical Physics* **1996**, *105*, 11024-11031.

(79) Wieczorek, R.; Haskamp, L.; Dannenberg, J. J. *Journal of Physical Chemistry A* **2004**, *108*, 6713-6723.

(80) Kobko, N.; Dannenberg, J. J. *Journal of Physical Chemistry A* **2001**, *105*, 1944-1950.

(81) Dannenberg, J. J.; Kobko, N. *Abstracts of Papers, 220th ACS National Meeting, Washington, DC, United States, August 20-24, 2000* **2000**, COMP-123.

(82) Simon, S.; Duran, M.; Dannenberg, J. J. *Journal of Physical Chemistry A* **1999**, *103*, 1640-1643.

(83) Masunov, A.; Dannenberg, J. J. *Journal of Physical Chemistry A* **1999**, *103*, 178-184.

(84) Turi, L.; Dannenberg, J. J. *Journal of Physical Chemistry* **1993**, *97*, 2488-90.

(85) Simon, S.; Duran, M.; Dannenberg, J. J. *Journal of Chemical Physics* **1996**, *105*, 11024-11031.

(86) Perdew, J. P.; Burke, K.; Ernzerhof, M. *Physical Review Letters* **1996**, *77*, 3865-3868.

(87) Wang, W. H. *Chemical Physics Letters* **2005**, *402*, 54-56.

(88) Zhao, Y.; Truhlar, D. G. *Journal of Chemical Theory and Computation* **2005**, *1*, 415-432.

(89) Zhao, Y.; Truhlar, D. G. *Journal of Physical Chemistry A* **2005**, *109*, 6624-6627.

(90) Cerny, J.; Hobza, P. *Physical Chemistry Chemical Physics* **2005**, *7*, 1624-1626.

(91) (a) Check, C. J. O. C., 70, 9828; (b) Yao, X; J Phys Chem A 2003, 107, 9991; (c) Izgorodina, E; J Phys Chem A 2005, 109, 7558;; (d) Grimme, S. A. C., Int Ed 2006, 45, 4460; (e) Wodrich, M; Org Lett 2006, 8, 3631; (f) Schreiner, P; Org Lett 2006, 8, 3635; (g) Zhao, Y; Org Lett 2006, 8, 5753; (h) Grimme, S; J Chem Theory Comput 2007, 3, 42; (i) Carlier, P; J Org Chem 2006, 71, 1592; (j) Zhao, Y; J Org Chem 2007, 72, 295; (k) Kafafi, S; J Phys Chem A 1998, 102, 10404; (l) Woodcock, H; J Phys Chem A 2002, 106, 11923; (m) Zhao, Y; J Phys Chem A 2006, 110, 10478; (n) Grimme, S; J Org Chem 2007, 72, 2118; (o) Riley, K; J Chem Theory Comput 2007, 3, 407.

(92) (a) Raghavachari, K. M. P., 91, 555;(b) Curtiss, L; J Chem Phys 1997, 106, 1063; (c) Curtiss, L; J Chem Phys 2000, 112, 7374; (d) Saeys, M. J. P. C. A., 107, 9147.

(93) (a) Feng, Y. J. C. I. C. S., 43, 2005; (b) Fu, Y; Chin J Chem 2005, 23, 474.

(94) Wodrich, M. D.; Corminboeuf, C.; Schreiner, P. R.; Fokin, A. A.; Schleyer, P. R. *Org Lett* **2007**, *9*, 1851-4.

(95) Lukin, O.; Leszczynski, J. *Journal of Physical Chemistry A* **2002**, *106*, 6775-6782.

(96) Guerra, C. F.; Bickelhaupt, F. M.; Snijders, J. G.; Baerends, E. J. *Journal of the American Chemical Society* **2000**, *122*, 4117-4128.

(97) Rablen, P. R.; Lockman, J. W.; Jorgensen, W. L. *Journal of Physical Chemistry A* **1998**, *102*, 3782-3797.

(98) Scheiner, S. *Hydrogen bonding : a theoretical perspective*; Oxford University Press: New York, 1997.

(99) Yung-fou Chen, R. V. a. J. J. D. *Journal of Physical Chemistry A*.

(100) Kobko, N.; Dannenberg, J. J. *Journal of Physical Chemistry A* **2003**, *107*, 6688-6697.

(101) Krimm, S.; Abe, Y. *Proc Natl Acad Sci U S A* **1972**, *69*, 2788-92.

(102) Frisch, M. J. T., G. W.; Schlegel, H. B.; Scuseria, G. E.; Robb, M. A.; Cheeseman, J. R.; Montgomery, J. A., Jr.; Vreven, T.; Kudin, K. N.; Burant, J. C.; Millam, J. M.; Iyengar, S. S.; Tomasi, J.; Barone, V.; Mennucci, B.; Cossi, M.; Scalmani, G.; Rega, N.; Petersson, G. A.; Nakatsuji, H.; Hada, M.; Ehara, M.; Toyota, K.; Fukuda, R.; Hasegawa, J.; Ishida, M.; Nakajima, T.; Honda, Y.; Kitao, O.; Nakai, H.; Klene, M.; Li, X.; Knox, J. E.; Hratchian, H. P.; Cross, J. B.; Bakken, V.; Adamo, C.; Jaramillo, J.; Gomperts, R.; Stratmann, R. E.; Yazyev, O.; Austin, A. J.; Cammi, R.; Pomelli, C.; Ochterski, J. W.; Ayala, P. Y.; Morokuma, K.; Voth, G. A.; Salvador, P.; Dannenberg, J. J.; Zakrzewski, V. G.; Dapprich, S.; Daniels, A. D.; Strain, M. C.; Farkas, O.; Malick, D. K.; Rabuck, A. D.; Raghavachari, K.; Foresman, J. B.; Ortiz, J. V.; Cui, Q.; Baboul, A. G.; Clifford, S.; Cioslowski, J.; Stefanov, B. B.; Liu, G.; Liashenko, A.; Piskorz, P.;

Komaromi, I.; Martin, R. L.; Fox, D. J.; Keith, T.; Al-Laham, M. A.; Peng, C. Y.; Nanayakkara, A.; Challacombe, M.; Gill, P. M. W.; Johnson, B.; Chen, W.; Wong, M. W.; Gonzalez, C.; Pople, J. A. Gaussian 03, revision C.02; Gaussian, Inc.: Wallingford, CT, 2004.; Revision C.02 ed. 2004.

(103) Linda. Scientific. Computing Associates, N. H.

(104) Becke, A. D. *Journal of Chemical Physics* **1993**, *98*, 5648-52.

(105) Lee, C.; Yang, W.; Parr, R. G. *Physical Review B: Condensed Matter and Materials Physics* **1988**, *37*, 785-9.

(106) Tsai, C. J.; Zheng, J.; Nussinov, R. *Plos Computational Biology* **2006**, *2*, 311-319.

(107) Paramonov, S. E.; Jun, H. W.; Hartgerink, J. D. *Journal of the American Chemical Society* **2006**, *128*, 7291-7298.

(108) Ashkenasy, N.; Horne, W. S.; Ghadiri, M. R. *Small* **2006**, *2*, 99-102.

(109) Amorin, M.; Castedo, L.; Granja, J. R. *Chemistry-a European Journal* **2005**, *11*, 6543-6551.

(110) Zhang, S. G.; Marini, D. M.; Hwang, W.; Santoso, S. *Current Opinion in Chemical Biology* **2002**, *6*, 865-871.

(111) Baker, E. N.; Hubbard, R. E. *Progress in Biophysics & Molecular Biology* **1984**, *44*, 97-179.

(112) Jeffrey, G. A.; Saenger, W. *Hydrogen bonding in biological structures*; Springer-Verlag: Berlin ; New York, 1991.

(113) Jeffrey, G. A.; Saenger, W. *Hydrogen bonding in biological structures*; Study ed.; Springer-Verlag: Berlin ; New York, 1994.

(114) Gao, X.; Matsui, H. *Advanced Materials (Weinheim, Germany)* **2005**, *17*, 2037-2050.

(115) Gorbitz, C. H. *Chemical Communications* **2006**, 2332-2334.

(116) Kol, N.; Adler-Abramovich, L.; Barlam, D.; Shneck, R. Z.; Gazit, E.; Rousso, I. *Nano Letters* **2005**, *5*, 1343-1346.

(117) Ghadiri, M. R. *Advanced Materials* **1995**, *7*, 675-677.

(118) Turi, L.; Dannenberg, J. J. *Journal of Physical Chemistry* **1993**, *97*, 12197-204.

(119) Colominas, C.; Teixido, J.; Cemeli, J.; Luque, F. J.; Orozco, M. *Journal of Physical Chemistry B* **1998**, *102*, 2269-2276.

(120) Gomez Marigliano, A. C.; Varetti, E. L. *Journal of Physical Chemistry A* **2002**, *106*, 1100-1106.

(121) Harmony, M. D.; Laurie, V. W.; Kuczkowski, R. L.; Schwendeman, R. H.; Ramsay, D. A.; Lovas, F. J.; Lafferty, W. J.; Maki, A. G. *Journal of Physical and Chemical Reference Data* **1979**, *8*, 619-721.

(122) Nahringbauer, I. *Acta Crystallographica, Section B: Structural Crystallography and Crystal Chemistry* **1978**, *B34*, 315-18.

(123) Turi, L. *Journal of Physical Chemistry* **1996**, *100*, 11285-11291.

(124) Asensio, A.; Kobko, N.; Dannenberg, J. J. *Journal of Physical Chemistry A* **2003**, *107*, 6441-6443.

(125) Hazra, M. K.; Chakraborty, T. *Journal of Physical Chemistry A* **2005**, *109*, 7621-7625.

(126) Jaravine, V. A.; Alexandrescu, A. T.; Grzesiek, S. *Protein Sci* **2001**, *10*, 943-50.

(127) Juranic, N.; Moncrieffe, M. C.; Likic, V. A.; Prendergast, F. G.; Macura, S. *J Am Chem Soc* **2002**, *124*, 14221-6.

(128) Miller, J. S.; Kennedy, R. J.; Kemp, D. S. *J Am Chem Soc* **2002**, *124*, 945-62.

(129) Raczynska, E. D.; Darowska, M.; Dabkowska, I.; Decouzon, M.; Gal, J. F.; Maria, P. C.; Poliart, C. D. *Journal of Organic Chemistry* **2004**, *69*, 4023-4030.

(130) Kriz, J.; Dybal, J.; Brus, J. *J Phys Chem B Condens Matter Mater Surf Interfaces Biophys* **2006**, *110*, 18338-46.

(131) Cardenas-Jiron, G. I.; Masunov, A.; Dannenberg, J. J. *Journal of Physical Chemistry A* **1999**, *103*, 7042-7046.

(132) Dannenberg, J. J. *Journal of Molecular Structure* **2002**, *615*, 219-226.

(133) Dannenberg, J. J.; Kobko, N. *Abstracts of Papers, 226th ACS National Meeting, New York, NY, United States, September 7-11, 2003* **2003**, PHYS-225.

(134) Wieczorek, R.; Dannenberg, J. J. *Journal of the American Chemical Society* **2003**, *125*, 8124-8129.

(135) Salvador, P.; Dannenberg, J. J. *Journal of Physical Chemistry B* **2004**, *108*, 15370-15375.

(136) Viswanathan, R.; Asensio, A.; Dannenberg, J. J. *Journal of Physical Chemistry A* **2004**, *108*, 9205-9212.

(137) Wieczorek, R.; Dannenberg, J. J. *Journal of the American Chemical Society* **2004**, *126*, 14198-14205.

(138) Guo, H.; Gresh, N.; Roques, B. P.; Salahub, D. R. *Journal of Physical Chemistry B* **2000**, *104*, 9746-9754.

(139) Zhao, Y. L.; Wu, Y. D. *Journal of the American Chemical Society* **2002**, *124*, 1570-1571.

(140) Goedert, M.; Spillantini, M. G. *Science* **2006**, *314*, 777-81.

(141) Hardy, J.; Selkoe, D. J. *Science* **2002**, *297*, 353-6.

(142) Prusiner, S. B. *Science* **1997**, *278*, 245-51.

(143) Matsui, H.; Pan, S.; Gologan, B.; Jonas, S. H. *Journal of Physical Chemistry B* **2000**, *104*, 9576-9579.

(144) Gao, X. Y.; Matsui, H. *Advanced Materials* **2005**, *17*, 2037-2050.

(145) Ranganathan, D.; Lakshmi, C.; Karle, I. L. *Journal of the American Chemical Society* **1999**, *121*, 6103-6107.

(146) Engels, M.; Bashford, D.; Ghadiri, M. R. *Journal of the American Chemical Society* **1995**, *117*, 9151-9158.

(147) Jagannadh, B.; Reddy, M. S.; Rao, C. L.; Prabhakar, A.; Jagadeesh, B.; Chandrasekhar, S. *Chemical Communications* **2006**, 4847-4849.

(148) Adler-Abramovich, L.; Reches, M.; Sedman, V. L.; Allen, S.; Tendler, S. J. B.; Gazit, E. *Langmuir* **2006**, *22*, 1313-1320.

(149) Matsumura, S.; Uemura, S.; Mihara, H. *Molecular Biosystems* **2005**, *1*, 146-148.

(150) Fukasaku, K.; Takeda, K.; Shiraishi, K. *Journal of the Physical Society of Japan* **1997**, *66*, 3387-3390.

(151) Lewis, J. P.; Pawley, N. H.; Sankey, O. F. *Journal of Physical Chemistry B* **1997**, *101*, 10576-10583.

(152) Fukasaku, K.; Takeda, K.; Shiraishi, K. *Journal of the Physical Society of Japan* **1998**, *67*, 3751-3760.

(153) Okamoto, H.; Nakanishi, T.; Nagai, Y.; Kasahara, M.; Takeda, K. *Journal of the American Chemical Society* **2003**, *125*, 2756-2769.

(154) Ferrante, F.; La Manna, G. *Journal of Physical Chemistry A* **2003**, *107*, 91-96.

(155) Nagai, Y.; Nakanishi, T.; Okamoto, H.; Takeda, K.; Furukawa, Y.; Usui, K.; Mihara, H. *Japanese Journal of Applied Physics Part 1-Regular Papers Brief Communications & Review Papers* **2005**, *44*, 7654-7661.

(156) Lin, J. Q.; Luo, S. W.; Wu, Y. D. *J Comput Chem* **2002**, *23*, 1551-8.

(157) Seto, C. T.; Whitesides, G. M. 1993; Vol. 115, p 905-916.

(158) Brunet, P.; Simard, M.; Wuest, J. D. 1997; Vol. 119, p 2737-2738.

(159) Muller, A.; Talbot, F.; Leutwyler, S. *Journal of Chemical Physics* **2000**, *112*, 3717-3725.

(160) Viswanathan, R.; Asensio, A.; Dannenberg, J. J. *Journal of Physical Chemistry A* **2004**, *108*, 9205-9212.

(161) Charmant, J. P. H.; Norman, N. C.; Starbuck, J. In *Acta Crystallographica Section E* 2002; Vol. 58, p m144-m146.

(162) (a) Gilli, P. B., V.; Ferretti, V.; Gilli, G. J. Am. Chem. Soc.1994, 116, 909. (b) Gilli, G.; Bellucci, F.; Ferretti, V.; Bertolasi, V. J. Am.; Chem. Soc. 1989, 1023. (c) Bertolasi, V.; Gilli, P.; Ferretti, V.; Gilli, G. J. Am. Chem. Soc. 1991, 113, 4917. (d)

Gilli, P.; Ferretti, V.; Bertolasi, V.; Gilli, G. In AdVances in Molecular Structure Research; Hargittai, I.,Hargittai, M., Eds.; JAI Press, Inc.: Greenwich, CT, 1996; Vol. 2, p 67.(e) Gilli, G.; Bertolasi, V.; Ferretti, V.; Gilli, P. Acta Crystallogr. 1993, B49, 564. (f) Bertolasi, V.; Gilli, P.; Ferretti, V.; Gilli, G. Chem. Eur. J.; 1996, 925. (g) Gilli, P.; Ferretti, V.; Gilli, G. In Fundamental Principles of Molecular Modeling; Gans, W., Amann, A., Boeyens, J. C. A., Eds.;; Plenum Press: New York, h. G., G.; Gilli, P. J. Mol. Struct. 2000,552, 1.

(163) Whitesides, G. M.; Simanek, E. E.; Mathias, J. P.; Seto, C. T.; Chin, D. N.; Mammen, M.; Gordon, D. M. *Accounts of Chemical Research* **1995**, *28*, 37-44.

(164) Shi, X. X.; Barkigia, K. M.; Fajer, J.; Drain, C. M. *Journal of Organic Chemistry* **2001**, *66*, 6513-6522.

(165) Brunet, P.; Simard, M.; Wuest, J. D. *Journal of the American Chemical Society* **1997**, *119*, 2737-2738.

(166) Park, T.; Todd, E. M.; Nakashima, S.; Zimmerman, S. C. *Journal of the American Chemical Society* **2005**, *127*, 18133-18142.

(167) Dannenberg, J. J. *Peptide Solvation and H-Bonds* **2006**, *72*, 227-+.

(168) Sheridan, R. P.; Lee, R. H.; Peters, N.; Allen, L. C. *Biopolymers* **1979**, *18*, 2451-2458.

(169) Turi, L.; Dannenberg, J. J. *Journal of Physical Chemistry* **1992**, *96*, 5819-5824.

(170) Turi, L.; Dannenberg, J. J. *Journal of the American Chemical Society* **1994**, *116*, 8714-21.

(171) Torii, H.; Tatsumi, T.; Kanazawa, T.; Tasumi, M. *Journal of Physical Chemistry B* **1998**, *102*, 309-314.

(172) Ismer, L.; Ireta, J.; Boeck, S.; Neugebauer, J. *Physical Review E* **2005**, *71*, -.

(173) Xiang, T.; Goss, D. J.; Diem, M. *Biophysical Journal* **1993**, *65*, 1255-1261.

(174) Diep, V.; Dannenberg, J. J.; Franck, R. W. *Journal of Organic Chemistry* **2003**, *68*, 7907-7910.

(175) Scott, A. P.; Radom, L. *Journal of Physical Chemistry* **1996**, *100*, 16502-16513.

(176) Mehler, E. L. *J Am Chem Soc* **1980**, *102*, 4051-4056.

(177) Torii, H.; Tasumi, M. *Journal of Raman Spectroscopy* **1998**, *29*, 81-86.

(178) Torii, H.; Tasumi, M. *International Journal of Quantum Chemistry* **1998**, *70*, 241-252.

(179) Bour, P.; Kubelka, J.; Keiderling, T. A. *Biopolymers* **2000**, *53*, 380-95.

(180) Bour, P.; Keiderling, T. A. *J Am Chem Soc* **1993**, *115*, 9602-9607.

(181) Silva, R. A.; Yasui, S. C.; Kubelka, J.; Formaggio, F.; Crisma, M.; Toniolo, C.; Keiderling, T. A. *Biopolymers* **2002**, *65*, 229-43.

(182) Bour, P.; Kubelka, J.; Keiderling, T. A. *Biopolymers* **2002**, *65*, 45-59.

(183) Bour, P.; Keiderling, T. A. *J Phys Chem B Condens Matter Mater Surf Interfaces Biophys* **2005**, *109*, 5348-57.

(184) Kubelka, J.; Keiderling, T. A. *Journal of Physical Chemistry A* **2001**, *105*, 10922-10928.

(185) Kubelka, J.; Keiderling, T. A. *J Am Chem Soc* **2001**, *123*, 12048-58.

(186) Myshakina, N. S.; Asher, S. A. *J Phys Chem B* **2007**, *111*, 4271-9.

(187) Brauner, J. W.; Dugan, C.; Mendelsohn, R. *J Am Chem Soc* **2000**, *122*, 677-683.

(188) Huang, R.; Kubelka, J.; Barber-Armstrong, W.; Silva, R. A.; Decatur, S. M.; Keiderling, T. A. *J Am Chem Soc* **2004**, *126*, 2346-54.

(189) Hilario, J.; Kubelka, J.; Syud, F. A.; Gellman, S. H.; Keiderling, T. A. *Biopolymers* **2002**, *67*, 233-6.

(190) Cha, S. Y.; Ham, S. H.; Cho, M. H. *Journal of Chemical Physics* **2002**, *117*, 740-750.

(191) Viswanathan, R.; Wieczorek, R.; Dannenberg, J. J. In *unpublished results* 2006.

(192) Dannenberg, J. J.; Haskamp, L.; Masunov, A. *Journal of Physical Chemistry A* **1999**, *103*, 7083-7086.

(193) Salvador, P.; Kobko, N.; Wieczorek, R.; Dannenberg, J. J. *Journal of the American Chemical Society* **2004**, *126*, 14190-14197.

(194) Etter, M. C.; Urbanczyklipkowska, Z.; Jahn, D. A.; Frye, J. S. *Journal of the American Chemical Society* **1986**, *108*, 5871-5876.

(195) Buemi, G. *Journal of the Chemical Society-Faraday Transactions Ii* **1989**, *85*, 1771-1778.

(196) Buemi, G.; Gandolfo, C. *Journal of the Chemical Society-Faraday Transactions Ii* **1989**, *85*, 215-227.

(197) Dannenberg, J. J.; Rios, R. *Journal of Physical Chemistry* **1994**, *98*, 6714-18.

(198) Xu, S. J.; Park, S. T.; Feenstra, J. S.; Srinivasan, R.; Zewail, A. H. *Journal of Physical Chemistry A* **2004**, *108*, 6650-6655.

(199) Iijima, K.; Ohnogi, A.; Shibata, S. *Journal of Molecular Structure* **1987**, *156*, 111-118.

(200) Lowrey, A. H.; George, C.; D'Antonio, P.; Karle, J. *Journal of the American Chemical Society* **1971**, *93*, 6399-403.

(201) Caminati, W.; Grabow, J. U. *Journal of the American Chemical Society* **2006**, *128*, 854-857.

(202) De Loze, C.; Baron, M. H.; Fillaux, F. *Journal de Chimie Physique et de Physico-Chimie Biologique* **1978**, *75*, 631-49.

(203) Fillaux, F.; De Loze, C. *Journal de Chimie Physique et de Physico-Chimie Biologique* **1972**, *69*, 36-44.

(204) Jeffrey, G. A.; Piniella, J. F.; North Atlantic Treaty Organization. Scientific Affairs Division. *The application of charge density research to chemistry and drug design*; Plenum Press: New York, 1991.

(205) Krimm, S.; Reisdorf, W. C. *Faraday Discussions* **1994**, 181-197.

(206) Yoder, G.; Keiderling, T. A.; Formaggio, F.; Crisma, M.; Toniolo, C.; Kamphuis, J. *Tetrahedron: Asymmetry* **1995**, *6*, 687-90.

(207) Yoder, G.; Pancoska, P.; Keiderling, T. A. *Biochemistry* **1997**, *36*, 15123-33.

(208) Schweitzer-Stenner, R.; Eker, F.; Huang, Q.; Griebenow, K. *J Am Chem Soc* **2001**, *123*, 9628-9633.

(209) Chirgadze, Y. N.; Brazhnikov, E. V.; Nevskaya, N. A. *J Mol Biol* **1976**, *102*, 781-792.

(210) Chirgadze, Y. N.; Nevskaya, N. A. *Biopolymers* **1976**, *15*, 607-625.

(211) Chirgadze, Y. N.; Nevskaya, N. A. *Biopolymers* **1976**, *15*, 627-636.

(212) Rubtsov, I. V.; Hochstrasser, R. M. *Journal of Physical Chemistry B* **2002**, *106*, 9165-9171.

(213) Watson, T. M.; Hirst, J. D. *Physical Chemistry Chemical Physics* **2004**, *6*, 998-1005.